ALFRED-WEGENER-INSTITUT
HELMHOLTZ-ZENTRUM FÜR POLAR- UND MEERESFORSCHUNG

Universität Bremen

Predicting the future of northern North Atlantic shallow water ecosystems from fossil bio-archives

Dissertation zur Erlangung des Grades eines
Doktors der Naturwissenschaften
– Dr. rer. nat. –

vorgelegt von

Lars Beierlein

Universität Bremen, August 2014

Prüfungsausschuss

1. Gutachter:	Prof. Dr. Thomas Brey Alfred-Wegener-Institut für Polar- und Meeresforschung Funktionelle Ökologie – Bremerhaven
2. Gutachter:	Prof. Dr. Bernd R. Schöne Johannes Gutenberg-Universität Mainz Institut für Geowissenschaften
3. Prüfer:	Prof. Dr. Claudio Richter Alfred-Wegener-Institut für Polar- und Meeresforschung Bentho-Pelagische Prozesse – Bremerhaven
4. Prüfer:	Dr. Helge Meggers Alfred-Wegener-Institut für Polar- und Meeresforschung Dynamik des Paläoklimas – Bremerhaven

ALFRED-WEGENER-INSTITUT
HELMHOLTZ-ZENTRUM FÜR POLAR- UND MEERESFORSCHUNG

Universität Bremen

Predicting the future of northern North Atlantic shallow water ecosystems from fossil bio-archives

Voraussagen zur Zukunft von Flachwasserökosystemen im nördlichen Nord Atlantik anhand fossiler Bio-Archive

Dissertation zur Erlangung des Grades eines
Doktors der Naturwissenschaften
– Dr. rer. nat. –

Fachbereich 2 Biologie/Chemie
Universität Bremen

vorgelegt von

Lars Beierlein

Bremen, August 2014

"*An expert is a person who has made all the mistakes that can be made in a very narrow field.*"

– Niels Bohr, Danish physicist and Nobel Prize winner

Abstract

A comprehensive understanding of past climates and environmental conditions is essential for our ability to successfully predict the likely impacts of future climate change and to effectively employ adaptation and mitigation strategies. The continued improvement and verification of numerical global circulation models (GCMs) is our best tool for predicting future climate scenarios. However, longer time-scale reconstructions particularly rely on archives (e.g., ice cores, sediment cores) that contain preserved records of past conditions (proxies) in their biogenic hard parts (e.g., shells, bones, teeth) or non-biogenic deposits/accumulations (e.g., lake varves, layers in stalagmites or ice cores).

The marine bivalve *Arctica islandica* is one such versatile and commonly used biogenic archive. Its key advantages are its longevity (up to 500 years old), its wide distribution throughout the North Atlantic and its abundance in the fossil record (back to 20 Ma). Variability in shell growth and the biogeochemistry of its shell carbonate (aragonite) enable reconstructions of, for example, large-scale ocean-atmosphere phenomena such as the North Atlantic Oscillation and sub-annual (seasonal) absolute water temperatures (based on stable oxygen isotopes). This well understood and well-calibrated archive has most commonly been used for environmental reconstructions in the last 2,000 years but its full potential for climate reconstructions further back in time has not yet been fully exploited. Therefore, this thesis aims to thoroughly assess the potential of sub-fossil (up to 10,000 years old) and fossil *A. islandica* shell specimens as a palaeo-archive that records the environmental conditions of the North Atlantic during past warm phases.

The use of any proxy data from fossil specimens presents challenges that can significantly impact upon palaeo-environmental interpretations. I firstly present a new methodology using confocal Raman microscopy (CRM) as a powerful sclerochronological tool for assessing preservation and identifying taphonomic alterations in the original shell carbonate. Diagenetic modifications to the shell make it challenging to visualize the internal growth patterns and typically render the specimen unusable for biogeochemical analysis (e.g., stable isotope or trace elemental analyses). The CRM mapping approach outlined here proves that CRM leads to comparable and even superior results when compared to commonly used growth increment visualization techniques on both modern and particularly on fossil shell material (*A. islandica* and *Pygocardia rustica*; both Pliocene). I also clearly demonstrate the

significant impact that the recrystallization of metastable shell aragonite to calcite can have on isotopic signatures within the shell carbonate. $\delta^{18}O$ and $\delta^{13}C$ signatures in recrystallized shell sections of a Pliocene *A. islandica* (Iceland) show tremendous changes from the pristine shell. Preservation state, which is often overlooked, therefore has a substantial impact on isotope records and serious implications for environmental and climatic interpretation. I therefore strongly emphasise the crucial need for preservation assessment prior to sampling for any proxy record and that CRM is an ideal tool with which to do this.

This thesis presents a reconstruction of high latitude (Svalbard) seasonality during the last warmer-than-today phase based on the archive *A. islandica*. Meticulously discussing all relevant considerations (e.g., shell preservation, palaeo-water depth, palaeo-water chemistry, ice volume effect, etc.), I show that seasonal temperatures in a fjord setting during the Holocene Climate Optimum (HCO) were considerably higher than today (+6°C on average), which impressively identifies past polar amplification (expected HCO global mean temperature +3°C). This presents a first indication of the possible impacts of future climate change in high latitude marine regions (IPCC, 2013 stating up to +3.7°C global temperatures until CE 2100).

The further analysis of internal shell growth patterns of HCO *A. islandica* specimens from Svalbard detect a pronounced and significant 11-year oscillation using tools of spectral frequency analysis. Such a signal has been previously reported in other archives and has most often been associated to the 11-year solar sunspot cycle (Schwabe cycle). Solar-climate interactions remain a debated issue, as present data is temporally and spatially insufficient to decipher any hypothetical links. Therefore no previous studies propose any explanation for a mechanistic link between shell growth in biogenic marine archives and solar activity. In this thesis I propose a first possible link between solar activity and shell growth via a biological amplifying mechanism – UV radiation and phytoplankton productivity. I emphasize that the strongly simplified hypothetical explanation presented does not claim to be conclusive. It is instead a first explanation that is intended to fuel debate and discussion on this vitally important topic that has been so far overlooked.

This study shows that growth and biogeochemical proxies recorded in the shells of *A. islandica* are a powerful archive of past climate conditions and variability on sub-annual to multi-centennial timescales. The seasonal environmental record of past warm intervals presented is a particularly valuable result, showing that northern North

Atlantic shallow marine ecosystems may experience amplified warming under future global mean climate scenarios. The importance of understanding the mechanistic links between climate drivers and growth in biogenic archives cannot be underestimated and is a priority for future research. It is hoped that the methodological advances presented here will additionally lead to significant improvements in the quality of geochemical and growth increment based biogenic proxy data produced by the sclerochronological community by facilitating preservation assessment prior to any analysis.

Zusammenfassung

Ein umfassendes Verständnis vergangener Klima- und Umweltbedingungen ist eine Grundvoraussetzung für die erfolgreiche Vorhersage zukünftiger Klimaveränderungen sowie die erfolgreiche Entwicklung von Klimaschutzstrategien. Globale Zirkulationsmodelle (GCM, aus dem Englischen) sind zur Zeit die beste Möglichkeit zur Vorhersage zukünftiger Klimaszenarien. Eine Verbesserung der Genauigkeit solcher GCMs ist nur mit Klimainformationen aus der Vergangenheit möglich. Für Zeiträume, die länger als 250 Jahre zurückliegen kann diese nur mit Hilfe von Archiven (z.B. Eisbohrkerne, Sedimentkerne) rekonstruiert werden. Verschiedene Archive speichern dabei (indirekte) vergangene Umweltbedingungen (so genannte Proxies) in biogenen Hartteilen (z.B. Muscheln, Knochen, Zähne) oder nicht-biogenen Ablagerungen (z.B. Warven, Stalagmiten oder Eisbohrkerne).

Die marine Muschel *Arctica islandica* ist ein vielseitiges und häufig genutztes Bio-Archiv. Die größten Vorteile dieses Archivs liegen dabei in der Langlebigkeit (bis zu 500 Jahre alt), der großräumigen Verbreitung im Nordatlantik und darin, dass sie relativ häufig fossil nachgewiesen wurde (für die vergangenen 20 Millionen Jahre). Schwankungen im Schalenwachstum sowie die Geochemie des Schalenkarbonats (Aragonit) ermöglichen zum Beispiel die Rekonstruktion großräumiger Ozean- und Atmosphärenphänomene wie der Nordatlantischen Oszillation oder saisonaler Wassertemperaturen (Sauerstoffisotopie). Dieses gut untersuchte Bio-Archiv wurde bislang überwiegend für Umweltrekonstruktionen der vergangenen 2000 Jahre genutzt. Das wahre Potential in Bezug auf Klimarekonstruktionen weiter zurückliegender Zeiträume wurde bisher noch nicht voll ausgeschöpft. Das Ziel der vorliegenden Arbeit liegt folglich darin, das Potential von sub-fossilen (bis zu 10000 Jahre alt) und fossilen *A. islandica* Schalen zu testen und auf seine Eignung hin als ein Umweltarchiv vergangener Warmphasen im Nordatlantik zu beurteilen.

Die Verwendung von fossilen Proxydaten bringt dabei eine Reihe verschiedener Herausforderungen mit sich, welche einen erheblichen Einfluss auf die resultierenden Paläo-Umweltrekonstruktionen haben können. In dieser Arbeit präsentiere ich eine Studie, welche das konfokale Raman Mikroskop als ein leistungsstarkes, sklerochronologisches Werkzeug darstellt mit dessen Hilfe sich der Erhaltungszustand als auch taphonomische Veränderungen im Schalenkarbonat bewerten lassen. Im Allgemeinen bedingen diagenetische Veränderungen der Schale, dass die internen Wachstumsstrukturen nicht mehr sichtbar gemacht bzw. visualisiert werden können

und die Schale nicht für geochemische Analysen geeignet ist (z.B. Isotope oder Spurenelemente). Die hier präsentierte Methode führt im Vergleich mit herkömmlichen Visualiserungsmethoden zu vergleichbaren oder sogar besseren Ergebnissen. Dies trifft auf rezentes aber vor allem auch auf fossiles Schalenmaterial zu (*A. islandica* und *Pygocardia rustica*; beide Pliozän). Zudem ist es mir möglich, den erheblichen Einfluss auf die Isotopensignatur des Schalenkarbonats zu zeigen, den der Rekristallisationsprozeß von Aragonit zu Kalzit in der Schale mit sich bringt. Die Isotopenwerte ($\delta^{18}O$ und $\delta^{13}C$) der rekristallisierten Schalenabschnitte einer pliozänen *A. islandica* unterscheiden sich dabei deutlich von denen des ursprünglichen (aragonitischen) Schalenkarbonats. Der Erhaltungszustand kann daher einen großen Einfluß auf die Isotopenzusammensetzung in der Schale und folglich weitreichende Auswirkungen auf die darauf basierenden Klima- und Umweltrekonstruktionen haben. Auf Grund dessen ist es mir ein bedeutendes Anliegen, die Wichtigkeit der Schalenerhaltung zu betonen und in diesem Zusammenhang die Vorzüge des konfokalen Raman Mikroskops hervorzuheben.

Diese Arbeit beinhaltet zudem eine Rekonstruktion saisonaler Wassertemperaturen zur Zeit der letzten Warmphase (wärmer als heute), rekonstruiert anhand von *A. islandica* Schalen (Spitzbergen). Nach einer ausgiebigen Diskussion und Berücksichtigung aller relevanten Faktoren (z.B. der Erhaltung der Schalen, der Wassertiefe, der Wasserchemie und Veränderungen des Eisvolumens) ist es mir möglich zu zeigen, dass saisonale Wassertemperaturen in einem Fjord während der Holozänen Warmphase (HCO, aus dem Englischen) deutlich höher waren als heute (+6°C im Durchschnitt), was auf beeindruckende Weise die polare Amplifikation zeigt (globale Rekonstruktionen gehen von +3°C aus). Dies gibt einen ersten Eindruck im Hinblick auf mögliche zukünftige Klimaänderungen für marine Polargebiete (der IPCC Report von 2013 sagt einen globalen Temperaturanstieg von bis zu 3.7°C für das Jahr 2100 voraus).

Anhand einer spektralen Frequenzanalyse konnte ich in den Wachstumsstrukturen der holozänen *A. islandica* Schalen von Spitzbergen ein signifikantes 11 Jahre Signal identifizieren. Ein solches Signal wurde schon früher von verschiedenen anderen Archiven beschrieben und zumeist mit dem 11 Jahre Sonnenfleckenzyklus auf der Sonnenoberfläche in Verbindung gebracht (Schwabe-Zyklus). Der Einfluß der Sonne auf das Klima der Erde ist ein vieldiskutiertes Thema. Da heutige Daten gleichwohl zeitlich als auch räumlich begrenzt vorliegen, ist es momentan nicht möglich diese Frage abschließend zu klären. Bisher liegen noch keine

Studien vor, welche einen Erklärungsansatz für den möglichen kausalen Zusammenhang zwischen Schalenwachstum und Sonnenaktivität anbieten. Insofern beschreibe ich in dieser Arbeit eine erste mögliche indirekte Verbindung, welche über einen biologischen Verstärkungsmechanismus wirkt und dabei UV Strahlung als auch Phytoplankton mit einschließt. Dabei möchte ich zu bedenken geben, dass dieser stark vereinfachte und theoretische Erklärungsansatz nicht den Anspruch hat unwiderlegbar zu sein oder als einzig möglicher Erklärungsansatz verstanden werden möchte. Vielmehr soll eine erste Erklärung der Zusammenhänge gegeben werden, welche als Grundlage zur Diskussion dieses Themas dienen soll.

Meine Untersuchungen zeigen, dass Schalenwachstum und geochemische Proxies der Muschel *A. islandica* ein vielseitiges Archiv zur Rekonstruktion vergangener Klimabedingungen auf einer saisonalen bis hin zu einer jahrhundertelangen Zeitskala darstellen. Die hier präsentierte Rekonstruktion saisonaler Umweltbedingungen stellt dabei eine besonders wichtige Erkenntnis dar. Sie legt nahe, dass unter der Annahme einer zukünftigen globalen Erwärmung in marinen Flachwasserökosystemen im nördlichen Nordatlantik mit einer verstärkten Erwärmung zu rechnen sein wird. Die Identifizierung aller relevanten Umweltfaktoren in Bezug auf das Schalenwachstum biogener Archive sollte eine wichtige Rolle in zukünftigen Studien spielen. Es ist daher wünschenswert, dass die hier vorgelegten Fortschritte und Ergebnisse zu einer Verbesserung von Wachstums- als auch geochemischen Analysen führen, sowie zu einer verbesserten Beurteilung der Erhaltung von fossilem Schalenmaterial beitragen können.

Acknowledgements

Auf diesem Wege möchte ich mich (kurz) bei allen bedanken, die mich in den letzten drei Jahren (und zum Teil auch schon davor) auf meinem wissenschaftlichen Weg begleitet haben. Ohne euch wäre diese Arbeit so nicht zustande gekommen und ihr seid der Grund dafür, dass ich die kompletten drei Jahre ununterbrochen lang Spaß an meinem Projekt hatte. Es sei kurz erwähnt, dass ich meiner Familie und meinen Freunden nicht minder dankbar bin und ihr Anteil an dieser Arbeit mindestens (!) genauso groß ist. Ich habe mich allerdings dafür entschieden diese Danksagung rein wissenschaftlich und AWI bezogen zu halten.

Zu allererst ein riesiger Dank an meinen Doktorvater, **Prof. Dr. Thomas Brey**. Du hast mir vom allerersten Tag an vollstes Vertrauen geschenkt, mich wirklich immer und bei allem zu 100% unterstützt und mir in diesen drei Jahren so Vieles ermöglicht. Das ist alles andere als selbstverständlich und ich bin dir wirklich mehr als dankbar.

Einen großen Dank an **Prof. Dr. Bernd Schöne** dafür, dass du mir in den letzten drei Jahren, wie schon davor, immer mit Rat und Tat zur Seite gestanden hast, dass du mehrfach den Weg nach Bremerhaven gefunden hast und Teil meines PhD Komitees warst und nun auch als Zweitgutachter für meine Doktorarbeit zur Verfügung stehst. Außerdem möchte ich dir dafür danken, dass ich durch dich die Wissenschaft der 'sclerochronology' für mich entdeckt habe, welche mich seit jeher fasziniert.

Vielen Dank an **Prof. Dr. Claudio Richter** und **Dr. Helge Meggers** für das Interesse an meiner Arbeit und dafür, dass ihr euch beide bereit erklärt habt, Mitglieder meines Prüfungsausschusses zu sein.

Dir Helge, genauso wie **Dr. Klaus Grosfeld**, **Stefanie Klebe**, **Dr. Ludvig Löwemark** so wie allen **ESSReS Studenten** ein großes Dankeschön für euer Engagement und eure Hingabe im Rahmen der ESSReS graduate school. An dieser Stelle möchte ich mich auch nochmals bei Klaus und **Dr. Angelika Dummermuth** bedanken, durch die ich die Möglichkeit hatte bei der Organisation und Durchführung der 'summer school' im Sommer 2012 mitwirken zu dürfen.

Als nächstes möchte ich mich gerne bei **Dr. Gernot Nehrke** bedanken, mit dem ich viel Zeit im Labor verbringen durfte und dabei sehr viel gelernt habe. Du warst Teil meines PhD Komitees, du hast mich mit dem Raman Mikroskop vertraut gemacht und mir wissenschaftlich vieles mit auf den Weg gegeben. Vielen Dank dafür.

Danke an **Prof. Dr. Gerrit Lohmann** für die Einsichten in die Welt der Klimamodellierungen und warum Archive wie *A. islandica* und proxies zur Saisonalität so gut zusammen passen. Danke für die Diskussionen, als Teil meines PhD Komitees, aber auch unabhängig davon.

Bei **Dr. Torsten Bickert** möchte ich mich dafür bedanken, dass er ein Teil meines PhD Komitees war, mehrfach den Weg nach Bremerhaven gefunden hat und auch Zeit für mich am MARUM hatte. Ein besonderer Dank an dich dafür, dass du mir im richtigen Moment aufgezeigt hast, die Projekte in Richtung Manuskripte zu lenken. An jenem Tag eine zugegeben nicht ganz einfache Lektion, aber ich bin dir wirklich sehr dankbar dafür.

Bei **Prof. Dr. Andreas Mackensen** und **Lisa Schönborn** möchte ich mich ganz herzlich für die Zusammenarbeit bei den Messungen meiner stabilen Isotope bedanken. Ich weiß, ich habe euch ganz gut auf Trapp gehalten, aber wir wurden mit wunderbaren Ergebnissen belohnt. Dir Andreas auch noch ein Dankeschön für dein offenes Ohr in Sachen postdoc in Norwegen.

Nun ein ganz großer Dank an meine Arbeitsgruppe: Danke **Kerstin Beyer** und Danke **Petra Steffens**. Ob im Labor, beim Organisatorischen oder all den anderen, kleinen Dingen des Lebens; ohne euch zwei und ohne eure Unterstützung hätte ich das niemals so hinbekommen. Danke!

Im Weiteren (und leider viel zu kurz) möchte ich mich bei folgenden AWIanern bedanken, dass sie mir in den vergangenen drei Jahren positiv und hilfreich zur Seite gestanden haben: Annika Mackensen (Danke, Danke, Danke), Laura Jensen, Stephan Dietrich, Marlene Wall, Kristina Stemmer, Kristina Kunz, Katharina Klein, Horst Bornemann, Jürgen Laudien, Jacqueline Krause-Nehring, Michael Seebeck, Jelle Bijma, Andrea Eschbach, Ruth (Dr. House) Alheit und alle die ich vergessen habe.

Zudem in Kürze, aber von Herzen: Danke an Kristina Kunz und Gotje von Leesen, dass ihr euch bereit erklärt habt meiner Prüfung beizusitzen. Danke an Jan Fietzke und Marlene Wall, für eure Zeit und Hilfe an der Mikrosonde am Geomar in Kiel. Danke an Dr. Ragnhild Asmus und Dr. Harald Asmus, sowie Marieke Feis für einen unglaublich produktiven Aufenthalt auf Sylt. Thank you Liz Nunn, for all you taught me during my diploma thesis; still benefitting from it a lot. Thanks to all (guest) students I had the pleasure of working with during my time at AWI, in particular Sol Bayer, Tamara Trofimova, Michaela Deininger and Gotje von Leesen.

Contents

List of Figures

Please note that Figures listed here do not include Figures from Manuscripts (Section 4).

Abbreviations & Acronyms

ACIA	Arctic Climate Impact Assessment
ACRI	Arctic Climate Regime Index
AMO	Atlantic Multidecadal Oscillation
AMS	Accelerator Mass Spectrometry
AO	Arctic Oscillation
AW	Atlantic Water
BWT	Bottom Water Temperature
cal yrs BP	Calibrated years before present (present = 1950)
CE	Common Era (equivalent to 'Anno Domini' (AD))
CRM	Confocal Raman Microscopy
CTD	Conductivity, Temperature and Depth
DNA	Deoxyribonucleic Acid
dog	direction of growth
EBSD	Electron Backscatter Diffraction
EGC	East Greenland Current
ENSO	El Niño-Southern Oscillation
EOF	Empirical Orthogonal Function
ESC	East Spitsbergen Current
FESOM	Finite Element Sea Ice-Ocean Model
FL	Fluorescence microscopy
GCM	General Circulation Model
GCR	Galactic Cosmic Radiation
GI	Growth Index
GISP	Greenland Ice Sheet Project
GRIP	Greenland Ice Core Project
HCO	Holocene Climate Optimum
ICP-MS	Inductively Coupled Plasma Mass Spectroscopy
IPCC	Intergovernmental Panel on Climate Change
IRMS	Isotope Ratio Mass Spectrometry
LA-ICP-MS	Laser Ablation ICP-MS

LGM	Last Glacial Maximum
LIG	Last Interglacial
LSG	Line of Strongest Growth
MEM	Maximum Entropy Method
MPWP	Mid-Pliocene Warm Period
MTM	Multi-Taper Method
NAC	Norwegian Atlantic Current
NAO	North Atlantic Oscillation
NCC	Norwegian Coastal Current
ppm	parts per million
RCP	Representative Concentration Pathway
REE	Rare Earth Elements
rpm	revolutions per minute
SEM	Scanning Electron Microscope
SGI	Standardized Growth Index
SIM	Spectral Irradiance Monitor
SIMS	Secondary Ion Mass Spectrometry
SLP	Sea Level Pressure
SSA	Singular Spectrum Analysis
SST	Sea Surface Temperature
TSI	Total Solar Irradiance
UV	Ultraviolet
VSMOW	Vienna Standard Mean Ocean Water
VPDB	Vienna Pee Dee Belemnite
WSC	West Spitsbergen Current
XRD	X-Ray Diffraction

1 Introduction

This chapter highlights the importance of detailed knowledge about past climatic and environmental conditions in the northern North Atlantic and explains why and how such conditions are linked to future climate change. Different palaeo-archives and proxies are introduced, including an emphasis on the exceptional biogenic archive *Arctica islandica* (Bivalvia), which has been utilized in all studies of this thesis.

1.1 Past climate variability and its link to future climate change

The consequences of future climate change will probably be one of the greatest challenges faced by present and future generations. The burning of fossil fuels is leading to rapidly increasing levels of atmospheric CO_2, which is causing elevated global mean surface temperatures (+1.0°C to +3.7°C by CE 2100; Figure 1a; IPCC, 2013), melting ice caps and retreating sea-ice extent (e.g., Comiso et al., 2008), rising global mean sea level (+0.4 m to +0.63 m until CE 2100; Figure 1b; IPCC, 2013) and increasing ocean acidification (–0.06 to –0.32 pH units by CE 2100; Figure 1c; Doney et al., 2009; IPCC, 2013). These changes are expected to be amplified towards the Subarctic and Arctic regions (ACIA, 2004; IPCC, 2013). Climate change will also severely affect all aspects of human livelihoods and society (Manuscript VI). Health will be affected by the spread of infectious diseases linked to climate fluctuations (Craig et al., 2004; Patz et al., 2005) and increased mortality linked to high temperatures and extreme weather events (Huynen et al., 2001; Koppe, 2005). Freshwater quality and water security will become a serious issue in the future (Vörösmarty et al., 2000; Hurd et al., 2004). Rising sea levels are expected to inundate low lying regions such as The Netherlands, the Dead Sea and some Pacific islands, as well as densely populated coastal cities around the world, causing millions of people to migrate in the future (Wetherald and Manabe, 2002; Meehl et al., 2005). The occurrence of extreme weather events will increase (e.g., storms, droughts, extreme precipitation; c.f., Meehl et al., 2000; IPCC, 2013), with implications for economics and insurance (Mills, 2005; De Sherbinin et al., 2007) as well as impacts on natural systems (e.g., live-stocks (e.g., fish), agriculture, coral reefs and forests), on which the livelihoods of billions of people depend (e.g., Stenevik and Sundby, 2007). However, quantifying the actual

anthropogenic contribution to historical and modern global warming remains challenging (IPCC, 2013).

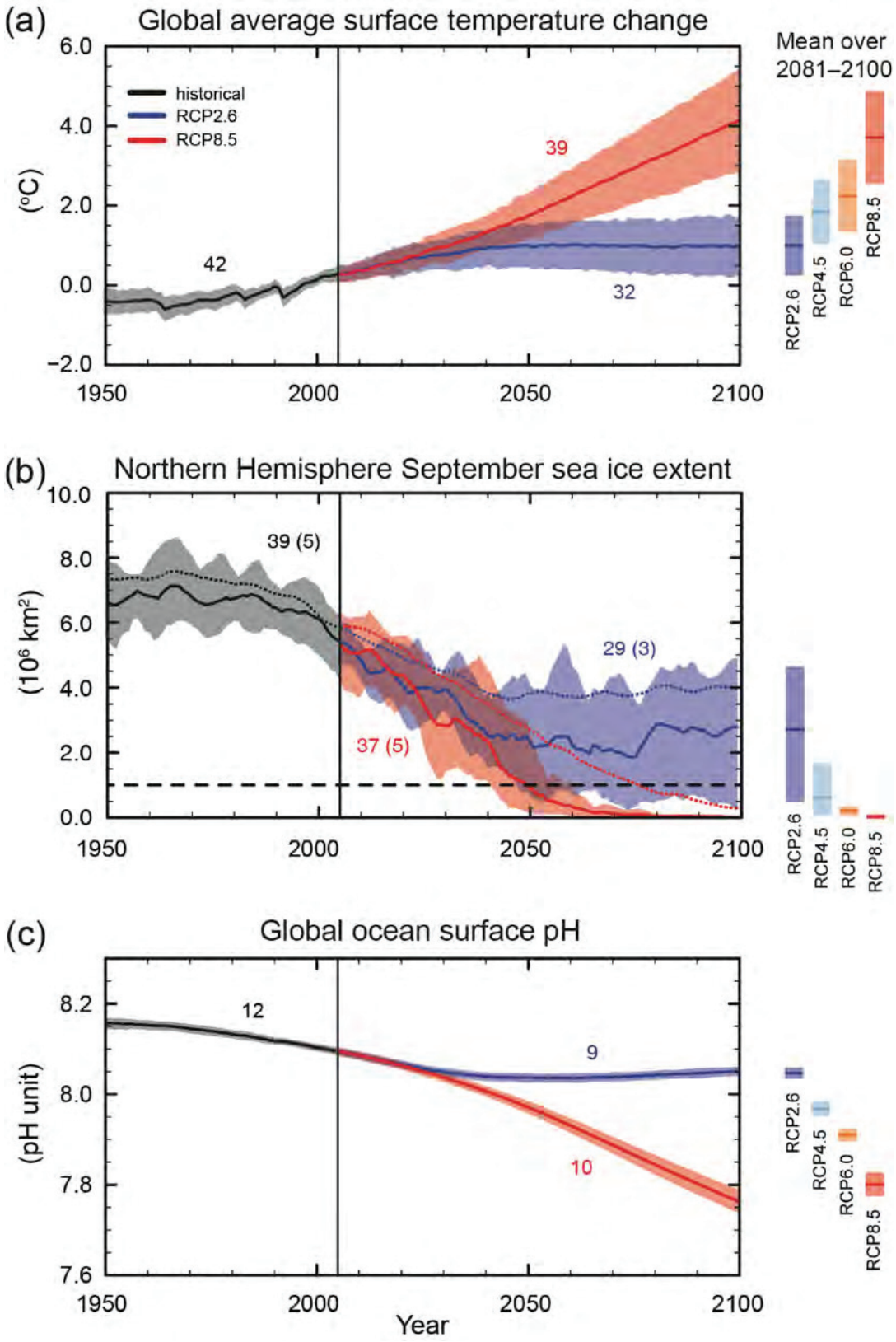

Figure 1 (previous page). Future climate scenarios. (a) Global mean surface temperature, (b) Northern Hemisphere September sea-ice extent and (c) global ocean pH under four future scenarios, given as representative concentration pathways (RCP) associated with different cumulative CO_2 emissions and 2100 CO_2 concentrations: RCP2.6 'mitigation scenario' (with mean 270 GtC from CE 2012 to 2100, 421 ppm), RCP4.5 and RCP6.0 'stabilization scenarios' (780 GtC, 538 ppm and 1060 GtC, 670 ppm respectively) and RCP8.5 'high greenhouse gas emission scenario' (1685 GtC, 936 ppm). Note that 1 GtC equals 3.67 $GtCO_2$. Number of contributing models is displayed on each graph. From IPCC, 2013.

Climate is defined as an average of weather conditions (including temperature, precipitation, humidity, wind stress and cloud cover) over a period of 30 years or more. The incoming solar energy and the resulting heat transport from the equator towards the poles via the oceans and atmosphere is a fundamental driver of climate (e.g., Petit et al., 1999). However, long-term climate changes are mainly driven by changes within the Earth–ocean–atmosphere system. Here, the main driving mechanisms are the global carbon cycle (marine and terrestrial carbon storage, the release of volcanic aerosols and gases into the atmosphere and the development of carbonate platforms), palaeo-geography and continental configuration, and vegetation patterns (Schönwiese, 1992; Shindell et al., 2003; Fluteau et al., 2007; Frank et al., 2010; Figure 2).

A crucial aspect of our understanding of the likely impacts of future climate change on natural environmental systems comes from our ability to understand system responses during warm periods in the geological past. Frequently quoted as "The past is the key to the future", environmental data from palaeo-climatic reconstructions are essential to calibrate, verify and greatly improve the accuracy and confidence of such climate models that are used for future climate projections.

The warmest interval of the Holocene interglacial (red square marked 'H' in Figure 2) and the most recent warmer-than-today phase was the Holocene Climate Optimum (HCO), lasting from approximately 10,500 to 8,200 yrs BP in the Arctic with 1–3°C warmer temperatures globally (Salvigsen et al., 1992; Rasmussen et al., 2012). Sea-ice expanse was reduced and the strength of the northernmost extension of the gulfstream also resembled expected future conditions (Ebbesen et al., 2007; IPCC, 2013). The similarities between the climate of the HCO and future temperature predictions make this a particularly important interval for understanding the mechanisms of climate change in the high latitudes and better predicting the impacts of future global warming on the natural environment. The mid-Pliocene Warm Period (MPWP; ca. 3.3–3.0 Ma) is a second ideal analogue for the future environmental conditions (e.g., Kalis et al., 2003; Salzmann et al., 2011) that may be expected according to IPCC modelling projections (IPCC, 2013).

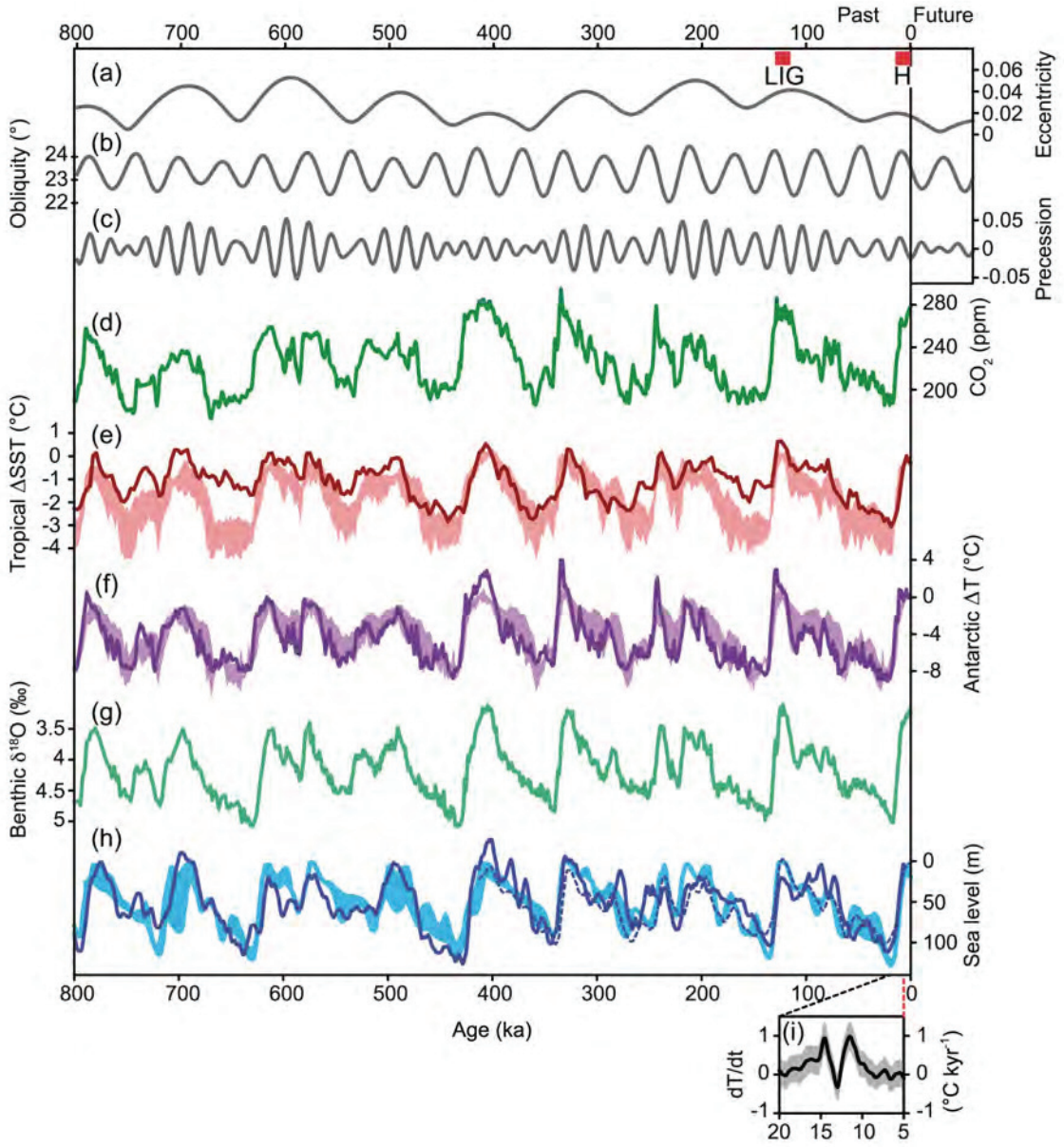

Figure 2. Long-term climate variability for the last 800 ka in comparison to (a–c) orbital Milankovitch cycles (eccentricity, obliquity, precession), (d) atmospheric CO_2 concentrations, (e) tropical SST anomalies, (f) Antarctic temperature anomalies, (g) changes in benthic $\delta^{18}O$ values and (h) sea level changes (from IPCC, 2013). Red square 'H' marks the Holocene. Red square 'LIG' marks last interglacial.

General circulation models (GCMs) are currently the most reliable tools to mathematically simulate the general circulation of the atmosphere and ocean and explore feedbacks between them, the land surface and the cryosphere. They depend mostly on observational and instrumental data (e.g., satellite data), which is available as far back as about 350 years (with the longest instrument-based temperature record, the Central England Temperature record, dating back to CE 1659). For information on climatic and environmental conditions and variabilities further back in time however (Figure 2), GCMs rely on multiple archives and proxies (Section 1.2; Figure 3). Palaeo-

climatic and palaeo-environmental information is therefore of greatest importance for the verification and assessment of these numerical models, which are the only method we have to predict future changes and enable society to successfully mitigate and adapt to a rapidly changing world.

1.2 Archives, proxies and sclerochronology

Natural archives allow climate scientists to reconstruct past climate and environmental conditions prior to the instrumental era (Figure 3) and to utilize this information in numerical climate models for a better understanding of future climate change (e.g., Felis et al., 2004). For the terrestrial realm, several biogenic (e.g., trees) and non-biogenic (e.g., ice cores, lake varves, stalagmites) archives have been successfully used, while for the marine realm, biogenic archives such as corals, coralline algae, fish otoliths and bivalves, and non-biogenic archives such as sediment cores can be utilised. All of these archives indirectly record ambient environmental conditions at the time of their growth or deposition in the form of proxies.

A proxy provides information on environmental conditions at a specific locality through records of a physical, biological or chemical response to those conditions (e.g., benthic foraminiferal $\delta^{18}O$ values recording deep-sea temperature). For most biogenic archives this information is stored within the accretionally-grown hard parts of the organism (e.g., shell) in two different ways: via anatomical-morphological features of the skeletal hard parts (i.e., shell growth increment width) and via the mineral biogeochemistry of bio-carbonate or bio-apatite (i.e., stable isotope values such as $\delta^{18}O$, $\delta^{13}C$, $\delta^{11}B$; trace and minor elemental ratios such as Sr/Ca, Mg/Ca, Li/Ca, Ba/Ca, Pb, Cd, Fe, Mn), which can be used as proxies for water temperature, salinity, pH, pollution or upwelling (e.g., Matthews et al., 2008; Hetzinger et al., 2009; Chan et al., 2011; Hahn et al., 2012; Krause-Nehring et al., 2012). The methods used to retrieve this information have improved greatly in the past few decades.

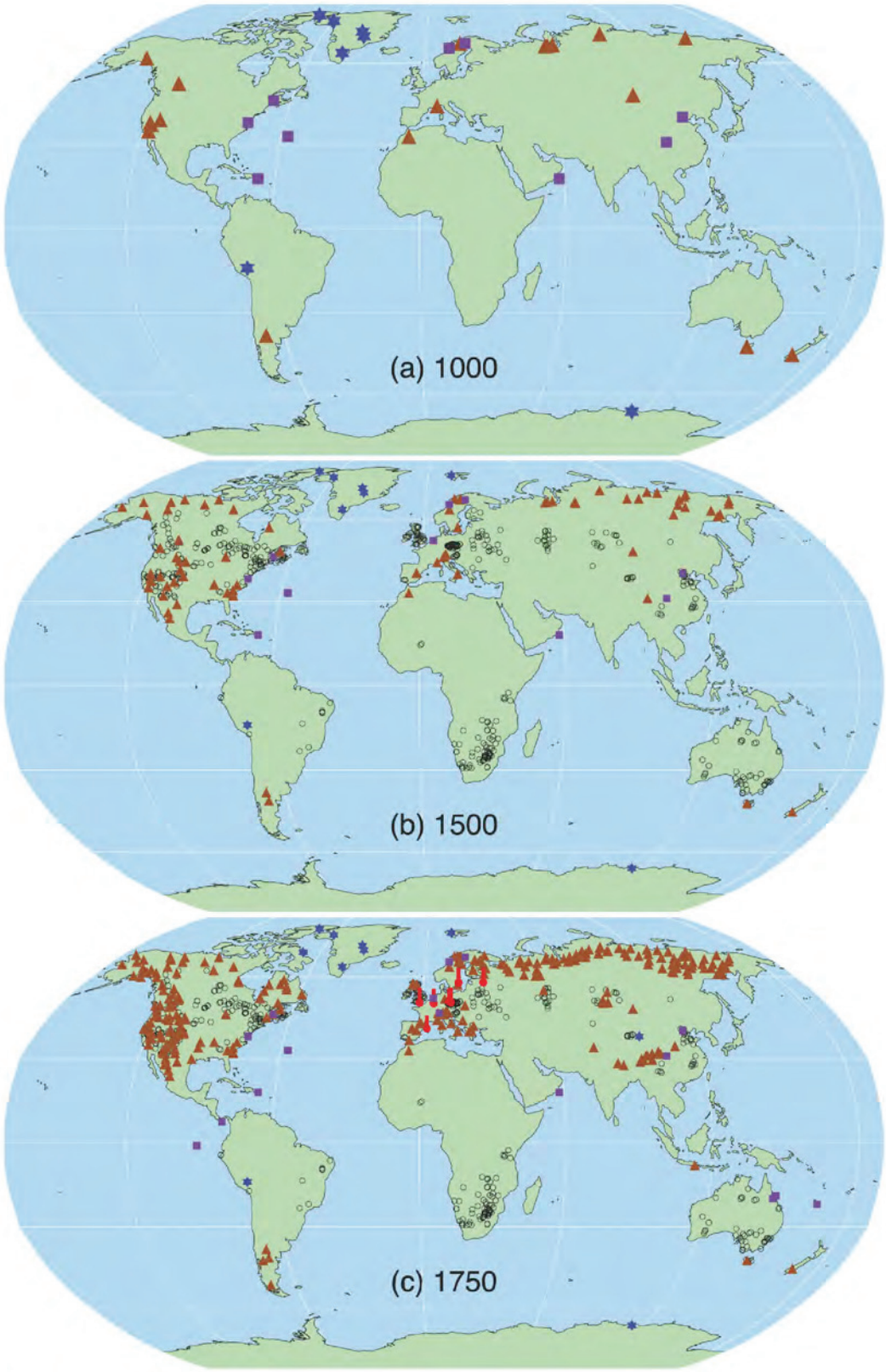

Figure 3. Global geographic distribution of temperature-sensitive proxy records back to (a) CE 1000, (b) 1500 and (c) 1750. Available archives become extremely limited, even as far back as the last 1000 years. Brown triangles = tree rings; black circles = boreholes; blue stars = ice core; purple squares = other records (from Solomon et al., 2007).

Nevertheless, almost all proxy data have both spatial and seasonal biases (Schöne, 2008). Therefore, a multi-proxy approach to past climate reconstruction is needed to provide more rigorous estimates (Black, 2009). However, one should not forget that no method is infallible and that replication and cross-verification are essential. Best results can be expected when compiling multi-archive records of a single proxy, or multi-proxy records from a single archive and combining these results for more reliable assessments of past environmental conditions.

Sclerochronology usually comprises all methods concerning the physical and chemical composition of biological hard tissues in incrementally growing organisms (c.f., Buddemeier et al., 1974; Hudson et al., 1976; Jones, 1983). The skeletal hard parts are usually derived from molluscs (including bivalves and gastropods), brachiopods, corals, coralline algae, unicellular organisms (e.g., foraminifera, coccoliths, conodonts or ostracods), pollen, spores or fish otoliths.

1.3 The importance of the northern North Atlantic

The northern North Atlantic has significant importance in the global climate system (Marshall et al., 2001), for example through its role in deep-water formation (Elliot et al., 2002). It is host to sensitive cold terrestrial environments, such as tundra and permafrost, as well as sea-ice and permanent continental ice, which support a diverse array of polar wildlife (e.g., Beaugrand et al., 2002; Beaugrand, 2004). The marine system is highly productive, supporting key fisheries (Myers et al., 1996) and playing a crucial role in global biogeochemical cycles (Gruber et al., 2002). It is additionally a region where high concentrations of anthropogenic carbon dioxide are drawn into the deep ocean (e.g., Sabine et al., 2004). The impact of future climate change on these ecosystem services could therefore be severe and far-reaching.

The North Atlantic and Arctic marine systems are also important drivers of European weather and climate (e.g., Rodwell et al., 1999; Hurrell et al., 2002; Scaife et al., 2008), which can have an impact on weather and climate globally through teleconnections (Giannini et al., 2001; Castanheira and Graf, 2003). As such, ocean-atmosphere phenomena like the North Atlantic Oscillation (NAO; Hurrell et al., 2003), which is defined as the atmospheric pressure difference between the Icelandic low and Azores high, have a significant influence on the weather and therefore on marine and

terrestrial ecosystems, mainly by influencing the strength and pathways of westerly winds (Trigo et al., 2002).

Climate change has a more pronounced impact at high northern latitudes compared to low latitudes, a phenomenon known as polar amplification (Serreze and Francis, 2006; Miller et al., 2010). High-latitude regions are subsequently more sensitive to climate variability. Palaeo-proxy data and climate model reconstructions both identify polar amplification in the past (Manuscript IV; Section 5.4) and it is highly likely to happen in the future (c.f., IPCC, 2013). This can be clearly seen in Figure 4, the results of a Finite Element Sea Ice-Ocean Model (FESOM) run for the North Atlantic area during the last warmer-than-today phase, the early Holocene Climate Optimum (HCO). SST surface anomalies for the early Holocene (9,000 years BP) are most pronounced in the northern high latitudes (red colours indicating warmer temperatures).

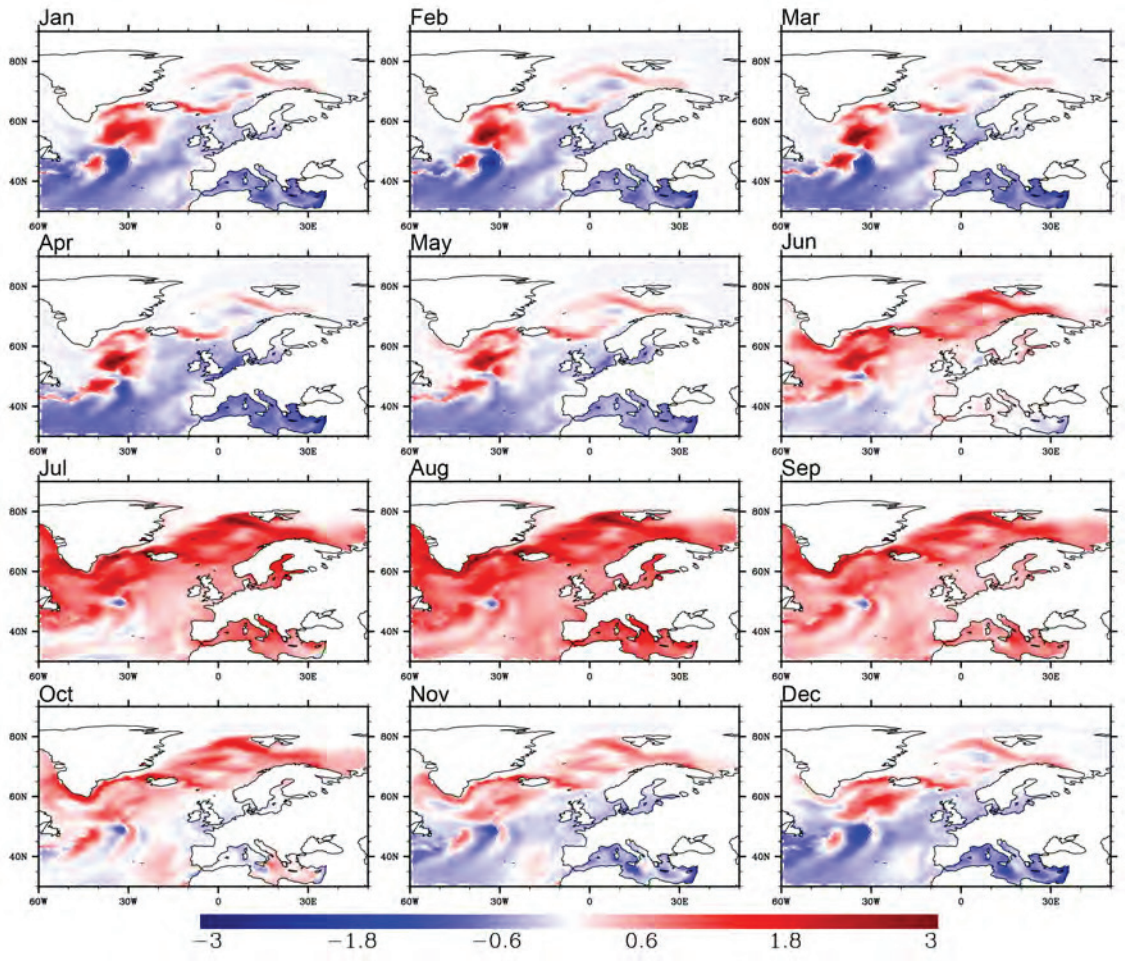

Figure 4. SST anomalies (°C) given as monthly data for North Atlantic region from the Finite Element Sea Ice-Ocean Model (FESOM) model run for 9,000 years BP. Higher impact of warming (intensity of red colours) towards higher latitudes indicates polar amplification. Data generated and provided by Gerrit Lohmann and Xiaoxu Shi (both AWI Bremerhaven).

The shifting configuration of the continental and oceanic plates has a significant impact on ocean circulation, deep-water formation, and heat distribution and storage (e.g., Roth, 1986). These are therefore important considerations when working on geological time-scales and with fossil biogenic archives. For the last 5 million years however (the time interval within which specimens from the following Manuscripts lived), the terrestrial geography and the ocean basin configuration within the North Atlantic realm remain comparable to its modern configuration (Scotese et al., 1988). This qualifies the HCO interval for detailed analysis of past climatic conditions. Since the HCO occurred after the last glacial maximum (LGM), we can also estimate with some confidence the palaeo-water chemistry (MacLachlan et al., 2007; Rasmussen et al., 2012), which is an essential prerequisite for any absolute water temperature reconstruction using stable oxygen isotopes ($\delta^{18}O$; c.f., Manuscript IV and Section 5.2).

1.4 The bivalve *Arctica islandica*: an exceptional bio-archive

In order to further our understanding of past natural climate change in the North Atlantic region, climate archives with higher temporal resolution are urgently needed. The only high-latitude archive that records environmental data on a seasonal timescale are bivalves. Bivalves are a class of molluscs, which can be found in almost every aquatic system worldwide. They typically build two bilaterally symmetrical valves of calcium carbonate, $CaCO_3$, as either aragonite or calcite (two of three varieties of $CaCO_3$). In some cases, shells are composed of both, and in some rare cases, they are composed of vaterite (the third variety of $CaCO_3$; e.g., Spann et al., 2010; Nehrke et al., 2012). The accretion of $CaCO_3$ is mainly controlled by temperature (Pannella and MacClintock, 1968; Jones et al., 1978), nutrients (Coe, 1948; Witbaard, 1996), water quality (Koike, 1980) and the timing of reproduction (Jones, 1980), and periodically reduces to a minimum. This makes it possible to obtain an exact calendar dating for every shell portion.

By applying sclerochronological techniques, a great variety of data can be retrieved from bivalve shells. Information about palaeo-environmental and palaeo-climatic conditions is stored within the shell in several ways (see Manuscript I for an introduction for the broader audience): the relative growth increment width, the isotopic composition of the shell material and the crystal fabric of the skeletal hard parts (Davenport, 1938; Craig and Hallam, 1963; Jones et al., 1989; Schöne et al.,

2013). Bivalves produce regular annual growth lines (Ropes et al., 1984; Brey and Mackensen, 1997) formed when growth is reduced to a minimum or stops completely ('growth cessation') in times of colder temperatures or reproduction (Aldridge, 1999). In most cases these can be identified as lines of darker colouration within shell cross-sections under reflected light, or as translucent lines in thin-sections when viewed under transmitted light. The relative thickness of these growth increments can be used in conjunction with stable isotope data to reconstruct temperature and environmental conditions (Manuscripts I, III, IV and V). Depending on the genus and the resolution of the applied method, very detailed reconstructions are achievable. Seasonal variability (Goewert and Surge, 2008; Manuscript IV), reproduction cycles (Jones, 1980), tidal rhythms (Evans, 1972), day and night cycles (Clark, 1975) and even circalunidian/circatidal increments (showing high tides twice a day; Hallmann et al., 2009) have been determined for different bivalve species.

Modern weather records typically date back 250 years or less. However, this duration is far too short to reveal long-term climate signals. Because of their longevity, some bivalves can record details of temperature and growth conditions in their surrounding environment over centuries (Jones, 1983; Forsythe et al., 2003; Butler et al., 2010). Furthermore, long-term climate signals, like the North Atlantic Oscillation (NAO; Schöne et al., 2003b) and the El Niño-Southern Oscillation (ENSO; Carré et al., 2005; Schöne et al., 2007), have been recorded and detected in marine molluscs, demonstrating their excellent suitability for the study of past climates on very short to decadal and longer timescales.

By applying cross-dating techniques to individual specimens, master chronologies can also be generated. So far, there has been limited application of this approach to bivalve shells (e.g., Marchitto et al., 2000; Forsythe et al., 2003; Schöne et al., 2003a; Butler et al., 2013). However, dendrochronological master chronologies already cover the entire Holocene, showing the great potential of this technique (Friedrich et al., 2004).

Arctica islandica is a long-lived (more than 400 years) species of marine bivalve that is widely distributed in the North Atlantic region and has an extensive fossil record (20 Ma to present), making it an ideal biogenic archive for coastal marine ecosystems (e.g., Brey et al., 1990; Dahlgren et al., 2000; Schöne et al., 2005b). *A. islandica* records ambient environmental conditions such as water temperature within oxygen isotopes ($\delta^{18}O$) incorporated into shell carbonate (Figure 5; Manuscript IV; Weidman et

al., 1994), while food availability and temperature are the main limiting factors that determine the width of daily and annual growth increments (Manuscript V; Witbaard, 1996; Witbaard et al., 1997).

Modern *A. islandica* specimens have proved to be highly sensitive to temperature changes when compared to instrumental data. In Schöne et al. (2005d) shell carbonate derived water temperatures have been compared to ambient North Sea instrumental temperature measurements resulting in a precision error of 0.25 to 0.4°C (Figure 5). Schöne et al. (2005b) compared a 374-year shell growth record of an *A. islandica* specimen to known climatic and environmental conditions and events during its lifetime (Figure 6) and found years of reduced shell growth that coincided with major volcanic eruptions (e.g., Mount Tambora, CE 1815). Furthermore, periods of strong growth variability (CE 1550–1620) have been shown to correspond with the culmination of the Little Ice Age (Figure 6). Manuscript IV gives the first records of high-resolution seasonal temperature variability from *A. islandica* during the HCO in Svalbard.

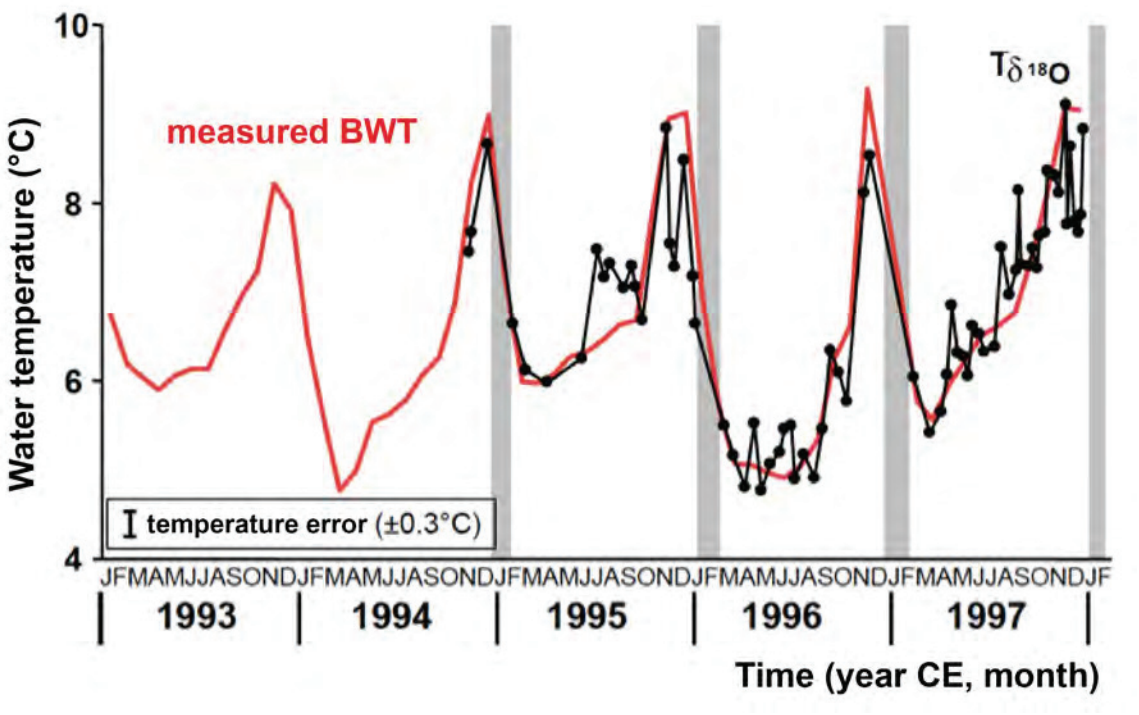

Figure 5. North Sea temperatures derived from oxygen isotopes ($\delta^{18}O$) within *A. islandica* shell carbonate (black) closely match instrumentally measured bottom water temperatures (BWT; red). Precision error is 0.25 to 0.4°C (from Schöne et al., 2005d).

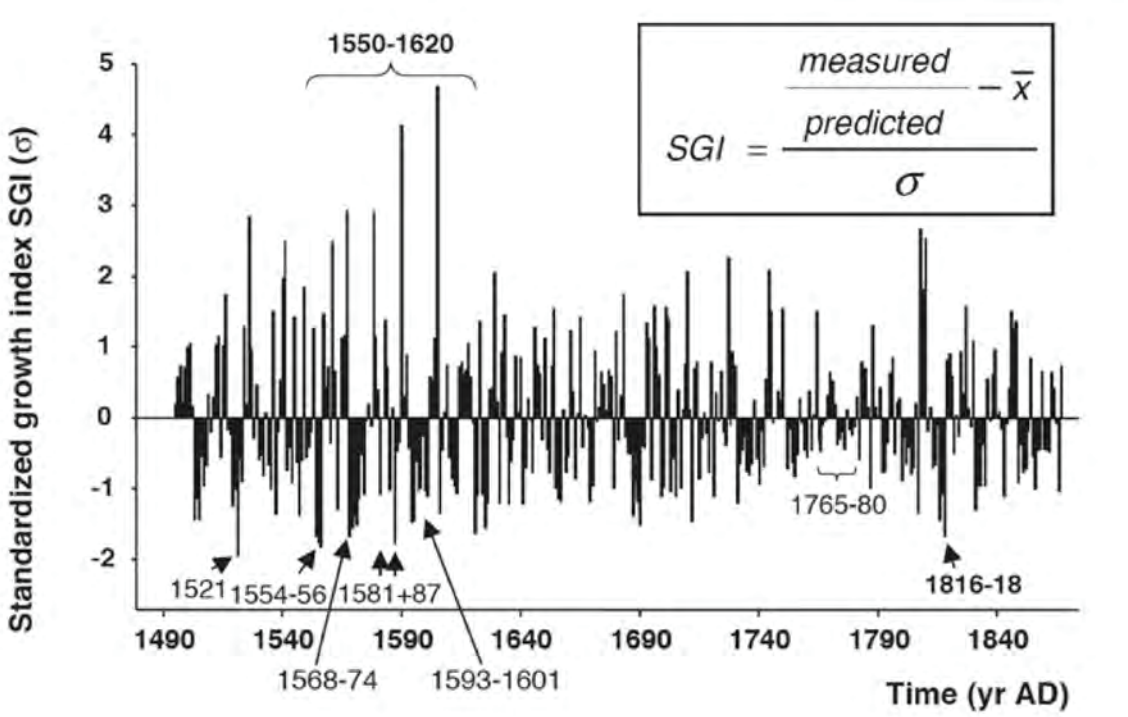

Figure 6. Annual shell growth record of a 374-year old *A. islandica* specimen from Iceland. Dimensionless standardized growth index (SGI) coincides with the dates of volcanic eruptions and the culmination of the Little Ice Age (from Schöne et al., 2005b). AD being equivalent to CE.

Working with fossil shell material does present some challenges and addressing these is a major emphasis of this thesis. To successfully obtain results based on shell increment widths, such as seen in Figure 6 or Manuscript V, a key pre-condition is that internal growth increments can be visualized (e.g., by Mutvei´s solution staining; Schöne et al., 2005a) and measured. This can be rather challenging in fossil and sub-fossil (up to 10,000 years old) specimens due to taphonomic processes. Manuscript II details a new methodology that uses confocal Raman microscopy (CRM) to visualize internal growth increments based on the vibrational modes of the shell carbonate (see Section 3.3 and Manuscript II). Furthermore, the reconstruction of absolute water temperatures (as seen in Figure 5) based on stable oxygen isotopes from fossil specimens (Section 3.5; Manuscript IV) is complicated by issues of preservation or recrystallization of the shell carbonate (Manuscript III), the associated palaeo-$\delta^{18}O_{seawater}$ value and palaeo-water depth (Manuscript IV).

2 Aims & Objectives

The primary aim of this thesis was to assess to what extent fossil and sub-fossil shells of *Arctica islandica* can be used for palaeo-environmental and palaeo-climatic reconstructions in the northern North Atlantic region. As highlighted in Section 1.4, working on fossil shell material presents a variety of challenges and uncertainties. To achieve this aim and investigate these challenges in detail, three main objectives each address a crucial topic in the context of palaeo-climatic and palaeo-environmental studies based on biogenic archives and proxies. Specific aims and objectives raised here will investigated in the corresponding manuscripts (Section 4) and further discussed in Section 5.

2.1 Main Objective A: Preservation & Taphonomy

Fossil biogenic archives, such as bivalve shells, contain environmental information in the form of varying increment growth widths (i.e., internal growth record) recorded within their skeletal hard parts (Sections 3.5 and 3.6; Richardson, 2001). However, deciphering the internal growth record from fossil specimens and revealing the palaeo-environmental information contained within it can be difficult. This is simply due to the fact that visualizing growth increments in fossil specimens is challenging, such as seen in a weaker staining effect of the Mutvei´s solution treatment on fossil shells (Schöne et al., 2005a). This might be explained through taphonomic alteration processes, which could lead to reduced amounts of polysaccharides in the fossil shell material (c.f., Schöne et al., 2005a) and therefore reducing the increment contrast that can be achieved. Consequently, an approach that can improve the achievable increment visualization in fossil shells is needed. Question A1 (below) will provide the basis for the investigations undertaken into the new proposed technique using confocal Raman microscopy and presented in Manuscript II (Section 4), which will be further discussed in Section 5.1.

Question A1

Is confocal Raman microscopy (CRM) a valid tool for the visualization of internal growth patterns in modern and fossil bivalve shells?

Another crucial aspect when working on fossil shell material is its preservation and a check for diagenetic alterations is necessary. *A. islandica* builds its three shell layers out of aragonite (e.g., Schöne, 2013). Pressure, heat and/or the presence of hydrothermal fluids within the surrounding sediment layer can cause fossil biogenic aragonite to recrystallize to calcite over time (the more stable polymorph of calcium carbonate; e.g., Maliva, 1998), affecting the original isotope signal of the carbonate. Even though it is commonly agreed that recrystallized shell material should not be considered for any kind of biogeochemical analysis (e.g., stable isotope or trace element analyses), the direct impact of recrystallization in *A. islandica* has never been described. From this I raise Question A2, which is the topic of Manuscript III (Section 4). A final assessment is presented in Section 5.1.

Question A2

Does the recrystallization from pristine aragonite to calcite affect the stable isotope ($\delta^{18}O$ & $\delta^{13}C$) composition of a fossil *A. islandica* shell? What influence will this have on palaeo-temperature reconstructions?

2.2 Main Objective B: Seasonal Palaeo-temperatures

Existing Holocene climate records for the North Atlantic region based on ice-rafted debris (e.g., Hald et al., 2004), benthic and planktonic foraminifera (e.g., Rasmussen et al., 2012), diatoms (e.g., Birks and Koc, 2002) and plant macrofossils (e.g., Birks, 1991) have limited temporal resolution, with 10–70 years in ice and sediment cores (e.g., Sarnthein et al., 2003) at best. However, annual and seasonal temperatures are crucial components of climate variability. In particular, climate modellers require these data with which to calibrate future model scenarios (c.f., Section 1). This is of utmost importance because the extent and duration of Arctic sea-ice, phenology of biological activity and severity of weather patterns all depend critically on the seasonal difference in temperature and precipitation (Weslawski et al., 1988). In order to further our understanding of natural climate change in the North Atlantic region, climate archives with higher temporal (sub-annual) resolution, such as bivalve shells, are of greatest importance. Manuscript IV therefore addresses Question B1 in order to assess if stable oxygen isotope ($\delta^{18}O$) measurements on the shell carbonate can reconstruct

information on seasonality for the early Holocene Climate Optimum (HCO). A final assessment is given in Section 5.2.

Question B1

Did sub-fossil *A. islandica* shells from the Dicksonfjord, Svalbard, record palaeo-water temperatures in their shell carbonate ($\delta^{18}O$)? If so, what are the reconstructed absolute water temperatures and seasonal amplitude for the early Holocene Climate Optimum?

2.3 Main Objective C: Decadal Variability

Despite using biogeochemical approaches such as stable oxygen isotope values ($\delta^{18}O$; Manuscript IV; Section 3.5) to reconstruct environmental conditions on a seasonal time scale, the internal growth record in *A. islandica* can (if successfully visualized; Sections 2.1 and 3.3; Manuscript II) be used for investigations into decadal- to centennial-scale climate variabilities (Schöne et al., 2005b; Butler et al., 2013). Significant oscillation patterns reconstructed from modern growth records can be correlated (e.g., by linear or multivariate regression analysis) to different environmentally and climatically derived time-series (e.g., water temperature, NAO) to identify the main drivers of shell growth variability. For fossil or sub-fossil shell growth records, which pre-date the observational era (last 250 years), a comparison to modern instrumental time-series is only feasible via frequency/spectral analysis (Section 3.6; Manuscript V). In an attempt to verify the potential of spectral analysis on sub-fossil *A. islandica* shell growth records, I hereby raise Question C1 and refer to the investigations in Manuscript V. Potential drivers on shell growth are carefully assessed in Section 5.3.

Question C1

Do early Holocene *A. islandica* shells from the Dicksonfjord, Svalbard contain significant year-to-year variabilities within the internal growth record? What are the most likely potential environmental/climate drivers of any identified oscillations in shell growth?

3 Sampling & Methodology

This Section gives an overview of the origin of the shell material used in the following manuscripts (Section 4), the fundamental preparation steps undertaken in the laboratory and a short rationale about the applied methods that form the basis for the work reported in Manuscripts I–VI. More specific information can be found in the relevant Material & Methods section of each Manuscript.

3.1 Origin of shell material

A total of 77 specimens (*Arctica islandica* (72); *Serripes groenlandicus* (3); *Pygocardia rustica* (2)) from seven geographical localities around the North Atlantic and the Mediterranean Sea dating back to the Oligocene (about 25 Ma) have been analysed during this PhD (Figure 7; Appendix 1). The PhD work presented in Manuscripts I to V focuses on a subset of the total number of specimens (Appendix 1) retrieved from six of the seven geographic localities throughout the North Atlantic (stars in Figure 7) and dating back to the Pliocene (approximately 3.5 Ma). All shell specimens (almost exclusively *A. islandica*), with the exception of the Pleistocene Mediterranean specimens from Stirone River (Italy), were derived from past warm periods. Detailed information on the origin of each specific specimen reported in Section 4 can be found in the respective Material & Method sections of each Manuscript.

All shell material has been provided by different international collaborators (see Appendix 1), which are hereby thankfully acknowledged. I am grateful for the support from each collaborator in providing detailed geological and stratigraphic knowledge on the associated locality and associated palaeo-environmental and palaeo-climatic information.

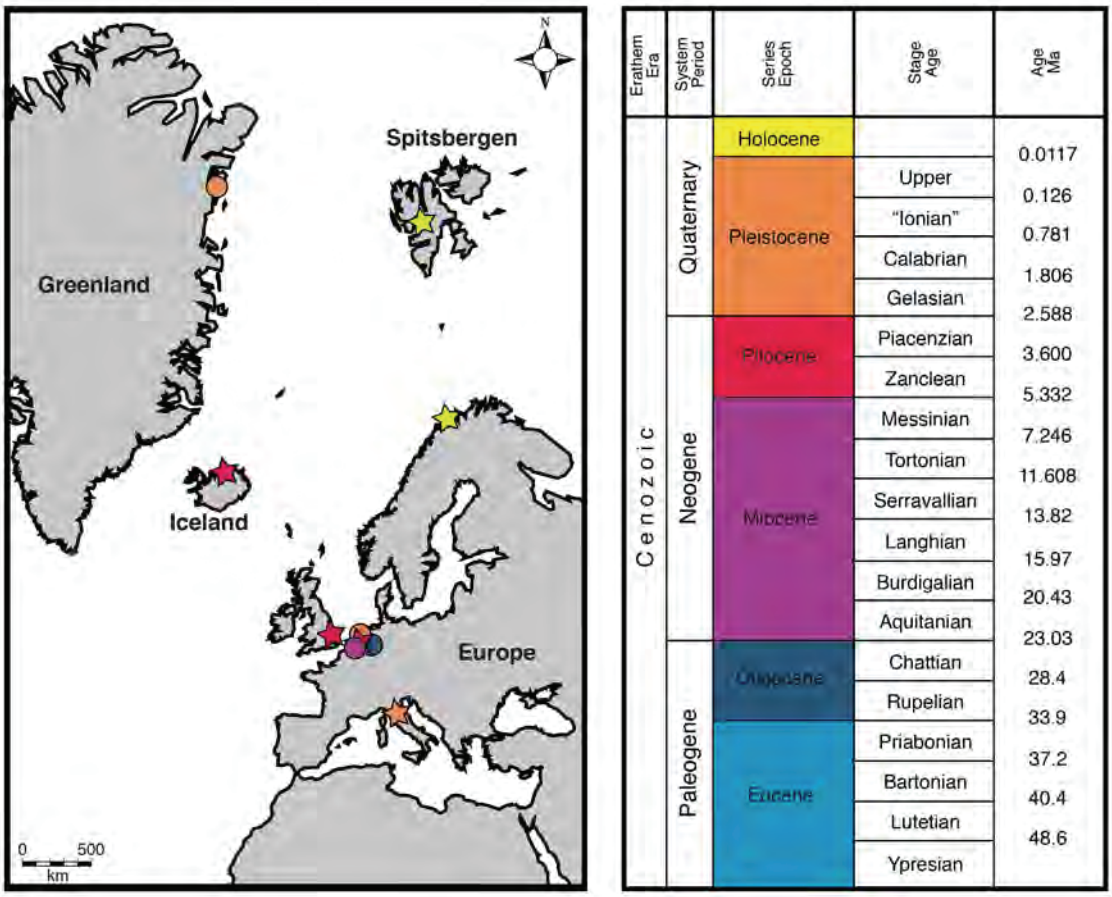

Figure 7. Map of the northern North Atlantic (left), based on a modern continental configuration, showing the origin of shell material for this study (circle symbols) and shell material used in one of the manuscripts (star symbols; Section 4). Cenozoic time scale (right) gives additional information on the geological age of shell material. For illustration purposes, colour-coding does not follow the conventions of the international stratigraphic chart.

3.2 Preparation of shell material

All shells were externally strengthened with an epoxy resin cover to prevent them from breakage. For each specimen, a 5 mm (for geochemical analysis, e.g., oxygen isotopes; see Section 3.5) and a 3 mm (internal growth record analysis; see Section 3.3 and 3.6) cross-section were prepared by sawing along the line of strongest growth (LSG; running perpendicular to the growth lines; Figure 8a) using a low-speed precision saw (Buehler, IsoMet) equipped with a 0.4 mm diamond-coated saw blade. Cross-sections were then ground using a manual grinder (Buehler, Phoenix Alpha) and sand paper with three different grain sizes (15 µm, 10 µm and 5 µm). The 3 mm cross-sections were stained in Mutvei´s solution (Schöne et al., 2005a) for 23 minutes at constant 38°C (Figure 8c) unless otherwise stated in the Material & Methods sections of the Manuscripts.

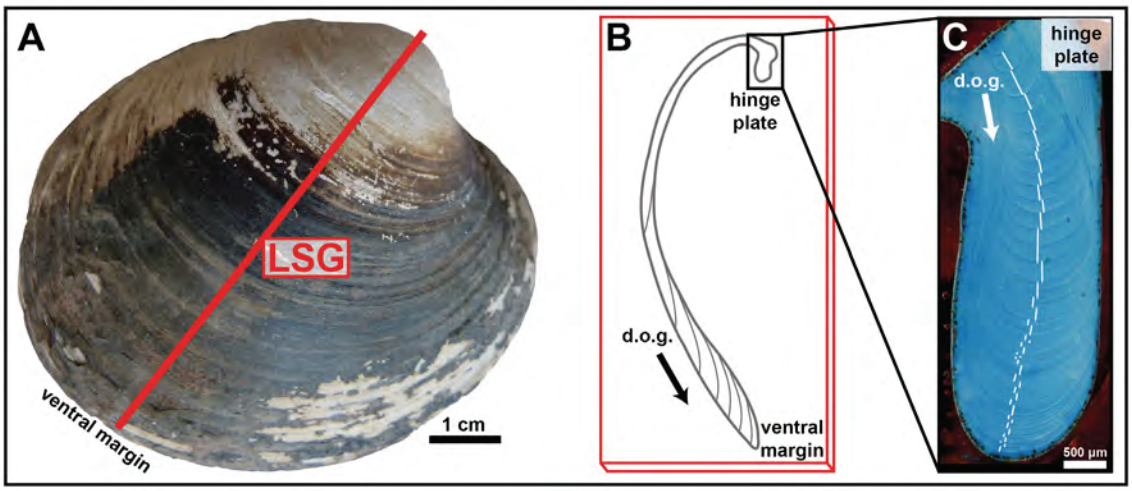

Figure 8. Preparation of 3 mm *A. islandica* shell cross-section for growth trend analysis. (A) Shell is cut along the line of strongest growth (LSG; red line) perpendicular to the growth lines. (B) Cross-section is glued onto a glass-slide and stained in Mutvei´s solution (not shown). (C) Individual increment widths have been measured along the hinge plate of the shell (indicated by white lines). Blue shell colouration derives from Mutvei treatment. Arrows gives direction of growth (d.o.g.).

3.3 Preservation & Visualization: Confocal Raman microscopy

In order to identify and investigate taphonomic and diagenetic alterations it is crucial to test the preservation state of fossil and sub-fossil shell specimens (Section 1.4 and 2.1). The physical state of preservation of the shells used in this study (Figure 9) range from very good (Holocene shells from Svalbard; Figure 9d) to very poorly preserved (abraised, fragmented and discoloured; e.g., Pleistocene shells from Greenland; Figure 9i). The state of preservation (physical and chemical) determines which geochemical and shell growth width derived reconstructions are feasible.

Post-depositional alterations in carbonate fossils can take several forms, including both flattening and chemical changes (e.g., infiltration by diagenetic minerals or recrystallization). Chemical changes are often caused by dissolved chemicals in solution passing through the sediment containing the fossils and either replacing the original shell material (molecule-for-molecule) or precipitating secondary material within the mineral matrix. Elevated temperatures and/or increased pressure can also convert skeletal material to a more thermodynamically stable form, thereby changing the crystal structure (e.g., Tütken and Vennemann, 2011). All of these processes can occur very soon after or a long time after burial (Benton and Harper, 2009). One of the most common diagenetic processes in aragonitic mollusc shells is the conversion of metastable aragonite to more stable calcite (both polymorphs of $CaCO_3$; e.g., Bathurst,

1964; Manuscript III), a process called recrystallization. Additional diagenetic processes that can occur in mollusc fossils include the formation of carbonate concretions, pyrite (FeS_2), phosphatisation or silicification.

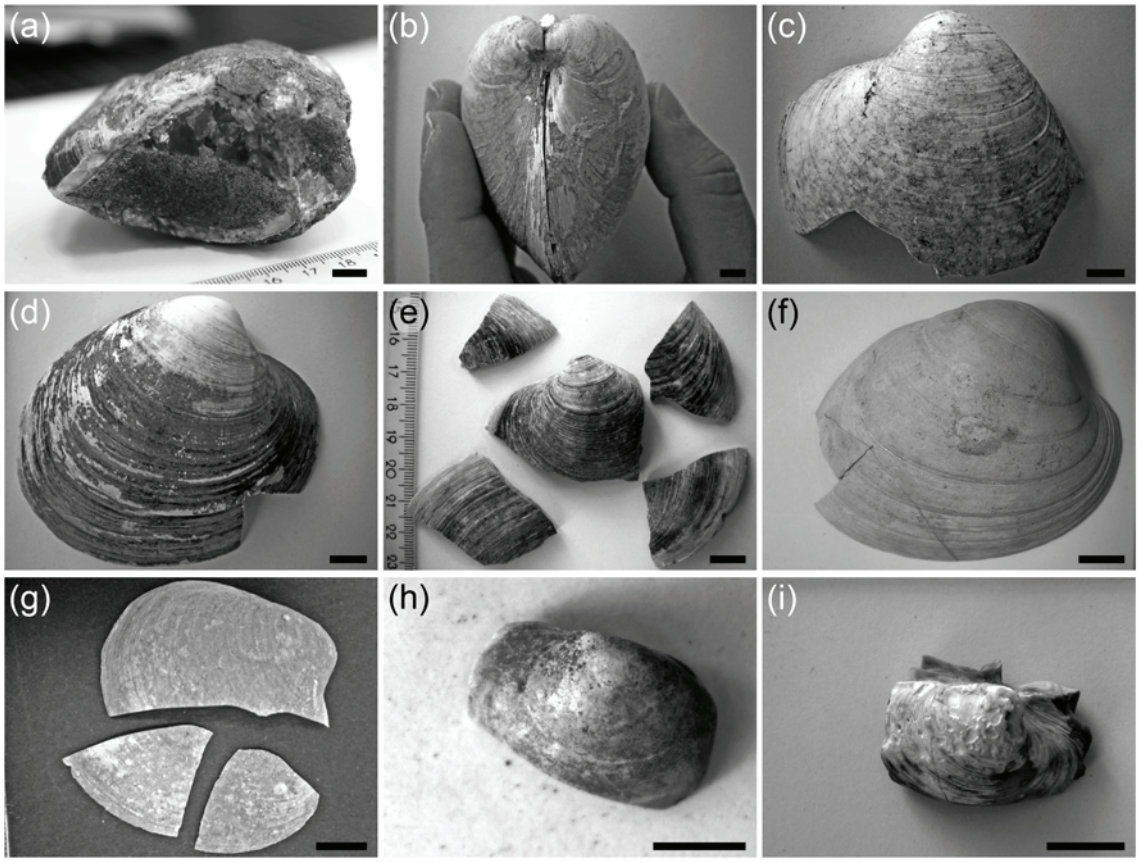

Figure 9. Different types of preservation in shells analysed for this thesis. (a) *A. islandica* from Tjörnes Beds, Iceland (AI-TjBe-01). (b) *A. islandica* from Stirone River, Italy (AI-StRi1-BK2c). (c) *A. islandica* from Coralline Crag, UK (AI-CoCr-02). (d) *A. islandica* from the Dicksonfjord, Svalbard (AI-DiFj-01). (e) *A. islandica* from Stirone River, Italy (AI-StRi2-BK1h). (f) *Pygocardia rustica* from Antwerp, Belgium (RGM609.096). (g) *A. islandica* from Eggum, Norway (AI-EgLo-03). (h) *A. islandica* from Tjörnes Beds, Iceland (AI-TjBe-07). (i) *A. islandica* from Ile de France, Greenland (AI-IdFr-03). All scale bars are 1 cm.

Raman microscopy is one method that identifies the mineral composition of a specimen and can therefore be used to identify whether the original aragonite has been recrystallized into calcite (Manuscript III). The molecules within each mineral, and polymorph of each mineral, have a specific molecular vibration that depends on the crystal structure and the number of bonds between each of the molecules. When light is incident onto the specimen, the majority of this light is scattered back elastically (Rayleigh scattering), but a small fraction of the light is scattered inelastically, known as Raman scattering (Figure 10; Raman and Krishnan, 1928). The confocal Raman microscope (CRM) identifies the material depending on the difference in frequency

between the irradiated and scattered light (Stokes shift). Each mineral and mineral polymorph has a characteristic spectrum of frequency peaks that can be used for material identification (Figure 11; e.g., Smith and Dent, 2005).

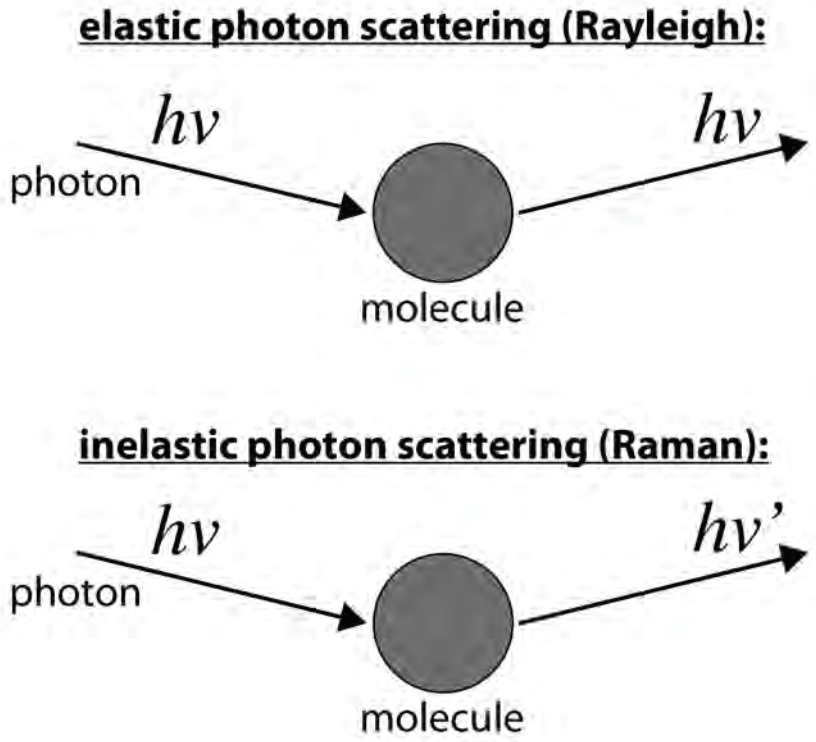

Figure 10. Differences in Rayleigh and Raman photon scattering. While the main portion of incident light is scattered elastically (Rayleigh; upper image), a small fraction of incident light is scattered inelastically (Raman; lower image) depending on the molecular vibration of molecules and can therefore be used for material identification (c.f., Figure 11). hv stands for photon energy.

The differences in Raman spectra of aragonite and calcite are illustrated in Figure 11 (blue line and red line respectively). Both forms of $CaCO_3$ have coincident peaks at 152 cm^{-1} and 1085 cm^{-1} but each spectrum also has a peak that does not occur at the same frequency in the other polymorph (compare dotted lines in Figure 11). CRM can identify mineral and organic phases in marine biogenic carbonates at a high spatial resolution (several hundred nm), allowing the detailed identification of taphonomic changes in the carbonate structure (Manuscript III; Nehrke and Nouet, 2011; Cuif et al., 2012). The high spatial resolution achievable also makes CRM a valuable tool to identify and visualize growth increments within accretionally precipitated carbonate skeletons of marine organisms such as bivalves (Manuscript II), especially where commonly used dyeing techniques (e.g., Mutvei´s solution; Schöne et

al., 2005a) are inefficient in fossil biogenic carbonates with low organic content. CRM is therefore highly successful in revealing shell formation processes at a very high spatial resolution, even in shell material that is several million years old (Manuscript II). Additionally, this method is ideal to detect possible contaminations that might result from shell preparation in the laboratory (e.g., by epoxy resin or super glue).

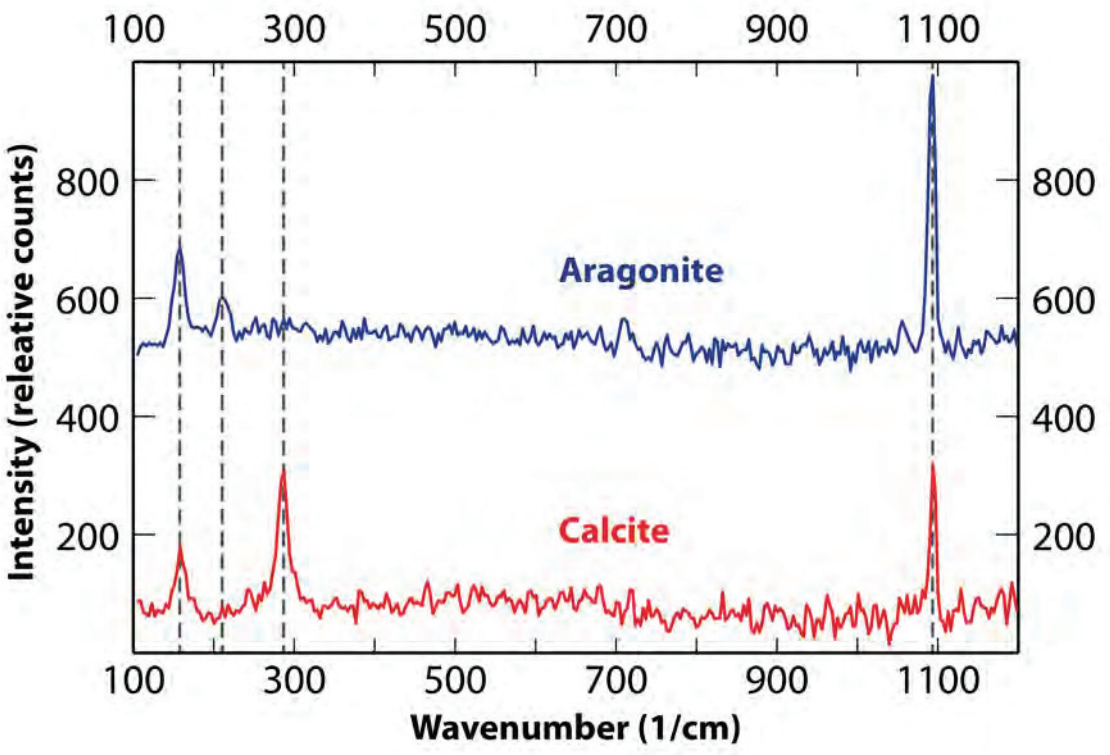

Figure 11. Raman spectra for two calcium carbonate polymorphs aragonite (blue) and calcite (red), illustrating the differences in specific Stokes shift peaks. Polymorphs are identified based on two lattice modes (translation mode, 152 cm^{-1} and liberation mode, 206 cm^{-1}) and the two vibration modes (C–O symmetric stretch, 1085 cm^{-1} and C–O in-plane bending, 705 cm^{-1}).

3.4 Dating of shell material

Dating is an essential step to assign fossil shell material to a specific geological time. Consequently, all shells for the Holocene time period (Manuscripts IV and V) have been radiocarbon ($^{14}C_{AMS}$) dated, while older shell material (Manuscripts II and III) has been dated based on the stratigraphy of the specific outcrop/locality. As an example, Figure 12 illustrates how the Pleistocene shell material from the Stirone River locality in Italy (e.g., Figure 9b and e) has been retrieved. The geological age of 1.81 Ma to 0.78 Ma (Middle Calabrian) is based on the sediment layering (see yellow marked A to D sequence in upper image) and extensive work on the bio-stratigraphy of this outcrop

(c.f., Bertolani Marchetti et al., 1979; Mary et al., 1993), which has for example been used in Manuscript II.

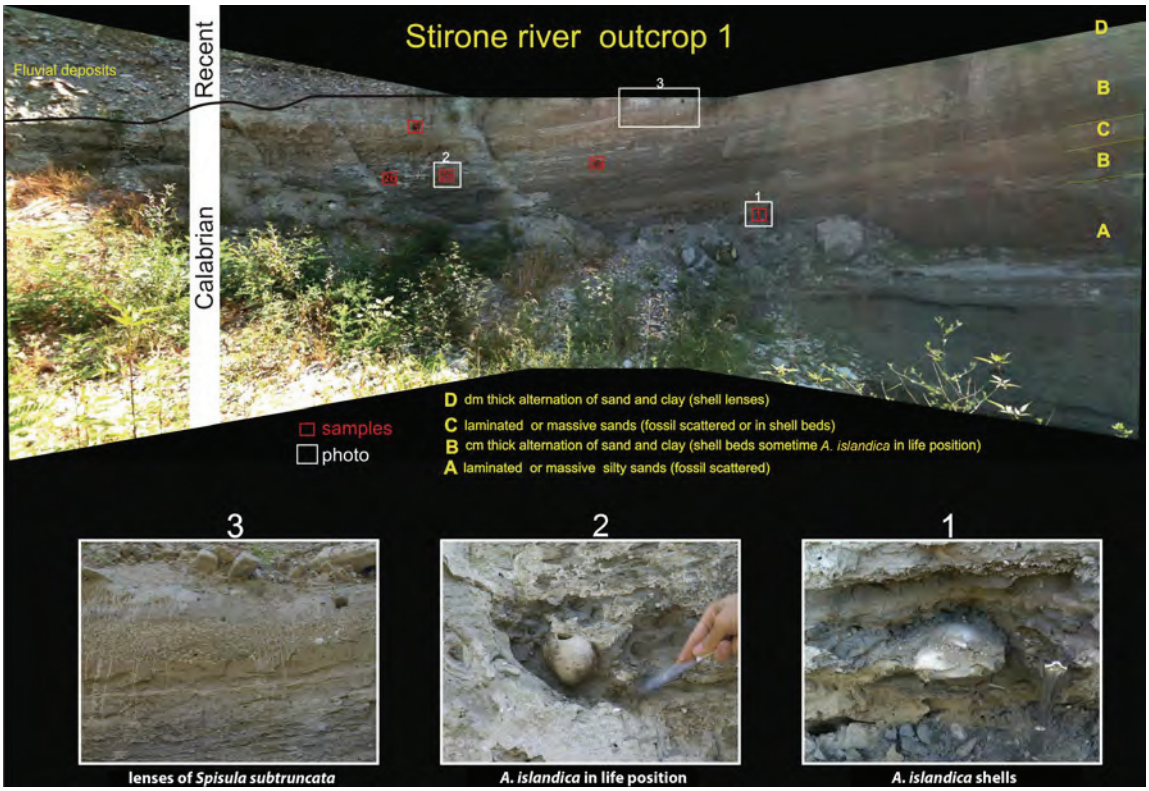

Figure 12. Pleistocene outcrop at Stirone River, Italy. Images giving information on stratigraphic classification, origin of provided shell material, preservation and outcrop conditions (image and shell material kindly provided by Daniele Scarponi and Sergio Raffi, University of Bologna, Italy).

3.5 Stable oxygen ($\delta^{18}O$) isotopes: Seasonal variability

In recent decades, a large number of different biogeochemical proxies have been developed and calibrated for biogenic archives (e.g., based on isotopes: $\delta^{18}O$, $\delta^{13}C$, $\delta^{15}N$, $\delta^{34}S$, $^{87}Sr/^{86}Sr$, $^{143}Nd/^{144}Nd$, δD; elemental ratios: Mg/Ca, Sr/Ca; or membrane lipids: TEX_{86},) allowing for the reconstruction of different environmental parameters (e.g., water temperature, salinity, water pollution). Some proxies are still not yet fully calibrated but have significant potential for palaeo-climate studies (e.g., boron isotopes $\delta^{11}B$, calcium isotopes $\delta^{44}Ca$ or clumped isotopes Δ_{47}).

The aragonitic shells of *A. islandica* incorporate oxygen isotopes that are in equilibrium with the surrounding water (e.g., Weidman et al., 1994). As this process involves no biological fractionation, the stable oxygen isotope composition of the accretionally accumulated aragonite records an environmental signal of the ambient

water at the moment of precipitation and can therefore be used as a palaeo-environmental proxy. Higher temperatures facilitate the incorporation of the lighter oxygen isotope (^{16}O) and shell material accreted during relatively warm periods is relatively depleted in the heavier oxygen isotope ^{18}O (Grossman and Ku, 1986). The $\delta^{18}O$ proxy is defined as the relative abundance of $^{18}O/^{16}O$. This results in an inverse linear relationship between $\delta^{18}O_{shell}$ and water temperature (Grossman and Ku, 1986). If the isotopic composition of the surrounding water ($\delta^{18}O_{water}$) is known, the precipitation temperature of the biogenic carbonate can be calculated, by using an empirically determined temperature relationship for aragonite, for example Grossman and Ku (1986). In general, a change of 1‰ within the $\delta^{18}O_{shell}$ values equates to a temperature change of 4.3°C. Palaeo-temperatures in Manuscripts I, III and IV have been calculated following the descriptions in Dettman et al. (1999) and applying a modification to the SMOW scale:

(Equation 1) $$T°C = 20.6 - 4.34 (\delta^{18}O_{shell} - (\delta^{18}O_{water} - 0.27))$$

Oxygen isotopes ($\delta^{18}O$) in *A. islandica* have been successfully used to provide information on water temperatures (Buchardt and Simonarson, 2003; Schöne et al., 2004; Schöne et al., 2005b; Wanamaker Jr et al., 2008), including the reconstruction of seasonality (Schöne et al., 2005d; Schöne and Fiebig, 2009; Wanamaker Jr et al., 2011; Manuscript IV). However, when applied to sub-fossil and fossil specimens, this approach has not yet been exploited to its full potential. In this regard, Manuscripts III and IV assess and report aspects associated with the potential risks (recrystallization) and benefits (palaeo-seasonality for past warm phases) of the $\delta^{18}O$ proxy. Samples for oxygen isotopes in this study have been taken manually from *A. islandica* specimens using the micro-milling approach (Figure 13; Dettman and Lohmann, 1995), which is considered to result in a superior resolution (i.e., higher sample density per ontogenetic year) than the more commonly used micro-drilling or automated MicroMill approaches.

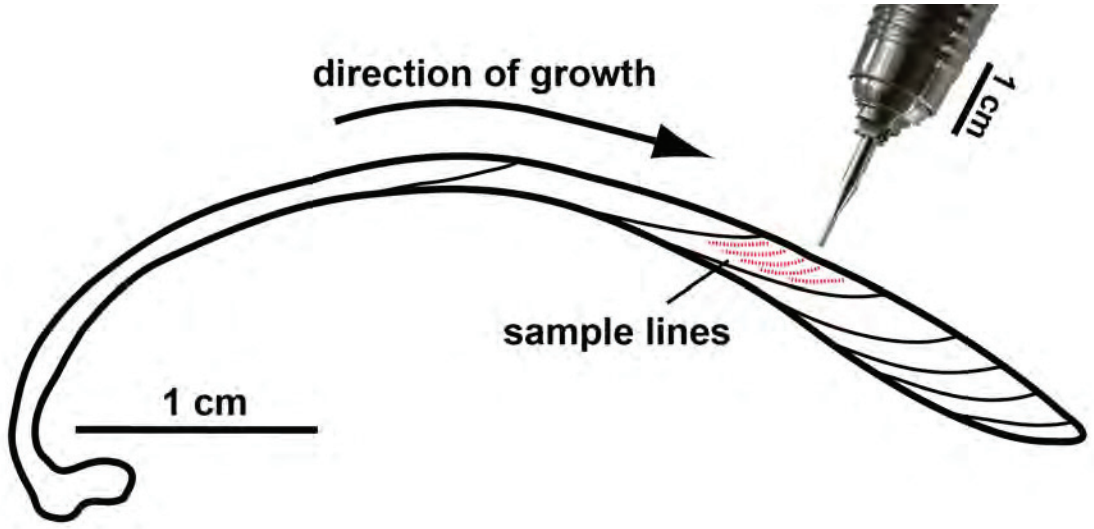

Figure 13. Schematic illustration of micro-milling approach as applied for stable oxygen analysis in this study (c.f., Manuscripts I, III and IV). Samples were taken in the direction of growth (arrow) parallel to internal growth lines (indicated by red dotted lines).

3.6 Spectral frequency analysis: Decadal variability

One of the biggest advantages of *A. islandica* as a biogenic archive is it longevity and therefore its suitability to identify intra-annual variability over long time-scales. The measured widths of the annual growth increments (Figure 14a and b) can be used to calculate a dimensionless standardized growth index (SGI) that shows whether growth in any particular ontogenetic year is above or below that which would be expected (Figure 14c). As shell growth (i.e., shell increment width) is regulated by environmental factors (e.g., water temperature and food availability; Schöne, 2013), which are in turn influenced by larger scale ocean and/or atmosphere processes, the spectral analysis of this index can be used to identify the frequencies of sub-decadal to multi-centennial variability in weather and climate (Butler et al., 2013). This study follows the two spectral analysis procedures described in Schöne et al. (2005b) and Butler et al. (2010) (c.f., discussion in Schöne, 2013).

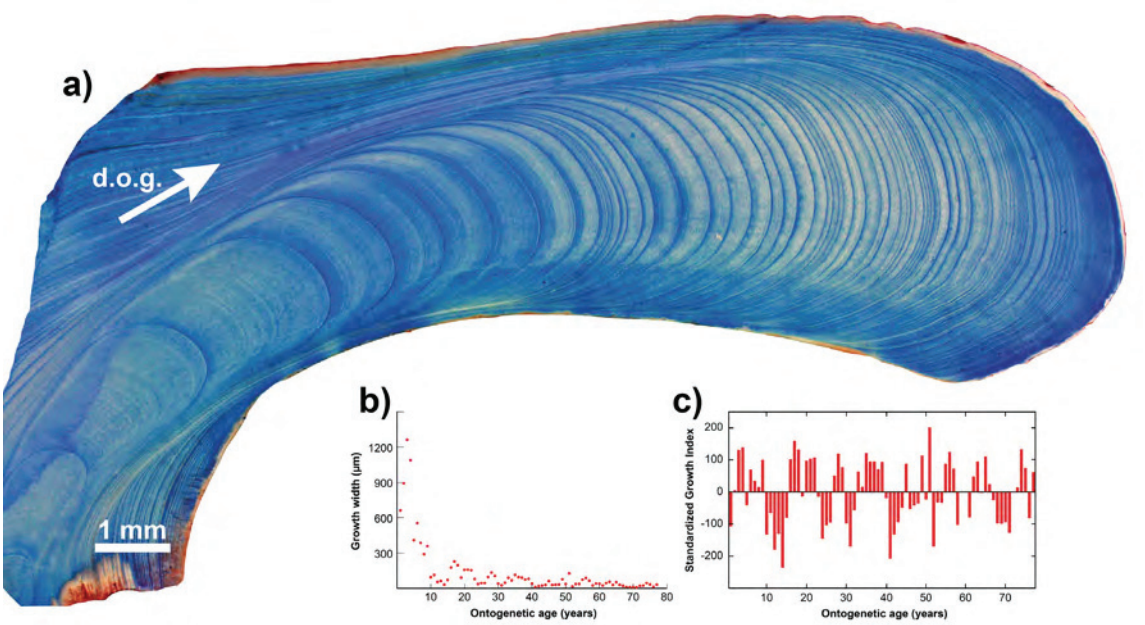

Figure 14. Shell growth width analysis of an *A. islandica* specimen from the Dicksonfjord, Svalbard (ID: AI-DiFj-08; c.f., Manuscript V). (a) Mutvei´s solution stained (blue colouration) hinge plate showing annual growth increments. Arrow giving direction of growth (d.o.g.). (b) Measured growth increment widths showing an exponential decline throughout ontogeny. (c) Dimensionless standardized growth index (SGI) for specimen AI-DiFj-08 indicating years with above expected average growth (positive values) and years of below expected average growth (negative values).

For modern biogenic growth records that overlap with observational data (past 250 years), methods such as regression analysis using linear regression (response of one environmental parameter; Manuscript V), multivariate regression (simultaneous response of multiple parameters; e.g., Schöne et al., 2005c) and/or spatial regression (i.e., pattern matching e.g., Lohmann and Schöne, 2012) have been employed in addition to spectral analysis (c.f., Manuscript V). However, since fossil growth records do not overlap in time with the instrumental record, the tools of spectral analysis (see Manuscript V for details on Singular Spectrum Analysis (SSA; Figure 15a), Multi-Taper Method (MTM; Figure 15b) and Maximum Entropy Method (MEM)) are often the only possible way to identify and associate past shell growth signals to known oscillations in modern climatic and environmental signals. It is also possible to determine the stationarity of significant quasi-periodic signals through time in both modern and fossil SGI time-series using continuous wavelet transformation (Figure 15c; see Manuscript V for details and application; Torrence and Compo, 1998).

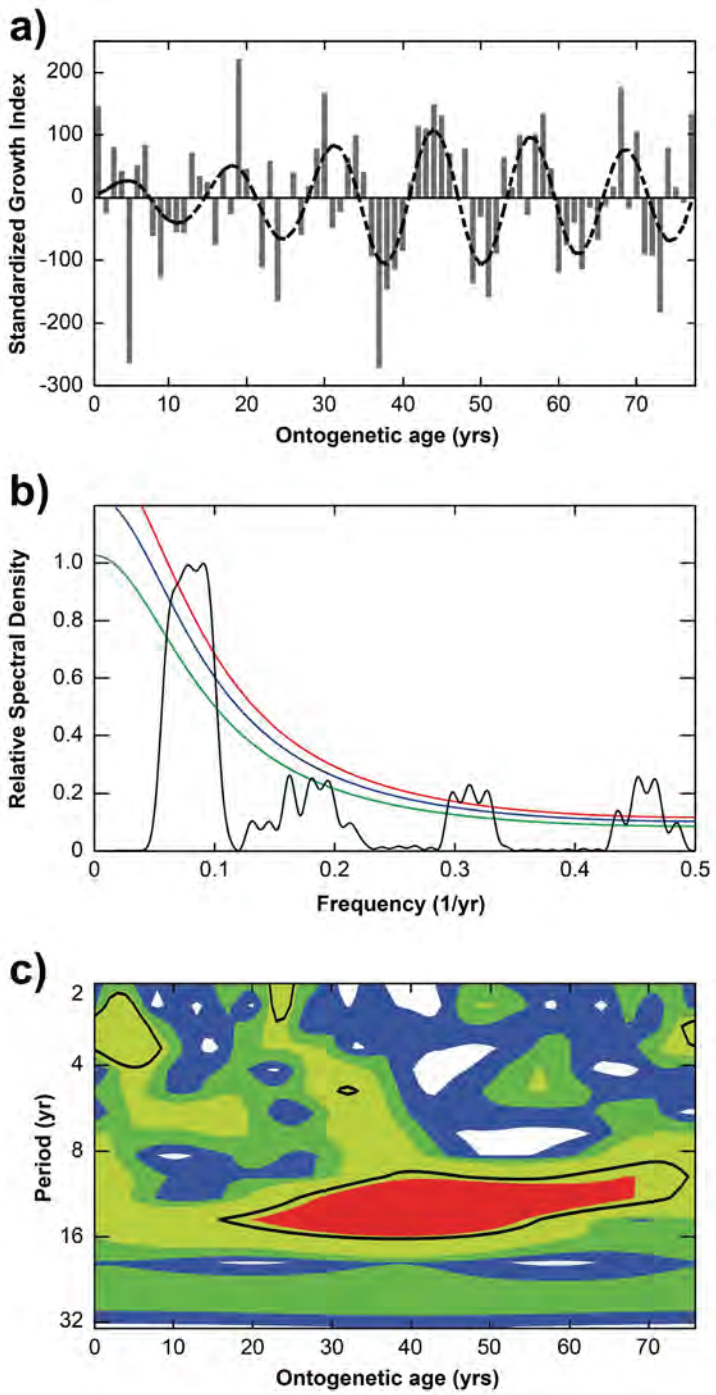

Figure 15. Spectral frequency analysis on early Holocene *A. islandica* specimen AI-DiFj-04 from the Dicksonfjord, Svalbard (c.f., Manuscript V). (a) Standardized growth index (SGI, bars) with reconstructed 11-year component (dashed line) as identified by SSA analysis. (b) Multi-Taper Method (MTM) used on SGI in (a) to identify significant frequencies and signals. Green (90%), blue (95%) and red (99%) lines give significance levels, identifying significant signals at ~0.09 yr^{-1} (= 11 years), ~0.19 yr^{-1} (= 5.3 years), ~0.32 yr^{-1} (= 3.1 years) and 0.47 yr^{-1} (= 2.1 years). (c) Continuous wavelet transformation providing information about the stationarity (i.e., strength of a certain signal over time). Red area confirms a significant 11-year signal but shows that the signal is not equally strongly pronounced over time.

3.7 Storage of material and accessibility of data

All remaining shell materials that were analysed in this study are currently stored at the Alfred Wegener Institute, Bremerhaven, Germany. Data storage and accessibility for all data used and created in manuscripts II to V (Section 4) will be provided using PANGAEA (www.pangaea.de) after final publication (press) of these manuscripts in peer-reviewed journals.

4 Manuscripts

The following summarises the division of work for each of the six manuscripts that constitute my thesis, stating where appropriate any contributions by co-authors. Each manuscript is also briefly summarised in context to the 'bigger picture' (i.e., palaeo-environmental and palaeo-climatic reconstructions based on proxy analysis from bivalve shells). A more detailed synthesis and evaluation of the key results and conclusions of each manuscript can be found in Section 5.

Manuscript I

Beierlein L, Nehrke G, Trofimova T and Brey T (2014, accepted for publication). Bivalve shells – unique high-resolution archives of the environmental past. *Springer Briefs in Earth System Sciences*.

Division of work: I developed the concept of the manuscript in discussion with TB, carried out the statistical analysis and had the lead in writing the manuscript. Raman microscopy measurements were done by me, with assistance by GN. Isotope samples were taken by TT and measured at AWI Bremerhaven (A. Mackensen).

Context: This manuscript gives an overview and a general introduction into sclerochronological approaches and the palaeo-environmental information that can be retrieved from bivalve shells. In this model study, seasonal information derived from stable oxygen isotopes ($\delta^{18}O$) of the shell carbonate is combined with a multi-year shell-growth derived frequency analysis to show the potential of bivalve shells as recorders of environmental variability on a sub-annual to a decadal time-scale.

Manuscript II

Beierlein L, Nehrke G and Brey T (2014, submitted). Confocal Raman microscopy in sclerochronology: a powerful tool to visualize environmental information in recent and fossil biogenic archives. *Geochemistry, Geophysics, Geosystems*.

Division of work: Raman measurements were done by me together with and in discussion with GN. I wrote the manuscript (with revisions by GN and TB), carried out all increment measurements and the statistics of the study. Extensive discussions on how to best present this calibration study with both TB and GN.

Context: Even though Raman spectroscopy is a well established method in geosciences and biosciences, the approach of using CRM as a mapping tool has scarcely been exploited, especially not in sclerochronology. Using it as a tool to visualize growth patterns in modern and fossil shell material presents new perspectives and possibilities in climatic and environmental reconstructions based on biogenic and non-biogenic archives.

Manuscript III

Beierlein L, Brey T, Nehrke G, Schöne BR, Bickert T and Mackensen A (manuscript, in preparation). From aragonite to calcite: Impacts of recrystallization on stable isotope ($\delta^{18}O$ & $\delta^{13}C$) composition of the commonly used bio-archive *Arctica islandica*. *Palaeogeography, Palaeoclimatology, Palaeoecology* (intended).

Division of work: Initial idea for the project, shell preparation, manuscript writing, sampling for stable isotope measurements was performed by me. TBrey, BRS, TBickert and GN all contributed to discussions about all conducted results and the significance for the sclerochronological community in general. CRM and additional EMP measurements (not presented in this manuscript) were undertaken together with and in discussion with GN. AM provided useful discussion about results of stable isotopes and conduction of measurements.

Context: *A. islandica* plays a major role in sclerochronological studies that aim to reconstruct past climate and environmental conditions. Stable oxygen isotopes ($\delta^{18}O$) are the most commonly used and best calibrated biogeochemical proxy, allowing for reconstructions of water temperatures (and salinity). The effect of recrystallization on the isotopic composition of *A. islandica* has never been reported before. Micro-milling a semi-recrystallized shell resolves this issue and illustrates the challenges associated with potential temperature reconstructions.

Manuscript IV

Beierlein L, Salvigsen O, Schöne BR, Mackensen A and Brey T (2014, accepted with minor revisions). The seasonal water temperature cycle in the Arctic Dicksonfjord (Svalbard) during the Holocene Climate Optimum derived from sub-fossil *Arctica islandica* shells. *The Holocene*.

Division of work: Initial project idea conceived by TB, OS and me. Shell material provided by OS. I took all samples for stable isotope measurements, which were measured by AM. Results of isotope measurements were discussed with BRS, AM and TB. I carried out CRM measurements with the assistance of G. Nehrke. Radiocarbon dating samples were taken by me, with discussion on calibration with BRS, AM and TB. Reconstruction of HCO (and modern) fjord conditions at Svalbard were assisted by OS. Palaeo-water temperature reconstructions were performed by me, with help of BRS and TB. I lead the writing of the manuscript, which was revised by all authors.

Context: To test the full potential of the archive *A. islandica*, the commonly used proxy stable oxygen isotopes ($\delta^{18}O$) were measured in sub-fossil HCO shells from Svalbard. Resulting $\delta^{18}O$ values taken with high spatial resolution (micro-milling) are subsequently discussed with great care before a first palaeo-temperature reconstruction is presented. The retrieved data on seasonality is unique for Arctic HCO, impressively identifying polar amplification.

Manuscript V

Beierlein L, Dima M, Schöne BR, Salvigsen O and Brey T (manuscript, to be submitted in September 2014). A pronounced 11-year oscillation in high Arctic marine bivalve shells during the early Holocene Climate Optimum. *PLOS ONE*.

Division of work: HCO shell material was provided by OS. I conceived the initial project idea, carried out statistics, increment measurements, took samples for radiocarbon dating and led the manuscript writing. Spectral analysis was performed by myself together with and in discussion with MD. BRS and TB contributed to discussion about potential mechanistic links and biological amplification.

Context: An 11-year signal has previously been reported from different biogenic and non-biogenic archives and is usually associated with solar activity. However, explanations on the mechanistic links between solar activity and the archive are hardly ever given. The pronounced 11-year oscillation in the growth pattern of the HCO *A. islandica* shells presented here shall serve as a basis for a discussion on how solar activity might influence shell growth on a decadal scale.

Manuscript VI

Beierlein L and Sheward RM (2013). Climate Service – Definition and Function. *Berichte zur Polar- und Meeresforschung, Alfred Wegener Institute for Polar and Marine Research 662, 72–75*.

Division of work: I wrote the manuscript in discussion with and edited by RS.

Context: Climate change will play an increasingly important role for humankind in the future. To best adapt and mitigate to such changes, a concept called 'climate services' has been conceived. Its fundamental objective is to help society to cope with climate risks and opportunities, strengthening the cooperation between (climate change) sciences and different interested parties that rely on climatic and scientific information.

Manuscript I

Bivalve shells – unique high-resolution archives of the environmental past

Lars Beierlein[1], Gernot Nehrke[1], Tamara Trofimova[2] and Thomas Brey[1]

[1]Alfred Wegener Institute Helmholtz Centre for Polar and Marine Research, Bremerhaven, Germany

[2]Saint Petersburg State University, St. Petersburg, Russia

Accepted for publication in: "Towards an interdisciplinary approach in Earth System Science: Advances of a Helmholtz Graduate Research School". Lohmann, G., Meggers, H., Unnitan, V., Wolf-Gladrow, D., Notholt, J. and Bracher, A. (editors). *Springer Briefs in Earth System Sciences.*

Abstract

Understanding the climate of the past is essential for anticipating future climate change. Palaeo-climatic archives are the key to the past, but few marine archives (including tropical corals) combine long recording times (decades to centuries) with high temporal resolution (decadal to intra-annual). In temperate and polar regions carbonate shells can perform the equivalent function as a proxy archive as corals do in the tropics. The bivalve *Arctica islandica* is a particularly unique bio-archive owing to its wide distribution throughout the North Atlantic and its extreme longevity (up to 500 years).

This paper exemplifies how information at intra-annual and decadal scales is derived from *A. islandica* shells and combined into a detailed picture of past conditions. Oxygen isotope analysis ($\delta^{18}O$) provides information on the intra-annual temperature cycle while frequency analysis of shell growth records identifies decadal variability such as a distinct 5-year signal, which might be linked to the North Atlantic Oscillation.

Keywords: sclerochronology, *Arctica islandica*, frequency analysis, Raman microscopy, stable oxygen isotopes, palaeoceanography, intra-annual, decadal.

1 Introduction

Current predictions of future climate change (e.g., IPCC, 2013) are based on global circulation models (GCM) to a large extent. Such models incorporate observational and instrumental data of the oceans, continents and atmosphere. Instrumental data are available for the last two centuries at best, but we need climate and environmental data prior to the instrumental era in order to improve and verify such climate models. Therefore, climate sciences rely on climate archives such as sediment cores and ice cores. Such archives contain 'proxies', i.e., physical, chemical or biological properties that correlate to certain environmental parameters and hence allow reconstructions of such parameters at the time of the formation of the archive. The relationship between water temperature and $\delta^{18}O$ is thought to be the most important relationship between an environmental parameter and its proxy.

Accretionally growing hard parts of aquatic organisms (e.g., corals, fish and squid otoliths, coralline algae, bivalve shells) are being used as climate archives with increasing frequency, providing environmental information on daily to multi-centennial time-scales (Schöne et al., 2005b; Hallmann et al., 2009; Butler et al., 2010). For this purpose, analyses of the anatomical-morphological features of the skeletal hard parts – such as growth patterns and crystal structures – are commonly combined with geochemical analyses (e.g., stable isotopes, trace elements). Due to its wide distribution throughout the North Atlantic (Dahlgren et al., 2000) and its longevity (500 years and more, Butler et al., 2013), the bivalve *Arctica islandica* represents an exceptional bio-archive for northern temperate regions.

A. islandica forms annual growth rings (increments), which can be measured and used as a calendar (Jones, 1980). However, when working with fossil specimens, the state of preservation is an essential aspect to consider prior to any kind of geochemical analysis (e.g., stable oxygen isotopes ($\delta^{18}O$) as a proxy for water temperature and salinity). Confocal Raman microscopy (CRM) is a non-destructive method, which allows a test for diagenetic alteration on the same sample that will later be used for the geochemical measurement.

The annual growth rate of bivalves mainly depends on ambient water temperature and food quality and availability (e.g., Witbaard et al., 1997) which vary on a regional scale, but may be affected by large-scale ocean-atmosphere phenomena, too (Schöne et al., 2003a), like the North Atlantic Oscillation (NAO). The frequency

analysis of the growth record of just a single *A. islandica* shell can identify such decadal signals (several years to decades) in a time window corresponding to the animal's lifetime.

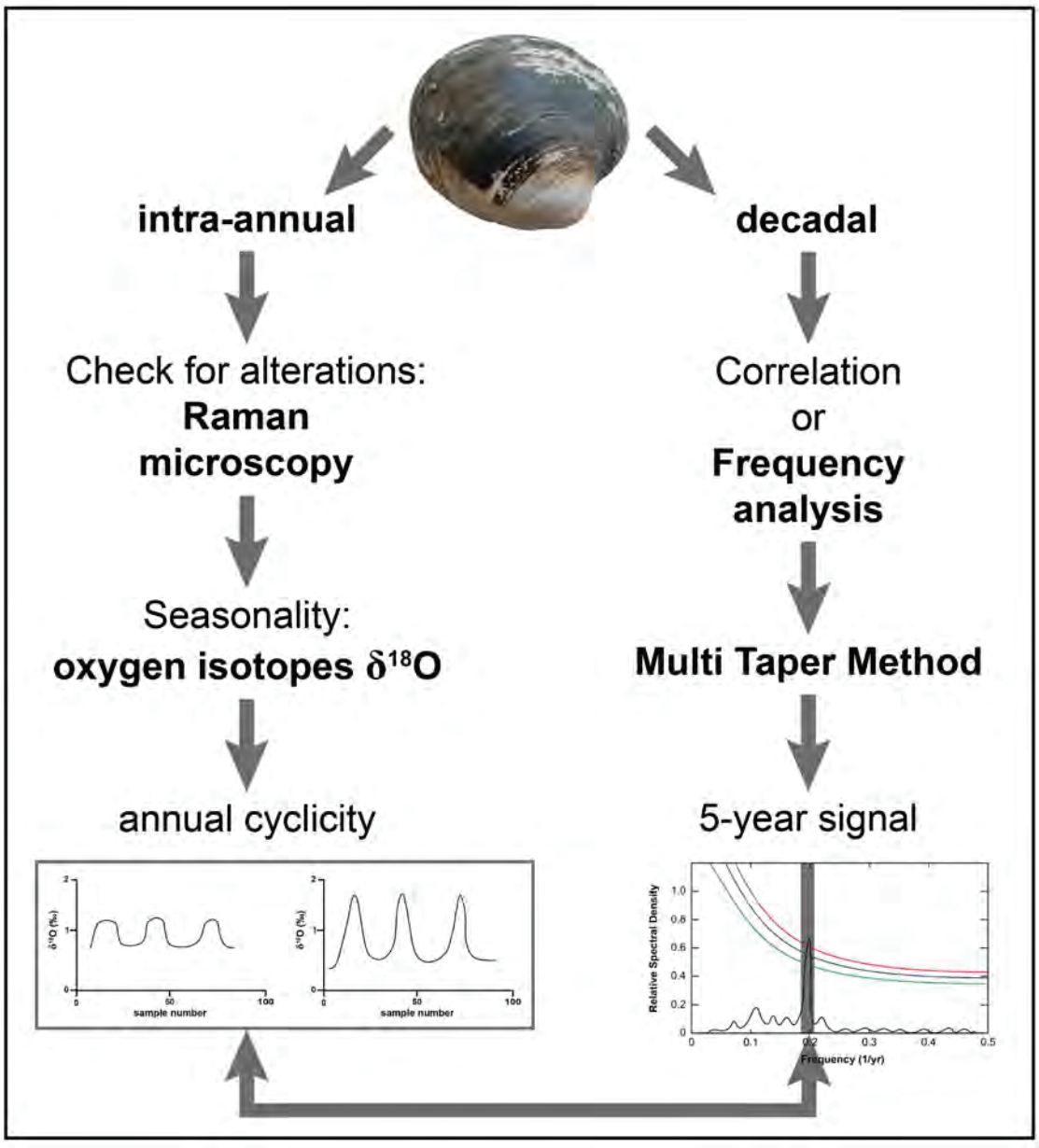

Figure 1. Flow chart illustrating potential reconstruction techniques on various time-scales for bivalve shells. Geochemical analyses, such as $\delta^{18}O$ as a proxy for water temperatures, allow reconstructions on an intra-annual level. A test for preservation in fossil specimens – e.g., by using CRM – should be obligatory. The shell of *A. islandica* can additionally be used for a frequency analysis (e.g., Multi Taper Method) of the annual growth pattern, allowing the identification of decadal variabilities, such as a 5-year quasi-periodic signal.

For demonstration purposes we combine the results from modern and fossil shell material to emphasise the unique character of the bio-archive *A. islandica*. We demonstrate its outstanding potential in terms of intra-annual (stable oxygen isotopes) as well as decadal (frequency analysis) climatic and environmental reconstructions and show how these can be combined to inform our understanding of climate in the past (Figure 1).

2 Methods

2.1 Shell origin and laboratory work

We use three *A. islandica* specimens of different geological age (see Table 1 for details) to demonstrate how sclerochronological analyses at intra-annual and decadal scale fit together. The CRM approach has been applied on Pliocene specimen AI-TjBe-01, which was removed from the biostratigraphically dated Tjörnes Bed formation, Iceland. Specimen AI-EgLo-02 has been found dead in beach deposits at the Lofoten, Norway, and used for the frequency analysis. Further, specimen Ai24568 has been live-collected in Tromsø, Norway in 2006 and used for the $\delta^{18}O$ approach.

Shell ID	Length (mm)	Height (mm)	Width (mm)	Locality	Geological age	Ontogenetic age (yrs)	Applied method
Ai24568	86.7	82.0	23.2	Tromso, Norway	Modern	71	Oxygen isotope analysis
AI-EgLo-02	53.3	46.6	14.0	Lofoten, Norway	Found dead, beach deposit	45	Frequency analysis
AI-TjBe-01	57.2*	84.0	24.4*	Tjörnes, Iceland	Pliocene	*not determined*	Raman microscopy

Table 1. Shell information. Information on shell morphology, shell origin, geological and ontogenetic ages as well as applied methods are given. Measurements marked with (*) for specimen AI-TjBe-01 give values for partly fragmented shell portions.

In the laboratory, all specimens were cleaned using a paintbrush, deionized water and an ultrasonic bath. Afterwards, shells were externally strengthened with an epoxy resin and cut along the line of strongest growth (LSG, Figure 2). The cut shell sections were glued onto glass slides and ground on sandpaper with varying grain sizes of 15 µm, 10 µm and 5 µm respectively.

To improve the visibility of the individual growth increments, the thick-section intended for the frequency analysis (shell ID: AI-EgLo-02) was stained with Mutvei´s solution (Schöne et al., 2005a). Digital images were taken under a stereo-microscope (Olympus, SZX12) attached to a CCD camera (Olympus) and increment width was measured using the image processing software analySIS (Olympus, version 5.1).

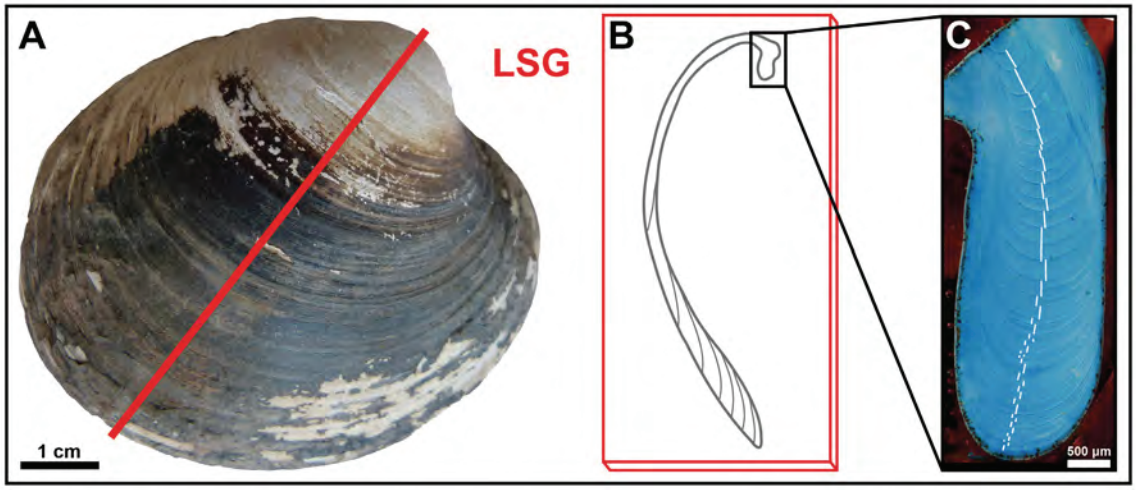

Figure 2. Cutting axis and location of shell increments in *A. islandica*. A) Right valve of an *A. islandica* specimen with line of strongest growth (LSG, equals cutting axis). B) Graphical illustration of an *A. islandica* thick-section after cutting through the LSG (red). Black box indicates the umbonal area shown in C. C) Magnification of the umbonal area, stained in Mutvei´s solution and showing annual growth increments. Growth band widths are measured perpendicular to the increments, as indicated by the white lines.

2.2 State of preservation

The shells of *A. islandica* consist of aragonite ($CaCO_3$), trace elements and organics (e.g., Schöne, 2013). After burial and in terms of fossilisation, several factors such as heat and pressure at depth, as well as hydrothermal fluids, can cause alterations in the shell carbonate, e.g., recrystallization from pristine aragonite to the more stable $CaCO_3$ polymorph calcite (e.g., Bathurst, 1964). In most cases the recrystallization process involves a dissolution and recrystallization process (neomorphism, e.g., Maliva, 1998), which would replace the pristine stable oxygen isotope value within the carbonate and erase the associated environmental signal in the shell (e.g., Hendry et al., 1995).

Due to its high spatial resolution of a few hundred nm CRM provides an ideal tool for shell carbonate analysis. For our measurements on Pliocene specimen AI-TjBe-01 we used a WITec alpha 300 R instrument, equipped with a diode laser

(excitation wavelength 532 nm) and a 20x Zeiss objective. Details on the measurements can be found in Nehrke et al. (2012).

2.3 Frequency analysis

The growth record of shell AI-EgLo-02 was detrended using a cubic spline (JMP software, version 9.0.1 by SAS Institute Inc. 2007), and a standardized growth index (SGI) was calculated following Butler et al. (2010). The subsequent frequency analysis was conducted using kSpectra software (version 3.4 by SpectraWorks) with settings according to Ivany et al. (2011) and applying a Singular Spectrum Analysis (SSA) and the Multi Taper Method (MTM). Furthermore, we used wavelet transformation to examine whether quasi-periodic signals were stationary over time (http://ion.researchsystems.com/IONScript/wavelet/), following Torrence and Compo (1998). Growth records of specimens Ai24568 and AI-TjBe-01 have not been analysed.

2.4 Stable oxygen isotopes ($\delta^{18}O$)

During shell formation, *A. islandica* incorporates oxygen isotopes in equilibrium with the surrounding seawater (Weidman and Jones, 1994). Since the incorporation of lighter oxygen isotopes is facilitated during higher temperatures (Grossman and Ku, 1986), the oxygen isotope value $\delta^{18}O$ of most bivalve species provides information on water temperatures (e.g., Schöne et al., 2005c) and salinity (e.g., Schöne et al., 2003b) at the moment of shell formation. In general, the modified temperature equation by Dettman et al. (1999) is used for *A. islandica*, which is based on the empirically determined relationship between temperature and $\delta^{18}O$ for aragonite by Grossman and Ku (1986).

Carbonate samples were milled by hand (Dettman and Lohmann, 1995) using a 700 µm drill bit (Komet/Gebr. Brasseler GmbH & Co. KG) mounted onto an industrial high precision drill (Minimo C121, Minitor Co., Ltd.) and attached to a binocular microscope. Measurements were performed on a Thermo Finnigan MAT 253 isotope ratio mass spectrometer and calibrated against a NBS-19 standard with a precision error of 0.08‰ for oxygen. Shell-derived water temperatures have been compared to SST measurements reported online (www.seatemperature.org/europe/norway/tromso).

3 Results

3.1 State of preservation

From the Raman scan it can be seen that the area of the fossil *A. islandica* shell (shell ID: AI-TjBe-01) marked in Figure 3A consisted of both aragonite and calcite. An area scan of 520x500 µm (Figure 3B), partly covering the potentially recrystallized shell portion, indicates the distribution of (pristine) aragonite and (recrystallized) calcite within the shell carbonate. Both polymorphs share carbonate-specific peaks at 155 cm^{-1} and 1085 cm^{-1} in their Raman spectra (Figure 3C). The aragonite-specific peak at ~206 cm^{-1} (blue line in Figure 3C) is shifted towards ~280 cm^{-1} in (recrystallized) calcite (red line in Figure 3C).

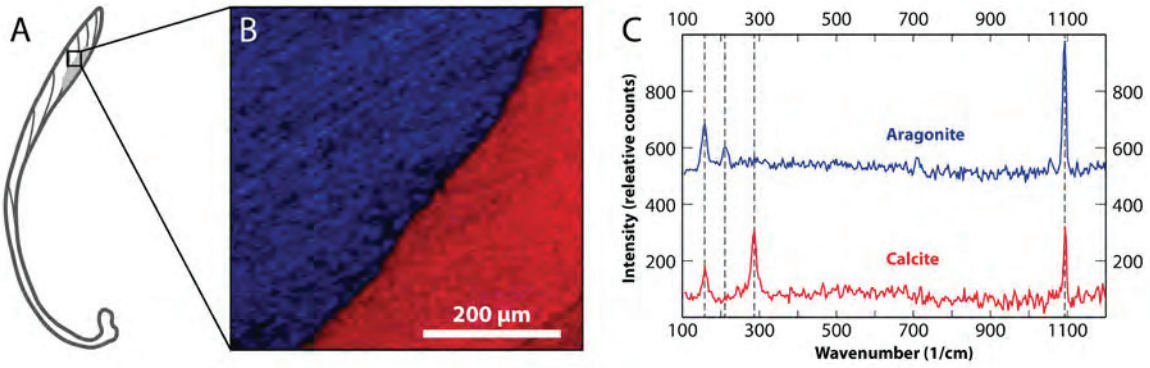

Figure 3. State of preservation tested by confocal Raman microscopy. A) Schematic illustration of a (fossil) *A. islandica* specimen. Light grey colour exemplary indicates area of potential recrystallization. B) Areal CRM scan in specimen AI-TjBe-01 close to the altered shell portion and as indicated in A. Two different materials have been identified. C) Raman spectra for two different polymorphs of calcium carbonate explaining colour coding in B. Intensity differences in liberation modes (peaks at ~206 cm^{-1} for aragonite and ~280 cm^{-1} for calcite) in single spot Raman spectra identify pristine aragonite (blue) and recrystallized calcite (red).

3.2 Frequency analysis

The frequency analysis of the SGI (Figure 4A) in specimen AI-EgLo-02 indicates a significant (95% level) 5-year signal (Figure 4B). Additionally, a signal at 2.7 years was significant at the 90% level. The wavelet transformation shows the variability of the indicated signals over time. Strength of the 5-year signal varies distinctly over time and is most prominent between ontogenetic years 20 and 30 (Figure 4C).

3.3 Stable oxygen isotopes ($\delta^{18}O$)

Oxygen isotope values of three consecutively sampled ontogenetic years in modern *A. islandica* specimen Ai24568 show three distinct sinusoidal patterns (summer peaks and winter troughs) with amplitudes of about 2‰ each (Figure 4D). Assuming a constant modern $\delta^{18}O_{seawater}$ value of 0‰ during shell formation, the measurements translate into water temperatures between 15°C and 6°C (Figure 4D).

4 Discussion and Conclusions

When working on fossil shell material, the state of preservation must be evaluated prior to geochemical analysis (e.g., stable oxygen isotopes) to avoid serious errors and bias. Here, CRM represents a powerful, time-effective and non-destructive tool for the examination of shell carbonate polymorphs (Figure 3).

In *A. islandica* shells it is possible to check the growth record for decadal variability throughout the life of the animal. In specimen AI-EgLo-02 (Lofoten, Norway) frequency analysis identified a significant 5-year signal, which, however, is not stationary over time (Figures 4A–C). Since the date of death is unknown, a direct correlation to observational or instrumental time-series is not feasible. This would, however, be an essential step to unambiguously link our 5-year signal to the NAO (c.f., Wunsch, 1999). A number of studies have shown indeed *A. islandica* shell growth patterns to correlate with known ocean-atmosphere oscillations such as NAO (Schöne et al., 2003a; Wanamaker Jr et al., 2009). Nevertheless, further investigations of additional shell material as well as of local forcing mechanisms are required.

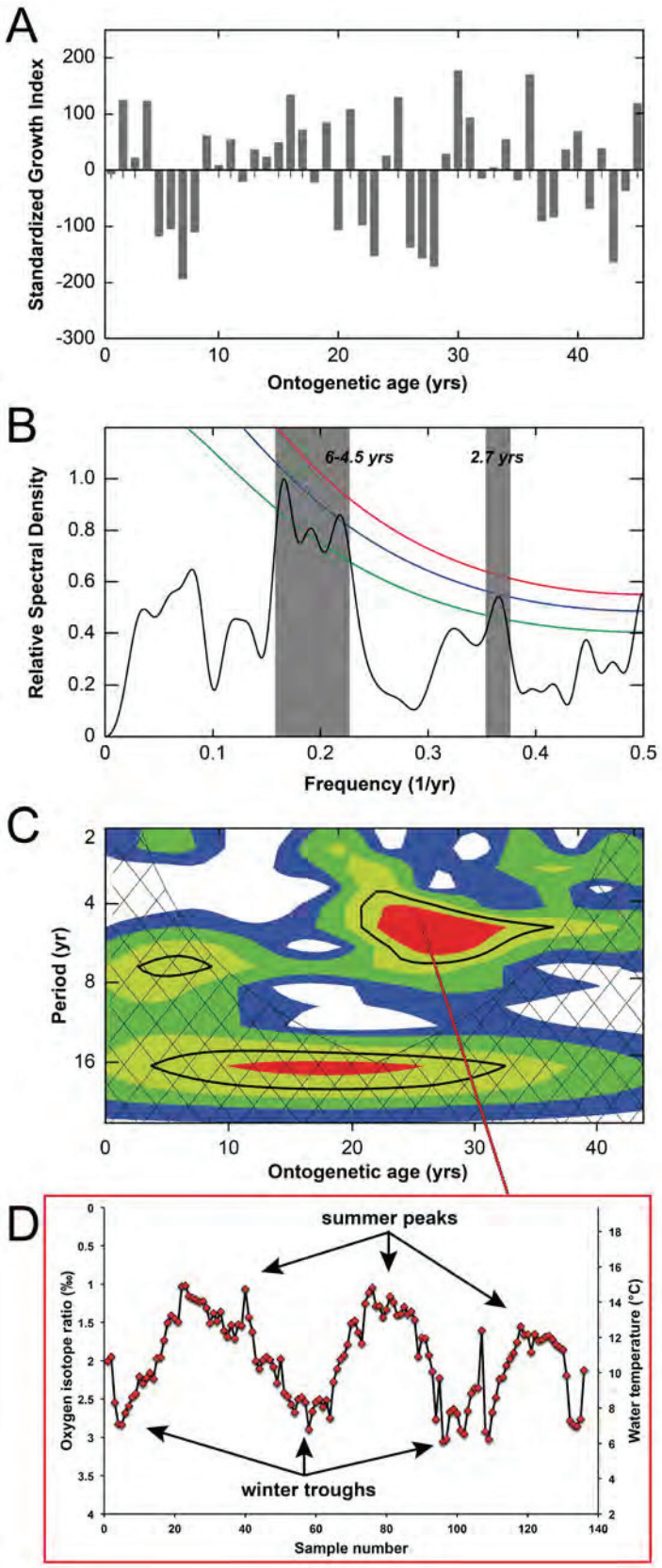
A
Standardized Growth Index
200
100
0
-100
-200
-300
0
10
20
30
40
Ontogenetic age (yrs)
B
Relative Spectral Density
6-4.5 yrs
2.7 yrs
1.0
0.8
0.6
0.4
0.2
0
0
0.1
0.2
0.3
0.4
0.5
Frequency (1/yr)
C
Period (yr)
2
4
8
16
0
10
20
30
40
Ontogenetic age (yrs)
D
summer peaks
winter troughs
Oxygen isotope ratio (‰)
Water temperature (°C)
Sample number
0
20
40
60
80
100
120
140

Figure 4 (previous page). Frequency analysis on *A. islandica* growth pattern. A) Standardized growth index (SGI) giving relative information on positive (above 0) or negative (below 0) deviations from average shell growth. B) Multi Taper Method (MTM) applied to the SGI shown in A. Red, blue and green lines represent significance levels of 99%, 95% and 90%, respectively. The significant (95%) signal at the frequency of 0.197 (1/yr) corresponds to a 5-year signal (combined SSA and MTM analysis). C) Wavelet transformation giving information on the stationarity of quasi-periodic signals identified by SSA and MTM. The strength of the 5-year quasi-periodic signal varies over time, being more prominent from ontogenetic year 20 onwards. D) Results for the $\delta^{18}O$ analysis in three ontogenetic years throughout the pronounced phase of the 5-year signal, as indicated in C. $\delta^{18}O$ values have been translated into water temperatures according to Dettman et al. (1999) assuming a $\delta^{18}O_{seawater}$ value of 0‰. Arrows indicate summer peaks and winter troughs.

$\delta^{18}O$ derived water temperatures (6–15°C, Figure 4D) in specimen Ai24568 correspond well to SST measurements (2.8–13.7°C) for Tromsø, Norway. However, our temperature reconstruction does not account for seasonal changes in salinity and assumes a global average $\delta^{18}O_{seawater}$ value of 0‰, which would need verification by on-site measurements. Further, an assumed growing season from February/March to September (Schöne et al., 2004) in *A. islandica* might explain truncated winter minimum temperatures.

Conclusively, for demonstrating purposes, we combined the results from the frequency and $\delta^{18}O$ analyses from two different shell specimens to give an exemplary perspective on the potential of *A. islandica* as a recorder of the environmental past. Accordingly, if *A. islandica* growth increment series can be synchronized with the external forcing signal (e.g., NAO) intra-annual analysis techniques (such as $\delta^{18}O$) can be used to analyse whether intra-annual patterns differ between weak and strong phases of shell growth oscillation. In our example, $\delta^{18}O$ analysis allowed to link a seasonal water temperature amplitude of about 9°C to the most prominent phase of the 5-year periodic signal (Figures 4C and D). The high temporal resolution combined with an exceptional longevity distinguish *A. islandica* shells from all other marine archives and show the great potential and uniqueness of *A. islandica* for climatic and environmental reconstructions on various time-scales.

Acknowledgements

We would like to thank Salma Begum (AWI Bremerhaven), Carin Andersson Dahl (Bjerknes Centre for Climate Research, Uni Research), Lovísa Ásbjörnsdóttir (Icelandic Institute of Natural History) for providing the shell material. Further, Andreas Mackensen, Lisa Schönborn and Kerstin Beyer (all AWI Bremerhaven) are thanked for their help and advice with the stable oxygen isotope measurements.

References

(Please note that references have been formatted according to style of journal)

Bathurst, R.G.C.: The replacement of aragonite by calcite in the molluscan shell wall. In: Imbrie, J. and Newell, N.O. (eds.) Approaches to Paleoecology, pp. 357–376. John Wiley & Sony, New York (1964).

Butler, P.G., Richardson, C.A., Scourse, J.D., Wanamaker Jr, A.D., Shammon, T.M., Bennell, J.D.: Marine climate in the Irish Sea: analysis of a 489-year marine master chronology derived from growth increments in the shell of the clam *Arctica islandica*. Quaternary Science Reviews 29, 1614–1632 (2010).

Butler, P.G., Wanamaker Jr, A.D., Scourse, J.D., Richardson, C.A., Reynolds, D.J.: Variability of marine climate on the North Icelandic Shelf in a 1357-year proxy archive based on growth increments in the bivalve *Arctica islandica*. Palaeogeography, Palaeoclimatology, Palaeoecology 373, 141–151 (2013).

Dahlgren, T.G., Weinberg, J.R., Halanych, K.M.: Phylogeography of the ocean quahog (*Arctica islandica*): influences of paleoclimate on genetic diversity and species range. Marine Biology 137, 487–495 (2000).

Dettman, D., Lohmann, K.C.: Microsampling Carbonates for Stable Isotope and Minor Element Analysis: Physical Separation of Samples on a 20 Micrometer Scale. Journal of Sedimentary Research 65A, 566–569 (1995).

Dettman, D.L., Reische, A.K., Lohmann, K.C.: Controls on the stable isotope composition of seasonal growth bands in aragonitic fresh-water bivalves (Unionidae). Geochimica et Cosmochimica Acta 63, 1049–1057 (1999).

Grossman, E.L., Ku, T.-L.: Oxygen and carbon isotope fractionation in biogenic aragonite: Temperature effects. Chemical Geology 59, 59–74 (1986).

Hallmann, N., Burchell, M., Schöne, B.R., Irvine, G.V., Maxwell, D.: High-resolution sclerochronological analysis of the bivalve mollusk *Saxidomus gigantea* from Alaska and British Columbia: techniques for revealing environmental archives and archaeological seasonality. Journal of Archaeological Science 36, 2353–2364 (2009).

Hendry, J.P., Ditchfield, P.W., Marshall, J.D.: Two-stage neomorphism of Jurassic aragonitic bivalves: implications for early diagenesis. Journal of Sedimentary Research 65, 214–224 (1995).

IPCC: Climate Change 2013: The Physical Science Basis. Contribution of Working Group I to the Fifth Assessment Report of the Intergovernmental Panel on Climate Change. Cambridge University Press, Cambridge, United Kingdom and New York, NY, USA (2013).

Ivany, L.C., Brey, T., Huber, M., Buick, D.P., Schöne, B.R.: El Niño in the Eocene greenhouse recorded by fossil bivalves and wood from Antarctica. Geophysical Research Letter 38, L16709 (2011).

Jones, D.S.: Annual Cycle of Shell Growth Increment Formation in Two Continental Shelf Bivalves and its Paleoecologic Significance. Paleobiology 6, 331–340 (1980).

Maliva, R.G.: Skeletal aragonite neomorphism – quantitative modelling of a two-water diagenetic system. Sedimentary Geology 121, 179–190 (1998).

Nehrke, G., Poigner, H., Wilhelms-Dick, D., Brey, T., Abele, D.: Coexistence of three calcium carbonate polymorphs in the shell of the Antarctic clam *Laternula elliptica*. Geochemistry, Geophysics, Geosystems 13, Q05014 (2012).

Schöne, B.R.: *Arctica islandica* (Bivalvia): A unique paleoenvironmental archive of the northern North Atlantic Ocean. Global and Planetary Change 111, 199–225 (2013).

Schöne, B.R., Dunca, E., Fiebig, J., Pfeiffer, M.: Mutvei's solution: An ideal agent for resolving microgrowth structures of biogenic carbonates. Palaeogeography, Palaeoclimatology, Palaeoecology 228, 149–166 (2005a).

Schöne, B.R., Houk, S.D., Freyre Castro, A.D., Fiebig, J., Oschmann, W., Kroncke, I., Dreyer, W., Gosselck, F.: Daily Growth Rates in Shells of *Arctica islandica*: Assessing Sub-seasonal Environmental Controls on a Long-lived Bivalve Mollusk. Palaios 20, 78–92 (2005b).

Schöne, B.R., Oschmann, W., Rössler, J., Castro, A.D.F., Houk, S.D., Kröncke, I., Dreyer, W., Janssen, R., Rumohr, H., Dunca, E.: North Atlantic Oscillation dynamics recorded in shells of a long-lived bivalve mollusk. Geology 31, 1037–1040 (2003a).

Schöne, B.R., Pfeiffer, M., Pohlmann, T., Siegismund, F.: A seasonally resolved bottom-water temperature record for the period AD 1866–2002 based on shells of *Arctica islandica* (Mollusca, North Sea). International Journal of Climatology 25, 947–962 (2005c).

Schöne, B.R., Tanabe, K., Dettman, D.L., Sato, S.: Environmental controls on shell growth rates and $\delta^{18}O$ of the shallow-marine bivalve mollusk *Phacosoma japonicum* in Japan. Marine Biology 142, 473–485 (2003b).

Schöne, B.R., Freyre Castro, A.D., Fiebig, J., Houk, S.D., Oschmann, W., Kröncke, I.: Sea surface water temperatures over the period 1884-1983 reconstructed from oxygen isotope ratios of a bivalve mollusk shell (*Arctica islandica*, southern North Sea). Palaeogeography, Palaeoclimatology, Palaeoecology 212, 215-232 (2004).

Torrence, C., Compo, G.P.: A Practical Guide to Wavelet Analysis. Bulletin of the American Meteorological Society 79, 61–78 (1998).

Wanamaker Jr, A., Kreutz, K., Schöne, B., Maasch, K., Pershing, A., Borns, H., Introne, D., Feindel, S.: A late Holocene paleo-productivity record in the western Gulf of Maine, USA, inferred from growth histories of the long-lived ocean quahog (*Arctica islandica*). International Journal of Earth Sciences 98, 19–29 (2009).

Weidman, C.R., Jones, G.A.: The long-lived mollusc *Arctica islandica*: A new paleoceanographic tool for the reconstruction of bottom temperatures for the continental shelves of the northern North Atlantic Ocean. Journal of Geophysical Research 99, 18305–18314 (1994).

Witbaard, R., Franken, R., Visser, B.: Growth of juvenile *Arctica islandica* under experimental conditions. Helgolaender Meeresuntersuchungen 51, 417–431 (1997).

Wunsch, C.: The Interpretation of Short Climate Records, with Comments on the North Atlantic and Southern Oscillations. Bulletin of the American Meteorological Society 80, 245–255 (1999).

Manuscript II

Confocal Raman microscopy in sclerochronology: a powerful tool to visualize environmental information in recent and fossil biogenic archives

Lars Beierlein[1], Gernot Nehrke[1] and Thomas Brey[1]

[1]Alfred Wegener Institute, Helmholtz Centre for Polar and Marine Research, Bremerhaven, Germany

Submitted to *Geochemistry, Geophysics, Geosystems* (August 2014).

Abstract

Biological hard-parts and skeletons of aquatic organisms often archive information of past environmental conditions. Deciphering such information forms an essential contribution to our understanding of past climate conditions and thus our ability to mitigate the climatic, ecological and social impacts of a rapidly changing environment. Several established techniques enable the visualization and reliable use of the information stored in anatomical features of such biogenic archives, i.e., its growth patterns. Here, we test whether confocal Raman microscopy (CRM) is a suitable method to reliably identify growth patterns in the commonly used archive *Arctica islandica* and the extinct species *Pygocardia rustica* (both Bivalvia). A modern *A. islandica* specimen from Norway has been investigated to verify the general feasibility of CRM, resulting in highly correlated standardized growth indices ($r > 0.96$; $P < 0.0001$) between CRM derived measurements and measurements derived from the established methods of fluorescence microscopy and Mutvei´s solution staining. This demonstrates the general suitability of CRM as a method for growth pattern evaluation and cross-dating applications. Moreover, CRM may be of particular interest for palaeo-environmental reconstructions, as it yielded superior results in the analysis of fossil shell specimens (*A. islandica* and *P. rustica*) compared to both Mutvei staining and fluorescence microscopy. CRM is a reliable and valuable tool to visualize internal growth patterns in both modern and fossil calcium carbonate shells that notably also facilitates the assessment of possible diagenetic alteration prior to geochemical analysis without geochemically compromising the sample. We strongly recommend the CRM approach for the visualization of growth patterns in fossil biogenic archives, where conventional methods fail to produce useful results.

Keywords: confocal Raman microscopy, sclerochronology, *Arctica islandica*, fluorescence, Mutvei´s solution, biogenic carbonate, palaeo-climate, palaeo-environment

1 Introduction

Detailed understanding of the global dynamics that have driven past environment and climate conditions prior to the era of instrumental and observational data (i.e., the last 200 years) is of utmost significance for proper forecasts of future climate development, e.g., by means of global coupled ocean-atmosphere models. Different archives of past climates contribute to this understanding of past climatic conditions and can subsequently be used to verify and improve models of future climate conditions. Commonly used archives such as sediment cores or ice cores cover long timespans (tens of thousands to millions of years, e.g., Petit et al., 1999) but have limited temporal resolution (annual at best, but usually in the range of decades to thousands of years, e.g., Hald et al., 2007). However, the reliability of palaeo-environmental/climate reconstructions and models can be greatly enhanced by including data on short-term variability at sub-decadal or even sub-annual (e.g., seasonal) scales. Such information can be derived from non-biogenic (e.g., speleothems) and biogenic (e.g., durable accretion parts of plants and animals) archives. Particularly, the aquatic realm is a rich resource of biogenic archives (mostly calcium carbonate) produced by long-lived organisms such as coralline algae, corals, molluscs and fish (otoliths). These archives provide high-resolution information on decadal (DeLong et al., 2007) and sub-annual (Halfar et al., 2008) scales, whilst individual specimens can reach ages of several centuries (Schöne et al., 2005b).

Bivalves constitute archives of increasing importance (Richardson, 2001; Schöne, 2013). They can be found in almost all aquatic systems worldwide, but notably in boreal and Polar regions they represent the only available long-lived biogenic information source (Schöne, 2013). Due to their annual resolution, analysis of the internal growth patterns in different bivalve species have been used successfully to identify multi-year and decadal oscillation patterns such as the North Atlantic Oscillation (NAO; Brocas et al., 2013), Arctic Climate Regime Index (ACRI; Carroll et al., 2011) or El Niño-Southern Oscillation (ENSO; Schöne et al., 2007). Bivalve sclerochronology has additionally been used to identify multi-decadal climate trends (Brey et al., 2011), sub-annual environmental patterns (Beierlein et al., 2014) and has successfully been applied in archaeological studies, where, for example, sub-fossil bivalve shells from shell-middens (mounds of discarded shell materials at pre-historic settlements) are used to identify seasonal patterns of resource procurement (Burchell et al., 2013; Hallmann et al., 2013).

The bivalve *Arctica islandica* is a unique biogenic archive of particular importance (Schöne, 2013) due to its longevity (400 years and more; Butler et al., 2013), its wide boreal distribution throughout the North Atlantic (Dahlgren et al., 2000) and the fact that it records environmental conditions of the ambient water on a sub-annual scale (Schöne and Fiebig, 2009).

To reliably utilize the climate and environmental information recorded within the shell, the internal growth pattern of the shell needs to be visualized. Changes in carbonate structure and/or shell organic matter content are formed at regular intervals, and it is crucial to successfully couple and interpret the temporal and physical/biological mechanisms involved in these successive growth increments (for example annual, lunar, daily, tidal periodicity) in order to make reliable interpretations about past environments.

It is therefore essential that the accretionally precipitated growth increments within the shell are identified reliably and unambiguously, measured and finally interpreted as a proxy for past environmental conditions. However, depending on the archive material (e.g., biogenic apatite or calcium carbonate), its age and preservation, it can be challenging to accurately and consistently reveal such information.

Several techniques have been established to visualize growth increments in sectioned bivalve shells. Common approaches are acetate peel replicas (Ropes, 1987) and treatment with Mutvei´s solution (Schöne et al., 2005a), which stains the organic compounds of the shell and simultaneously removes surface carbonate to create a relief structure. More technically sophisticated methods include fluorescence microscopy (Wanamaker Jr et al., 2009), which enhances contrast by inducing auto-fluorescence in organic compounds, backscattered electron microscopy (BSE; Karney et al., 2011), where the detection of backscattered high-energy electrons is used, and NanoSIMS (Karney et al., 2012), which identifies differences in composition of annual growth increments.

Each of these methods has inherent advantages and limitations. Most preparation techniques are considered time-consuming. Some are considered to make the unambiguous identification of growth increments difficult (acetate peels), require etching of the shell surface (i.e., the cross section will become unusable for geochemical analysis) or require different steps of shell pre-treatment (e.g., spattering). Mutvei´s solution uses glutaraldehyde (for chemical fixation of organic compounds), which is a hazardous respiratory toxin. In addition, most of the commonly used

techniques are only of limited use when applied to sub-fossil (up to 10,000 years old) and fossil shell material. This also applies for Mutvei´s solution, where smaller amounts of polysaccharides are present in the skeletons of older shells result in reduced contrast and lighter staining (Schöne et al., 2005a).

Raman spectroscopy is a commonly applied technique in geosciences (e.g., for the identification and characterization of minerals) and studies of biominerals (Nehrke and Nouet, 2011; Wall and Nehrke, 2012). Confocal Raman microscopy (CRM) has been employed in several biological studies involving molluscs, for example it has been used in studies to identify polyenes/pigments in several bivalve species (Barnard and de Waal, 2006; Hedegaard et al., 2006; Stemmer and Nehrke, 2014), to demonstrate that changes in the biomineralization of the Peruvian bivalve *Trachycardium procerum* are associated with El Niño events (Perez-Huerta et al., 2013), to document meteoric diagenesis involving syntaxial overgrowth of aragonite cement on late Pleistocene aragonitic freshwater bivalve bio-crystals (Webb et al., 2007), and for polymorph identification in marine and freshwater bivalve shells and pearls (Wehrmeister et al., 2010; Nehrke et al., 2012).

Here we test whether CRM is a suitable or even superior – in terms of resolution and efficiency – tool for visualizing internal shell growth patterns compared to Mutvei´s solution and fluorescence microscopy, using shells of *A. islandica* and *Pygocardia rustica* and with particular emphasis on fossil specimens. We additionally discuss and evaluate the advantages and limitations of CRM in comparison to other visualization techniques.

2 Materials and Methods

2.1 Origin and preparation of shell material

A total of four shell specimens have been analyzed in this study (for detailed information on shell material see Table 1). We test the CRM approach against the established methods of Mutvei staining and fluorescence microscopy (from here on referred as FL) using one modern *Arctica islandica* shell (ID: Ai1276R) from Tromsø, Norway. Then we compared the performance of the three methods with fossil shells, using two fossil *A. islandica* shells (IDs: AI-CoCr-01 from Sudbourne Park Pit, UK; AI-

StRi2-BK1b from Stirone River, Italy) and one fossil *Pygocardia rustica* shell (ID: RGM609.096 from Antwerp, Belgium).

A. islandica builds its three shell layers out of aragonite (Schöne, 2013) as does the extinct species *P. rustica*, which inhabited a similar ecological niche as *A. islandica* (Bosch and Wesselingh, 2006). Annual growth lines in both taxa are usually precipitated in autumn and winter (Ropes et al., 1984).

All four shells were initially covered with an epoxy resin and cut using a low-speed precision saw (Buehler, IsoMet) equipped with a 0.4 mm diamond-coated saw blade. Cross-sections of 3 mm thickness were cut perpendicular to the growth lines, glued on glass slides and ground using a manual grinder (Buehler, Phoenix Alpha) and sand paper with three different grain sizes (15 µm, 10 µm and 5 µm). All shells have been analyzed consecutively, starting with the FL method then the CRM method and finally the Mutvei staining approach.

2.2 Visualization Methods

2.2.1 Confocal Raman microscopy (CRM)

In contrast to elastic light scattering (also known as Rayleigh scattering), which applies to the main fraction of light, during inelastic light scattering (commonly termed Raman scattering) a very small fraction of incident light is scattered inelastically (Raman and Krishnan, 1928). The resulting difference in frequency between irradiated and scattered light (Stokes shift) depends on the specific molecular vibration of the molecules and can therefore be used for material identification (e.g., Smith and Dent, 2005). All shells analyzed in this study consist of aragonite, which is identified based on two lattice modes (translation mode, 152 cm^{-1} and liberation mode, 206 cm^{-1}) and the two vibration modes (C–O symmetric stretch, 1085 cm^{-1} and C–O in-plane bending, 705 cm^{-1}).

We used a confocal Raman microscope (CRM) (WITec alpha 300 R) with two different monochromatic light sources (diode lasers): a laser with an excitation wavelength of 488 nm and one of 785 nm in conjunction with a motorized scan table with a maximum scan range of 2.5 x 2.5 cm and a minimum step size of 100 nm. Raman maps were taken using 20x (Zeiss EC Epiplan, NA = 0.4) and 100x (Nikon, NA = 0.9) objectives. Raman signals were detected using a UHTS300 ultra high throughput spectrometer (WITec GmbH, Ulm, Germany) in which the spectrometer for

532 nm excitation wavelengths used a 600 mm^{-1} grating and a 500 nm blaze while the spectrometer for 785 nm excitation wavelength used a 600 mm^{-1} grating and a 750 nm blaze. Subsequent spectral analysis and processing of digital images was conducted using WITecProject software (version 2.10, WITec GmbH, Ulm, Germany). Integration time was chosen to 0.1 s, while all measurements have been conducted at room temperature.

In order to establish whether the obtained results from Raman mapping are comparable to more commonly used techniques such as fluorescence microscopy (Wanamaker Jr et al., 2009) and staining with Mutvei´s solution (Schöne et al., 2005a) a mapping approach was applied (c.f., Nehrke and Nouet, 2011; Nehrke et al., 2012; Wall and Nehrke, 2012; Stemmer and Nehrke, 2014), where each pixel consists of a single spectrum containing the entire spectral information (Figure 1). Raman maps in this study are large area scans showing the relative intensity difference of the fluorescence signal between wavenumbers of 2000 cm^{-1} and 2400 cm^{-1} before any background subtraction was applied (Figure 1a). Consequently, and following descriptions in Nehrke and Nouet (2011) and Wall and Nehrke (2012), we use the fluorescence intensity distribution to map the distribution of organic components. Intensity colour-coding has been chosen as orange and red (compare Figure 1b).

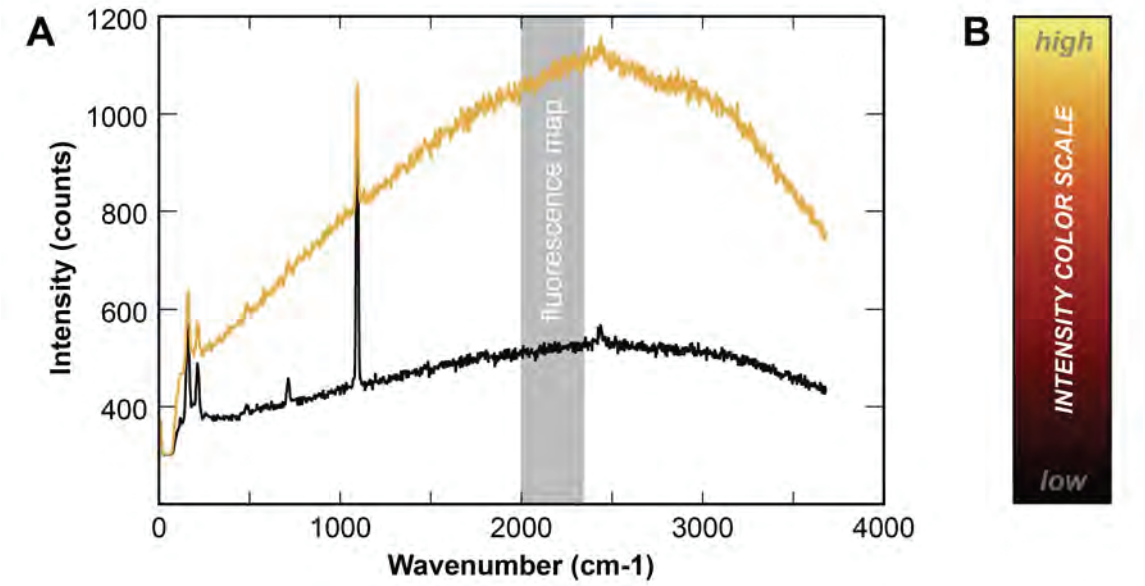

Figure 1. Colour-coding in CRM fluorescence maps. (A) Two exemplary Raman-derived spectra for aragonite. The relative intensity difference in the spectral region 2000–2400 cm^{-1} is used to derive fluorescence maps. (B) High relative intensities (yellow) and low relative intensities (black) define the "colour-coding" range of the fluorescence maps (as seen in Figures 2, 3, 4 and 6).

2.2.2 Fluorescence microscopy

Following the recommendations in Wanamaker Jr et al. (2009), we used the 'blue light spectrum' where internal growth lines of the hinge plate become most prominent. An excitation filter (BP 460–490; excitation 460–490 nm, emission 515 nm) and a barrier filter (BA510IF), filtering the reflected light, were used. Images were taken in analySIS docu software (Olympus, version 5.1) using a stereo-microscope (Olympus, SZX12) attached to a CCD camera (Olympus, U-CMAD).

2.2.3 Mutvei´s solution

The application of Mutvei´s solution to shells or skeletons simultaneously causes chemical etching (acetic acid), histochemical staining (alcian blue) and chemical fixation (glutaraldehyde). Cross-sections of three shell specimens (IDs: Ai1276R, AI-CoCr-01 and RGM609.096) were stained with Mutvei´s solution according to the procedure described in Schöne et al. (2005a). An immersion time of 23 minutes at 37–40°C has been applied. Due to unsatisfactory results in the fossil specimens, immersion times were stepwise increased to 46 minutes in specimen RGM609.096 and 60 minutes in specimen AI-CoCr-01. Digital images of Mutvei stained cross sections were taken using an Olympus SZX12 stereo-microscope equipped with an Olympus U-CMAD CCD camera and analySIS docu software (Olympus, version 5.1).

2.3 Growth increment measurements

We determined increment widths in the aragonitic hinge plates of three shells, a modern *A. islandica* (ID: Ai1276R; Figure 2), a fossil *A. islandica* (ID: AI-CoCr-01; Figure 3) and a fossil *P. rustica* (ID: RGM609.096; Figure 4). Increment width in CRM maps as well as in Mutvei and FL derived images was measured using Panopea image processing software (© Peinl & Schöne). Mutvei and FL derived images were processed with Adobe Photoshop (version CS5.1) in order to enhance contrast and guarantee comparable results. Increment series were transformed into standardized growth index (SGI) series by means of detrending using a cubic spline (λ = 150; JMP statistical software, version 9.0.1, SAS Institute Inc. 2007) and subsequent calculation of SGI following Schöne et al. (2005b). We compared the SGI series obtained by CRM, FL and Mutvei staining, following the approach of Wanamaker Jr et al. (2009).

3 Results

3.1 CRM verification with modern *A. islandica* shell

We were able to identify, count and measure internal growth increments throughout the entire hinge plate of the modern *A. islandica* shell specimen Ai1276R (Figure 2) on digital photographs derived from the Mutvei and FL approaches as well as on CRM maps. The corresponding growth increment time-series (Figure 5a) were detrended and standardized growth indices (SGI) were calculated (Figure 5b). The CRM SGI series correlates strongly with the FL series ($r = 0.98$; $P < 0.0001$; $N = 57$; age 5–62) and the Mutvei series ($r = 0.96$; $P < 0.0001$; $N = 57$; age 5–62) and the same applies to the Mutvei and FL series ($r = 0.97$; $P < 0.0001$; $N = 57$; age 5–62). Specimen Ai1276R became 65 ontogenetic years old, covering a life span from 1942–2006 (Figure 5a and 5b). For the verification approach, the time span from 1946–2003 was chosen.

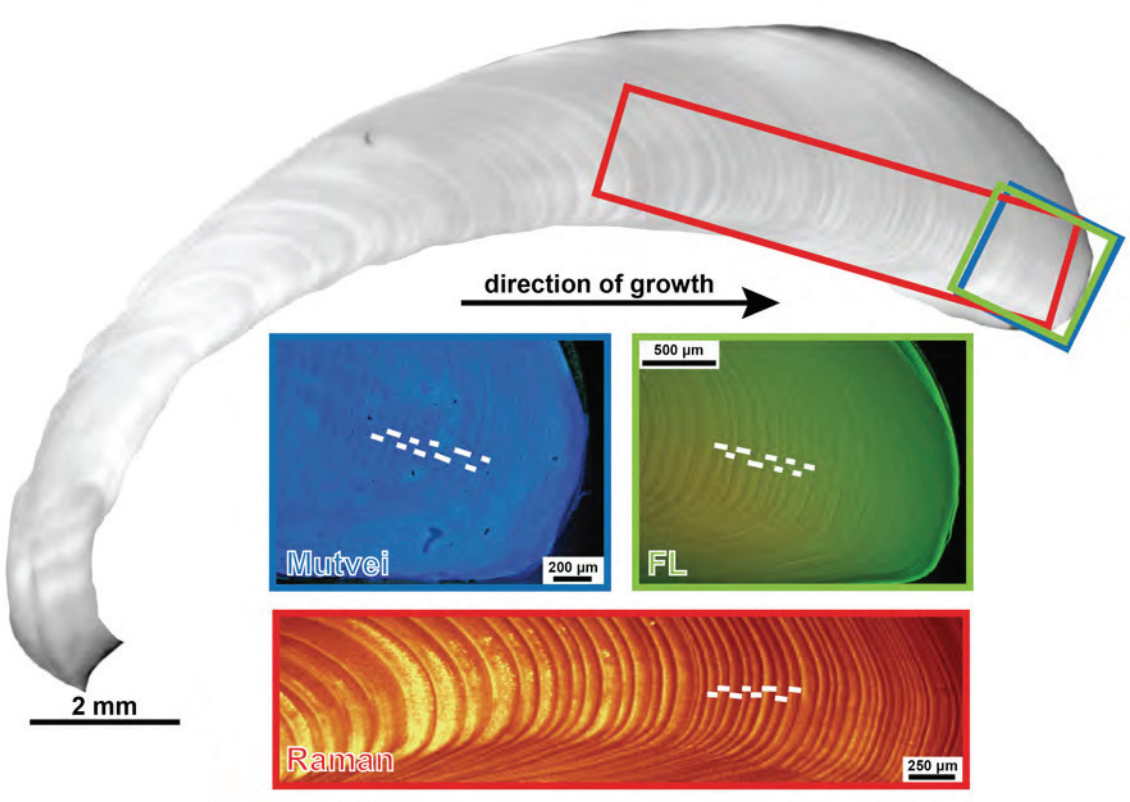

Figure 2. Verification approach: Growth increments in the hinge plate of the modern *A. islandica* shell specimen (ID: Ai1276R) were successfully visualized, counted and measured using Mutvei staining (blue), FL (green) and CRM mapping (red). White lines indicate increment widths, perpendicular to the annual growth lines.

3.2 Application to fossil *A. islandica* and *P. rustica*

CRM maps clearly show annual growth increments throughout the entire hinge plate (Figures 3 and 4). Based on these maps, the Pliocene *A. islandica* specimen (AI-CoCr-01) reached an ontogenetic age of 31 years (Figure 5c) while the Pliocene *P. rustica* specimen (ID: RGM609.096) reached an age of 17 years (Figure 5e). The FL and Mutvei staining approaches of both fossil specimens resulted in digital images of very low contrast (Figures 3 and 4). Particularly in the ontogenetically older areas, where growth increments become most narrow, a clear distinction between increments was no longer possible. Consequently, it was not possible to reliably measure the internal growth pattern over the entire hinge plate (Figures 5c–5f). The Mutvei treatment revealed the first 22 ontogenetic years only, and the FL treatment the first 17 years in the fossil *A. islandica* specimen (Figures 5c and 5d). In the fossil *P. rustica* specimen (ID: RGM609.096) both Mutvei and FL treatment showed the first five ontogenetic years only (Figures 5e and 5f). In the Pliocene *A. islandica* specimen (AI-CoCr-01), SGI series obtained by CRM and Mutvei (22 years; $r = 0.95$; $P < 0.0001$) as well as by CRM and FL (17 years; $r = 0.86$; $P < 0.0001$) are strongly correlated (Figure 5d). The short increment series obtained with FL and Mutvei treatments did not allow for a corresponding SGI series comparison for Pliocene *P. rustica* specimen (Figure 5f).

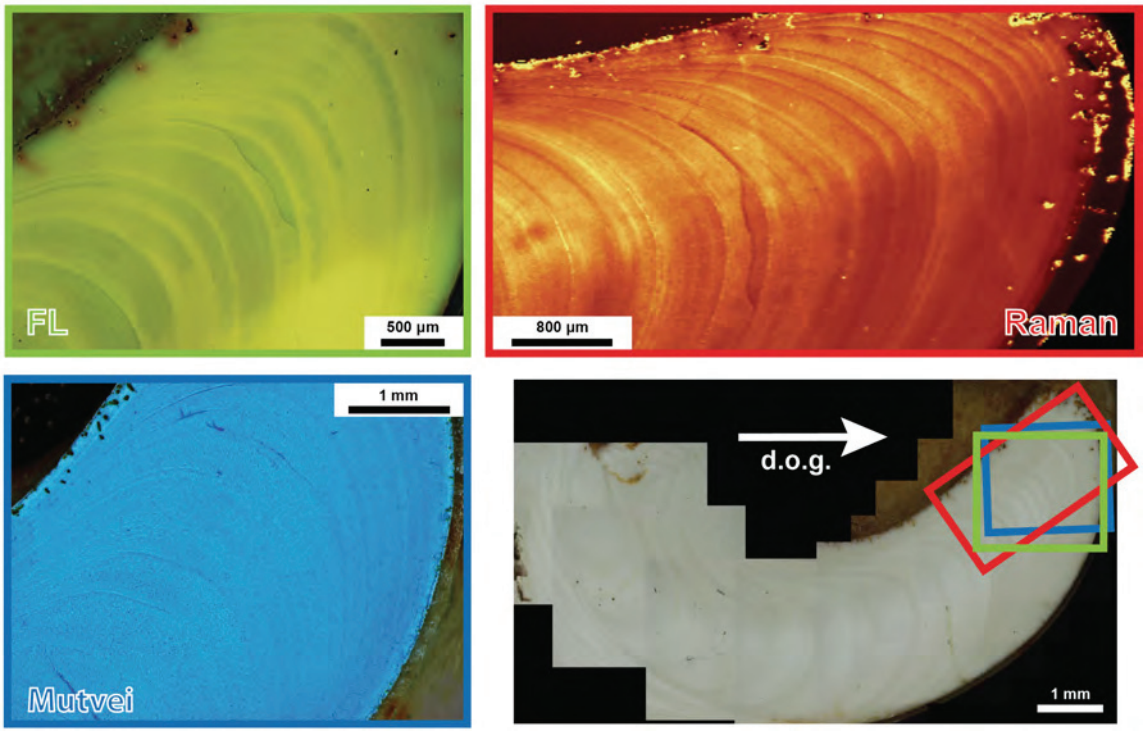

Figure 3 (previous page). Hinge plate of fossil *A. islandica* specimen AI-CoCr-01 analyzed by FL (green), Mutvei staining (blue) and CRM mapping (red). FL and Mutvei staining approaches do not allow for distinction of growth increments in the ontogenetically oldest parts of the shell carbonate, but CRM maps do. Arrow indicates direction of growth (d.o.g.).

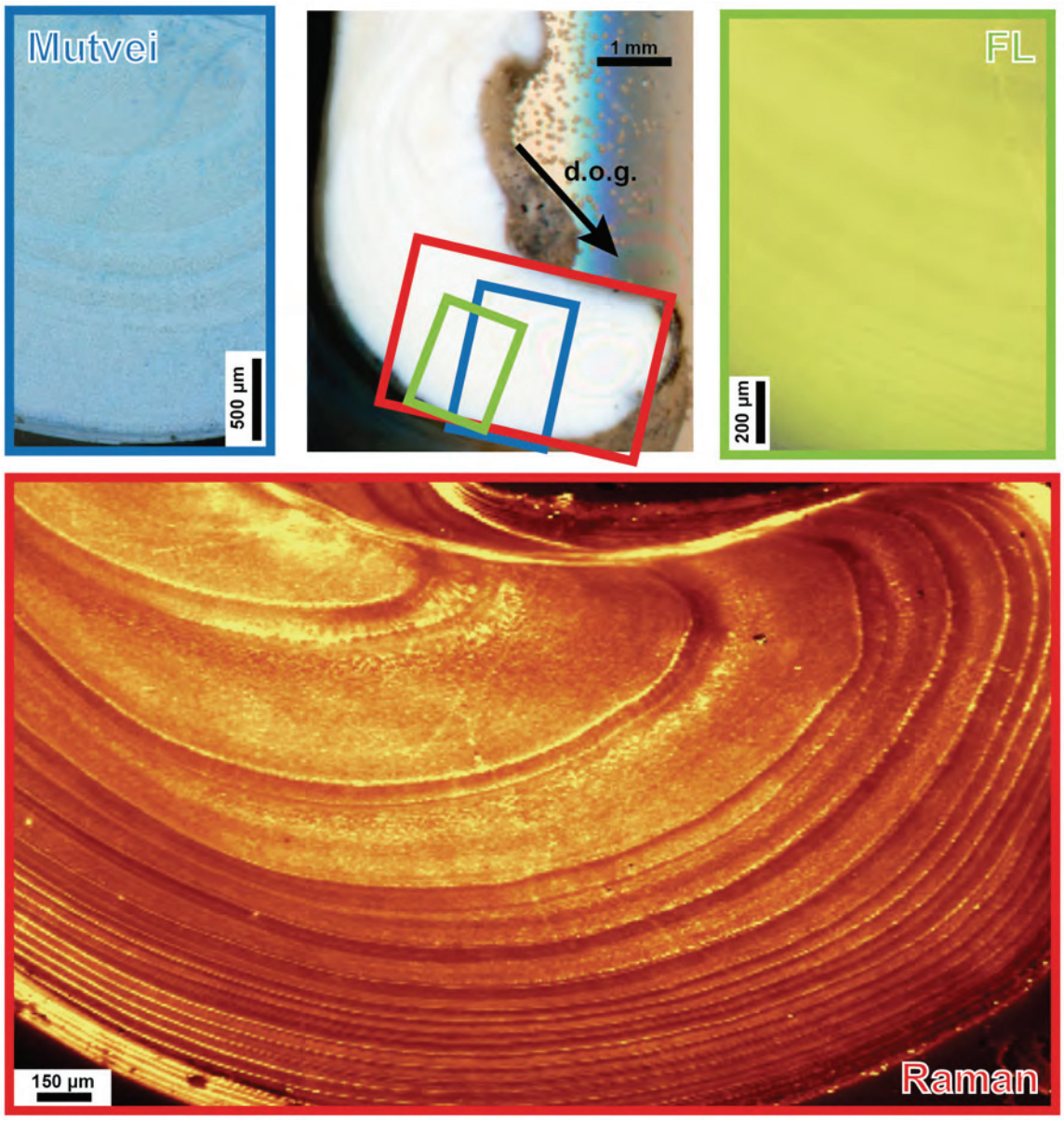

Figure 4. Hinge plate of fossil *P. rustica* specimen RGM609.096 analyzed by Mutvei staining (blue), FL (green) and CRM mapping (red). FL and Mutvei staining approaches do not allow for distinction of growth increments in the ontogenetically oldest parts of the shell carbonate, but CRM maps do. Arrow indicates direction of growth (d.o.g.).

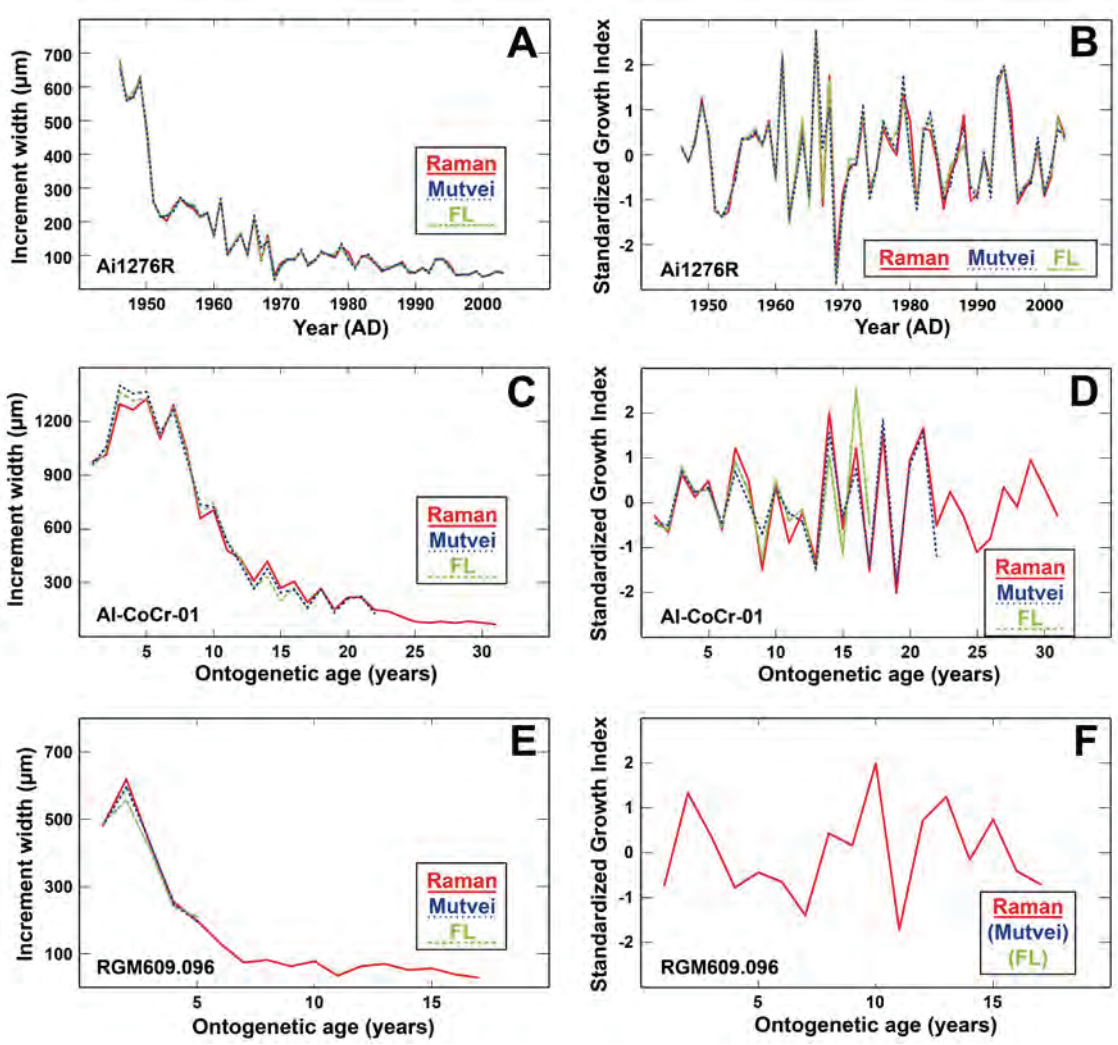

Figure 5. Comparison of growth increment series in modern *A. islandica* (ID: Ai1276R) (A), fossil *A. islandica* (ID: Al-CoCr-01) (C) and fossil *P. rustica* (ID: RGM609.096) (E) as determined by means of FL (green dashed line), Mutvei staining (blue dotted line) and CRM (red solid line). SGI series for Ai1276R (N = 57; age 5–62; B) correlate significantly between CRM and FL ($r = 0.98$; $P < 0.0001$), between CRM and Mutvei ($r = 0.96$; $P < 0.0001$) and between Mutvei and FL ($r = 0.97$; $P < 0.0001$). SGI series for Al-CoCr-01 (D) correlate significantly between CRM (31 years) and FL (17 years) for the first 17 years ($r = 0.86$; $P < 0.0001$) and between Mutvei (22 years) and CRM for the first 22 years ($r = 0.95$; $P < 0.0001$). Due to short FL (5 years) and Mutvei staining (5 years) derived time-series in RGM609.096, SGI (F) has only been calculated for CRM approach (solid red line). Colours and lines as A, C, E.

4 Discussion

4.1 Verification on modern *A. islandica*

The strong correlations ($r > 0.96$; $P < 0.0001$) between SGI series resulting from CRM, FL and Mutvei treatments (Figure 5b) confirm that the shell growth increment pattern visualized by CRM mapping is identical to the growth patterns detected by the established methods Mutvei staining and FL. Therefore CRM can be considered to be

an equally reliable method to visualize internal growth structures in aragonite shells. It is also suitable for cross-dating applications such as the compilation of master chronologies, where the growth records of single specimens with overlapping life spans are stacked to produce a compilation of environmental change that can cover time spans of up to several hundred years (Butler et al., 2010). Consequently, such archives allow for climatic reconstructions from a daily to a multi-decadal or even centennial time scale.

4.2 Analysis of fossil *A. islandica* and *P. rustica*

In both the fossil *A. islandica* (ID: AI-CoCr-01) and the fossil *P. rustica* (ID: RGM609.096) shell, the two commonly used techniques Mutvei staining and FL failed to visualize the complete shell growth pattern (Figures 5c–5f). The very low contrast of the preparations rendered it impossible to identify and measure increments in the ontogenetically oldest parts of the shells (Figures 3–5). Regarding the Mutvei treatment, even the extension of the exposure duration from 23 minutes to up to 60 minutes did not result in improved contrast. This finding confirms Schöne et al. (2005a), who state that Mutvei´s solution results in lighter shadings of blue in fossil material. Schöne et al. (2005a) hypothesize that the low contrast in fossil specimens might be associated with diagenetic alteration of the shell material. However, CRM analysis indicates that the measured shell material consist solely of aragonite. Hence, a strong diagenetic alteration, resulting in the transformation of aragonite into the more stable polymorph calcite (e.g., Maliva and Dickson, 1992), can be excluded. However, taphonomic alteration processes might have led to reduced amounts of polysaccharides in the fossil shell material (c.f., Schöne et al., 2005a) being a more likely explanation of the weaker effect of the Mutvei treatment on fossil shells.

So far, we do not fully understand the cause-and-effect mechanisms that underlie the extraordinarily good performance of CRM in fossil carbonate shell material. All three methods tested here rely in some way on the organic content of the shell. Since detailed studies of the organic composition of mollusc shells such as *A. islandica* and *P. rustica* are lacking, we cannot say which specific chemical compounds cause the fluorescence in FL and CRM. Scenarios with increasing organic composition (c.f., Wanamaker Jr et al., 2009; Karney et al., 2011) or mineralization (as described in Karney et al. (2011) for an elevated backscattered signal) prior to or

during the formation of growth lines seem plausible. Both Mutvei staining and FL performed poorly when applied to fossil shell material, most likely owing to the decay and loss of shell organic compounds over time. In contrast to Mutvei staining and FL, CRM mapping seems to be able to visualize organic-related shell structures even after the original organic components have already been strongly altered.

4.3 Potential of CRM in sclerochronology

4.3.1 Advantages and limitations of CRM

We show that confocal Raman microscopy (CRM) can visualize internal growth patterns in both modern and fossil biogenic carbonate structures, showing a performance as good or even better than the established methods Mutvei staining and FL. Compared to established methods, CRM mapping offers a unique combination of features that make it the most versatile approach:

(1) CRM analysis does not require chemical sample (pre-) treatment, i.e., the shell surface is neither contaminated nor destructed. This is in contrast to Mutvei staining, acetate peels (surface etching) and BSE (sputtering with carbon, gold or platinum), which modify the shell to enhance visibility of the micro-structures. Furthermore, no toxic/hazardous chemicals are involved such as glutaraldehyde (a respiratory toxin) and alcian blue in Mutvei´s solution. Consequently, shell cross-sections analyzed by CRM can be used for subsequent geochemical analysis (e.g., stable isotopes or trace/ minor elements as shown in Nehrke et al., 2012).

(2) The CRM mapping area is large. Larger areas can be scanned consecutively (by moving the sample) and maps can be stitched (to a mosaic) afterwards.

(3) CRM analysis can be conducted with high spatial resolution (down to several hundred nm), allowing the detection and identification of even finest growth structures (Figure 6). This is especially advantageous in the study of sub-annual variability.

Nevertheless, CRM has some limitations, too:

(1) The confocal Raman microscope represents a relatively expensive instrument that may not yet be available easily.

(2) Depending on scan area, resolution and integration time, a single scan can take several hours. Hence, at the current technical level, CRM mapping may not become

the standard tool for growth increment analysis, but may serve best in cases where standard methods fail.

(3) Caution is advised when exposing organic-rich samples to a laser source. Repeated measurements may dampen the Raman signal significantly. Furthermore, shell coatings such as polyvinyl alcohol (PVA) might burn when exposed to a monochromatic light source.

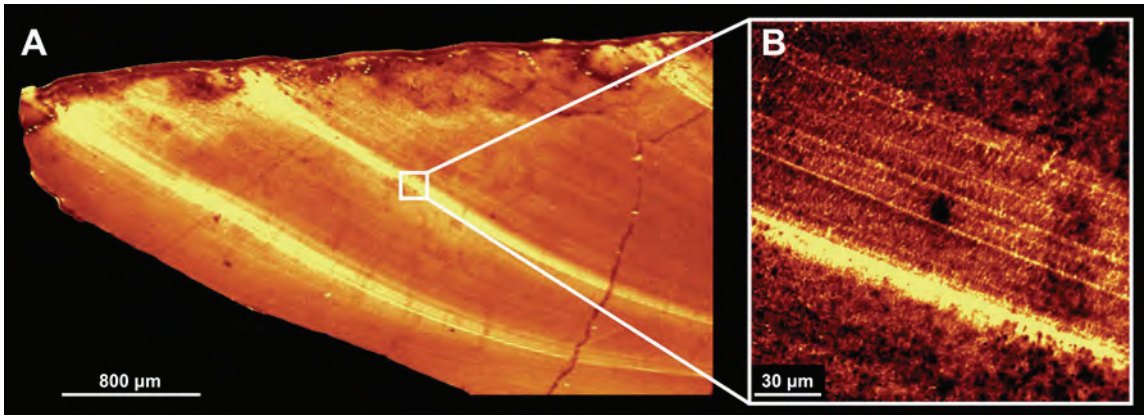

Figure 6. CRM maps of ventral shell margin in fossil *A. islandica* specimen AI-StRi2-BK1b. (A) CRM map using a 20x magnification and showing two pronounced annual winter growth lines (yellow) at the (broken) ventral margin of the shell. (B) High-resolution CRM map of the area indicated in (A) using a 100x magnification and showing intra-annual growth patterns within a single winter line.

4.3.2 Check for diagenesis and contamination

A check for taphonomic alteration (e.g., recrystallization from pristine aragonite to secondary calcite) in marine biogenic carbonates should be a mandatory step prior to any kind of biogeochemical analysis such as stable isotopes or trace elemental ratios of fossil samples. Therefore, CRM mapping can play a crucial role in the quality control of biogenic carbonate studies. Nehrke et al. (2012) highlighted the potential of CRM mapping in the identification of three different calcium carbonate polymorphs in the hinge plate of a modern marine bivalve species from Antarctica. In combination with electron microprobe (EMP) analysis they were able to show that trace element incorporation differs with calcium carbonate polymorph (e.g., for magnesium and strontium). CRM may be helpful, too, in detecting contamination of shell material that might result from laboratory preparation (e.g., from glue or polishing residuals). Again, this check should be a mandatory step prior to any geochemical analysis.

5 Conclusions

In this study we show that CRM is a reliable and valuable tool to visualize internal growth patterns in modern (Figures 2, 5a and 5b) and fossil bivalve shell specimens of *A. islandica* (Figures 3, 5c, 5d and 6) and *P. rustica* (Figures 4, 5e and 5f). CRM performs as good as established methods (Mutvei staining and FL) in modern shells. Therefore, CRM based growth data are considered suitable for cross-dating applications, such as those used to compile master chronologies from multiple specimen archives. Regarding fossil shells, CRM reveals growth patterns where established methods fail, thus enabling a much more precise record of annual and even sub-annual growth increments (Figure 6) and the interpretation of their palaeo-environmental information (Figures 5d and 5f). Furthermore, CRM constitutes an alternative non-destructive approach (as described for FL in Wanamaker Jr et al., 2009) that does not required any pre-treatment of the shell cross-section and makes the preparation of a second cross section for geochemical analysis redundant.

We strongly recommend the use of CRM in samples where further geochemical analysis will be undertaken and as the best technique available for the imaging of annual growth increments in fossil bivalve shells. We emphasize that CRM should be considered a powerful tool for assessing the absence or degree of diagenetic alteration in sub-fossil and fossil carbonate shell specimens prior to any geochemical analysis.

6 Outlook

Future studies based on CRM mapping in sclerochronology should test for the potential to utilize high-resolution scans as shown in Figure 6 to visualize (daily or tidal) micro-increments (Schöne et al., 2005c). The role and function of polyenes and pigments in the biomineralization processes of modern and sub-fossil mollusc specimens needs to be better understood and their potential in terms of visualization of internal growth patterns needs to be tested. The method described here should also be applied to *A. islandica* specimens of older ontogenetic ages (100+ years), in the ventral portion of the shell and combined with studies on the organic content of *A. islandica* to decipher the origin of fluorescence variability. Application of this technique on additional mollusc taxa, both modern and fossil, and on non-carbonate palaeo-archives such as modern and fossil biogenic apatites (bones and teeth) or

speleothems should be undertaken to fully test and exploit the potential of this versatile tool in archaeology and geosciences, as well as in climate-related proxy reconstructions.

Acknowledgments

The first author (LB) was financed by the “Earth System Science Research School (ESSReS)”, an initiative of the Helmholtz Association of German Research Centres (HGF) at the Alfred Wegener Institute (AWI), Helmholtz Centre for Polar and Marine Research. We would like to thank Peter E. Long (University of Leicester), Daniele Scarponi, Sergio Raffi (both University of Bologna) and Frank Wesselingh (Naturalis Museum, Leiden) for providing the shell material. Further thanks to Rosie Sheward (NOC, Southampton) for suggestions that improved the written quality of the manuscript.

Shell ID	Species	Ontogenetic age (years)	Locality	Epoch / Stage / Age	Collected in	Shell provider
Ai1276R	*A. islandica*	65	Tromsø, Norway	Modern	2006	S. Begum (AWI Bremerhaven)
AI-CoCr-01	*A. islandica*	31	Sudbourne Park Pit, UK	Pliocene / Coralline Crag / Ramsholt Member	1974/1975	P. E. Long (Univ. of Leicester)
AI-StRi-BK1b	*A. islandica*	*not determined*	Stirone River, Italy	Pleistocene / Middle Calabrian	2011	D. Scarponi, S. Raffi (Univ. of Bologna)
RGM609.096	*P. rustica*	17	Antwerp, Belgium	Pliocene / Piacenzian / Lillo Formation, Oorderen Member	1958	F. Wesselingh (Naturalis, Leiden)

Table 1. Modern and fossil shell specimens analyzed in this study.

References

(Please note that references have been formatted according to style of journal)

Barnard, W., and D. de Waal (2006), Raman investigation of pigmentary molecules in the molluscan biogenic matrix, *Journal of Raman Spectroscopy*, *37*, 342–352.

Beierlein, L., O. Salvigsen, B. R. Schöne, A. Mackensen, and T. Brey (2014), The seasonal water temperature cycle in the Arctic Dicksonfjord (Svalbard) during the Holocene Climate Optimum derived from sub-fossil *Arctica islandica* shells, *The Holocene*, *(accepted for print, with minor revisions)*.

Bosch, J., and F. Wesselingh (2006), On the stratigraphic position of the Delden Member (Breda Formation, Overijssel, the Netherlands) with implications for the taxonomy of *Pygocardia* (Mollusca, Bivalvia), *Cainozoic Research*, *4*, 109–117.

Brey, T., M. Voigt, K. Jenkins, and I.-Y. Ahn (2011), The bivalve *Laternula elliptica* at King George Island – A biological recorder of climate forcing in the West Antarctic Peninsula region, *Journal of Marine Systems*, *88*, 542–552.

Brocas, W. M., D. J. Reynolds, P. G. Butler, C. A. Richardson, J. D. Scourse, I. D. Ridgway, and K. Ramsay (2013), The dog cockle, *Glycymeris glycymeris* (L.), a new annually-resolved sclerochronological archive for the Irish Sea, *Palaeogeography, Palaeoclimatology, Palaeoecology, 373*, 133–140.

Burchell, M., A. Cannon, N. Hallmann, H. P. Schwarcz, and B. R. Schöne (2013), Inter-site variability in the season of shellfish collection on the central coast of British Columbia, *Journal of Archaeological Science, 40*, 626–636.

Butler, P. G., A. D. Wanamaker Jr, J. D. Scourse, C. A. Richardson, and D. J. Reynolds (2013), Variability of marine climate on the North Icelandic Shelf in a 1357-year proxy archive based on growth increments in the bivalve *Arctica islandica*, *Palaeogeography, Palaeoclimatology, Palaeoecology*, *373*, 141–151.

Butler, P. G., C. A. Richardson, J. D. Scourse, A. D. Wanamaker Jr, T. M. Shammon, and J. D. Bennell (2010), Marine climate in the Irish Sea: analysis of a 489-year marine master chronology derived from growth increments in the shell of the clam *Arctica islandica*, *Quaternary Science Reviews*, *29*, 1614–1632.

Carroll, M. L., W. G. Ambrose Jr, B. S. Levin, S. K. Ryan, A. R. Ratner, G. A. Henkes, and M. J. Greenacre (2011), Climatic regulation of *Clinocardium ciliatum* (bivalvia) growth in the northwestern Barents Sea, *Palaeogeography, Palaeoclimatology, Palaeoecology*, *302*, 10–20.

Dahlgren, T. G., J. R. Weinberg, and K. M. Halanych (2000), Phylogeography of the ocean quahog (*Arctica islandica*): influences of paleoclimate on genetic diversity and species range, *Marine Biology*, *137*, 487–495.

DeLong, K. L., T. M. Quinn, and F. W. Taylor (2007), Reconstructing twentieth-century sea surface temperature variability in the southwest Pacific: A replication study using multiple coral Sr/Ca records from New Caledonia, *Paleoceanography*, *22*, PA4212.

Hald, M., C. Andersson, H. Ebbesen, E. Jansen, D. Klitgaard-Kristensen, B. Risebrobakken, G. R. Salomonsen, M. Sarnthein, H. P. Sejrup, and R. J. Telford (2007), Variations in temperature and extent of Atlantic Water in the northern North Atlantic during the Holocene, *Quaternary Science Reviews*, *26*, 3423–3440.

Halfar, J., R. S. Steneck, M. Joachimski, A. Kronz, and A. D. Wanamaker (2008), Coralline red algae as high-resolution climate recorders, *Geology*, *36*, 463–466.

Hallmann, N., M. Burchell, N. Brewster, A. Martindale, and B. R. Schöne (2013), Holocene climate and seasonality of shell collection at the Dundas Islands Group, northern British Columbia, Canada – A bivalve sclerochronological approach, *Palaeogeography, Palaeoclimatology, Palaeoecology, 373*, 163–172.

Hedegaard, C., J.-F. Bardeau, and D. Chateigner (2006), Molluscan Shell Pigments: An In Situ Resonance Raman Study, *Journal of Molluscan Studies*, *72*, 157–162.

Karney, G. B., P. G. Butler, J. D. Scourse, C. A. Richardson, K. H. Lau, J. T. Czernuszka, and C. R. M. Grovenor (2011), Identification of growth increments in the shell of the bivalve mollusc *Arctica islandica* using backscattered electron imaging, *Journal of microscopy*, *241*, 29–36.

Karney, G. B., P. G. Butler, S. Speller, J. D. Scourse, C. A. Richardson, M. Schröder, G. M. Hughes, J. T. Czernuszka, and C. R. M. Grovenor (2012), Characterizing the microstructure of *Arctica islandica* shells using NanoSIMS and EBSD, *Geochemistry, Geophysics, Geosystems*, *13*, Q04002.

Maliva, R. G., and J. A. D. Dickson (1992), The mechanism of skeletal aragonite neomorphism: evidence from neomorphosed mollusks from the upper Purbeck Formation (Late Jurassic-Early Cretaceous), southern England, *Sedimentary Geology*, *76*, 221–232.

Nehrke, G., and J. Nouet (2011), Confocal Raman microscope mapping as a tool to describe different mineral and organic phases at high spatial resolution within marine biogenic carbonates: case study on *Nerita undata* (Gastropoda, Neritopsina), *Biogeosciences*, *8*, 3761–3769.

Nehrke, G., H. Poigner, D. Wilhelms-Dick, T. Brey, and D. Abele (2012), Coexistence of three calcium carbonate polymorphs in the shell of the Antarctic clam *Laternula elliptica*, *Geochemistry, Geophysics, Geosystems*, *13*, Q05014.

Perez-Huerta, A., M. F. Etayo-Cadavid, C. F. T. Andrus, T. E. Jeffries, C. Watkins, S. C. Street, and D. H. Sandweiss (2013), El Niño Impact on Mollusk Biomineralization – Implications for Trace Element Proxy Reconstructions and the Paleo-Archeological Record, *PLOS ONE*, *8*, e54274.

Petit, J. R., J. Jouzel, D. Raynaud, N. I. Barkov, J.-M. Barnola, I. Basile, M. Bender, J. Chappellaz, M. Davisk, G. Delaygue, M. Delmotte, V. M. Kotlyakov, M. Legrand, V. Y. Lipenkov, C. Lorius, L. Pepin, C. Ritz, E. Saltzmank, and M. Stievenard (1999), Climate and atmospheric history of the past 420,000 years from the Vostok ice core, Antarctica, *Nature*, *399*, 429–436.

Raman, C. V., and K. S. Krishnan (1928), A new type of secondary radiation, *Nature*, *121*, 501–502.

Richardson, C. A. (2001), Molluscs as archives of environmental change, *Oceanography and Marine Biology: an Annual Review*, *39*, 103–164.

Ropes, J. W. (1987), Preparation of acetate peels of valves from the ocean quahog, *Arctica islandica*, for age determinations, *NOAA Technical Report NMFS*, *50*, 1–5.

Ropes, J. W., D. S. Jones, S. A. Murawski, F. M. Serchuk, and A. Jearld Jr (1984), Documentation of annual growth lines in ocean quahogs, *Arctica islandica* Linné, *Fishery Bulletin*, *82*, 1–19.

Schöne, B. R. (2013), *Arctica islandica* (Bivalvia): A unique paleoenvironmental archive of the northern North Atlantic Ocean, *Global and Planetary Change*, *111*, 199–225.

Schöne, B. R., and J. Fiebig (2009), Seasonality in the North Sea during the Allerød and Late Medieval Climate Optimum using bivalve sclerochronology, *International Journal of Earth Sciences*, *98*, 83–98.

Schöne, B. R., E. Dunca, J. Fiebig, and M. Pfeiffer (2005a), Mutvei's solution: An ideal agent for resolving microgrowth structures of biogenic carbonates, *Palaeogeography, Palaeoclimatology, Palaeoecology*, *228*, 149–166.

Schöne, B. R., N. Page, D. Rodland, J. Fiebig, S. Baier, S. Helama, and W. Oschmann (2007), ENSO-coupled precipitation records (1959–2004) based on shells of freshwater bivalve mollusks (*Margaritifera falcata*) from British Columbia, *International Journal of Earth Sciences*, *96*, 525–540.

Schöne, B. R., J. Fiebig, M. Pfeiffer, R. Gle, J. Hickson, A. L. A. Johnson, W. Dreyer, and W. Oschmann (2005b), Climate records from a bivalved Methuselah (*Arctica islandica*, Mollusca; Iceland), *Palaeogeography, Palaeoclimatology, Palaeoecology*, *228*, 130–148.

Schöne, B. R., S. D. Houk, A. D. Freyre Castro, J. Fiebig, W. Oschmann, I. Kröncke, W. Dreyer, and F. Gosselck (2005c), Daily growth rates in shells of *Arctica islandica*: Assessing sub-seasonal environmental controls on a long-lived bivalve mollusk, *Palaios*, *20*, 78–92.

Smith, E., and G. Dent (Eds.) (2005), Modern Raman Spectroscopy – A Practical Approach, John Wiley, Hoboken, N. J., pp. 201.

Stemmer, K., and G. Nehrke (2014), The distribution of polyenes in the shell of *Arctica islandica* from North Atlantic localities: A confocal Raman microscopy study, *Journal of Molluscan Studies*, doi:10.1093/mollus/eyu033.

Wall, M., and G. Nehrke (2012), Identification of two organic bands showing different chemical composition within the skeleton of *Porites lutea*: a confocal Raman microscopy study, *Biogeosciences Discussions*, *9*, 8273–8306.

Wanamaker Jr, A. D., A. Baker, P. G. Butler, C. A. Richardson, J. D. Scourse, I. Ridgway, and D. J. Reynolds (2009), A novel method for imaging internal growth patterns in marine mollusks: A fluorescence case study on the aragonitic shell of the marine bivalve *Arctica islandica* (Linnaeus), *Limnology And Oceanography: Methods*, *7*, 673–681.

Webb, G. E., G. J. Price, L. D. Nothdurft, L. Deer, and L. Rintoul (2007), Cryptic meteoric diagenesis in freshwater bivalves: Implications for radiocarbon dating, *Geology*, *35*, 803–806.

Wehrmeister, U., D. E. Jacob, A. L. Soldati, N. Loges, T. Häger, and W. Hofmeister (2010), Amorphous, nanocrystalline and crystalline calcium carbonates in biological materials, *Journal of Raman Spectroscopy*, *42*, 926–935.

Manuscript III

From aragonite to calcite: Impacts of recrystallization on stable isotope ($\delta^{18}O$ & $\delta^{13}C$) composition of the commonly used bio-archive *Arctica islandica*

Lars Beierlein[1], Thomas Brey[1], Gernot Nehrke[1], Bernd R. Schöne[2], Torsten Bickert[3] and Andreas Mackensen[1]

[1]Alfred Wegener Institute Helmholtz Centre for Polar and Marine Research, Bremerhaven, Germany

[2]Institute of Geosciences, University of Mainz, Germany

[3]MARUM, University of Bremen, Germany

Manuscript in preparation (To be submitted to *Palaeogeography, Palaeoclimatology, Palaeoecology*).

Abstract

The bivalve *Arctica islandica* is a commonly used biogenic archive for reconstructing past environmental conditions. Stable oxygen isotopes ($\delta^{18}O$) values from the shells of well-preserved *A. islandica* specimens are a frequently used proxy for water temperatures (and salinity), recording ambient environmental conditions at exceptionally high-resolution (up to sub-seasonal scale). This species therefore has significant potential to improve our understanding of seasonal temperature dynamics in the past.

We present the first stable isotope ($\delta^{18}O$ & $\delta^{13}C$) analysis on a fossil semi-recrystallized *A. islandica* shell from the Tjörnes Beds of Iceland (Pliocene). Confocal Raman microscopy is used to identify areas of pristine aragonite and recrystallized calcite shell, which were then sampled by high-resolution micro-milling. Stable oxygen isotope values from both recrystallized and non-recrystallized portions of the shell are used to calculate palaeo-water temperatures to highlight and discuss the impacts of taphonomic alterations on a micro-scale and its implications for palaeo-environmental reconstructions. We stress the need for careful interpretation of carbonate-based water temperature reconstructions, as small-scale diagenesis can significantly modify the original stable oxygen isotopes and substantially distort the derived palaeo-climatic or palaeo-environmental signals.

Keywords: sclerochronology, *Arctica islandica*, neomorphism, recrystallization, biogenic calcium carbonate.

1 Introduction

Bivalve shells are very important archives of palaeo-environmental and palaeo-climatic information (Richardson, 2001; Schöne, 2013). *Arctica islandica* (Bivalvia) is a commonly used biogenic archive (Schöne, 2013) due to its exceptional longevity of up to 500 years (Butler et al., 2013) and its broad distribution throughout the North Atlantic (Dahlgren et al., 2000). Reconstructions of past climatic conditions can be assembled from the internal growth record of the shell (i.e., individual growth increment width). Through this technique, *A. islandica* shells have enabled the reconstruction of ocean-atmosphere phenomena, such as the North Atlantic Oscillation (Schöne et al., 2003; Wanamaker Jr et al., 2009).

A. islandica shells also record environmental information as a geochemical proxy in the form of stable oxygen isotope values ($\delta^{18}O_{shell}$; e.g., Schöne et al., 2004; Beierlein et al., 2014). Oxygen isotopes (^{16}O, ^{18}O) are incorporated into the shell carbonate in equilibrium with the ambient water (Schöne, 2013). If the oxygen isotope composition of the ambient water ($\delta^{18}O_{seawater}$) is known, the $\delta^{18}O_{shell}$ can be used for the reconstruction of absolute water temperatures for the water mass and depth at which the organism lived (e.g., Schöne and Fiebig, 2009). This presents a challenge when working with sub-fossil and fossil specimens, as $\delta^{18}O_{seawater}$ must be estimated instead of directly measured, providing potentially larger error susceptibility. This species is one of the few that records exceptionally high-resolution proxies, up to sub-seasonal scale and therefore has significant potential to improve our understanding of seasonal temperature dynamics in the past. Therefore it is of greatest importance that, despite the necessary estimation of past $\delta^{18}O_{seawater}$, we fully utilise the environmental records incorporated into these shells.

A. islandica shells comprise of three layers, all of which are the metastable polymorph of calcium carbonate ($CaCO_3$) aragonite (Schöne, 2013). The outer shell layer is used for isotopic analysis in palaeo-environmental studies. More information on shell formation and growth can be found in Ropes et al. (1984) and Schöne (2013). A crucial primary step in the use of sub-fossil (up to 10,000 years old) or fossil shells prior to geochemical analysis should be a precise and detailed examination of their state of preservation. Taphonomic and diagenetic processes, triggered by exposure to pressure, heat and/or hydrothermal fluids over time (i.e., when exposed to meteoric vadose and phreatic conditions; c.f., Wardlaw et al., 1978) can cause the shell aragonite to recrystallize to the more stable polymorph calcite (Bathurst, 1964), as can

also be observed in limestone (Friedman, 1964; Folk, 1965) and speleothems (Folk and Assereto, 1976; Zhang et al., 2014).

Subsequent to this recrystallization process, two scenarios can occur: the original C and O atoms remain present in their original isotopic proportions or an exchange occurs, where the original C and/or O atoms are substituted with atoms from solutions or gases. The latter scenario results in a change in isotopic composition, whereby it no longer characterises the original environmental conditions at the time of shell formation (c.f., Hudson, 1977). The transition from aragonite to calcite can occur through two main processes. Solid diffusion, which is a very slow process and requires temperatures of 200°C, is rather unlikely to be the cause of recrystallization in shell material (Fyfe and Bischoff, 1965; Anderson, 1969; Hudson, 1977). It is more likely that the recrystallization involves a solution followed by re-precipitation along a thin solution film of less than 10 nm (e.g., Wardlaw et al., 1978) and no substantial voids produced (e.g., Martin et al., 1986). This assumed solution film however has to our knowledge never been observed and remains a theoretical construct. In general, if the effective water-to-rock ratio is high, the system is seen as 'open', resulting in solution-precipitation and isotopic reorganization. This newly precipitated carbonate will not have the same isotopic composition as the proto-carbonate and the oxygen isotopic composition of recrystallized carbonate will reflect the ambient conditions during transformation, rather than the environmental conditions during (shell) formation (c.f., Tan and Hudson, 1974; Hudson, 1977). Assessment of the degree of recrystallization in each specimen is therefore essential to confirm that the isotopic record in the shell material is the original, primary environmental signal that is sought for palaeo-climatic reconstruction.

Previous studies on carbonates (Machel, 1997) and mollusc shells (Kendall, 1975; Wardlaw et al., 1978; Hendry et al., 1995) have used and coined the term 'neomorphism' to describe all important aspects relating to carbonate recrystallization. To our knowledge however, there is a severe lack of acknowledgement and discussion in literature regarding ‘neomorphism’ in more recent sclerochronological studies that use carbonate archives such as bivalve shells and corals. The community must ensure that steps are taken to assess the degree of ‘neomorphism’ in specimens assigned for (bio)geochemical analysis in order to guarantee that isotope analysis is preferentially performed on material that has not undergone any recrystallization for the most accurate results. Although it is commonly agreed that recrystallized shell material can still yield highly useful information for many aspects of geology (Hudson, 1977), it has

not been shown the extent to which these recrystallization processes influence the isotopic composition ($\delta^{18}O$ & $\delta^{13}C$) in *A. islandica*, which is frequently used for palaeo-reconstructions based on isotope analysis.

Here we present the first stable isotope ($\delta^{18}O$ & $\delta^{13}C$) analysis on a fossil semi-recrystallized *A. islandica* shell from the Tjörnes Beds of Iceland (Pliocene). Confocal Raman microscopy is used to identify pristine aragonite and recrystallized calcite shell portions, which were then sampled by high-resolution micro-milling and drilling. Stable oxygen isotope values from both recrystallized and non-recrystallized portions of the shell are then used to calculate palaeo-water temperatures to discuss and highlight the impacts of taphonomic alterations on a micro-scale and its implications for palaeo-environmental reconstructions based on this versatile, high-resolution biogenic proxy.

2 Materials and Methods

2.1 Shell origin and shell preparation in the laboratory

The *A. islandica* shell specimen (ID: AI-TjBe-01) analysed in this study was collected in summer 2011 from Hallbjarnarstaðakambur, Iceland. Biostratigraphy dates the Tjörnes Beds layers within which it was situated to 3.5 Ma. The specimen was found with both shell valves articulated and the internal cavity is filled with sediment and blocky, amber-coloured secondary calcite (Figure 1). Since *A. islandica* is a well-calibrated archive and it is known that oxygen isotopes are incorporated in equilibrium with the ambient seawater (Schöne, 2013), anomalies in the isotopic composition or temperature reconstructions can be linked directly to 'neomorphism', as metabolic effects can be excluded as an explanation.

The shell specimen was embedded whole within epoxy resin to prevent it from breaking during the sawing process. After setting the resin for 24 h in a dry oven at about 40°C it was cut along the line of strongest growth (LSG), perpendicular to the growth lines using a water-cooled geological rock cutting saw. Three cuts resulted in two thick-sections of about 3 cm thickness. The inner sides (i.e., the surface towards the LSG) of both the thick-sections were then ground using a manual grinder (Buehler, Phoenix Alpha) and sand paper with three different grain sizes (15 µm, 10 µm and 5 µm).

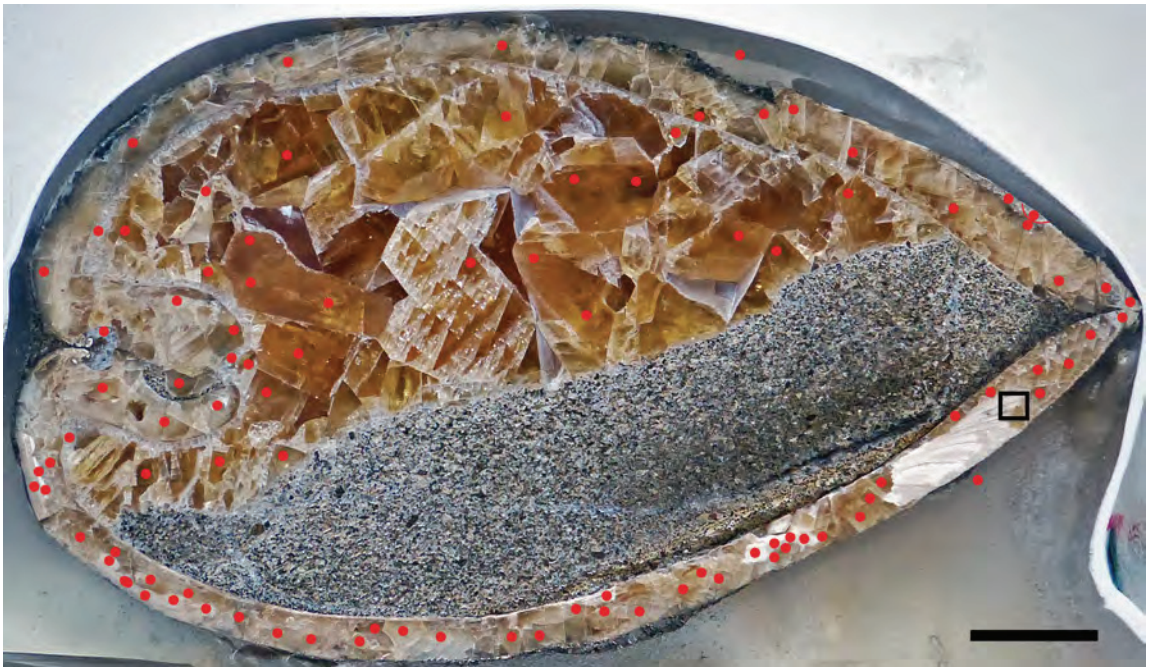

Figure 1. Thick-section of *A. islandica* specimen AI-TjBe-01 from the Tjörnes Beds, Iceland. Shell has been embedded in epoxy resin (transparent surrounding at outer edges) to prevent the shell from damage during the sawing process. Both shells are still articulated, while the internal cavity has been filled with sediment (grey in the lower cavity half) and secondary blocky crystals (amber coloured in the upper part), which have been identified as calcite based on CRM analysis (Section 3.1). Shell mainly consists of amber coloured crystals (calcite; c.f., Section 3.1) with white patches of aragonite. Red dots give locations for isotopes samples taken by drilling. Black square gives location for CRM map shown in Figure 2. Adjacent area is used for isotope milling approach (Section 3.2.1) and shown with higher magnification in Figure 4. Scale bar is 1 cm.

2.2 Check for recrystallization: Confocal Raman microscopy

We use a confocal Raman microscope (CRM) (WITec alpha 300 R), equipped with a diode laser (excitation wavelength 152 nm) and a 20x Zeiss objective to examine the mineralogy of the shell. Instrumental settings and procedure follow Nehrke et al. (2012). Single spot measurements (i.e., single spectrum analysis) and Raman maps (c.f., Nehrke and Nouet, 2011; Wall and Nehrke, 2012; Stemmer and Nehrke, 2014; Beierlein et al., 2014) have been used to identify different mineral phases in the shells and in the internal cavity in order to distinguish polymorphs of calcium carbonate (c.f., Nehrke et al., 2012).

2.3 Stable isotope ($\delta^{18}O$ & $\delta^{13}C$) measurements: drilling & milling

Carbonate samples were taken manually by drilling (in spots indicated by red dots in Figure 1) in order to verify the entire range of isotopic variability within the shell and infilled secondary calcite material. Milling samples were also taken (along the transect

in Figure 4a) to assess the impact of recrystallization through the direct transition from calcite to aragonite (Dettman and Lohmann, 1995). Drill and mill bits were mounted onto an industrial high precision drill (Minimo C121, Minitor Co., Ltd.) and attached to a binocular microscope. Stable isotope measurements of carbon and oxygen were conducted on a Thermo Finnigan MAT 253 isotope ratio mass spectrometer coupled with an automated carbonate preparation device (Kiel IV). Measurements were calibrated against the international NBS-19 standard and reported in δ-notation versus VPDB (Vienna Peedee Belemnite). The long-term precision of this instrumentation based on an internal laboratory standard (Solnhofen limestone) measured over a one-year period together with samples was better than ±0.08‰.

$\delta^{18}O_{shell}$ values are influenced by both ambient water temperature and changes in global ice volume (Beierlein et al., 2014). Therefore changes in ice volume over geological timescales must be considered when calculating palaeo-temperatures from fossil shell carbonate. Our reconstructed palaeo-temperatures for 194 individual samples from the milling approach (Figure 1) were calculated according to Dettman et al. (1999) and based on Grossman and Ku (1986) for aragonite (see Section 4.4 for discussion and potential temperatures derived for this approach). We applied a $\delta^{18}O_{seawater}$ value range from −0.2‰ to −0.5‰ following Buchardt and Simonarson (2003) in order to guarantee comparability between our results and those previously published, and to provide an error estimate.

3 Results

3.1 Check for recrystallization: Confocal Raman microscopy

Single spot CRM spectra were used to identify amber-coloured blocky crystals (Figure 1) as calcite and white patches within the shells as aragonite. Further, this information was used to divide all measurements taken by the drilling approach (red dots in Figure 1) into four categories for further analysis and distinction (Section 3.2) – secondary calcite filling; calcite shell; mixed zone (aragonite & calcite); aragonite (c.f., Section 3.2 and Figure 3). Aragonite and calcite occur in direct contact within the shell, as can be seen in Figure 2. Reflected-light microscopy (Figure 2a) identifies white shell areas with visible shell growth patterns and darker homogeneous shell areas (here dark blue,

amber-coloured in Figure 1). CRM mapping (c.f., Nehrke and Nouet (2011) for detailed explanation on method) has been used to visualize aragonitic areas (Figure 2b) and calcitic (Figure 2c) areas within the shell. The carbonate polymorphs growth structure become visible in both aragonite (blue) and calcite (red) areas when all spectral information is used to compile a stacked image (Figure 2d).

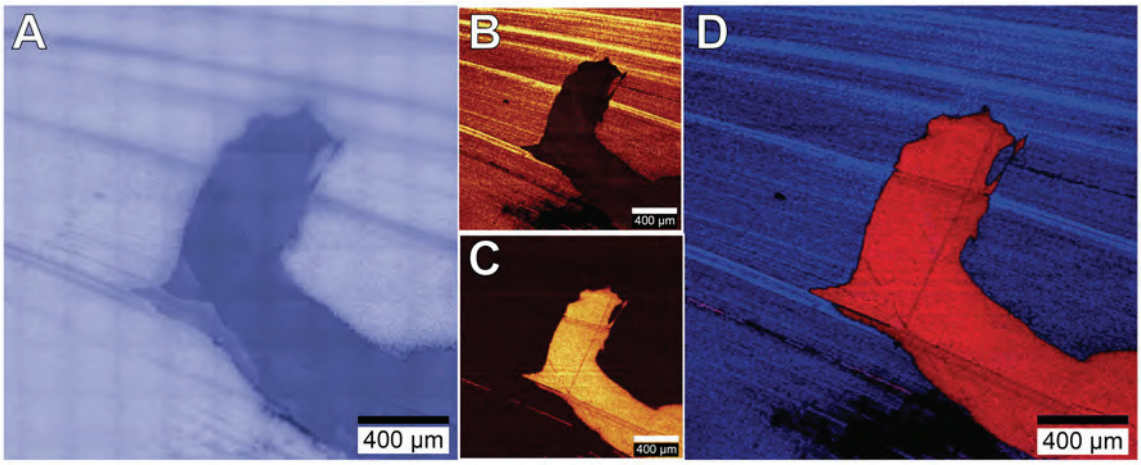

Figure 2. Shell section as indicated by black square in Figure 1 shown by reflected-light microscopy (a) and means of CRM analysis (b-d). Raman map solely visualizing aragonite-derived information (b) and calcite-derived information is used to create stacked information (d) showing entire spectral information with aragonite in blue and calcite in red. Note that aragonitic as well as calcitic parts in CRM maps (c and d) show shell growth lines.

3.2 Stable isotope ($\delta^{18}O$ & $\delta^{13}C$) measurements

3.2.1 Stable isotope ($\delta^{18}O$ & $\delta^{13}C$) measurements drilling

Based on the division into four categories (secondary calcite filling, calcite shell, mixed zone and aragonite), results for 80 out of the 96 single spot stable isotope drilling approach have been plotted by colour (c.f., Figure 3). For $\delta^{13}C$, a maximum value of 2.13‰ and a minimum value of −16.37‰ were measured. For $\delta^{18}O$, a maximum value of 1.21‰ and a minimum value of −17.20‰ have been measured. The most negative $\delta^{18}O$ values and negative $\delta^{13}C$ values are found in the secondary calcite filling the internal cavity (Figure 3; c.f., Figure 1). $\delta^{13}C$ values within the shell are predominantly negative, while $\delta^{18}O$ values are slightly more positive than for the filling calcite. Mixed zone values (i.e., values that could not be reliably associated to calcite or aragonite) understandably result in a wide range of both $\delta^{18}O$ and $\delta^{13}C$ values. Single spot measurements classified as aragonite show the most positive $\delta^{18}O$ and $\delta^{13}C$ values, varying by about 4‰ in both.

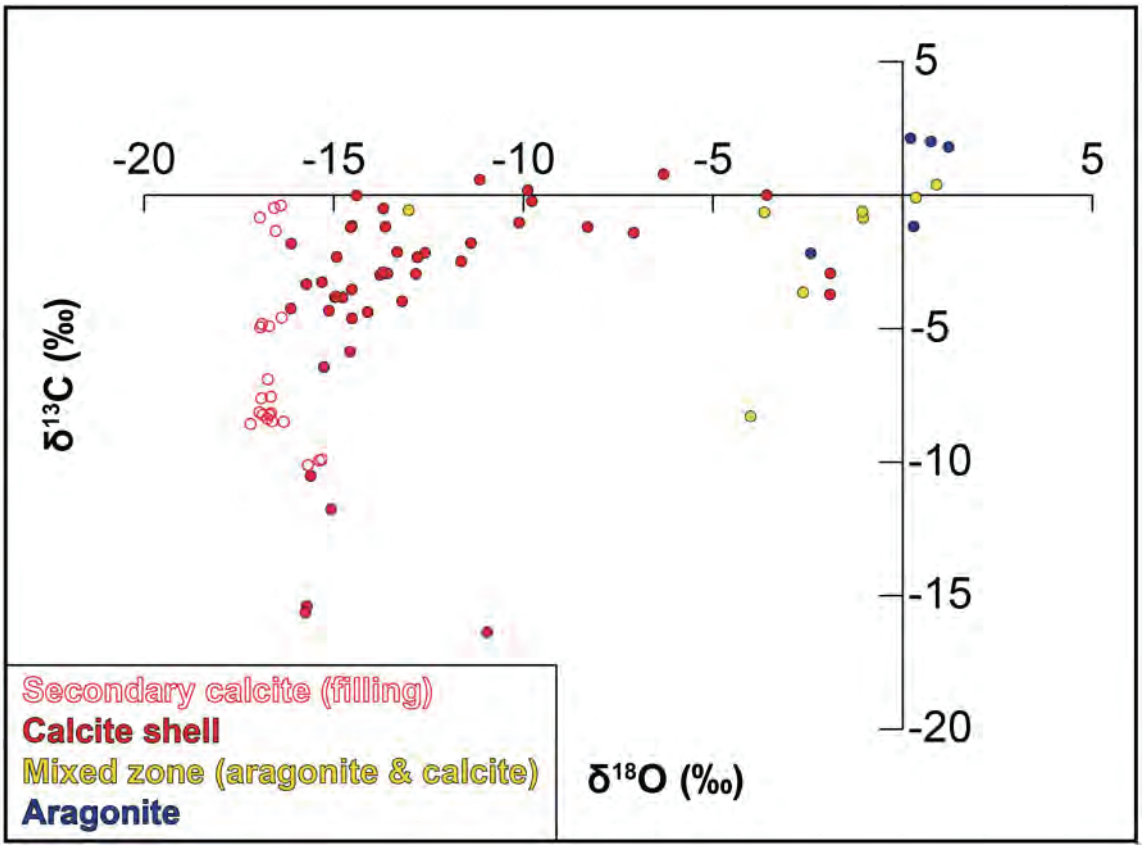

Figure 3. Results for stable isotope ($\delta^{18}O$ and $\delta^{13}C$) measurements taken by drilling in spots indicated in Figure 1. Division into four categories based on naked eye observations and CRM analysis (see text for explanation).

3.2.2 Stable isotope ($\delta^{18}O$ & $\delta^{13}C$) measurements milling

Measurements for the milling approach resulted in a maximum value of 2.35‰ and a minimum value of −11.42‰ for $\delta^{18}O$ within the indicated area in Figure 4a. For $\delta^{13}C$, a maximum value of 2.44‰ and a minimum value of −10.15‰ were measured. Based on the results of CRM analysis and naked eye observations during manual micro-milling, the entire section shown in Figure 4a has been divided into subsections (labelled from A to I) that represent three polymorph compositions – Subsection A is entirely calcitic, subsections B, C and I are mixed aragonite and calcite, and subsections D to H are entirely aragonitic.

Subsection A (entirely calcite) shows negative $\delta^{13}C$ values and the most negative $\delta^{18}O$ values observed in the transect, which in both cases is followed by an upward trend through subsections B and C (mixed) towards positive values of $\delta^{18}O$ and $\delta^{13}C$ (Figure 4). Subsections D to H show positive values for $\delta^{18}O$ and $\delta^{13}C$ throughout, with the exception of during the transitions between subsections E/F and

F/G. Both of these transitions are associated with a return to more negative values, with the most negative $\delta^{13}C$ values of the entire transect measured at the F/G transition. Towards subsection I (mix of aragonite and calcite) $\delta^{18}O$ values become negative again.

In general, this supports the observations in Hudson (1977) that carbon isotopes are likely to be less liable to diagenetic processes since the solutions circulating within sedimentary layers contain more O compared to C.

4 Discussion

4.1 Check for recrystallization: Confocal Raman microscopy

CRM has proven to be an ideal tool to identify preservational information on calcium carbonate polymorphs on a small spatial scale (few hundred nm), which is a precondition for any biogeochemical analysis (such as stable isotopes) undertaken on fossil shell material. Further, CRM is able to visualize growth structures in calcitic parts of the shell, which are not visible to the naked eye or through reflected-light microscopy. These 'ghost structures' (i.e., relict textures) have been reported repeatedly (Folk, 1965; Dodd, 1966; Sandberg and Hudson, 1983; Martin et al., 1986; Maliva et al., 2000) and are seen as an indicator for very slow (molecule for molecule) solution-precipitation transformation from aragonite to calcite in association with thin solution film (e.g., Wardlaw et al., 1978). It is most remarkable that these structures remain, considering that recrystallization involves solution and re-precipitation processes (e.g., Wardlaw et al., 1978) and that the transformation from aragonite to calcite is associated with an increase in volume by about 8% (e.g., Wardlaw et al., 1978). The depletion over time of organics within biogenic carbonates may account for this, as the volume increase fills in those gaps left by organic material. This may also explain why winter growth lines are especially pronounced under CRM, as they are organic-rich when formed and remain as an artefact in the re-precipitated calcite (Thompson and Chow, 1955).

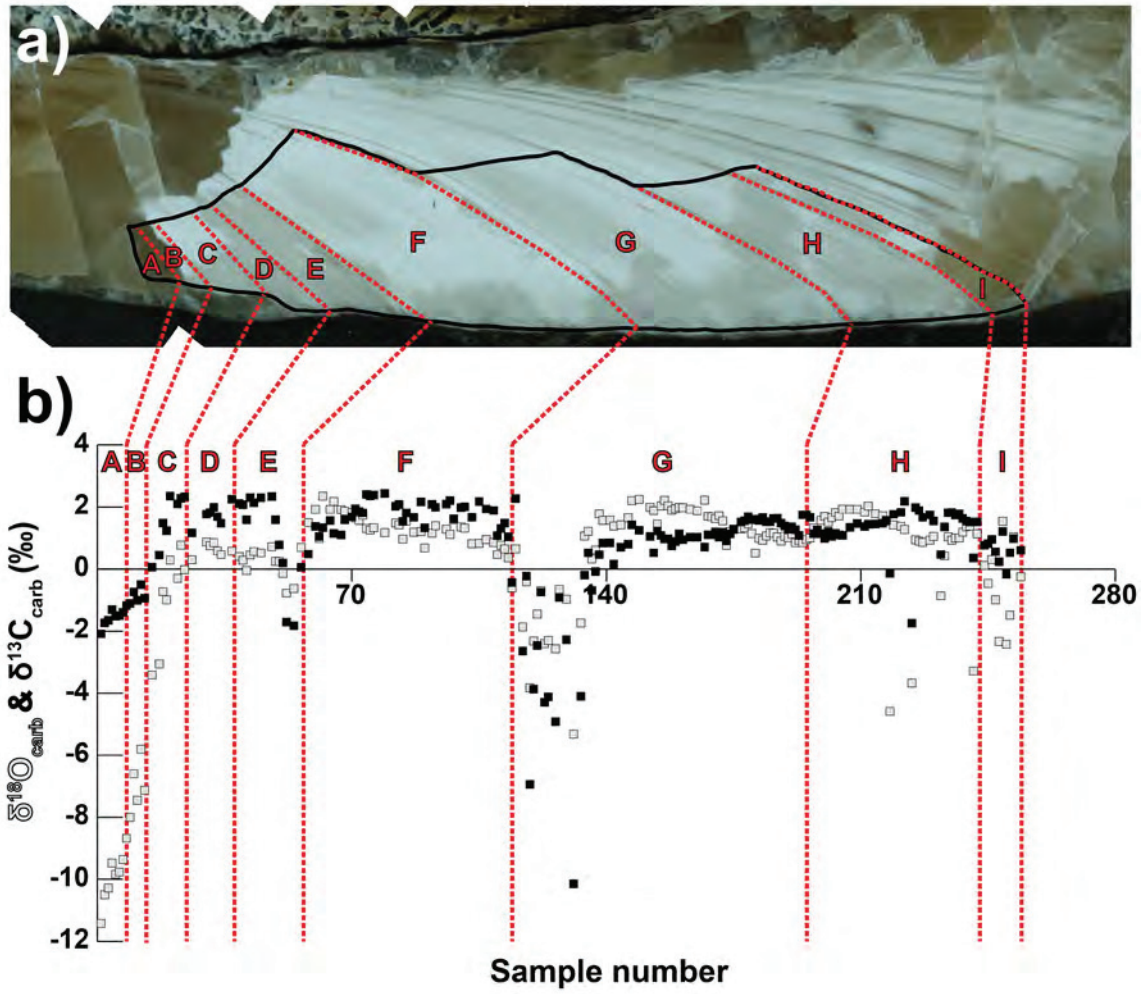

Figure 4. Transect for the micro-milling approach in *A. islandica* specimen AI-TjBe-01 (a), which has been subdivided into subsections A to I, based on polymorph composition (for description see text). Associated $\delta^{18}O$ and $\delta^{13}C$ values for 194 single measurements (b) both showing variability of more than 13‰.

4.2 Stable isotope ($\delta^{18}O$ & $\delta^{13}C$) measurements drilling

The blocky calcite of the cavity filling can be distinguished from the calcite in the recrystallized shell, as both $\delta^{18}O$ and $\delta^{13}C$ values are considerably more negative in cavity calcite. This most probably represents the end member and the isotopic composition of the circulating fluid from which this secondary calcite precipitated (Walderhaug and Bjorkum, 1992; Maliva, 1998). Since the shell and cavity calcite do not share exactly the same isotopic signature, it is likely that a small amount of the dissolved pristine aragonite has been mixed with the end member before re-precipitation. This argues for very different isotopic compositions of pristine shell carbonate compared to secondary calcite (i.e., different reservoirs) and therefore an open system.

$\delta^{18}O$ values as negative as −17.20‰ in the calcite parts argue that a meteoric water reservoir is the most likely origin of the recrystallized oxygen isotopes, since such negative values do not represent the isotopic signature of oceanic water (about 0‰) or any typical rock type (granite rocks as negative as −7‰; c.f., Hoefs, 1997). It is not possible to clarify the origin of the $\delta^{13}C$ signature in the calcite, as it shows similarities with known signatures from carbonatites, freshwater carbonates, atmospheric CO_2, marine and non-marine organisms and sedimentary organic material (e.g., coal, petroleum) (c.f., Hoefs, 1997). We assume that the isotopic values from the remaining aragonite represent the original shell signature and that the mixed zone is accordingly a mix of reservoir/end member calcite and pristine aragonite.

4.3 Stable isotope ($\delta^{18}O$ & $\delta^{13}C$) measurements milling

In general, the milling approach records comparable isotope results as the drilling approach (Section 4.2) for the pure calcitic parts, the mixed zone and the pure aragonitic parts of the shell. However, the milling approach represents a consecutive sequence of samples taken from calcite into aragonite and back into the calcite (c.f., Figure 4). Even though CRM analysis and naked eye observations identified the surface of subsections D to H as aragonite, isotope measurements taken with high-spatial resolution reveal possible contamination or micro-neomorphism processes that appear to start along the annual growth line of the bivalve shell. This is most probably due to the fact that the growth lines are typically produced in autumn/winter and contain relatively more organic material than the lighter spring and summer precipitated shell increments. These inter-crystalline organic molecules decay over time, leading to depletion and leaving gaps in the carbonate structure, which most likely represent pathways into and within the shell for circulating fluids in the sediment. 'Neomorphism' is therefore much more likely to take place along autumn/winter growth lines (Martin et al., 1986). It is very likely that the subsections F, G and H represent annual increments and that associated isotope measurements represent a seasonal cycle.

4.4 Implications for palaeo-temperature reconstructions

In order to test if the measured oxygen isotope measurements represent pristine values, we calculated water temperatures assuming the $\delta^{18}O_{seawater}$ range for the

Pliocene proposed by Buchardt and Simonarson (2003). The thickness of the red line in Figure 5 represents this range, which translates into a temperature range of 1.3°C for every measurement. Reconstructed temperatures for the entire sequence vary from 68.1°C (66.8°C) to 8.4°C (7.1°C) in −0.2‰ (−0.5‰) scenario. When compared to stable oxygen isotope profiles from well preserved *A. islandica* shells (e.g., Schöne and Fiebig, 2009), it becomes obvious that here, growth lines are not associated with positive peaks in isotope values (colder water temperatures during winter season) as would be expected (c.f., inverse relationship between oxygen isotopes in biogenic carbonates and temperature in Grossman and Ku, 1986). On the contrary, growth lines (i.e., transitions from subsections E to G are associated with strongly negative peak values, which translates into warmer water temperatures (up to 40°C), which is considered lethal for *A. islandica* and unrealistic for any palaeo-environmental reconstruction of past conditions.

This reveals a crucial consideration in terms of any palaeo-environmental reconstruction based on isotopic composition of fossil biogenic shell carbonate. If, as usual, XRD is used for check for preservation (where a bulk powder is analysed and as done by Buchardt and Simonarson (2003)), the aragonitic parts in this shell would have definitely been identified as pure aragonite (as did the CRM analysis for the surface shell bit in this study). Samples subsequently taken for isotope measurements by drilling and/or by averaging larger shell areas, such as by Buchardt and Simonarson (2003), and not by the high-resolution micro-milling with a sub-annual resolution approach undertaken in this study are extremely likely to record a mix of isotope signals. It is very unlikely that the true, pristine signal can be distinguished from taphonomic alterations on a micro-scale, which can significantly impact and invalidate the results of a palaeo-environmental study.

To illustrate this, we averaged all measurements indicated by the grey bar in Figure 5 and calculated one average temperature for the entire section (as described in Section 2.3). Please note that this grey area includes palaeo-temperatures of up to 40°C (for winter conditions), which clearly indicates a diagenetic overprint. If averaged, this area results in a water temperature of 14.7°C. In Buchardt and Simonarson (2003) fossil *A. islandica* shells giving water temperatures more than 16°C are not rejected, but are interpreted as palaeo-environmental signals. As such, our 14.7°C shell area might as well have served as indicator for a warmer Mactra or Tapes Zones (c.f., Figure 9 in Buchardt and Simonarson, 2003).

Furthermore, if we follow the methodology of Buchardt and Simonarson (2003) and calculate water temperatures based on a calcite relationship, even though *A. islandica* is aragonitic, water temperatures averaged from the grey area would be 6.7°C, but range from –5.1°C to 191.2°C. This clearly shows the problem of average values in association with minor recrystallization in the fossil shells, as an average water temperature of 6.7°C perfectly matches our assumptions for the preferred living conditions of *A. islandica* (Schöne, 2013) and previous temperature reconstructions based on oxygen isotopes from modern *A. islandica* shells (Schöne and Fiebig, 2009; Beierlein et al., 2014).

Calcite-based water temperature reconstructions are likely to indicate recrystallization temperatures at the time of 'neomorphism', which might be of interest from a geological perspective (e.g., to observe diagenesis and reconstruct burial history in sedimentary rocks; Hudson, 1977) or even in a climatic perspective (c.f., Hays and Grossman, 1991) but is certainly not desirable for palaeo-temperature reconstructions.

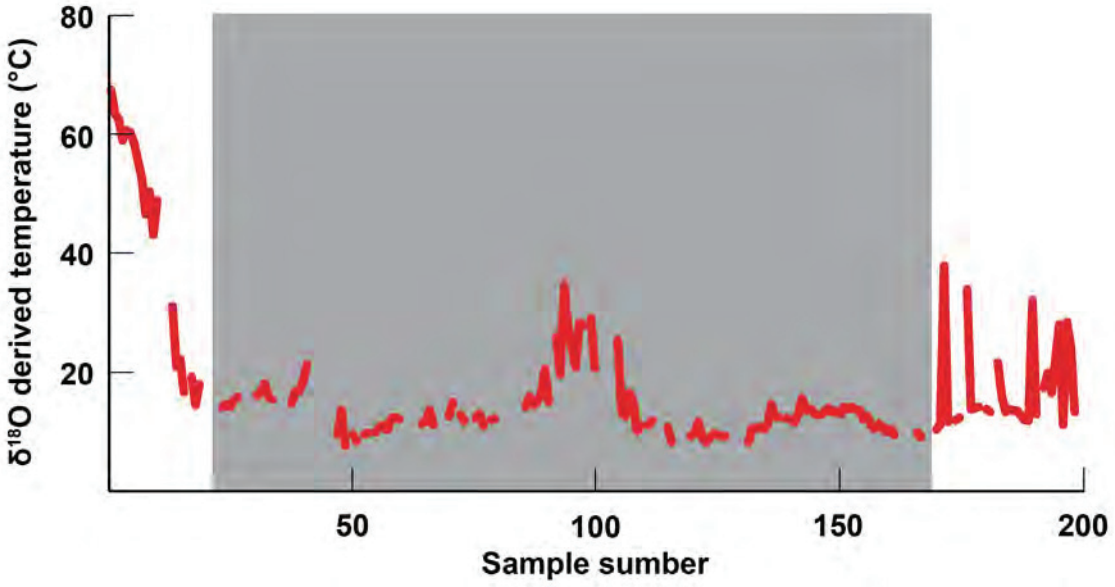

Figure 5. Water temperature calculated from $\delta^{18}O$ measurements throughout the shell transect by the micro-milling approach (Figure 4a). Line thickness (i.e., upper and lower margin) represents the temperature range that results from assumption of maximum and minimum $\delta^{18}O_{seawater}$ values as given by Buchardt and Simonarson (2003) (c.f., Section 2.3). Grey area indicates the water temperature values that have been averaged for the example discussed in Section 4.3 and result in an average temperature value of 14.7°C (6.7°C based on calcite temperature-isotope relationship used in Buchardt and Simonarson, 2003).

5 Conclusions

- CRM is an ideal tool to identify recrystallization in carbonate shells and identify carbonate polymorphs on small spatial scales.
- CRM maps can identify growth related structures in recrystallized shell calcite, referred to as 'ghost structures' in the literature, which indicate a slow recrystallization process. These are suggested to be associated with organic-depleted winter growth lines that provide pathways through the shell material for diagenetic fluids.
- Isotope values ($\delta^{18}O$ and $\delta^{13}C$) argue for an open system recrystallization process with a circulating reservoir of more negative values. Meteoric water is the most likely source of strongly negative $\delta^{18}O$ values in recrystallized calcite.
- Pristine aragonite appears to preserve the original isotopic composition, in contrast to recrystallized calcite, which reflects the isotopic composition of the substituting fluid.
- We stress the need for careful interpretation of carbonate-based water temperature reconstructions, as small-scale diagenesis can significantly impact results and substantially distort the derived palaeo-climatic or palaeo-environmental signals.

Acknowledgements

The first author (LB) was financed by the “Earth System Science Research School (ESSReS)”, an initiative of the Helmholtz Association of German Research Centres (HGF) at the Alfred Wegener Institute (AWI), Helmholtz Centre for Polar and Marine. Lisa Schönborn and Kerstin Beyer (both AWI Bremerhaven) are thanked for their help with the isotope measurements. Michael Seebeck is thanked for helping with initial shell preparation in the geosciences lab. We thank Lovísa Ásbjörnsdóttir (Icelandic Institute of Natural History, Gardabaer, Iceland) for providing the shell material.

References

Anderson, T.F., 1969. Self-diffusion of carbon and oxygen in calcite by isotope exchange with carbon dioxide. Journal of Geophysical Research 74, 3918–3932.

Bathurst, R.G.C., 1964. The replacement of aragonite by calcite in the molluscan shell wall. Approaches to Paleoecology, 357–376.

Beierlein, L., Salvigsen, O., Schöne, B.R., Mackensen, A., Brey, T., 2014. The seasonal water temperature cycle in the Arctic Dicksonfjord (Svalbard) during the Holocene Climate Optimum derived from sub-fossil *Arctica islandica* shells. The Holocene (accepted for print with minor revisions).

Buchardt, B., Simonarson, L.A., 2003. Isotope palaeotemperatures from the Tjörnes beds in Iceland: evidence of Pliocene cooling. Palaeogeography, Palaeoclimatology, Palaeoecology 189, 71–95.

Butler, P.G., Wanamaker Jr, A.D., Scourse, J.D., Richardson, C.A., Reynolds, D.J., 2013. Variability of marine climate on the North Icelandic Shelf in a 1357-year proxy archive based on growth increments in the bivalve *Arctica islandica*. Palaeogeography, Palaeoclimatology, Palaeoecology 373, 141–151.

Dahlgren, T.G., Weinberg, J.R., Halanych, K.M., 2000. Phylogeography of the ocean quahog (*Arctica islandica*): influences of paleoclimate on genetic diversity and species range. Marine Biology 137, 487–495.

Dettman, D.L., Lohmann, K.C., 1995. Microsampling carbonates for stable isotope and minor element analysis: Physical separation of samples on a 20 micrometer scale. Journal of Sedimentary Research 65A, 566–569.

Dettman, D.L., Reische, A.K., Lohmann, K.C., 1999. Controls on the stable isotope composition of seasonal growth bands in aragonitic fresh-water bivalves (unionidae). Geochimica et Cosmochimica Acta 63, 1049–1057.

Dodd, J.R., 1966. Processes of conversion of aragonite to calcite with examples from the Cretaceous of Texas. Journal of Sedimentary Research 36, 733–741.

Folk, R.L., 1965. Some aspects of recrystallization in ancient limestones. University of Texas, Austin, 1–35.

Folk, R.L., Assereto, R., 1976. Comparative fabrics of length-slow and length-fast calcite and calcitized aragonite in a Holocene speleothem, Carlsbad Caverns, New Mexico. Journal of Sedimentary Research 46, 486–496.

Friedman, G.M., 1964. Early diagenesis and lithification in carbonate sediments. Journal of Sedimentary Research 34, 777–813.

Fyfe, S.W., Bischoff, J.L., 1965. The calcite aragonite problem. University of California Berkeley, 1–11.

Grossman, E.L., Ku, T.-L., 1986. Oxygen and carbon isotope fractionation in biogenic aragonite: Temperature effects. Chemical Geology 59, 59–74.

Hays, P.D., Grossman, E.L., 1991. Oxygen isotopes in meteoric calcite cements as indicators of continental paleoclimate. Geology 19, 441–444.

Hendry, J.P., Ditchfield, P.W., Marshall, J.D., 1995. Two-stage neomorphism of Jurassic aragonitic bivalves: implications for early diagenesis. Journal of Sedimentary Research 65, 214–224.

Hoefs, J., 1997. Stable Isotope Geochemistry. Springer Berlin, pp. 201.

Hudson, J.D., 1977. Stable isotopes and limestone lithification. Journal of the Geological Society 133, 637–660.

Kendall, A.C., 1975. Post-compactional calcitization of molluscan aragonite in Jurassic limestone from Saskatchewan, Canada. Journal of Sedimentary Research 45, 399–404.

Machel, H.G., 1997. Recrystallization versus neomorphism, and the concept of 'significant recrystallization' in dolomite research. Sedimentary Geology 113, 161–168.

Maliva, R.G., 1998. Skeletal aragonite neomorphism – quantitative modelling of a two-water diagenetic system. Sedimentary Geology 121, 179–190.

Maliva, R.G., Missimer, T.M., Dickson, J.A.D., 2000. Skeletal aragonite neomorphism in Plio-Pleistocene sandy limestones and sandstones, Hollywood, Florida, USA. Sedimentary Geology 136, 147–154.

Martin, G.D., Wilkinson, B.H., Lohmann, K.C., 1986. The Role of Skeletal Porosity in Aragonite Neomorphism - *Strombus* and *Montastrea* from the Pleistocene Key Largo Limestone, Florida. Journal of Sedimentary Research 56, 194–203.

Nehrke, G., Nouet, J., 2011. Confocal Raman microscope mapping as a tool to describe different mineral and organic phases at high spatial resolution within marine biogenic carbonates: case study on *Nerita undata* (Gastropoda, Neritopsina). Biogeosciences 8, 3761–3769.

Nehrke, G., Poigner, H., Wilhelms-Dick, D., Brey, T., Abele, D., 2012. Coexistence of three calcium carbonate polymorphs in the shell of the Antarctic clam *Laternula elliptica*. Geochemistry, Geophysics, Geosystems 13, Q05014.

Richardson, C.A., 2001. Molluscs as archives of environmental change. Oceanography and Marine Biology: an Annual Review 39, 103–164.

Ropes, J.W., Jones, D.S., Murawski, S.A., Serchuk, F.M., Jearld Jr, A., 1984. Documentation of annual growth lines in ocean quahogs, *Arctica islandica* Linné. Fishery Bulletin 82, 1–19.

Sandberg, P.A., Hudson, J.D., 1983. Aragonite relic preservation in Jurassic calcite-replaced bivalves. Sedimentology 30, 879–892.

Schöne, B.R., 2013. *Arctica islandica* (Bivalvia): A unique paleoenvironmental archive of the northern North Atlantic Ocean. Global and Planetary Change 111, 199–225.

Schöne, B.R., Fiebig, J., 2009. Seasonality in the North Sea during the Allerød and Late Medieval Climate Optimum using bivalve sclerochronology. International Journal of Earth Sciences 98, 83–98.

Schöne, B.R., Freyre Castro, A.D., Fiebig, J., Houk, S.D., Oschmann, W., Kröncke, I., 2004. Sea surface water temperatures over the period 1884–1983 reconstructed from oxygen isotope ratios of a bivalve mollusk shell (*Arctica islandica*, southern North Sea). Palaeogeography, Palaeoclimatology, Palaeoecology 212, 215–232.

Schöne, B.R., Oschmann, W., Rössler, J., Castro, A.D.F., Houk, S.D., Kröncke, I., Dreyer, W., Janssen, R., Rumohr, H., Dunca, E., 2003. North Atlantic Oscillation dynamics recorded in shells of a long-lived bivalve mollusk. Geology 31, 1037–1040.

Stemmer, K., Nehrke, G., 2014. The distribution of polyenes in the shell of *Arctica islandica* from North Atlantic localities: a confocal Raman microscopy study. Journal of Molluscan Studies, in press.

Tan, F.C., Hudson, J.D., 1974. Isotopic studies on the palaeoecology and diagenesis of the Great Estuarine Series (Jurassic) of Scotland. Scottish Journal of Geology 10, 91–128.

Thompson, T.G., Chow, T.J., 1955. The strontium-calcium atom ratio in carbonate-secreting marine organisms. Papers in Marine Biology and Oceanography 3, 20–39.

Walderhaug, O., Bjorkum, P.A., 1992. Effect of meteoric water flow on calcite cementation in the Middle Jurassic Oseberg Formation, well 30/3-2, Veslefrikk Field, Norwegian North Sea. Marine and Petroleum Geology 9, 308–318.

Wall, M., Nehrke, G., 2012. Identification of two organic bands showing different chemical composition within the skeleton of *Porites lutea*: a confocal Raman microscopy study. Biogeosciences Discussions 9, 8273–8306.

Wanamaker Jr, A., Kreutz, K., Schöne, B., Maasch, K., Pershing, A., Borns, H., Introne, D., Feindel, S., 2009. A late Holocene paleo-productivity record in the western Gulf of Maine, USA, inferred from growth histories of the long-lived ocean quahog (*Arctica islandica*). International Journal of Earth Sciences 98, 19–29.

Wardlaw, N., Oldershaw, A., Stout, M., 1978. Transformation of aragonite to calcite in a marine gasteropod. Canadian Journal of Earth Sciences 15, 1861–1866.

Zhang, H., Cai, Y., Tan, L., Qin, S., An, Z., 2014. Stable isotope composition alteration produced by the aragonite-to-calcite transformation in speleothems and implications for paleoclimate reconstructions. Sedimentary Geology, in press.

Manuscript IV

The seasonal water temperature cycle in the Arctic Dicksonfjord (Svalbard) during the Holocene Climate Optimum derived from sub-fossil *Arctica islandica* shells

Lars Beierlein[1], Otto Salvigsen[2], Bernd R. Schöne[3], Andreas Mackensen[1] and Thomas Brey[1]

[1]Alfred Wegener Institute, Helmholtz Centre for Polar and Marine Research, Bremerhaven, Germany

[2]Department of Geosciences, University of Oslo, Norway

[3]Institute of Geosciences, University of Mainz, Germany

Accepted, with minor revisions in *The Holocene*.

Abstract

Future climate change will have significant effects on ecosystems worldwide and on Polar regions in particular. Hence, palaeo-environmental studies focusing on the last warmer-than-today phase (i.e., the early Holocene) in higher latitudes are of particular importance to understand climate development and its potential impact in polar systems. Molluscan bivalve shells constitute suitable bio-archives for high-resolution palaeo-environmental reconstructions. Here, we present a first reconstruction of early Holocene seasonal water temperature cycle in an Arctic fjord based on stable oxygen isotope ($\delta^{18}O_{shell}$) profiles in shells of *Arctica islandica* (Bivalvia) from raised beach deposits in the Dicksonfjord, Svalbard, dated at 9,954–9,782 cal yrs BP. Reconstructed maximum and minimum bottom palaeo-water temperatures for the assumed shell growth period between April and August of 15.2°C and 2.8°C imply a palaeo-seasonality of about 12.4°C for the early Holocene. In comparison to modern temperatures this indicates that average temperature declined by 6°C and seasonality narrowed by 50%. This first palaeo-environmental description of a fjord setting during the Holocene Climate Optimum at Spitsbergen exceeds most previous global estimates (+ 1–3°C) but confirms studies indicating an amplified effect (+ 4–6°C) at high northern latitudes.

Keywords: *Arctica islandica*, sclerochronology, palaeo-seasonality, palaeo-temperature, Holocene Climate Optimum, Svalbard, polar amplification

1 Introduction

Environmental and ecological consequences of future climate change will be most pronounced at high latitudes, as the ice covered polar systems are particularly sensitive to a rise in temperature. A statistically significant warming trend of 0.09°C per decade has already been observed in mean surface temperature over the last century in the Arctic polar region (ACIA, 2004). Temperature and sea level rise across the Arctic Ocean are expected to be considerably higher (ACIA, 2004; Spielhagen et al., 2011; IPCC, 2013) than global average rise of up to 3.7°C and 0.63 m (IPCC, 2013) predicted by global circulation models (GCMs) for the year 2100.

The Holocene Climatic Optimum (HCO), approximately 10,500 to 8,200 years BP in the Arctic region, was the warmest interval of the Holocene interglacial, followed by a general cooling trend into the modern (Hald et al., 2004; Ebbesen et al., 2007; Rasmussen et al., 2012). It was associated with an 8% higher maximum insolation anomaly (Berger and Loutre, 1991), 1–3°C warmer temperatures and an increased seasonality compared to modern (e.g., Kutzbach and Guetter, 1986; Salvigsen et al., 1992; Koc et al., 1993; Sarnthein et al., 2003; ACIA, 2004; Rasmussen et al., 2012). The similarities between the climate of the HCO and predictions for the forthcoming centuries therefore make this a particularly important interval for predicting and understanding the mechanisms and impacts of future global warming.

The archipelago of Svalbard is located north of the Arctic Circle at 74°–84°N (Figure 1). The West Spitsbergen Current (WSC), the northernmost extension of the Norwegian Atlantic Current (NAC) (e.g., MacLachlan et al., 2007), transports relatively warm and salty Atlantic water (AW) polewards along the western coasts of Svalbard and produces the distinct hydrography of the coastal and fjord waters. In addition, modern fjord hydrography is seasonally influenced by cold Arctic surface waters of the East Spitsbergen Current (ESC) and glacial meltwater input (e.g., Saloranta and Svendsen, 2001; Tverberg and Nøst, 2009). This general pattern (Figure 1) is presumed to have existed during the entire Holocene (Salvigsen, 2002; Slubowska-Woldengen et al., 2007). However, the early Holocene is associated with reduced (or even completely absent) glacial conditions at Svalbard, a reduced expansion of sea-ice from the north and an enhanced WSC (Svendsen and Mangerud, 1997; Salvigsen, 2002; Sarnthein et al., 2003; Hald et al., 2004). This setting is considered to resemble future conditions (Ebbesen et al., 2007; IPCC, 2013), making Svalbard an ideal site to investigate the climate of the HCO as an analogue to predicted future conditions.

Of the climate proxies available for the Arctic HCO, e.g., ice-rafted debris (Bond et al., 2001; Hald et al., 2004), benthic and planktonic foraminifera (Rasmussen et al., 2012), diatoms (Koc Karpuz and Jansen, 1992; Birks and Koc, 2002) or plant macrofossils (Birks, 1991), most have a very limited temporal resolution (e.g., 10–70 years in ice cores and sediment cores; Bond et al., 2001; Sarnthein et al., 2003; Hald et al., 2007; Reusche et al., 2014). Here, we examine three sub-fossil specimens of the marine bivalve *Arctica islandica* derived from raised beach deposits (~5 m above sea level) at Kapp Nathorst inside the Dicksonfjord (Figure 1b), a side-fjord of the Isfjord, the largest fjord on Spitsbergen (Nilsen et al., 2008). The longevity of *A. islandica* (225 to more than 500 years; Ropes and Murawski, 1983; Schöne et al., 2005a; Butler et al., 2013), its wide northern boreal distribution as well as its abundance in the fossil record (Dahlgren et al., 2000) qualifies this particular species for palaeo-environmental and palaeo-climatic reconstructions on decadal as well as on sub-annual time scales (Wanamaker Jr et al., 2011; Butler et al., 2013; Schöne, 2013). Previous studies on growth, physiology (e.g., Begum et al., 2010; Morton, 2011) and shell formation (e.g., Witbaard et al., 1999; Stemmer et al., 2013) make *A. islandica* a well-calibrated and understood high-resolution bio-archive for palaeo-climate studies. *A. islandica* precipitates its shell carbonate in isotopic equilibrium with ambient seawater (Weidman et al., 1994), and previous studies e.g., by Peacock (1989), Buchardt and Simonarson (2003) and Schöne et al. (2004), have successfully used stable oxygen isotope values ($\delta^{18}O_{shell}$) in *A. islandica* to reconstruct annual and sub-annual water temperatures. *A. islandica* is extinct in modern Svalbard, as mean summer water temperatures of about 5–6°C (see Table 1 for summary) are considerably below the range of about 9–16°C required by this species for successful reproduction and recruitment (Golikov and Scarlato, 1973; Lutz et al., 1982; Peacock, 1989).

We measure stable oxygen isotope values ($\delta^{18}O_{shell}$) in carbonate sampled with high spatial resolution along the growth trajectory in *A. islandica* shells to reconstruct palaeo-temperatures and palaeo-seasonality during the HCO interval. We present a high-resolution insight into the climatic conditions that may be experienced in the Polar region by the end of the century under current modelling projections and demonstrate the power of this bio-archive for accurate and sub-seasonal environmental reconstructions. We discuss the reliability of these results with respect to possible fluctuations of salinity and associated variations in seawater chemistry ($\delta^{18}O_{seawater}$), and to changes in ice volume as well as in the length of the growing season.

2 Material and Methods

2.1 Shell origin and preparation

A. islandica shells were collected during fieldwork (O. Salvigsen) in 1991 and were found in life-position in sub-littoral layers in raised beach deposits (about 5 m above sea level) at Kapp Nathorst on the eastern shore of the Dicksonfjord (78°46'41N, 15°24'21E, Figure 1). The landmasses of most of Svalbard experienced considerable relative uplift during the Holocene due to reduced ice load after the last glacial maximum and shells of different molluscs are commonly revealed in raised beach deposits following erosion by the sea or small rivers. Sub-fossil specimens of *A. islandica* appear to be more frequent in the Dicksonfjord than in other localities in Svalbard, particularly at Kapp Nathorst where these specimens were retrieved (c.f., Feyling-Hanssen, 1955). This post-glacial uplift has been dated in many places by age determinations of driftwood and whale bones found on these raised beaches (e.g., Forman, 1990; Bondevik et al., 1995; Landvik et al., 1998; Salvigsen and Høgvard, 2006) and a minimum value of 70 m is considered as a safe estimate for the post-glacial marine limit in the Dicksonfjord based on field observations. The depth at which these shells lived during the Holocene is discussed in Section 4.2.

After collection, the shells were air-dried and kept in storage until 2011. Three shells (shell IDs: AI-DiFj-02, AI-DiFj-03 and AI-DiFj-04) were selected for analysis and were externally strengthened with an epoxy resin cover to prevent them from breakage. A 5 mm cross-section was prepared by sawing along the line of strongest growth (running perpendicular to the growth lines) using a low-speed precision saw (Buehler, IsoMet) equipped with a 0.4 mm diamond-coated saw blade. Cross-sections were then ground using a manual grinder (Buehler, Phoenix Alpha) and sand paper with three different grain sizes (15 µm, 10 µm and 5 µm).

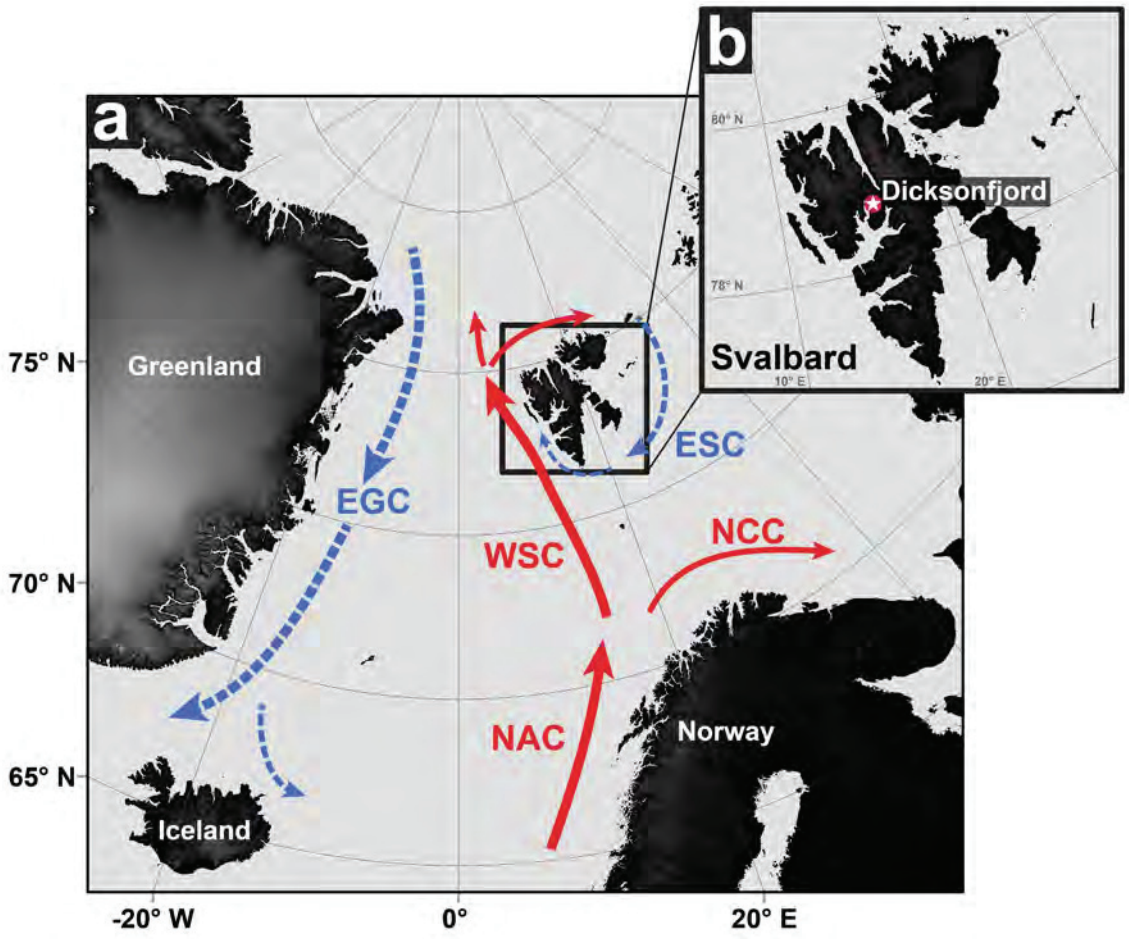

Figure 1. Map of Svalbard and the Nordic Seas showing major ocean currents. (a) Map illustrating the locality of the Svalbard archipelago between the northern North Atlantic Ocean and the Arctic Ocean. Solid arrows indicate the transport of relatively warm and salty water masses northwards via the Norwegian Atlantic Current (NAC), which subdivides into the Norwegian Coastal Current (NCC) and West Spitsbergen Current (WSC). Dashed arrows indicate southward flows of relatively cold water, i.e., East Greenland Current (EGC) and East Spitsbergen Current (ESC). (b) Map of Svalbard indicating the sample locality in the Dicksonfjord (star symbol) of *Arctica islandica* at about 79°N.

2.2 Preservation of shell material

When considering geochemical analyses on biogenic fossil and sub-fossil carbonate, a check for diagenetic alteration is a key step. *A. islandica* builds its three shell layers out of aragonite (e.g., Schöne, 2013). Depending on the existence of pressure, heat and/or hydrothermal fluids within the ambient sediment layer, fossil biogenic aragonite may recrystallize to calcite over time (the more stable polymorph of calcium carbonate; e.g., Maliva, 1998), affecting the original isotope signal of the carbonate. All shells in this study have been checked for recrystallization, using a confocal Raman microscope (CRM) (WITec alpha 300 R), equipped with a diode laser (excitation wavelength 488 nm) and a 20x Zeiss objective. CRM is a non-destructive method and provides a high spatial resolution (a few hundred nm). Instrumental settings and procedure follow

Nehrke et al. (2012). In each of the three 5 mm shell cross-sections dedicated for stable oxygen isotope analysis, the sampling areas were checked by CRM scans and single spot measurements.

2.3 Dating of shell material

All three sub-fossil shells in this study have been radiocarbon dated ($^{14}C_{AMS}$) at the Poznań Radiocarbon Laboratory in Poland. The periostracum and any adhering sediment were carefully removed from the outer surface of the shells using a hand drill device (Type Proxxon Minimot 40/E) and 50 mg samples of shell carbonate were taken for analysis. $^{14}C_{AMS}$ results were corrected using the program CALIB version 6.1.0 (Stuiver and Reimer, 1993, http://calib.qub.ac.uk/calib/) and the Marine09 calibration curve (Reimer et al., 2009). For Svalbard, a regional correction value (ΔR) of 93±23 years has been applied, following the descriptions in Slubowska-Woldengen et al. (2007) and Ebbesen et al. (2007).

2.4 Stable oxygen isotope analysis ($\delta^{18}O$)

Carbonate samples were manually taken from the outer shell layer (Dettman and Lohmann, 1995) using a 700 µm mill bit (Komet/Gebr. Brasseler GmbH & Co. KG) mounted onto an industrial high precision drill (Minimo C121, Minitor Co., Ltd.) and attached to a binocular microscope. Two identical consecutive ontogenetic years have been sampled in each of the three shells to assure comparability between individuals. Measurements were conducted on a Thermo Finnigan MAT 253 isotope ratio mass spectrometer coupled with an automated carbonate preparation device (Kiel IV). Measurements were calibrated against the international NBS-19 standard and reported in δ-notation versus VPDB (Vienna Peedee Belemnite). The long-term precision based on an internal laboratory standard (Solnhofen limestone) measured over a one-year period together with samples was better than ±0.08‰. The average sample weight for all 796 samples was ~48 µg, while the average spatial sampling resolution was ~50 µm (Table 3).

When calculating palaeo-temperatures from sub-fossil shell carbonate it is important to consider changes in ice volume over geological time-scales as this affects marine $\delta^{18}O_{seawater}$ values. Based on the work of Fairbanks (1989), $\delta^{18}O_{shell}$ values were

corrected with individual factors for each of the three specimens (Table 3) to make them comparable to modern measurements. Finally, we calculated palaeo-temperatures for all six individual ontogenetic years according to Dettman et al. (1999), which takes into account that the assumed $\delta^{18}O_{seawater}$ value of 0.20‰ as given by MacLachlan et al. (2007) for transformed AW in the Kongsfjord at water depths between 6 and 52 m was reported against VSMOW (Vienna Standard Mean Ocean Water). This $\delta^{18}O_{seawater}$ value is confirmed by a $\delta^{18}O_{seawater}$ value of 0.19‰ measured in water, from close to the mouth of the Isfjord (77.85°N, 11.9°E, T=3.36°C, S=34.48 psu) at a water depth of 52.5 m on 6 September 2001 (A. Mackensen, unpublished data). For the error estimate we assume the modern $\delta^{18}O_{seawater}$ variability (based on MacLachlan et al., 2007), which results in uncertainties of 0.87°C (+0.20‰) for highest and 0.61°C (–0.14‰) for lowest temperature estimates, respectively (legend in Figure 4).

2.5 Modern water temperature data from Svalbard

Modern long-term measurements of fjord water temperatures at West Spitsbergen are rare. Hence, information from different sources has been combined to obtain reliable estimates of seasonal maximum and minimum water temperatures (Table 1). According to this database, water temperatures below 2 m water depth range between –1°C in winter and 5–6°C in summer.

3 Results

3.1 Preservation of shell material

Confocal Raman microscope scans of the shell areas designated for oxygen isotope sampling indicated no traces of calcite. Hence, all shells were considered to be pristine aragonite and thus reliable in terms of radiocarbon dating ($^{14}C_{AMS}$) and stable oxygen isotope analysis ($\delta^{18}O$).

3.2 Dating of shell material

Calibrated radiocarbon ($^{14}C_{AMS}$) ages for the six shell specimens in this study cover a period from 9,954–9,782 cal yrs BP (Table 2). Therefore, all shells are assigned to the early Holocene (c.f., Hald et al., 2004; Kaufman et al., 2004). This is in good agreement with previously published radiocarbon ages for sub-fossil mollusc shells from Svalbard (see Salvigsen, 2002 for summary). Further, two recently reported age determinations of *A. islandica* shells from Hollendarbukta, outer Isfjord, revealed ages of 9,780±180 (sample ID: Lu-6992) and 9,670±80 (sample ID: GIN-14735) cal yrs BP respectively (Sharin et al., 2014).

3.3 Stable oxygen isotope analysis ($\delta^{18}O$) / Seasonal climate signal

$\delta^{18}O_{shell}$ profiles of all studied specimens (AI-DiFj-02, AI-DiFj-03, AI-DiFj-04) show two clear and distinct seasonal cycles (Figure 2). The darker winter bands within the shell carbonate (dashed lines in Figure 2) occur immediately before the most positive $\delta^{18}O_{shell}$ values (seen in the direction of growth). The $\delta^{18}O_{shell}$ values range from 1.4‰ to 4.3‰ in specimen AI-DiFj-02, from 1.3‰ to 4.0‰ in specimen AI-DiFj-03, and from 1.0‰ to 3.9‰ in specimen AI-DiFj-04 (Figure 2), i.e., they exhibit very similar absolute amplitudes of 2.7‰ to 2.9‰ in all three shells. Detailed information on the spatial sampling resolution as well as individual sample numbers in all six ontogenetic years is given in Table 3.

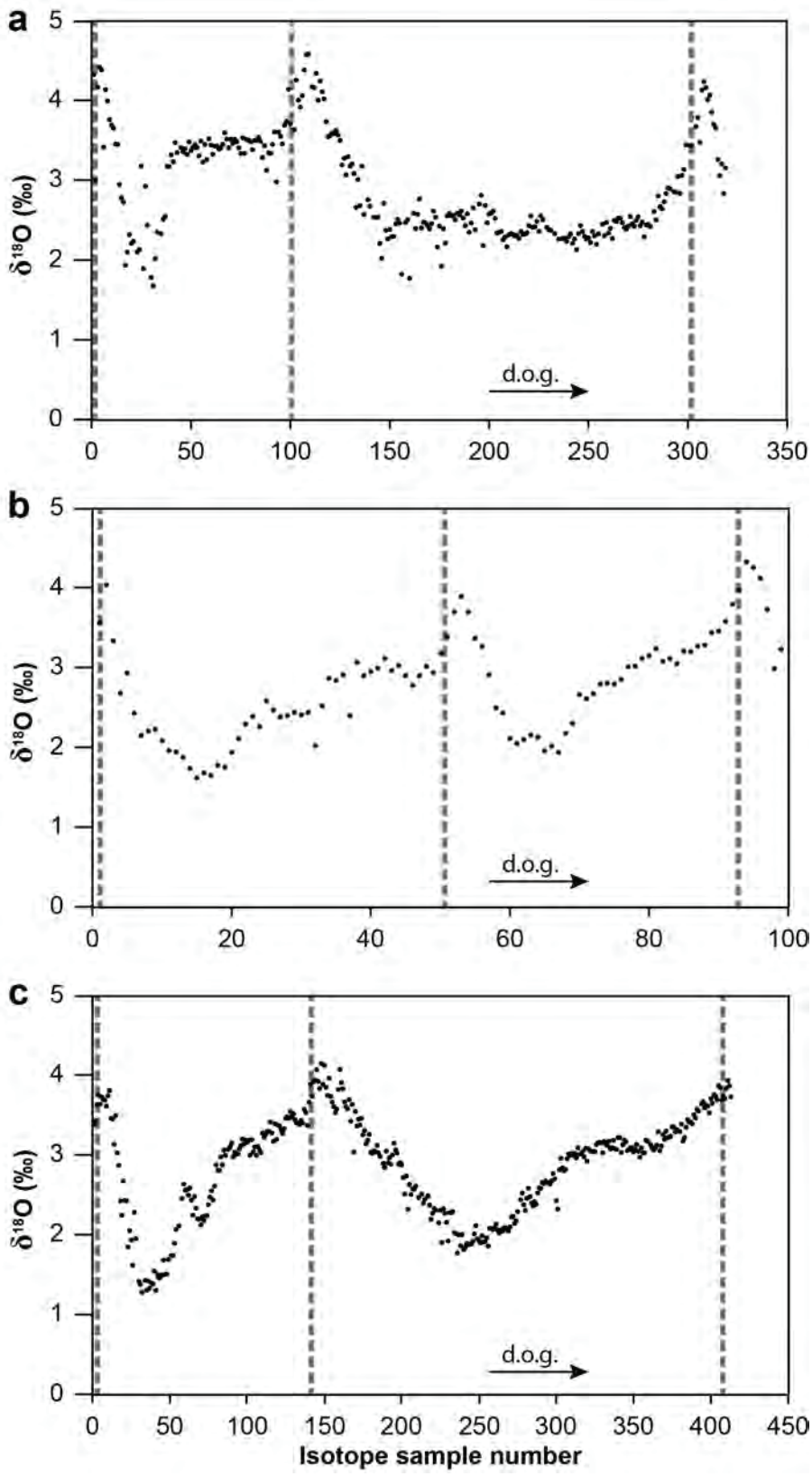

Figure 2. $\delta^{18}O_{shell}$ profiles in six ontogenetic years of *A. islandica*. Stable oxygen isotope ($\delta^{18}O_{shell}$) profiles from three early Holocene *A. islandica* specimens covering a period of two ontogenetic years each. All three profiles show two distinct annual cycles. Dotted lines indicate darker growth bands in the shell carbonate. d.o.g.: direction of growth. (a) Specimen AI-DiFj-02 with a total of 298 isotope measurements covers a range from 1.4‰ to 4.3‰. (b) Specimen AI-DiFj-03 with a total of 100 isotope measurements covers a range from 1.3‰ to 4.0‰. (c) Specimen AI-DiFj-04 with a total of 398 isotope measurements covers a range from 1.0‰ to 3.9‰.

4 Discussion

Since there is no living modern analogue of *Arctica islandica* at such high latitudes under present climate conditions against which to compare the isotope data, essential aspects concerning the observed $\delta^{18}O_{shell}$ signal have to be addressed prior to an interpretation. Firstly, we have to determine the time period represented by the analysed shell sections. Next, we need to infer the corresponding palaeo-water depth, and finally we have to discuss crucial environmental parameters such as salinity variability and $\delta^{18}O_{seawater}$ values. Only after a cautious evaluation of these issues we will proceed towards calculations for palaeo-water temperatures and estimates for palaeo-seasonality.

4.1 Season of growth

The exact duration of the season of growth, and therefore the time span of the annual temperature profile of each shell increment recorded during the year, is a crucial, albeit unknown factor for Holocene *A. islandica*. Shell growth depends primarily on water temperature and food availability (e.g., Witbaard et al., 1997). The annual growth line formation in this species occurs in late summer / autumn. However, the exact reasons for the regular slow-down of growth remain enigmatic (Schöne, 2013).

Studies of modern *A. islandica* populations indicate geographic variability in the duration of the growing season e.g., from February to September in the North Sea (Schöne et al., 2004), from January to August at the New Jersey coast (Jones, 1980) and from May to December near Cape Cod (Weidman et al., 1994). Seasonality in temperature and primary production (i.e., food availability) is predominantly driven by the annual cycle in day light hours, which is a function of geographical latitude. In the North Sea (54°N), daily light hours range between 7h and 17h, whereas at Spitsbergen (79°N) the range is 0h to 24h, with four months total darkness and four months 24h daylight (21 April – 21 August) per year. Correspondingly, the productive period is shorter in Spitsbergen (Hop et al., 2002), and hence the availability of fresh food for this bottom living deposit feeder is limited. Therefore it is most likely that the season of growth for Holocene *A. islandica* at Svalbard was shorter than at localities where this species occurs nowadays.

Today, the first phytoplankton bloom at Spitsbergen usually develops in April or May (Weslawski et al., 1988, Wassmann et al., 2006; Christensen, 2012) as sea-ice retreats and light conditions no longer limit growth (Sakshaug et al., 2009). During the early Holocene, however, sea-ice cover was greatly reduced (Svendsen and Mangerud, 1997), most probably causing phytoplankton production to be primarily coupled to sunlight availability. Thus we assume that the main growing season of early Holocene *A. islandica* at Spitsbergen ranged from approximately April to August, covering at least the period of constant daylight.

Whether this assumed April to August growing season would cover the whole annual temperature amplitude remains uncertain. However, modern maximum water temperatures are observed in July/August (e.g., Christensen, 2012, Table 1). We are therefore confident that the early Holocene shells record the maximum annual temperature. Modern minimum water temperatures of about –2°C to 0°C are measured until May, depending on locality and hydrography (e.g., Christensen, 2012). We therefore assume that the annual Holocene seasonal signal is most likely fully recorded by the *A. islandica* shells, although minimum winter temperatures are possibly truncated.

4.2 Water depth

For the palaeo-environmental reconstruction it is crucial to know the water depth from which the observed signals are derived, as this affects mean annual temperature and the degree of seasonality experienced by the organisms. We cannot determine directly whether Holocene *A. islandica* specimens lived above or below the thermocline and hence must rely on assumptions based on modern observations.

It is possible to estimate a minimum water depth value for the dated *A. islandica* shells at Kapp Nathorst based on the analysis of a whale cranium, which was radiocarbon dated to an age of 8,825±105 yrs BP (sample ID: T-17118; Borge et al., 2007) and was found at 25 m a.s.l. at Kapp Smith, on the western side of the Dicksonfjord. The following considerations and estimations are based mainly on the isobase pattern of Holocene shoreline as shown in Salvigsen (1984), Bondevik et al. (1995) and Landvik et al. (1998). The 25 m level of the whale cranium at Kapp Smith corresponds to an approximately 5 m higher level at Kapp Nathorst because the shoreline height rises east to west across the Dicksonfjord. The age difference

between our dated *A. islandica* shells at Kapp Nathorst (Table 2) and the whale cranium at Kapp Smith is approximately 400 years. In the Billefjord (the adjacent fjord to the Dicksonfjord) the average uplift between 10,000 and 8,000 yrs BP is estimated to 1.9 m per century (Salvigsen, 1984), equivalent to 7.6 m during 400 years. We therefore consider it reasonable to add an additional 5 m of uplift to the Dicksonfjord. Thus, the expected height from the contemporaneous shoreline to our *A. islandica* shells is reasoned to be at least 35 m a.s.l. As the shells at Kapp Nathorst were in fact found at approximately 5 m a.s.l. we therefore conclude that the palaeo-water depth at which these specimens lived was at least 30 m.

Estimating the palaeo-thermocline depth remains challenging. Modern long-term data on the temperature structure of different water columns in Spitsbergen fjords is scarce. MacLachlan et al. (2007) describe the thermocline at the Kongsfjord to be situated at approximately 5 m water depth in September. In the Dicksonfjord in August 2005 (Forwick, 2005) the uppermost water body, which was characterized by low salinities due to meltwater influx, extended to 10–20 m water depth. Even though water column stratification varies seasonally and between fjords, it appears to be a common feature of Svalbard coastal waters in summer. According to Rasmussen et al. (2014), a strong pycnocline existed in the West Svalbard shelf area (79°N) before 9,600 yrs BP, which argues for a stratified water column dominated by AW at the bottom. Reduced or even absent glaciers and sea-ice (e.g., Svendsen and Mangerud, 1997) resulted in reduced meltwater and freshwater influx, which led to an entirely AW occupied water column on the shelf between ca. 9,000 and 6,000 yrs BP (Rasmussen et al., 2014). Both scenarios would have led to much lower salinity fluctuations in bottom waters and more pronounced water column stratification during Holocene summer conditions at Spitsbergen (Hald et al., 2007; Rasmussen et al., 2012). Hence we assume that during the early Holocene, the water column in the Dicksonfjord remained stratified for the duration of the growing season (April to August) with a thermocline situated between 0 and 15 m water depth.

According to Schöne and Fiebig (2009) oxygen isotope profiles derived from shelf areas can indirectly indicate whether a bivalve lived above or below the thermocline. A saw-toothed shaped profile argues for a position below the thermocline, with rather stable conditions interrupted by “sudden” major winter mixing events. A more sinusoidal profile pattern argues for a position above or close to the

thermocline, as the water temperatures above the thermocline would have experienced greater seasonality.

In this study, isotope profiles of specimens AI-DiFj-02 and AI-DiFj-03 exhibit plateau-like intervals that are interjected by positive peaks in $\delta^{18}O_{shell}$ values (Figure 2a and b). This pattern indicates stable temperature and salinity conditions for most of the growing season, which are interrupted by deeper seasonal mixing. The $\delta^{18}O_{shell}$ profile of AI-DiFj-04 exhibits a more sinusoidal pattern but has the same range of $\delta^{18}O_{shell}$ values as the other two specimens (Figure 2c). However, the degree of consistency in $\delta^{18}O_{shell}$ values through an extraordinarily high sample density of 398 single samples in AI-DiFj-04 strongly argues against a life above the thermocline in a fjord setting. Furthermore, specimen AI-DiFj-04 recorded the warmest winter temperatures (3.6°C) of all three specimens. Presumably, the three specimens lived at slightly different geological times throughout the early Holocene (Table 2), and hence they may have inhabited slightly different water depths relative to the position of the thermocline. Therefore, the differences in the AI-DiFj-04 isotope profile might be explained by a vertical displacement of the seasonal thermocline (Schöne et al., 2005b). It should also be noted that Schöne and Fiebig (2009) describe isotope profiles for mid-latitude shelf area conditions, which are only of limited applicability to a high Arctic fjord setting such as Svalbard.

We therefore conclude that a living depth of at least 30 m b.s.l. for these sub-fossil *A. islandica* specimens from Spitsbergen would have been below the thermocline during the Holocene at this fjord.

4.3 (Sub-annual) salinity changes and $\delta^{18}O_{seawater}$

Palaeo-temperature reconstructions based on $\delta^{18}O_{shell}$ values should be interpreted with caution, as $\delta^{18}O_{seawater}$ values at the time of shell formation can vary on geological (ice volume) and sub-annual (seasonal) time-scales with changes in water temperature and salinity (Jansen, 1989; MacLachlan et al., 2007). To account for the effect on $\delta^{18}O_{seawater}$ of less global ice volume during the early Holocene, we applied correction values to $\delta^{18}O_{shell}$ based on the work of Fairbanks (1989) (Table 3). Sub-annual changes in salinity during the early Holocene in Spitsbergen fjords have not been determined thus far, but might have influenced $\delta^{18}O_{seawater}$ values. Our palaeo-salinity and palaeo-temperature estimates are therefore based on two assumptions:

(1) The correlation between salinity and $\delta^{18}O_{seawater}$ is nearly linear and latitude dependent (e.g., Azetsu-Scott and Tan, 1997; Mikalsen and Sejrup, 2000). For Spitsbergen, MacLachlan et al. (2007) established this correlation from modern annual $\delta^{18}O_{seawater}$ values and salinity data for the Kongsfjord, a fjord north of the Isfjord on the west coast of Spitsbergen, whose hydrology is considered to be similar to the Isfjord (Rasmussen et al., 2012). This allows the conversion of salinity measurements from fjords on Spitsbergen into $\delta^{18}O_{seawater}$ values. Accordingly, we assume a $\delta^{18}O_{seawater}$ value of 0.20‰ (ranging from 0.06‰ to 0.40‰) in our calculations. This is suggested by MacLachlan et al. (2007) for the outer fjord transformed AW at a depth of 6–52 m; the water mass that is considered most likely to resemble early Holocene, glacier-reduced water conditions. We assume the same annual salinity range of the Kongsfjord (from 34.02 to 34.59) for the early Holocene Dicksonfjord to provide an error estimate for our palaeo-temperature reconstructions (Figure 4). Additional average $\delta^{18}O_{seawater}$ values given in MacLachlan et al. (2007) for the inner fjord deep water (>2 m) of 0.10‰ and outer fjord AW (76–354 m) of 0.24‰ result in consistently increased (by 0.17°C for $\delta^{18}O_{seawater}$=0.24‰) or decreased (by 0.43°C for $\delta^{18}O_{seawater}$=0.10‰) water temperature values, both having comparable salinity ranges (0.7 for $\delta^{18}O_{seawater}$=0.10‰ and 0.48 for $\delta^{18}O_{seawater}$=0.24‰) and therefore not having an impact on the key findings in this study.

(2) During modern times and during the early Holocene, fjords along the west coast of Spitsbergen have strongly been influenced by the impact of AW, derived from the WSC (Peacock, 1989; Salvigsen et al., 1992; Salvigsen, 2002; Berge et al., 2005). On the western shelf of Svalbard (79°N), the development of a strong pycnocline in late spring separates low salinity surface water caused by meltwater influx from the warmer and more saline AW beneath (Rasmussen et al., 2014). Consequently, the influence of AW on bottom waters of the Isfjord would have been strongest during the summer growing season of *A. islandica* (see Section 4.1; Slubowska et al., 2005; Rasmussen et al., 2007; Slubowska-Woldengen et al., 2007; Skirbekk et al., 2010; Rasmussen et al., 2012). Although the modern hydrological summer conditions at the Isfjord are considered to be relatively stable (Berge et al., 2005), conditions during the early Holocene are presumed to have been even less variable (Ebbesen et al., 2007). Due to greatly reduced extent of glaciers and sea-ice (Svendsen and Mangerud, 1997; Salvigsen, 2002), pronounced water column stratification (Rasmussen et al., 2014) and a much enhanced WSC (Sarnthein et al., 2003; Hald et al., 2004), subsurface AW had a more distinct influence at the bottom than present (Koc and Jansen, 2002; Hald et al.,

2004; Rasmussen et al., 2014). Therefore, applying the modern salinity variability of 34.02 to 34.59 to the early Holocene (ca. 9,850 cal yrs BP) will likely overestimate Holocene variability in water chemistry. Our considerations imply that the benthos below 30 m water depth has been exposed to AW primarily, derived from the WSC. Consequently, we follow Lubinski et al. (2001) and Rasmussen et al. (2012) in expecting that Holocene benthic $\delta^{18}O_{shell}$ values from the west coast of Spitsbergen to reflect variations in temperature rather than in salinity.

4.4 Palaeo-temperatures and palaeo-seasonality

We present the first high temporal resolution snapshot of palaeo-temperature and palaeo-seasonality at ≥30 m water depth in an Arctic fjord setting during HCO. Due to the above-mentioned uncertainties in growing season, water depth, absolute $\delta^{18}O_{seawater}$ values and sub-annual salinity variability (see also Section 3.3), the reconstructed palaeo-temperatures are associated with a certain error. Nevertheless, they correspond very well with the preferred temperature range of modern *A. islandica* (Golikov and Scarlato, 1973; Witbaard et al., 1997). *A. islandica* is known to tolerate temperatures from about 20°C down to 1°C (Cargnelli et al., 1999) and occasionally below 0°C (Peacock, 1989). However, *A. islandica* growth may have paused during winter and thus the shell may have not recorded the true ambient minimum temperature.

The average minimum bottom water temperature (BWT) recorded is 2.8°C and thus about 4°C higher than modern minimum winter temperatures (Figure 3, Table 3). Furthermore, the maximum BWT amounts to 15.2°C, which is 8–10°C higher than modern maximum summer BWTs in this region (Figure 3, Table 3). Maximum BWTs represent peak values, occurring during the first half of the growing season in all six ontogenetic years (Figure 4). This might be due a down-mixing of low-salinity surface waters (associated with more negative $\delta^{18}O_{seawater}$ values) during thermocline formation at the beginning of the growing season. On the other hand, maximum BWTs in inner fjords may be higher in general compared to shelf regions, owing to "…atmospheric heating in sheltered areas and small inflow of cold water…" (Salvigsen et al., 1992). The early Holocene was associated with an 8% increased summer insolation (Berger and Loutre, 1991; Koc et al., 1993; ACIA, 2004), which may have caused stronger heating of the fjords during summer. Furthermore, glaciers, sea-ice and cold Arctic water influx were largely reduced compared to today (Salvigsen, 2002; Sarnthein et al.,

2003; Reusche et al., 2014), and due to an increased WSC, warmer AW dominated sub-surface waters on the shelf (Hald et al., 2004; Rasmussen et al., 2014) and therefore most probably also the hydrology inside the Isfjord/Dicksonfjord.

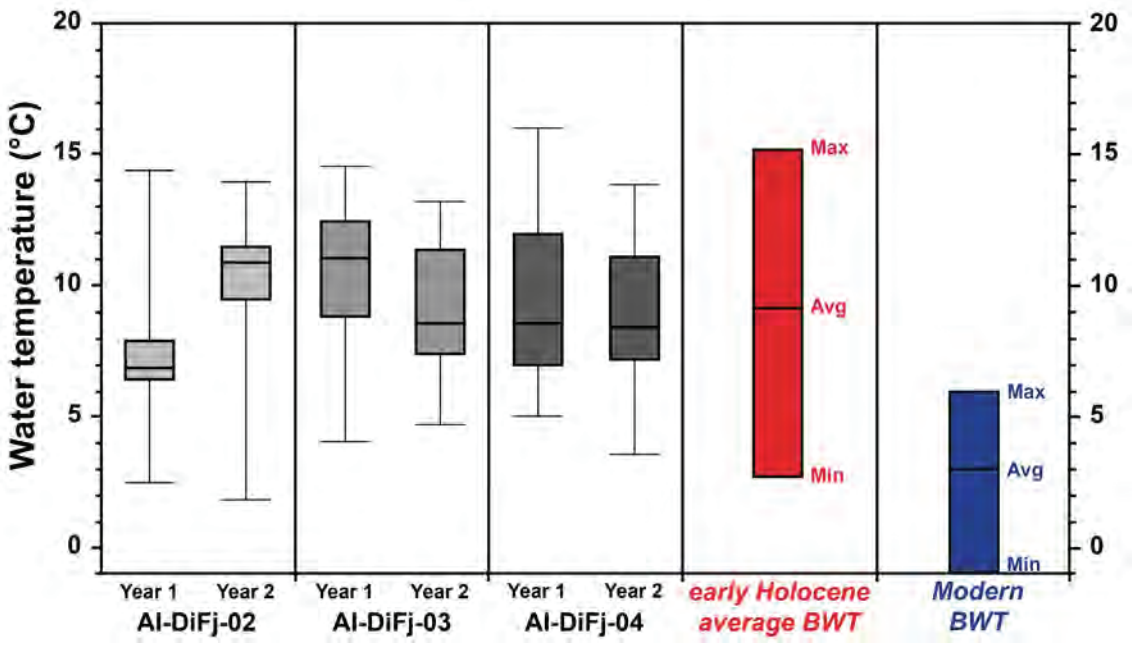

Figure 3. Reconstructed bottom water temperatures (BWTs) and palaeo-seasonality. Palaeo-temperatures derived from stable oxygen isotope values ($\delta^{18}O_{shell}$) of six individual ontogenetic years of specimens AI-DiFj-02, AI-DiFj-03 and AI-DiFj-04 (see Figure 2). Values have been individually corrected for ice volume changes (Table 3) and a modern $\delta^{18}O_{seawater}$ value of 0.20‰ has been assumed. Individual years are given as box-and-whisker plots with box giving the first quartile, median and third quartile (horizontal lines from top to bottom). Upper and lower whiskers give maximum and minimum of all data. Reconstructed early Holocene BWTs represent average values based on all six ontogenetic years (Table 3). Modern BWTs are based on references in Table 1.

Average BWT across all samples is 9.1°C, varying by ±0.3°C among the three specimens (Table 3). Since there are no long-term records of the Dicksonfjord water temperature, a direct modern analogue for comparison is lacking. A compilation of temperature data from a wider area (Table 1) indicates modern average water temperature of about 3°C at comparable water depth, which would indicate a decline in bottom water temperatures of about 6°C since the HCO. Furthermore, an average BWT of about 9°C satisfies the assumption that 9–10°C is the required summer minimum water temperature needed for spawning and reproduction in *A. islandica* (Golikov and Scarlato, 1973; Lutz et al., 1982; Peacock, 1989). All three shell specimens in this study recorded almost identical seasonal temperature amplitudes of 12.4°C (±0.4°C) (Figures 3 and 4; Table 3). Modern water temperatures at comparable depth (Table 1) range between −1°C and 5°C, i.e., the seasonal amplitude is about

6°C. Hence, average temperature has declined by 6°C since the HCO, and the seasonal amplitude has narrowed by 50%.

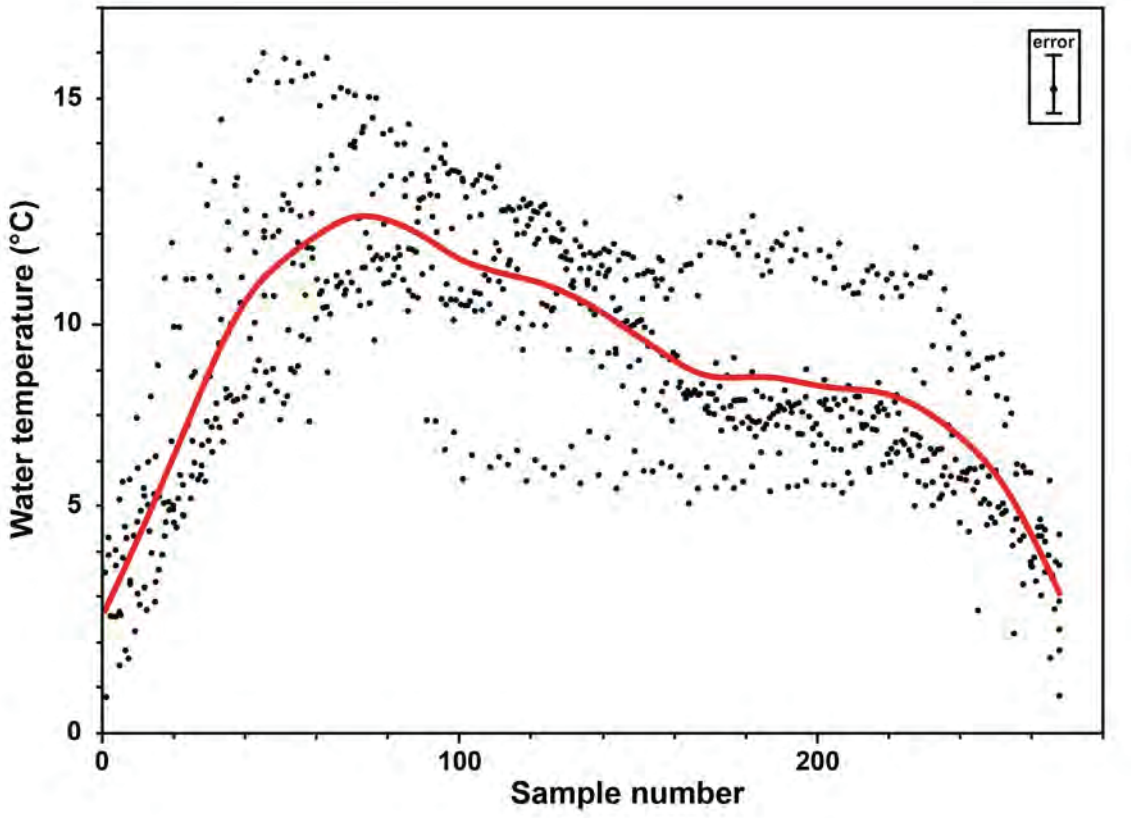

Figure 4. Seasonal temperature curve. Reconstructed water temperature based on all 796 stable oxygen isotope measurements. Spacing between individual data points has been adjusted to cover identical temporal ranges in all six ontogenetic years. Average line has been calculated using a cubic spline (λ=8000; statistical software JMP version 9.0.1, SAS Institute Inc. 2007). Error bar in inlay accounts for uncertainty due to modern seasonal salinity variation and applies for all single data points (see Section 3.3).

Even though the HCO period did not occur simultaneously throughout the Nordic Sea and Barents Sea areas, the 6°C higher HCO temperature found here is in very good agreement with previous palaeo-temperature reconstructions for the northern North Atlantic HCO derived from diatoms (+ 3–5°C in Birks and Koc (2002)) and foraminifera (+ 4–5°C in Sarnthein et al. (2003), + 6°C in Hald et al. (2004), + 6°C in Ebbesen et al. (2007), + 3–4°C in Rasmussen et al. (2014), and up to + 6°C for BWT based on oxygen isotope data) in sediment cores. Additionally, studies based on plant macrofossils (“at least” 1.5°C higher July air temperatures in Birks (1991)), mollusc shells (+ 4°C in Lubinski et al. (1999), based on the work of Salvigsen et al. (1992)) and insect data (+ 4–5°C summer air temperatures in Wohlfarth et al. (1995)) support our findings. The reconstructed temperatures and seasonal temperature range presented

here correspond very well (±0.1°C) to *A. islandica* derived southern North Sea water temperature values for the period 1884–1983 given in Schöne et al. (2004), where minimum temperatures of 2.9°C and maximum temperatures of 15.1°C result in a seasonal signal (February to September) of 12.2°C, which was also in good agreement with observational SST data. This suggests that recent southern North Sea conditions may be comparable to HCO conditions at Spitsbergen.

Given this substantiation, our results support the common assertion of polar region amplification associated with global warming (e.g., Serreze and Francis, 2006; Hald et al., 2007; Spielhagen et al., 2011) and the significant difference between global average values and actual regional impacts. Therefore, the presented temperatures might give an indication how an average increase in global temperatures by about 3.7°C, as suggested by the IPCC (2013) report, may be amplified on a regional scale such as the Svalbard archipelago.

5 Conclusions

We present a palaeo-environmental reconstruction for the early Holocene period in Svalbard, based on three sub-fossil shells of *A. Islandica* from the Dicksonfjord (Figure 1). Radiocarbon dating ($^{14}C_{AMS}$) has determined that these specimens lived during the early Holocene Climate Optimum (9,954–9,782 cal yrs BP, Table 2).

- Stable oxygen isotope ($\delta^{18}O_{shell}$) profiles of six ontogenetic years from three shells show distinct seasonal patterns with amplitudes of 2.7‰ to 2.9‰ (Figure 2);
- Reconstructed maximum and minimum palaeo-temperatures for the assumed shell growth period (April to August) of 15.2°C and 2.8°C imply a palaeo-seasonality of about 12.4°C for the early Holocene at Svalbard, giving a first unique palaeo-environmental description of a fjord setting during the Holocene Climate Optimum at Spitsbergen and coinciding with temperature requirements for *A. islandica* today (Table 3, Figures 3 and 4);
- An average bottom water temperature of 9.1°C argues for a + 6°C warmer HCO at Spitsbergen and hence our results distinctly exceed most previous global estimates (+ 1–3°C) but confirm studies indicating an amplified effect (+ 4–6°C) at high northern latitudes.

Climate archives with a sub-annual temporal resolution at high latitudes in the northern North Atlantic realm are rare. Due to changing climatic conditions over geological time-scales and related changes in the bio-geographic distribution of suitable archive species, it is challenging to provide continuous master chronologies for time spans such as the entire Holocene. However, this study demonstrates the potential of individual shell chronologies as well as of prospective cross-dated floating chronologies of the well-calibrated bio-archive *A. islandica* for providing valuable insights into palaeoceanographic and palaeo-environmental conditions at single points in time. However, special care has to be taken when interpreting these results as a proxy for the mean climate state of the early Holocene.

Acknowledgements

The first author (LB) was financed by the "Earth System Science Research School (ESSReS)", an initiative of the Helmholtz Association of German Research Centres (HGF) at the Alfred Wegener Institute (AWI), Helmholtz Centre for Polar and Marine Research. Kerstin Beyer and Lisa Schönborn (both AWI) are thanked for their help with the isotope measurements. Further thanks go to Gernot Nehrke (AWI) for help with the Raman microscope and Rosie Sheward (NOC, Southampton) for suggestions that improved the written quality of the manuscript.

Locality (Svalbard)	Latitude	Max temp. (°C)	Min temp. (°C)	Water mass/depth	Based on	Time	Reference
Hinlopenstretet	80°N	+4–5	---	---	CTD	Summer 1984	Koc et al., 2002
Kongsfjord	79°N	+7	–1	Bottom (11 m)	Ferrybox	Jul 2012 – Apr 2014	HZG/AWI (http://tsdata.hzg.de)
Kongsfjord	79°N	+7	–1	9 m (2 m above bottom)	CTD	Jul 2012 – Aug 2013	HZG/AWI (http://tsdata.hzg.de)
Kongsfjord	79°N	+7	–1.8	---	Logger	Sep 2009 – May 2011	Laudien, 2011
W Svalbard shelf	79°N	+5–6	+1	0–300 m	CTD	Aug 2005	Rasmussen et al., 2014
Kongsfjord	79°N	+7	–1	0–400 m	Mooring/CTD	2000-2003	Cottier et al., 2005
Kongsfjord shelf	79°N	+5	–1.5	0–400 m	CTD	Sep 2000, Apr 2002/2007	Tverberg and Nøst, 2009
Kongsfjord	79/78°N	+3	0	0–50 m	CTD	Jul 2002, Sep 2005	MacLachlan et al., 2007
W Spitsbergen shelf	79–77°N	+6	---	0–50 m	CTD	Sep 1998, 1999, 2000	Saloranta and Svendsen, 2001
Isfjord shelf/slope	78°N	+7	–1	0–300 m	CTD	Aug 2002, 2003, 2004	Berge et al., 2005
Isfjord shelf	78°N	+7.8	---	---	CTD	Aug 2004	Slubowska-Woldengen et al., 2007
Dicksonfjord	78°N	+8	–1.8	0–100 m	CTD	Jul/Aug 2005	Forwick, 2005
W Spitsbergen shelf	78°N	+5	–1	---	CTD	Jul/Aug 1981	Gammelsrød and Rudels, 1983
Billefjord	78°N	+7	–1.7	0–150 m	Mooring/CTD	Oct 2010 – Aug 2011	Christensen, 2012
W Spitsbergen,	78°N	+6	+2	0–600 m	---	Oct 2006, Aug 2007	Spielhagen et al., 2011
Isfjord shelf	78°N	+3.7	---	Modelled SST	NORA10	Jul–Sep average 1958 – 2009	Reistad et al., 2011
Hornsund	77°N	+3	–1.88	Near bottom water	Reverse thermometer	1984/1985	Weslawski et al., 1988

Table 1. Environmental data. Summary of published data on modern maximum and minimum water temperatures for the shelf area and fjords around Svalbard. Information given was used to estimate modern maximum, minimum and average water temperatures as well as the seasonal range for modern bottom water temperatures (BWTs). List does not claim to be complete.

Shell ID	Length (mm)	Height (mm)	Width (mm)	$^{14}C_{AMS}$ ages (raw data BP)	$^{14}C_{AMS}$ ages (cal yrs BP)	Ontogenetic age (yrs)
AI-DiFj-02	*not determined*	*not determined*	*not determined*	9,240 ± 70	9,954 ± 139	52
AI-DiFj-03	85.9	79.9	23.0	9,200 ± 50	9,838 ± 118	52
AI-DiFj-04	88.3	82.5	25.8	9,160 ± 50	9,782 ± 105	77

Table 2. Shell information. Information on shell morphology, radiocarbon ages (raw and calibrated, see Section 3.2 for details) and ontogenetic ages for all three sub-fossil shell specimens. Shell morphology of specimen AI-DiFj-02 has not been determined prior to shell coating in epoxy resin.

Shell ID	Ice Volume correction, $\delta^{18}O$ (‰)	Number of samples	Spatial sampling resolution ($\delta^{18}O$), year1/year2 (µm)	Average BWT (°C)	Minimum BWT (°C)	Maximum BWT (°C)	Seasonality (°C)
AI-DiFj-02	0.3138	298	67/31	9.0	1.8	14.4	12.6
AI-DiFj-03	0.2982	100	151/222	9.6	2.8	14.6	11.8
AI-DiFj-04	0.2907	398	27/24	9.1	3.6	16.0	12.4
AVERAGE	***---***	***796***	***50***	***9.1***	***2.8***	***15.2***	***12.4***

Table 3. Palaeo-temperatures and palaeo-seasonality. Summary of individual ice volume correction values (based on Fairbanks (1989)), total number of samples, spatial sampling resolutions for individual ontogenetic years and $\delta^{18}O_{shell}$-derived bottom water temperatures (BWTs) in specimens AI-DiFj-02, AI-DiFj-03 and AI-DiFj-04. All temperature calculations are based on Dettman et al. (1999) under the assumption of a modern $\delta^{18}O_{seawater}$ value of 0.20‰. An assumed modern salinity variability (minimum 34.02 to maximum 34.59, based on MacLachlan et al. (2007)) results in uncertainties of +0.87°C and −0.61°C on all temperature calculations respectively.

References

(Please note that references have been formatted according to style of journal)

ACIA (2004) *Impacts of a Warming Arctic – Arctic Climate Impact Assessment*. Cambridge: Cambridge University Press, pp. 1039.

Azetsu-Scott K and Tan FC (1997) Oxygen isotope studies from Iceland to an East Greenland Fjord: behaviour of glacial meltwater plume. *Marine Chemistry* 56: 239–251.

Begum S, Basova L, Heilmayer O et al. (2010) Growth and energy budget models of the bivalve *Arctica islandica* at six different sites in the Northeast Atlantic realm. *Journal of Shellfish Research* 29: 107–115.

Berge J, Johnsen G, Nilsen F et al. (2005) Ocean temperature oscillations enable reappearance of blue mussels *Mytilus edulis* in Svalbard after a 1000 year absence. *Marine Ecology Progress Series* 303: 167–175.

Berger A and Loutre MF (1991) Insolation values for the climate of the last 10 million years. *Quaternary Science Reviews* 10: 297–317.

Birks CJA and Koc N (2002) A high-resolution diatom record of late-Quaternary sea-surface temperatures and oceanographic conditions from the eastern Norwegian Sea. *Boreas* 31: 323–344.

Birks HH (1991) Holocene vegetational history and climatic change in west Spitsbergen-plant macrofossils from Skardtjørna, an Arctic lake. *The Holocene* 1: 209–218.

Bond G, Kromer B, Beer J et al. (2001) Persistent Solar Influence on North Atlantic Climate during the Holocene. *Science* 294: 2130–2136.

Bondevik S, Mangerud J, Ronnert L et al. (1995) Postglacial sea-level history of Edgeøya and Barentsøya, eastern Svalbard. *Polar Research* 14: 153–180.

Borge T, Bachmann L, Bjørnstad G et al. (2007) Genetic variation in Holocene bowhead whales from Svalbard. *Molecular Ecology* 16: 2223–2235.

Buchardt B and Simonarson LA (2003) Isotope palaeotemperatures from the Tjörnes beds in Iceland: evidence of Pliocene cooling. *Palaeogeography, Palaeoclimatology, Palaeoecology* 189: 71–95.

Butler PG, Wanamaker AD Jr, Scourse JD et al. (2013). Variability of marine climate on the North Icelandic Shelf in a 1357-year proxy archive based on growth increments in the bivalve *Arctica islandica*. *Palaeogeography, Palaeoclimatology, Palaeoecology* 373: 141–151.

Cargnelli LM, Griesbach SJ, Packer DB et al. (1999) Essential fish habitat source document: Ocean quahog, *Arctica islandica*, life history and habitat characteristics. *NOAA Technical Memorandum* 148, 1–12.

Christensen L (2012) Temporal variation of arctic marine picophytoplankton focusing on *Micromonas pusilla* (Mamiellophyceae). Master Thesis, University of Oslo, Norway.

Cottier F, Tverberg V, Inall M et al. (2005) Water mass modification in an Arctic fjord through cross-shelf exchange: The seasonal hydrography of Kongsfjorden, Svalbard. *Journal of Geophysical Research* 110: C12005.

Dahlgren TG, Weinberg JR and Halanych KM (2000) Phylogeography of the ocean quahog (*Arctica islandica*): influences of paleoclimate on genetic diversity and species range. *Marine Biology* 137: 487–495.

Dettman DL and Lohmann KC (1995) Microsampling carbonates for stable isotope and minor element analysis: Physical separation of samples on a 20 micrometer scale. *Journal of Sedimentary Research* 65A: 566–569.

Dettman DL, Reische AK and Lohmann KC (1999) Controls on the stable isotope composition of seasonal growth bands in aragonitic fresh-water bivalves (unionidae). *Geochimica et Cosmochimica Acta* 63: 1049–1057.

Ebbesen H, Hald M and Eplet TH (2007) Lateglacial and early Holocene climatic oscillations on the western Svalbard margin, European Arctic. *Quaternary Science Reviews* 26: 1999–2011.

Fairbanks RG (1989) A 17,000-year glacio-eustatic sea level record: influence of glacial melting rates on the Younger Dryas event and deep-ocean circulation. *Nature* 342: 637–642.

Feyling-Hanssen RW (1955) Stratigraphy of the marine late-Pleistocene of Billefjorden, Vestspitsbergen. *Norsk Polarinstitutt Skrifter* 107: 1–207.

Forman SL (1990) Post-glacial relative sea-level history of northwestern Spitsbergen, Svalbard. *Geological Society of America Bulletin* 102: 1580–1590.

Forwick M (2005) Marine-geological cruise to West Spitsbergen fjords on R/V Jan Mayen, July 29th – August 2nd 2005. Cruise report, University Of Tromsø, Norway.

Gammelsrød T and Rudels B (1983) Hydrographic and current measurements in the Fram Strait, August 1981. *Polar Research* 1: 115–126.

Golikov AN and Scarlato OA (1973) Method for indirectly defining optimum temperatures of inhabitancy for marine cold-blooded animals. *Marine Biology* 20: 1–5.

Hald M, Andersson C, Ebbesen H et al. (2007) Variations in temperature and extent of Atlantic Water in the northern North Atlantic during the Holocene. *Quaternary Science Reviews* 26: 3423–3440.

Hald M, Ebbesen H, Forwick M et al. (2004) Holocene paleoceanography and glacial history of the West Spitsbergen area, Euro-Arctic margin. *Quaternary Science Reviews* 23: 2075–2088.

Hop H, Pearson T, Hegseth EN et al. (2002) The marine ecosystem of Kongsfjorden, Svalbard. *Polar Research* 21: 167–208.

Intergovernmental Panel on Climate Change (2013) *Climate Change 2013: The Physical Science Basis. Contribution of Working Group I to the Fifth Assessment Report of the Intergovernmental Panel on Climate Change*. Cambridge: Cambridge University Press.

Jansen E (1989) The use of stable oxygen and carbon isotope stratigraphy as a dating tool. *Quaternary International* 1: 151–166.

Jones DS (1980) Annual cycle of shell growth increment formation in two continental shelf bivalves and its paleoecologic significance. *Paleobiology* 6: 331–340.

Kaufman DS, Ager TA, Anderson NJ et al. (2004) Holocene thermal maximum in the western Arctic (0–180°W). *Quaternary Science Reviews* 23: 529–560.

Koc Karpuz N and Jansen E (1992) A high-resolution diatom record of the last deglaciation from the SE Norwegian Sea: Documentation of rapid climatic changes. *Paleoceanography* 7: 499–520.

Koc N and Jansen E (2002) Holocene climate evolution of the North Atlantic ocean and the Nordic Seas – a synthesis of new results. In: Wefer G, Berger W, Behre KE et al. (eds) *Climate development and history of the North Atlantic realm*. Berlin Heidelberg: Springer, pp.165–173.

Koc N, Jansen E and Haflidason H (1993) Paleoceanographic reconstructions of surface ocean conditions in the Greenland, Iceland and Norwegian seas through the last 14 ka based on diatoms. *Quaternary Science Reviews* 12: 115–140.

Koc N, Klitgaard-Kristensen D, Hasle K et al. (2002) Late glacial palaeoceanography of Hinlopen Strait, northern Svalbard. *Polar Research* 21: 307–314.

Kutzbach JE and Guetter PJ (1986) The influence of changing orbital parameters and surface boundary conditions on climate simulations for the past 18,000 years. *Journal of the Atmospheric Sciences* 43: 1726–1759.

Landvik JY, Bondevik S, Elverhøi A et al. (1998) The last glacial maximum of Svalbard and the Barents Sea area: Ice sheet extent and configuration. *Quaternary Science Reviews* 17: 43–75.

Laudien J (2011) Physical oceanography at time series station Brandal in the Kongsfjorden (Spitsbergen, Arctic), 2009–09 to 2011–06. *Alfred Wegener Institute, Helmholtz Centre for Polar and Marine Research, Bremerhaven*. http://dx.doi:10.1594/PANGAEA.761660.

Lubinski DJ, Forman SL and Miller GH (1999) Holocene glacier and climate fluctuations on Franz Josef Land, Arctic Russia, 80°N. *Quaternary Science Reviews* 18: 85–108.

Lubinski DJ, Polyak L and Forman SL (2001) Freshwater and Atlantic water inflows to the deep northern Barents and Kara seas since ca 13 ^{14}C ka: foraminifera and stable isotopes. *Quaternary Science Reviews* 20: 1851–1879.

Lutz RA, Mann R, Goodsell JG et al. (1982) Larval and early post-larval development of *Arctica islandica*. *Journal of the Marine Biological Association of the United Kingdom* 62: 745–769.

MacLachlan SE, Cottier FR, Austin WEN et al. (2007) The salinity:δ^{18}O water relationship in Kongsfjorden, western Spitsbergen. *Polar Research* 26: 160–167.

Maliva RG (1998) Skeletal aragonite neomorphism – quantitative modelling of a two-water diagenetic system. *Sedimentary Geology* 121: 179–190.

Mikalsen G and Sejrup HP (2000) Oxygen isotope composition of fjord and river water in the Sognefjorden drainage area, Western Norway. Implications for paleoclimate studies. *Estuarine, Coastal and Shelf Science* 50: 441–448.

Morton B (2011) The biology and functional morphology of *Arctica islandica* (Bivalvia: Arcticidae): A gerontophilic living fossil. *Marine Biology Research* 7: 540–553.

Nehrke G, Poigner H, Wilhelms-Dick D et al. (2012) Coexistence of three calcium carbonate polymorphs in the shell of the Antarctic clam *Laternula elliptica*. *Geochemistry, Geophysics, Geosystems* 13: Q05014.

Nilsen F, Cottier F, Skogseth R et al. (2008) Fjord-shelf exchanges controlled by ice and brine production: The interannual variation of Atlantic Water in Isfjorden, Svalbard. *Continental Shelf Research* 28: 1838–1853.

Peacock JD (1989) Marine molluscs and late quaternary environmental studies with particular reference to the late-glacial period in Northwest Europe: A review. *Quaternary Science Reviews* 8: 179–192.

Rasmussen TL, Forwick M and Mackensen A (2012) Reconstruction of inflow of Atlantic Water to Isfjorden, Svalbard during the Holocene: Correlation to climate and seasonality. *Marine Micropaleontology* 94-95: 80–90.

Rasmussen TL, Thomsen E, Skirbekk K et al. (2014) Spatial and temporal distribution of Holocene temperature maxima in the northern Nordic seas: interplay of Atlantic-, Arctic- and polar water masses. *Quaternary Science Reviews* 92: 280–291.

Rasmussen TL, Thomsen E, Slubowska MA et al. (2007) Paleoceanographic evolution of the SW Svalbard margin (76°N) since 20,000 ^{14}C yr BP. *Quaternary Research* 67, 100–114.

Reimer PJ, Baillie MGL, Bard E et al. (2009) IntCal09 and Marine09 radiocarbon age calibration curves, 0–50,000 years cal BP. *Radiocarbon* 51: 1111–1150.

Reistad M, Breivik Ø and Dinessen F (2011) Ice, icing and temperature conditions around Svalbard. *Norwegian Meteorological Institute met.no report* 6: 1–82.

Reusche M, Winsor K, Carlson AE et al. (2014) ^{10}Be surface exposure ages on the late-Pleistocene and Holocene history of Linnébreen on Svalbard. *Quaternary Science Reviews* 89: 5–12.

Ropes JW and Murawski SA (1983) Maximum shell length and longevity in ocean quahogs, *Arctica islandica* Linné. *International Council for the Exploration of the Sea* K32: 1–8.

Sakshaug E, Johnsen G and Volent Z (2009) Light. In: Sakshaug E (ed) *Ecosystem Barents Sea*. Trondheim: Tapir Academic Press, pp.117–138.

Saloranta TM and Svendsen H (2001) Across the Arctic front west of Spitsbergen: high-resolution CTD sections from 1998–2000. *Polar Research* 20: 177–184.

Salvigsen O (1984) Occurrence of pumice on raised beaches and Holocene shoreline displacement in the inner Isfjorden area, Svalbard. *Polar Research* 2: 107–113.

Salvigsen O (2002) Radiocarbon-dated *Mytilus edulis* and *Modiolus modiolus* from northern Svalbard: climatic implications. *Norwegian Journal of Geography* 56: 56–61.

Salvigsen O and Høgvard K (2006) Glacial history, Holocene shoreline displacement and palaeoclimate based on radiocarbon ages in the area of Bockfjorden, north-western Spitsbergen, Svalbard. *Polar Research* 25: 15–24.

Salvigsen O, Forman SL and Miller GH (1992) Thermophilous molluscs on Svalbard during the Holocene and their paleoclimatic implications. *Polar Research* 11: 1–10.

Sarnthein M, Van Kreveld S, Erlenkeuser H et al. (2003) Centennial-to-millennial-scale periodicities of Holocene climate and sediment injections off the western Barents shelf, 75°N. *Boreas* 32: 447–461.

Schöne BR (2013) *Arctica islandica* (Bivalvia): A unique paleoenvironmental archive of the northern North Atlantic Ocean. *Global and Planetary Change* 111: 199–225.

Schöne BR and Fiebig J (2009) Seasonality in the North Sea during the Allerød and Late Medieval Climate Optimum using bivalve sclerochronology. *International Journal of Earth Sciences* 98: 83–98.

Schöne BR, Fiebig J, Pfeiffer M et al. (2005a) Climate records from a bivalved Methuselah (*Arctica islandica*, Mollusca; Iceland). *Palaeogeography, Palaeoclimatology, Palaeoecology* 228: 130–148.

Schöne BR, Freyre Castro AD, Fiebig J et al. (2004) Sea surface water temperatures over the period 1884–1983 reconstructed from oxygen isotope ratios of a bivalve mollusk shell (*Arctica islandica*, southern North Sea). *Palaeogeography, Palaeoclimatology, Palaeoecology* 212: 215–232.

Schöne BR, Houk SD, Freyre Castro AD et al. (2005b) Daily growth rates in shells of *Arctica islandica*: Assessing sub-seasonal environmental controls on a long-lived bivalve mollusk. *Palaios* 20: 78–92.

Serreze MC and Francis JA (2006) The Arctic on the fast track of change. *Weather* 61: 65–69.

Sharin VV, Kokin OV, Gusev EA et al. (2014) New geochronological data from Quaternary sediments of the Nordenskiold Land area (the Spitsbergen Archipelago). *Vestnik St. Petersburg State University Series* 7(1): 159–168.

Skirbekk K, Kristensen DK, Rasmussen TL et al. (2010) Holocene climate variations at the entrance to a warm Arctic fjord: evidence from Kongsfjorden trough, Svalbard. *Geological Society, London, Special Publications* 344: 289–304.

Slubowska MA, Koc N, Rasmussen TL et al. (2005) Changes in the flow of Atlantic water into the Arctic Ocean since the last deglaciation: Evidence from the northern Svalbard continental margin, 80°N. *Paleoceanography* 20: PA4014.

Slubowska-Woldengen M, Rasmussen TL, Koc N et al. (2007) Advection of Atlantic Water to the western and northern Svalbard shelf since 17,500 cal yr BP. *Quaternary Science Reviews* 26: 463–478.

Spielhagen RF, Werner K, Sorensen SA et al. (2011) Enhanced modern heat transfer to the Arctic by warm Atlantic water. *Science* 331: 450–453.

Stemmer K, Nehrke G and Brey T (2013) Elevated CO_2 Levels do not Affect the Shell Structure of the Bivalve *Arctica islandica* from the Western Baltic. *PloS ONE* 8: e70106.

Stuiver M and Reimer PJ (1993) Extended ^{14}C data base and revised CALIB 3.0 ^{14}C age calibration program. *Radiocarbon* 35: 215–230.

Svendsen JI and Mangerud J (1997) Holocene glacial and climatic variations on Spitsbergen, Svalbard. *The Holocene* 7: 45–57.

Tverberg V and Nøst OA (2009) Eddy overturning across a shelf edge front: Kongsfjorden, west Spitsbergen. *Journal of Geophysical Research* 114: C04024.

Wanamaker AD Jr, Kreutz KJ, Schöne BR et al. (2011) Gulf of Maine shells reveal changes in seawater temperature seasonality during the Medieval Climate Anomaly and the Little Ice Age. *Palaeogeography, Palaeoclimatology, Palaeoecology* 302: 43–51.

Wassmann P, Reigstad M, Haug T et al. (2006) Food webs and carbon flux in the Barents Sea. *Progress in Oceanography* 71: 232–287.

Weidman CR, Jones GA and Lohmann KC (1994) The long-lived mollusc *Arctica islandica*: A new paleoceanographic tool for the reconstruction of bottom temperatures for the continental shelves of the northern North Atlantic Ocean. *Journal of Geophysical Research* 99: 18305–18314.

Weslawski JM, Zajaczkowski M, Kwasniewski S et al. (1988) Seasonality in an Arctic fjord ecosystem: Hornsund, Spitsbergen. *Polar Research* 6: 185–189.

Witbaard R, Duineveld GCA and De Wilde PAWJ (1997) A long-term growth record derived from *Arctica islandica* (Mollusca, Bivalvia) from the Fladen Ground (northern North Sea). *Journal of the Marine Biological Association of the United Kingdom* 77: 801–816.

Witbaard R, Duineveld GCA and De Wilde PAWJ (1999) Geographical differences in growth rates of *Arctica islandica* (Mollusca: Bivalvia) from the North Sea and adjacent waters. *Journal of the Marine Biological Association of the United Kingdom* 79: 907–915.

Wohlfarth B, Lemdahl G, Olsson S et al. (1995) Early Holocene environment on Bjørnøya (Svalbard) inferred from multidisciplinary lake sediment studies. *Polar Research* 14: 253–275.

Manuscript V

A pronounced 11-year oscillation in high Arctic marine bivalve shells during the early Holocene Climate Optimum

Lars Beierlein[1], Mihai Dima[2], Bernd R. Schöne[3], Otto Salvigsen[4] and Thomas Brey[1]

[1]Alfred Wegener Institute, Helmholtz Centre for Polar and Marine Research, Bremerhaven, Germany

[2]Department of Matter Structure, Physics of the Atmosphere and Earth, University of Bucharest, Romania

[3]Institute of Geosciences, University of Mainz, Germany

[4]Department of Geosciences, University of Oslo, Norway

To be submitted to *PLOS ONE* (September 2014).

Abstract

Bivalve shells are reliable bio-archives for sub-annual to multi-decadal climate reconstructions. The well-established and calibrated bivalve species *Arctica islandica* is long-lived (500 years), abundant in the fossil record and widely distributed in the North Atlantic. The reconstruction of atmosphere-ocean phenomena, such as NAO, has been demonstrated successfully in this species. Here we present data from early Holocene (9,800 cal yrs BP) *A. islandica* specimens from Svalbard (79°N). All specimens exhibit a pronounced 11-year periodicity in their internal shell growth banding pattern. We hypothesise that this cycle is associated with insolation changes driven by the solar sunspot cycle and that quasi-decadal changes in UV radiation (and UV-B in particular) might act as an amplifying mechanism. In the high Arctic, where the summer bivalve growing season is characterised by 24-hour daylight, solar energy is the key limiting factor of plankton growth, the main food source for this species. Changes in plankton availability, as a direct result of varying solar radiation, are likely to be reflected in annual shell growth increments.

Keywords: *Arctica islandica*, sclerochronology, inter-annual variability, sunspot activity, Schwabe cycle

1 Introduction

Climate archives are of tremendous importance for the reconstruction of past climatic and environmental conditions and for the verification and improvement of climate models predicting future global change. The well-known archives of ice cores and sediment cores and well-established biogenic archives such as trees and corals have been complemented in recent decades by speleothems, coralline algae, otoliths and bivalve shells, providing crucial archives with sub-annual resolution. The application of different biogeochemical and anatomical proxies on these biogenic archives additionally facilitates environmental reconstructions from tidal (~12.4 h) to multi-centennial time-scales. This considerably improves upon the decadal to multi-decadal temporal resolution that can be achieved at best from ice or sediment cores (7–20 years and 100–1000s years resolution respectively).

Individual bivalve shells, such as *Arctica islandica* investigated in this study, record ambient environmental information in the growth rate of accreted shell material at a significantly higher temporal resolution. This provides sub-annual (circadian to seasonal) records of past climatic and environmental conditions (Schöne et al., 2005b; Schöne et al., 2005c). In addition, the application of cross-dating techniques to individual specimens, reaching ages of up to 500 years (e.g., Butler et al., 2013), can produce master chronologies that span several centuries (e.g., Butler et al., 2010; Butler et al., 2013), enabling palaeo-environmental reconstruction from sub-seasonal to multi-centennial timescales.

The high temporal resolution and decadal to centennial ontogenetic ages of bivalves such as *A. islandica* make them particularly well suited as recorders of inter-annual climate and atmospheric signals that cannot be captured in other lower resolution archives. Phenomena such as the North Atlantic Oscillation (NAO), Arctic Oscillation (AO) and El Niño-Southern Oscillation (ENSO) have been documented within the changes in bivalve shell growth (e.g., Schöne et al., 2003; Schöne et al., 2005c; Epplé et al., 2006; Wanamaker Jr et al., 2009; Ambrose et al., 2006; Brey et al., 2011).

In addition to these larger-scale, multi-annual ocean-atmosphere phenomena, solar irradiance is a fundamental driving component of Earth's energy balance and global climate (e.g., Haigh, 1996), although the extent of direct and indirect effects of the Sun on climate is still highly debated (e.g., Rind, 2002). Within many climate

archives, patterns in growth, accumulation or sedimentation have been found to correspond to specific periodicities associated with the Sun´s magnetic field: the Hale cycle (Hale, 1908) of ~22 years (e.g., tree rings; Raspopov et al., 2004b), sediment cores; Patterson et al., 2004), the Gleissberg cycle of ~90 years (e.g., sediment cores; Kern et al., 2013 or tree rings; Roig et al., 2001) or the ~220 year Suess (e.g., Suess, 1980) cycle (e.g., tree rings; Roig et al., 2001 or sediment cores; Cortese et al., 2005). The 11-year sunspot Schwabe cycle (e.g., Schwabe, 1844; Gnevyshev, 1977; Hathaway, 2010) has been less frequently identified within palaeo-archives due to their often limited temporal resolution and then exclusively from archives with annual or sub-annual temporal resolution (see Table 1 for overview; Figure 1).

Figure 1. Map of localities where 11-year signals have been reported in early Holocene *A. islandica* shells (X) and the source areas of modern bivalve chronologies (I–III) used in this study. Numbers 1–10 give localities for published studies reporting a solar-related 11-year signal in various archives. Detailed information on individual studies (1–10) is given in Table 1. Compilation does not claim to be complete.

Of these reported Sun-related periodicities, few studies have attempted to explain how solar activity is mechanistically linked to the climate archive in question (c.f., Frisia et al., 2003 for stalagmites in Italy). It is essential to understand how environmental parameters influenced by solar activity affect the growth of the biogenic archive in order to reliably associate variability in growth increment width, accumulation or sedimentation to the correct climatic driving mechanism. For most archives, solar periodicities are prominently manifested, although a direct link between total solar irradiance (TSI) and growth, accumulation or sedimentation patterns

appears to be unlikely (c.f., Gray et al., 2010). Since changes between a maximum and a minimum in the sunspot cycle only amount to a total TSI change of about 0.1% (Schlesinger and Ramankutty, 1992), an amplifying mechanism is potentially needed to intensify the initial TSI change. In bivalve growth records (e.g., Butler et al., 2013), a reported 11-year cyclicity was associated to solar activity, but with no further explanation on the mechanistic link between shell growth and sunspot activity. The simple observation and reporting of correlations is no longer sufficient to advance and fully exploit the use of bivalves as a proxy for past climate conditions. Investigations to systematically link internal and external climate drivers to environmental controls on bivalve shell growth level are now urgently required. Future studies on modern bio-archives must seek detailed knowledge on the growth-related processes required to differentiate precisely between natural and anthropogenic climate driving mechanisms.

We present the results of the frequency analysis of the growth records of six individual early Holocene (9,800 cal yrs BP) *A. islandica* bivalve shells, which have been derived from raised beach deposits in the Dicksonfjord, Svalbard (79°N). We carefully discuss the possible links between the pronounced 11-year periodicity identified in the growth of the shells to the solar sunspot cycle and propose a first theoretical explanation for a connection between Solar irradiance and bivalve growth via a potential amplifying mechanisms such as UV radiation.

2 Material and Methods

2.1 Shell origin and sample preparation

The six *A. islandica* shells analysed in this study have been derived from raised beach deposits in the Dicksonfjord, Svalbard. Further details on the sampling locality and the dating ($^{14}C_{AMS}$) of the shells are given in Beierlein et al. (2014). All shells were externally strengthened with an epoxy resin to prevent them from breaking while sawing. 3 mm cross-sections were prepared by sawing along the line of strongest growth (running perpendicular to the growth lines, Figure 2a, b) using a low-speed precision saw (Buehler, IsoMet) equipped with a 0.4 mm diamond-coated saw blade. Cross-sections were ground using a manual grinder (Buehler, Phoenix Alpha) and sand paper with three different grain sizes (15 µm, 10 µm and 5 µm). Afterwards, the 3 mm cross-

sections were stained in Mutvei´s solution (Schöne et al., 2005a) for 23 minutes at constant 38°C.

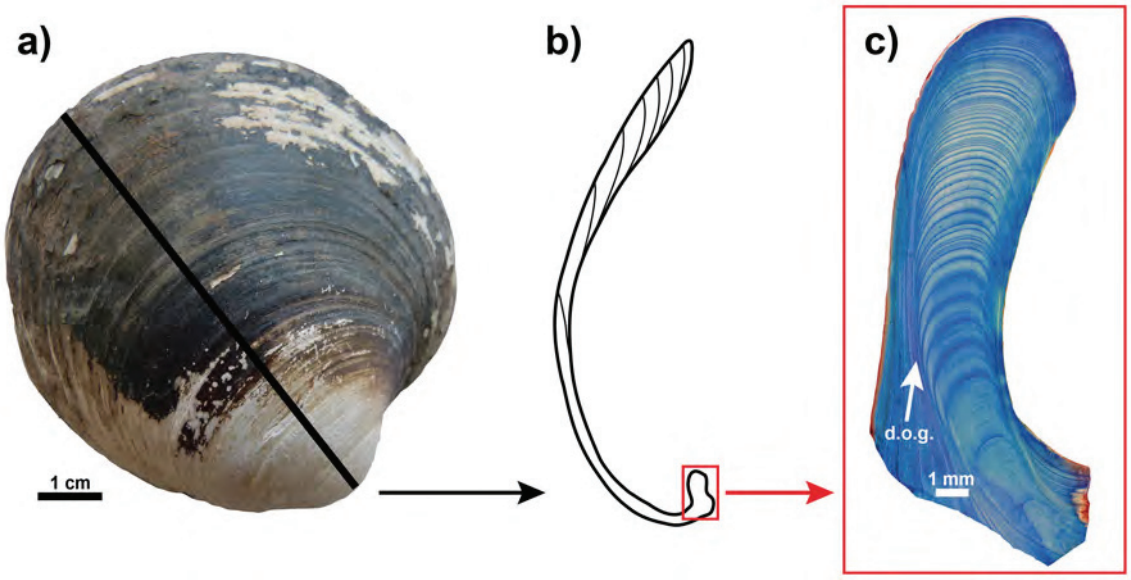

Figure 2. Shell of early Holocene *A. islandica* (ID: AI-DiFj-08) from the Dicksonfjord (A) giving the location of the cutting axis (black line) perpendicular to the growth increments. Sectioned shell in (B) illustrating the hinge plate of umbonal area (red box) in which growth increments have been counted and measured. Cross-sections have been stained in Mutvei´s solution to improve visibility of internal growth increments (C). Darker lines correspond to annual growth cessation in autumn/winter. Arrow gives direction of growth (d.o.g.) in hinge plate.

Digital images were taken using a stereo-microscope (Olympus, SZX12) attached to a CCD camera (Olympus, U-CMAD) and increment widths in all specimens were counted and measured in the hinge plate of the shells (Figure 2) using the image processing software analySIS (Olympus; version 5.1).

2.2 Shell growth records and statistical methods

Individual growth records were detrended using a cubic spline (λ = 500; statistical software JMP version 9.0.1, SAS Institute Inc. 2007) and dimensionless standardized growth indices (SGI) have been calculated following Butler et al. (2010). To check individual SGI time-series for quasi-periodic oscillation patterns (c.f., Ghil et al., 2002), we employ a two-step procedure following Ivany et al. (2011) starting with Singular Spectrum analysis (SSA; Allen and Smith, 1997) and followed by spectral density analysis using Multi-Taper method (MTM; Mann and Lees, 1996). In this regard, SSA has been used to reconstruct a 'filtered' SGI time-series based on the first ten SSA components to filter noise from the time-series. The associated relative spectral

densities (adjusted to the range of 0–1) for the first 10 SSA components were then considered for the MTM approach. MTM divides the spectral density into 512 equally spaced frequencies in the frequency range from 0 to 0.5. A composite frequency series (from hereon referred to as 'stacked MTM') has been computed from the resulting 512 frequencies x 6 individual shell time-series matrix to check for common/joint signals in the spectral domain. Subsequently, shared signals between individual shell records become more prominent while single signals, occurring only in individual time-series, are filtered out. Both methods (SSA and MTM) were conducted using kSpectra Toolkit software (version 3.4 by SpectraWorks) with settings chosen as described in Ivany et al. (2011).

A high percentage of explained total variance indicates a significant signal but does not necessarily indicate stationarity over time (c.f., Dima et al., 2005). To check prospective quasi-periodic signals within SGI time-series for stationarity over time, we computed continuous wavelet transformations using the online tool IONScript (http://ion.researchsystems.com/IONScript/wavelet/) as described by Torrence and Compo (1998).

2.3 Data on climate indices and sunspot activity

Northern hemisphere climate variability is assumed to exert significant influence on high Arctic environments such as Svalbard and thus may be reflected in *A. islandica* shell growth patterns. We therefore considered the frequency of oscillation patterns of modern climate oscillation indices, i.e., the North Atlantic Oscillation (NAO), the Arctic Oscillation (AO) and the Arctic Climate Regime Index (ACRI). Detailed information on each of the indices can be found in Hurrell et al. (2003), Jones et al. (1997) (NAO), Thompson and Wallace (1998) (AO) and Johnson et al. (1999) (ACRI). Data for the frequency analysis of NAO were obtained from (www.cru.uea.ac.uk/cru/data/nao/) and from (www.cpc.ncep.noaa.gov/products/) for AO. An updated index for ACRI has been provided by Proshutinsky (pers. comm.; Proshutinsky and Johnson, 1997).

Regarding sunspot activity, this study focuses exclusively on the solar cycle with an average duration of about eleven years (Schwabe cycle, e.g., Gnevyshev, 1977). The 11-year Schwabe sunspot cycle is a quasi-periodic signal associated with the magnetic field of the Sun (Schwabe, 1844; Hathaway, 2010). We therefore use a record of the raw numbers of sunspots, which has been published by the Solar

Influences Data Analysis Center (SIDC), Royal Observatory of Belgium (http://sidc.oma.be/sunspot-data/).

Spectral density analysis (SSA and MTM) on climate indices has been applied as described in Section 2.2 with window lengths chosen to be between 1/2 and 1/3 of the original time-series and considering the first ten SSA components, ranked by total variance explained, for the computation of a filtered time-series.

2.4 Modern and historical bivalve growth chronologies from the North Atlantic

In order to investigate a potential correlation between shell growth and solar activity, modern bivalve shell growth data from three different localities in the northern North Atlantic have been analysed. A 39-year long chronology covering the time period from CE 1969 to 2007 has been derived from *Ciliatocardium ciliatum* shells from the Barents Sea (I in Figure 1), which have been published in Carroll et al. (2014). All specimens comprising the chronology are influenced by Arctic water at a depth of about 100 m (c.f., Carroll et al., 2014) with individual years within the chronology represented by a minimum of 5 shells and a maximum of up to 16 shells. Further, a 41-year long time-series derived from growth records of *Mya* sp. from the east coast of Greenland (II in Figure 1) and covering CE 1960 to 2000 has been provided by Mikael Sejr (Aarhus University). Finally, the 1357-year long *A. islandica* chronology reported by Butler et al. (2013) from Iceland (http://hurricane.ncdc.noaa.gov/pls/paleox) has been analysed (III in Figure 1). Since this time-series extends the length of the sunspot time-series, correlation analysis is based on the time-period CE 1749 to 2005. All time-series have been analysed as described in Section 2.2.

3 Results

3.1 Inter-annual variability in early Holocene bivalve shells and the sunspot cycle

Ontogenetic ages ranged from 52 years in specimen AI-DiFj-02 to 87 years in specimen AI-DiFj-10 (see Table 2 for details). Within most specimens a distinct increase and decrease pattern within the internal hinge plate growth pattern is visible with the naked eye once stained (Figure 2c). SSA analyses identify significant frequencies in the range from 0.080 to 0.103 yr^{-1}, i.e., between about 9.7 and 12.5 years (from here on defined as the 11-year signal within the shell growth records), explaining between 19.3% and 39.8% of total variance in all six individual specimens (Figure 3, Table 2). Specific time empirical orthogonal functions (EOF) associated with the 11-year components are in quadrature, indicating a stable oscillation (c.f., Dima et al., 2005). Additionally, frequencies in the ranges 0.170–0.190 yr^{-1} (i.e., 5.2 to 5.9 years) and 0.350–0.390 yr^{-1} (i.e., 2.5 to 2.9 years) have been found, although these are not significant in all six specimens (MTMs in Figure 3). For illustrative purposes, reconstructed time-series for the regularly oscillating ~11 year components have been reconstructed using SSA (dashed lines in Figure 3a–f) and are shown with the initial SGI time-series (bars in Figure 3a–f). Continuous wavelet transformations (Figure 3m–r) confirm a ±11-year periodicity in all six shells specimens, but indicate that the strength of the signal is not equally pronounced throughout the time-series.

The stacked MTM spectrum of all six shell specimens combined (Figure 4a) shows significant (above 99% significance levels) frequency peaks at about 0.093 yr^{-1} (i.e., 10–11 years), ~0.187 yr^{-1} (i.e., 5–6 years) and ~0.364 yr^{-1} (i.e., 2–3 years). SSA and MTM analysis on the sunspot data identifies periodicities at ~0.092 yr^{-1} (i.e., 10–11 years) and ~0.188 yr^{-1} (i.e., 5–6 years) above the 99% significance level (Figure 4b).

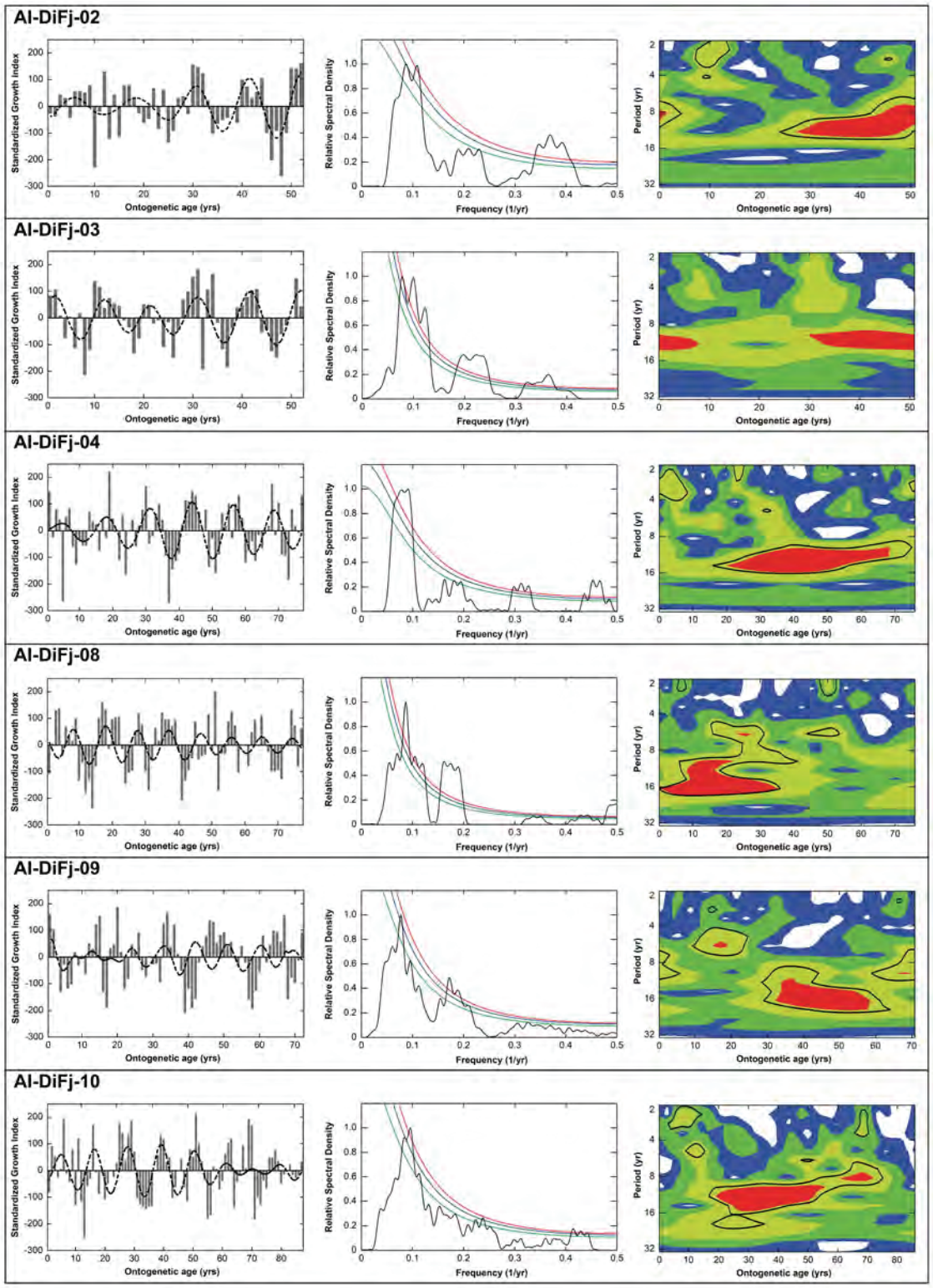

Figure 3. Spectral analysis of six early Holocene *A. islandica* specimens from the Dicksonfjord. For each individual shell-derived time-series a standardized growth index (SGI) has been calculated (grey bars in A–F). By applying a Single Spectrum Analysis (SSA), significant oscillations within the SGI time-series have been identified and for each the 11-year component has been reconstructed (dashed lines in A–F). Detailed information on explained total variance and exact frequency of reconstructed 11-year signal can be found in Table 2. Spectral density analysis by Multi-Taper method (MTM) of individual SGI time-series gives information on the significance of different oscillatory cycles (G–Q). Green (90%), blue (95%) and red (99%) lines being significance levels. Continuous wavelet transformations of individual SGI time-series, giving information on stationarity over time (M–R).

3.2 Correlation between modern bivalve shell growth and the sunspot cycle

SSA and MTM analyses of three modern shell-derived chronologies from three different bivalve species and from three different localities (Figure 1; Table 1) identify significant 11-year periodicities in all three chronologies (Figure 5). Further, the reconstructed 11-year signal has been correlated (without time-lag) to the sunspot data from the identical time-period (bars in Figure 5). Identified 11-year signals in the 39-year long chronology derived from *C. ciliatum* specimens from the Barents Sea as well as in the *Mya* sp. derived growth record of 41 years (1960–2000) for the east coast of Greenland both show strong negative correlations ($r = -0.84$; $P < 0.0001$ and $r = -0.77$; $P < 0.0001$ respectively) to the sunspot cycle. MTM analysis in the *A. islandica* derived chronology confirms the significant ~11-year component as reported in (Butler et al., 2013) (Figure 5). Further, the reconstructed signal in *A. islandica* (dashed line in Figure 5) is negatively correlated ($r = -0.29$; $P < 0.0001$) to the sunspot cycle for the time-period from 1749 to 2005.

4 Discussion

4.1 Inter-annual climate variability in early Holocene *A. islandica* growth records

All six SGI series derived from early Holocene *A. islandica* shells contain multiple significant frequencies (Figure 3). The most prominent frequency is a quasi-decadal periodic signal in the range 0.080 to 0.103 yr^{-1} occurring in all six shells (Table 2, Figure 3). Although these 11-year signals are significant (Figure 3g–x) and describe up to 39.8% of total variance (Table 2), they are not equally strong throughout the lifetime of the organism (Figure 3m–r). For further analysis, spectral information from all six individual shells (Figure 3g–q) has been averaged and a stacked MTM has been computed (Figure 4a). The shells share significant frequencies at ~0.093 yr^{-1}, ~0.187 yr^{-1} and ~0.364 yr^{-1}, which can be translated into oscillations of 10 to 11, 5 to 6 and 2 to 3 years (indicated by grey bars in Figure 4a). The 2–3 year oscillation will not be further discussed, since this signal can be associated with many different phenomena (e.g., NAO, ENSO) and is therefore not considered to be a distinctive feature.

Ideally, a correlation study should be supported by evidence in the form of inter time-series correlation and not based solely on spectral characteristics (c.f., Wunsch, 1999). However, a direct correlation of early Holocene growth records with modern observational data is not possible. Furthermore, due to colder modern water temperatures compared to the early Holocene, *A. islandica* cannot be found today at comparable latitudes to the Holocene specimens (Dahlgren et al., 2000). Hence, to assess the potential climate drivers of the observed 10–11 year and 5–6 year signals we compared spectral 'fingerprints' (MTM) of the stacked early Holocene records with the spectral 'fingerprints' (MTM) of modern ('internal') climate phenomena such as NAO, AO and ACRI, as well as ('external') solar activity time-series, that are likely to have affected ambient environmental conditions in the North Atlantic region. *A. islandica* has previously been shown to be a convenient recorder of inter-annual environmental signals such as the NAO (e.g., Schöne et al., 2003, Schöne et al., 2005c, Epplé et al., 2006, Wanamaker Jr et al., 2009). Additionally, effects of large-scale climate variability on shell growth have been found in a number of different bivalve species (e.g., ACRI in *Serripes groenlandicus* at Svalbard (Ambrose et al., 2006) or El Niño-Southern Oscillation (ENSO) at the Antarctic peninsula in *Laternula elliptica* (Brey et al., 2011)).

The stacked shell 'fingerprint' does not readily match the 'fingerprints' of these internal climate phenomena (not shown). However, the 5–6 year oscillation could correspond to a distinct 5-year oscillation (frequency: 0.200 yr^{-1}; 95% significance level) within the annual average NAO time-series. In comparison, the sunspot number MTM 'fingerprint' (Figure 4b) strongly resembles both the 5–6 year signal as well as the 10–11 year signal within the stacked shell MTM 'fingerprint' (Figure 4a). We therefore consider that sunspot activity is one likely explanation of the observed signals within these six early Holocene *A. islandica* shells.

When analysing strong and pronounced signals in frequency analysis, such signals can create so-called harmonics, with amplitudes inversely proportional to the initial frequency ('signal/2', 'signal/3', 'signal/4'; c.f., Lamb, 1972). Accordingly, in this study, predicted harmonics for a pronounced 0.093 yr^{-1} (= 10.8 year) frequency would be expected at 0.186 yr^{-1} (= 10.8/2 = 5.4 years), 0.279 yr^{-1} (= 10.8/3 = 3.6 years) and 0.372 yr^{-1} (= 10.8/4 = 2.7 years). Consequently, the identified signals at 5–6 years and 2–3 years (Figure 4a) could be considered harmonics of the initial 11-year signal rather than have a separate climatic or physical origin.

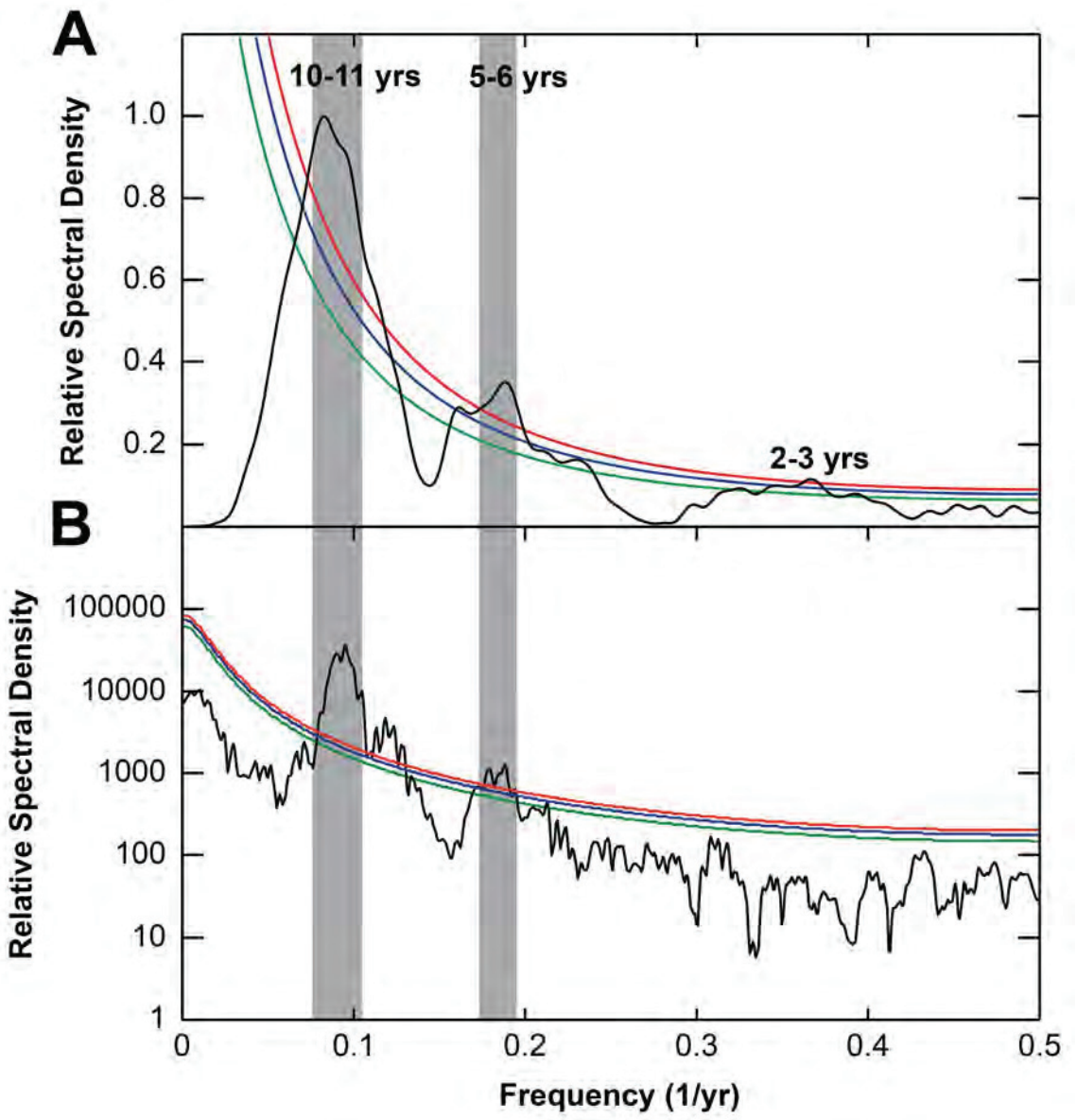

Figure 4. Comparison of spectral density 'fingerprints' in the form of stacked early Holocene *A. islandica* (all six shells) MTM (A) and sunspot number MTM (B) time-series (CE 1749–2012). Both MTMs share significant peaks at 11–10 years and 5–6 years respectively (highlighted by grey bars). Green (90%), blue (95%) and red (99%) lines being significance levels. Note that for illustration purposes the sunspot MTM has been plotted to a logarithmic scale.

Independent of the origin of these signals, this analysis is limited by the fact that these growth records represent early Holocene floating chronologies and therefore it cannot be excluded that a certain time lag existed between the signal recorded inside the shells and the output signal (source), as was found in Ambrose et al. (2006) and Witbaard et al. (2003). Hence, no evidence for a positive or negative correlation between the observed 11-year early Holocene shell signal and its potential output signal can be given.

4.2 Indications for a positive or negative correlation in modern bivalve growth records

Modern bivalve shell growth series from east Greenland, the Barents Sea and Iceland also exhibit significant 11-year signals (Figure 5), which are negatively correlated to the solar sunspot cycle ($r = -0.84$; $P < 0.0001$ for *C. ciliatum;* $r = -0.77$; $P < 0.0001$ for *Mya* sp.; $r = -0.29$; $P < 0.0001$ for *A. islandica*) when reconstructed by SSA from the original time-series. This argues for reduced bivalve growth during times of sunspot maxima associated with increased solar irradiance. However, despite this observed correlation, the mechanistic link remains unknown and it cannot be excluded that a certain time lag might have occurred.

4.3 Possible amplification mechanisms between sunspot activity and bivalve growth

The 0.1% difference in total solar irradiance (Schlesinger and Ramankutty, 1992) between a sunspot maximum and a sunspot minimum is unlikely to be sufficient to account for up to 40% of explained total variance in shell growth variability as observed in the early Holocene *A. islandica* specimens (Figure 3, Table 2). Consequently, the presumed effect of solar activity on growth in *A. islandica* is assumed to be solar influenced via an indirect atmosphere or oceanic feedback rather than solar forced (direct influence). Accordingly, an amplifying mechanism associated with the mechanisms of the internal atmosphere and ocean system (c.f., Meehl et al., 2009) would be required to intensify the 0.1% TSI change. Ruzmaikin (1999) for example, has shown that climate phenomena such as ENSO (2–7 years recurrence interval) are well suited to amplify the 11-year solar variability. Previous studies have successfully identified an 11-year periodicity in the surface temperature field (North et al., 2004) and in the sea surface temperatures (SSTs) of the upper ocean (White et al., 1997; van Loon et al., 2007). Such cyclicity has also been linked to the hydrological cycle and sedimentology, as 11-year cycles have been found in annually laminated sediment cores (e.g., Castagnoli et al., 1987) and the dust concentration of the Greenland GISP2 ice core (Ram et al., 1997; Figure 1; Table 1). On a global scale the effect of such indirect processes might be small, but the regional response to solar variability may be stronger.

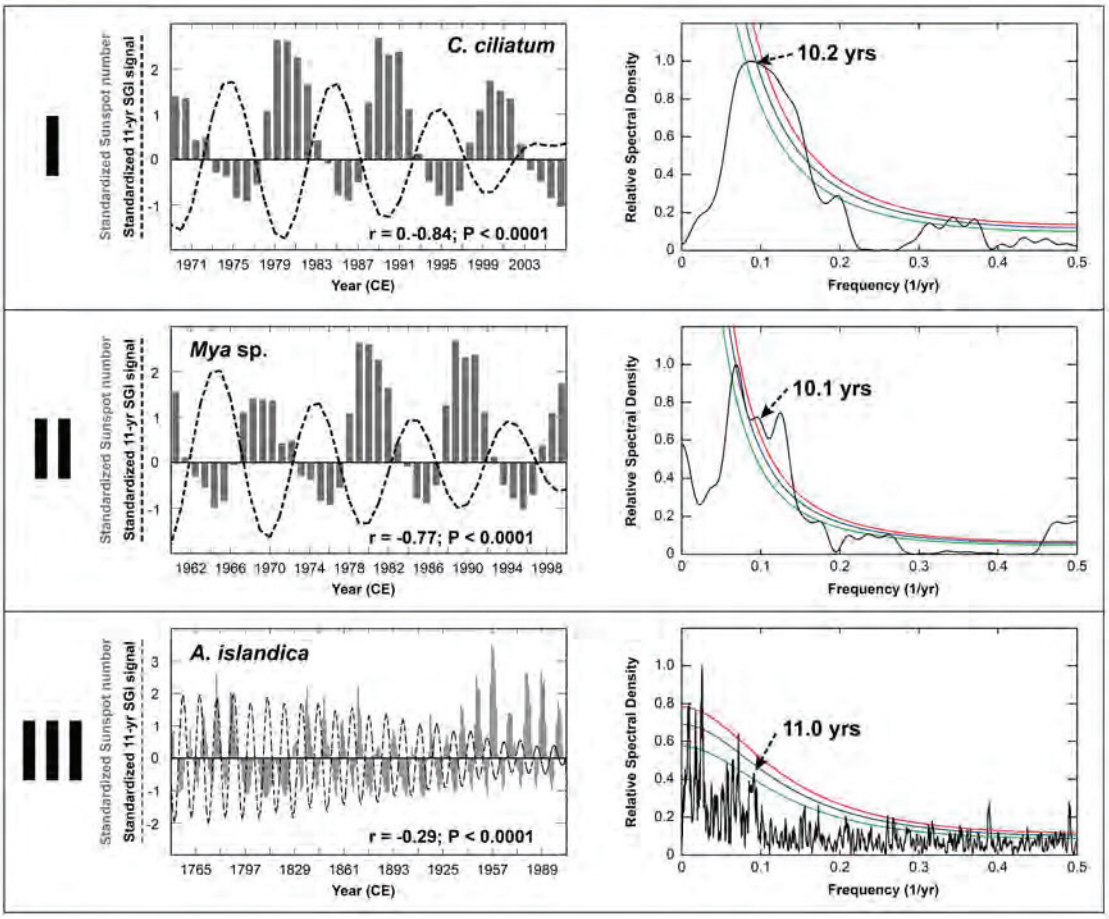

Figure 5. Correlation between modern bivalve shell chronologies and the sunspot cycle. Localities of chronologies are given in Figure 1 as I, II and III. (I, left) SSA-reconstructed 10.2-year signal from 39-year long *Ciliatocardium ciliatum* derived shell chronology from the Barents Sea (black dashed line) strongly negative correlated (r = –0.84; P < 0.0001) to sunspot number (grey bars). (I, right) MTM for SGI time-series, showing that SSA-reconstructed 10.2-year signal is significant. (II, left) SSA-reconstructed 10.1-year signal from 41-year long *Mya* sp. derived shell chronology from E Greenland (black dashed line) strongly negative correlated (r = –0.77; P < 0.0001) to the sunspot number (grey bars). (II, right) MTM for SGI time-series, showing that SSA-reconstructed 10.1-year signal is significant. (III, left) SSA-reconstructed 11-year signal from 260-year long *A. islandica* derived shell chronology from Iceland (black dashed line) negatively correlated (r = –0.29; P < 0.0001) to the sunspot number (grey bars). (III, right) MTM for SGI time-series, showing that SSA-reconstructed 11-year signal is significant. Green (90%), blue (95%) and red (99%) lines being significance levels.

Several studies have reported an 11-year cyclicity in various marine bio-archives (e.g., Halfar et al., 2007; Butler et al., 2013; Table 1) and associated it to solar activity. An 11-year cycle has additionally been identified in various other archives and biological organisms. Raspopov et al. (2004b), Lamb (1972), Damon et al. (1998) and Rodolfo Rigozo et al. (2007) have shown an 11-year cycle, as well as longer-term solar cycles, in the growth ring widths and $\Delta^{14}C$ measurements in tree-rings from Russia, Northern Scandinavia, the USA and Chile (Figure 1; Table 1). A Sun-related 11-year cycle has been found in freshwater phytoplankton blooms of Lake Baikal (Bondarenko and Evstafyev, 2006) and in the laminae thickness of speleothems from Italy (Frisia et

al., 2003). Although it is hypothesized that pronounced 11-year signals in these record are correlated with the 11-year Schwabe sunspot cycle, crucially to date, no explanation for a potential mechanistic links in marine biogenic archives has been explored. In order to foster debate on this important topic, we will present and discuss a feasible mechanistic link that includes potential amplifying mechanisms linking variability in shell growth to solar activity.

Shell growth is primarily limited by water temperature and food availability/ quality (e.g., Witbaard et al., 1999). Under the assumption that a direct link between solar activity and shell growth is not feasible, it seems most likely that a potential amplifying mechanism would impact shell growth via temperature and/or food. Under modern conditions, an insolation change of 0.1–0.2% (Willson and Hudson, 1991) would result in an average surface air temperature difference of about 0.1°K (Camp and Tung, 2007), which is considered undetectable in most proxy time-series and negligible compared to the daily and seasonal sea surface temperature variability experienced by many organisms. The most likely limiting factor in the growth of *A. islandica* in this context is therefore considered to be fluctuations in the availability of their food source, phytoplankton (Witbaard et al., 2003), which is also considered to be true for other benthic organisms (Christensen and Kanneworff, 1985; Brey et al., 1995; Ambrose et al., 2006). We subsequently discuss two amplification scenarios based on the link between solar irradiance and food source availability that provide a hypothetical explanation for the observed results from early Holocene and modern shell chronologies.

4.3.1 Cloud coverage, galactic cosmic radiation and atmospheric blocking events

Cloud cover is considered to be a potentially powerful climate feedback (IPCC, 2013) through its influence on the heat and radiation budget of the atmosphere and is thus a potential amplifying mechanism of TSI on Earth´s climate (Carslaw et al., 2002). Closely linked to this, a correlation between cosmic ray intensity and North Atlantic regional cloud cover (Marsh and Svensmark, 2000) suggests a link between atmospheric ionization by cosmic rays and the process of cloud nucleation (Kirkby, 2007), i.e., stronger solar winds associated with sunspot maxima result in less cosmic particles in the atmosphere and fewer clouds (Carslaw et al., 2002). One consequence of cloud cover is the significant impact of light availability on surface ocean primary production

(Sverdrup, 1953; Sakshaug et al., 2009b) and therefore the quality and quantity of food available to benthic deposit feeders such as *A. islandica*. We might therefore expect that intervals of solar maxima would be associated with reduced cloud cover and higher levels of incident irradiance to the surface ocean. This may result in increased primary production where light is a limiting factor for growth. Persistent reduced cloud cover may also act to strengthen the thermal stratification of the surface ocean, particularly during the summer (growing) season, which may also act to increase plankton biomass yields through greater light intensity, warmer SSTs and extending the duration of spring and autumn blooms. These processes would increase the food availability to benthic organisms. This mechanism is likely to be of greatest influence in the mid- to high-latitudes, where seasonal gradients in primary production are thought to be strongly influenced by light availability (Sakshaug et al., 2009b) and the available nutrients can support high phytoplankton yields (Sakshaug et al., 2009a). However, this explanation does not correspond to the inverse relationship that we observe between solar irradiance and modern shell growth chronologies (see Section 4.2).

4.3.2 Atmospheric processes and solar-induced impacts on winds and ocean mixing

The impact of solar activity and atmospheric heating can have a significant impact on the strength of large-scale atmospheric motion and wind stress. Fluctuations in the direction of flow and strength of dominant regional air masses are expected to effect the strength of ocean mixing, which is a crucial driver of nutrient delivery from sub-surface, nutrient-rich water to nutrient-deplete surface water. The influence of wind stress on ocean mixing has previously been documented in a number of studies investigating climate phenomena such as NAO and ENSO, which are the product of fluctuations in atmospheric pressure gradients and are thought to be driven in part by solar forcing (e.g., Huth et al., 2007; Kodera, 2003). The variability between solar minima and solar maxima may have a similar impact on mixing and nutrient supply, as the patterns in surface temperature and pressure during solar minima have been likened to the negative phases of NAO/AO (Ineson et al., 2011; Gray et al., 2005). Wind-driven changes in water mass mixing, nutrient delivery and subsequent plankton productivity were a suggested mechanism by which NAO-like oscillations were recorded in Norwegian Sea *A. islandica* growth records (Schöne et al., 2003). It is therefore possible that during solar minima, where the atmospheric system more

closely resembles the pressure fields of the negative phase of NAO, the weaker pressure gradient between high- and mid-latitudes results in weaker wind stresses over the North Atlantic region (Labitzke, 1987; Kodera, 1995; Kodera, 2002; Ineson et al., 2011). This reduces the extent of wind-driven surface ocean mixing and nutrient delivery to the surface is weaker. Subsequently, primary production is reduced during periods of solar minima, and may additionally be reduced by lower irradiance caused by increased cloud cover during solar minima. Again however, this explanation does not satisfy the inverse correlation observed between solar activity and shell growth. Conversely it is possible that, while increased mixing supplies more nutrients, the deepening of the mixed layer may results in reduced irradiance for much of the phytoplankton community and therefore reduces plankton yields during periods of solar maxima.

4.3.3 UV-B radiation and ozone

A solar maximum is associated with maximum irradiance in UV radiation in addition to a 0.1% increase in TSI (Schlesinger and Ramankutty, 1992). The amount of highly energetic UV-B radiation (280–315 nm; e.g., Aas et al., 2002) is subsequently also increased during solar maximums (Lean et al., 1995). While a significant portion of UV-B radiation is absorbed and scattered by the atmosphere/ozone layer, the small fraction of UV-B reaching Earth´s surface and penetrating the uppermost ocean to biologically significant depths (Helbling and Villafane, 2002) has a broad variety of mainly negative effects, such as impairment of photosynthesis, phytoplankton productivity and irreversible damage to phytoplankton photochemical systems (e.g., Häder et al., 2003; Häder et al., 2007), effects on Calvin cycle enzymes (e.g., Bischof et al., 2002), bleaching of photosynthetic pigments (Häder et al., 2003) or damage to DNA and membranes (Bischof et al., 2002; Häder et al., 2003). Furthermore, latest observation by Spectral Irradiance Monitor (SIM) satellite measurements indicate that variations in solar UV irradiance might be larger than previously assumed (Ineson et al., 2011; Harder et al., 2009). We therefore hypothesize a strongly simplified model (Figure 6) in which intervals of solar maximum, associated with a maximum in UV-B radiation penetrating the upper meters of the oceans, would result in the reduced quantity and nutritional quality of phytoplankton due to photoinhibition and damage to essential cell components. Food supply for the benthic community is reduced and subsequently results in relatively weak shell growth during solar maxima. Phytoplankton productivity

therefore acts as an amplifier of the initial irradiance change and explains the inverse correlation we found between TSI and growth increment width in the modern shell chronologies (Figure 5). To our knowledge, a correlation between the 11-year Schwabe cycle and primary production in the Arctic has not yet been published, mainly because observational data and measurements do not cover a time period long enough for detection. However, the component steps involved in this hypothetical model are very well described in the literature: a positive correlation between sunspot activity and UV-B radiation (Lean et al., 1995; Floyd et al., 2003), an inversely correlated dependence between UV-B radiation and phytoplankton productivity (Stuiver and Braziunas, 1993; Wängberg et al., 1998), especially at high latitudes (e.g., Sinha et al., 2001) and the positive correlation between phytoplankton productivity and shell growth rates at the benthos (e.g., Witbaard et al., 1999; Carroll et al., 2008).

Inter-annual variations in solar activity during the early Holocene solar maximum (8% more solar energy; Berger and Loutre, 1991) in the high Arctic, where irradiance is strongly seasonal (e.g., Rasmussen et al., 2012), are even more likely to have had an (indirect) impact on shell growth through this mechanism. Hence, due to its very direct influence on pelagic primary producers in a shallow water ecosystem such as a high Arctic fjord at Svalbard during the early Holocene solar maximum, decadal changes in UV-B radiation are considered the most likely explanation and amplifying mechanism in the early Holocene *A. islandica* shells so far.

Both processes – via atmospheric processes or UV radiation – described above would explain the negative correlation observed in the three modern shell master chronologies (Figure 5). However, it is equally conceivable that the signal could be positively correlated to another atmospheric and/or oceanic process and might also have occurred with a certain time lag. For example, an increase in solar energy might have prolonged the relative growing season of *A. islandica*: higher TSI may cause an extension of the period of thermal stratification and thus of pelagic primary production into spring (earlier onset) and as well as into autumn (later breakup) resulting in a longer growth period for benthic suspension feeders. Since long-term observational data is missing, the available results cannot clarify this issue or support our interpretation and we eagerly ask future studies on high temporal resolution archives to investigate and include observations on the potential processes involved.

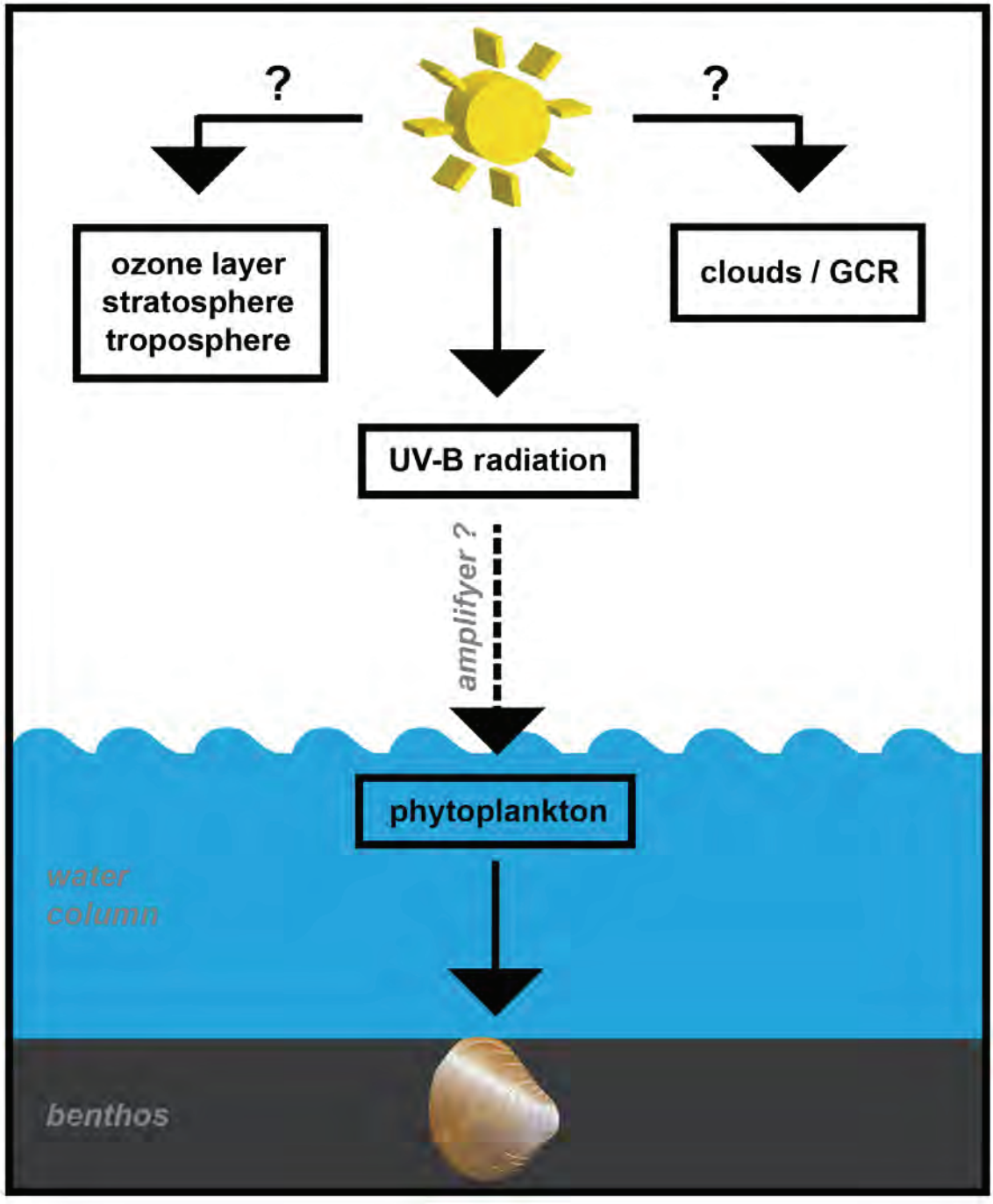

Figure 6. Schematic illustration showing hypothesized mechanistic/causal link between solar activity and marine bivalve shell growth. Decadal changes in UV-B radiation associated with the Schwabe sunspot cycle negatively influence phytoplankton productivity, i.e., the food source of the bivalve. In this model, phytoplankton inversely amplifies changes in solar activity. Phases of strong solar activity (maxima; high sunspot numbers) are associated with a maximum of emitted and incident solar irradiance and more UV-B radiation subsequently reaches Earth´s surface and penetrates the upper layer of the oceans. Since UV-B radiation in general has a negative effect on phytoplankton growth and abundance this results in reduced abundance and quality of food for benthic communities and particularly deposit feeders such as *A. islandica*, a main driver of shell growth. The illustrated scenario of high solar activity during a solar maximum would result in less strong bivalve shell growth.

If a causal link between TSI and high latitude pelagic primary production is valid, then other high latitude time-series (i.e., master chronologies) derived from biogenic archives that depend on pelagic primary production should also show solar cycles. Longer time-series should contain even longer manifestations of the solar cycles, such as the 22-year Hale cycle or the ~80–90 year Gleissberg cycle (Gleissberg, 1944; Raspopov et al., 2004a), as already shown for tree ring data in Lamb (1972) and Raspopov et al. (2004b). However, it is expected that there will be taxon-specific interactions with the mechanistic link we have described between 11-year cyclicity and benthos growth. It is also reasonable to assume that potential amplifying mechanisms might show biogeographic variability proportional to the characteristics of the surrounding regional ocean and atmosphere system and the local composition of primary producers. Furthermore, for archives such as coralline red algae (Halfar et al., 2007) or trees (Damon et al., 1998), where growth occurs directly as a consequence of photosynthesis, a possible direct link associated with insolation changes should be taken into consideration.

4.4 Latitude dependence

At ~79°N – both today and in the early Holocene – from October to February there is little to no sunlight during the day, while from May to August there is 24 h constant daylight. Consequently, sunlight availability limits the ecosystem much more at high latitudes than it does at lower latitudes (Sakshaug et al., 2009b), i.e., bivalve shell growth might be more irradiance-dependent at Svalbard than closer to the equator. Additionally, the shape of Earth´s magnetic field provides less protection against UV-B radiation at higher latitudes and might also therefore intensify the mechanism described above. Finally, and only valid for modern observations, the anthropogenic ozone depletion at both poles (Wessel et al., 1998) might additionally increase the effects described for UV-B above to due the inversely correlation between ozone amount and UV-B radiation (Dahlback, 2002). Since the ozone layer is mainly responsible for absorbing and reflecting the main portion of damaging UV-B radiation (e.g., Dahlback, 2002) depletion leads increased doses at the surface.

5 Conclusions

Our interpretation of the 11-year signal identified in early Holocene *A. islandica* shells tentatively investigates the potential indirect links between solar forcing and growth in benthic organisms. It is clear that variability in the Sun's energy is likely to impact upon a multitude of climatic, oceanographic and biological processes, each of which may cause an indirect physiological response in bivalves that is incorporated into their shells. Further work on high-resolution biogenic archives at the high latitudes is necessary to explore some of the potential connections highlighted in this study. In addition, longer time-series data from the instrumental period will hopefully in time shed light on physical climate and ocean mechanisms associated with solar cycles.

Our investigations on modern shell-derived chronologies argue for a negative correlation between shell growth and the 11-year Schwabe cycle (Figure 5). We propose a feasible mechanistic link between irradiance and shell growth via atmospheric processes, where UV-B radiation is negatively correlated to phytoplankton productivity, acting to amplify the initial TSI change during periods of solar maxima. However, we stress that this proposed causal link is a strongly simplified mechanism that should be seen as a basis for debate along the scientific community using biogenic archives for climatic and environmental reconstructions. This is a particularly important avenue of research considering the frequency with which 11-year and other solar signals have been identified within biological and non-biological climate archives with no further explanation for the mechanism linking the initial solar activity and the organism growth. It is essential to understand the potential factors influencing shell growth in order to reliably distinguish between the effects of natural versus anthropogenic climate change. We are confident that with a reliable and established explanation for the connection between solar activity and bivalve shell growth, shell records derived from high latitudes might also be used as potential proxy for past solar activity.

Acknowledgements

The first author (LB) was financed by the "Earth System Science Research School (ESSReS)", an initiative of the Helmholtz Association of German Research Centres (HGF) at the Alfred Wegener Institute (AWI), Helmholtz Centre for Polar and Marine Research. Otto Salvigsen (University of Oslo) is thanked for providing the shell material from the Dicksonfjord. Further, Michael Carroll (Akvaplan-niva, Tromsø, Norway), Mikael Sejr (Aarhus University, Denmark) and Paul Butler (Bangor University, UK) are thanked for providing chronology data from the Barents Sea, East Greenland and Iceland. Rosie Sheward (NOC, Southampton, UK) is thanked for improving the English of the manuscript.

Reference	Marking in Figure 1	Archive	Analysed on	Locality	Length of record
Ram et al., 1997	1	GISP2 ice core	Dust concentration	Greenland	100,000 yrs
Frisia et al., 2003	3	Stalagmites	Laminae thickness	N Italy	CE 1650–1713 CE 1798–1840
Damon et al., 1998	2	Tree-rings	Ring width	Sequoia National Forest, USA	CE 1065–1250
Bondarenko & Evstafyev, 2006	4	Lake water	Spring phytoplankton	Lake Baikal, Russia	CE 1943–2005
Halfar et al., 2007	5	Coralline red algae	Increment width	W Bering Sea/Aleutian Island region	Modern 117 yrs long
Carroll et al., 2014	I	Bivalve *C. ciliatum*	Increment width	Barents Sea	Modern 39 yrs long
Unpublished data M. Sejr	II	Bivalve *Mya* sp.	Increment width	East Greenland	Modern 41 yrs long
Berggren et al., 2010	6	Lake sediment	^{10}Be	Finland	CE 1900–2006
Vos et al., 2004	7	Lake sediment	Varve thickness	Holzmaar, Germany	10,000–9,000 cal. BP
Vos et al., 2004	8	GISP ice core	Accumulation rate	Greenland	10,000–9,000 cal. BP
Castagnoli et al., 1987	9	Sediment core	Thermoluminescence intensity	Ionian Sea	CE 1500–1974
Patterson et al., 2013	10	Sediment core	Varve thickness, diatoms	Vancouver Island, Canada	CE 1947–1993
Raspopov et al., 2004	11	Tree-rings	Ring width	Kola Peninsula	CE 1458–1975
Rodolfo Rigozo et al., 2007	12	Tree-rings	Ring width	Chile	CE 1587–1994
Stuiver and Quay, 1980	10, 13	Tree-rings	^{14}C	Washington Oregon, Vancouver Island, Canada	Modern 860 yrs long
Beer et al., 1998	14	Dye 3 ice core	^{10}Be	Greenland	CE 1783–1985
Berggren et al., 2009	15	NGRIP ice core	^{10}Be	Greenland	CE 1389–1994
Butler et al., 2013	III	Bivalve *A. islandica*	Increment width	North Icelandic Shelf	Modern 1357 yrs long

Table 1. Compilation of studies reporting an 11-year signal linked to solar activity in different archives worldwide. Localities of studies are illustrated in Figure 1. List does not claim to be complete.

Shell ID	$^{14}C_{AMS}$ ages (raw data BP)	$^{14}C_{AMS}$ ages (cal yrs BP)	Ontogenetic age (yrs)	Total variance explained by 11a signal (%)	Frequency of 11a signal (1/yr) (in SSA)
AI-DiFj-02	9,240 ± 70	9,954 ± 139	52	37.6	0.091
AI-DiFj-03	9,200 ± 50	9,838 ± 118	52	39.8	0.096
AI-DiFj-04	9,160 ± 50	9,782 ± 105	77	35.8	0.080
AI-DiFj-08	9,090 ± 50	9,648 ± 95	77	20.3	0.100
AI-DiFj-09	9,190 ± 50	9,815 ± 115	72	19.3	0.103
AI-DiFj-10	9,070 ± 50	9,623 ± 84	87	27.0	0.089

Table 2. Information on early Holocene *A. islandica* shell specimens from the Dicksonfjord. Further information for specimens AI-DiFj-02, AI-DiFj-03 and AI-DiFj-04 can be found in Beierlein et al. (2014).

References

Aas, E., Hokedal, J., Hojerslev, N.K., Sandvik, R., Sakshaug, E., 2002. Spectral properties and UV-attenuation in Arctic marine waters, UV Radiation and Arctic Ecosystems. In: UV Radiation and Arctic Ecosystems, Hessen, D.O. (Ed.), Springer Berlin, pp. 23–56.

Allen, M.R., Smith, L.A., 1997. Optimal filtering in singular spectrum analysis. Physics Letters A 234, 419–428.

Ambrose, W.G., Carroll, M.L., Greenacre, M., Thorrold, S.R., McMahon, K.W., 2006. Variation in *Serripes groenlandicus* (Bivalvia) growth in a Norwegian high-Arctic fjord: evidence for local- and large-scale climatic forcing. Global Change Biology 12, 1595–1607.

Beer, J., Steven, T., Weiss, N., 1998. An active Sun throughout the Maunder Minimum. Solar Physics 181, 237–249

Beierlein, L., Salvigsen, O., Schöne, B.R., Mackensen, A., Brey, T., 2014. The seasonal water temperature cycle in the Arctic Dicksonfjord (Svalbard) during the Holocene Climate Optimum derived from sub-fossil *Arctica islandica* shells. The Holocene (accepted for print with minor revisions).

Berger, A., Loutre, M.F., 1991. Insolation values for the climate of the last 10 million years. Quaternary Science Reviews 10, 297–317.

Berggren, A.M., Beer, J., Possnert, G., Aldahan, A., Kubik, P., Christl, M., Johnsen, S.J., Abreu, J., Vinther, B.M., 2009. A 600-year annual ^{10}Be record from the NGRIP ice core, Greenland. Geophysical Research Letters 36, L11801.

Berggren, A.M., Aldahan, A., Possnert, G., Haltia-Hovi, E., Saarinen, T., 2010. ^{10}Be and solar activity cycles in varved lake sediments, AD 1900–2006. Journal of Paleolimnology 44, 559–569.

Bischof, K., Hanelt, D., Wiencke, C., 2002. UV radiation and Arctic marine macroalgae, UV radiation and Arctic ecosystems. In: UV Radiation and Arctic Ecosystems, Hessen, D.O. (Ed.), Springer Berlin, pp. 227–243.

Bondarenko, N.A., Evstafyev, V.K., 2006. Eleven-and ten-year basic cycles of Lake Baikal spring phytoplankton conformed to solar activity cycles. Hydrobiologia 568, 19–24.

Brey, T., Pearse, J., Basch, L., McClintock, J., Slattery, M., 1995. Growth and production of *Sterechinus neumayeri* (Echinoidea: Echinodermata) in McMurdo Sound, Antarctica. Marine Biology 124, 279–292.

Brey, T., Voigt, M., Jenkins, K., Ahn, I.-Y., 2011. The bivalve *Laternula elliptica* at King George Island – A biological recorder of climate forcing in the West Antarctic Peninsula region. Journal of Marine Systems 88, 542–552.

Butler, P.G., Richardson, C.A., Scourse, J.D., Wanamaker Jr, A.D., Shammon, T.M., Bennell, J.D., 2010. Marine climate in the Irish Sea: analysis of a 489-year marine master chronology derived from growth increments in the shell of the clam *Arctica islandica*. Quaternary Science Reviews 29, 1614–1632.

Butler, P.G., Wanamaker Jr, A.D., Scourse, J.D., Richardson, C.A., Reynolds, D.J., 2013. Variability of marine climate on the North Icelandic Shelf in a 1357-year proxy archive based on growth increments in the bivalve *Arctica islandica*. Palaeogeography, Palaeoclimatology, Palaeoecology 373, 141–151.

Camp, C.D., Tung, K.K., 2007. Surface warming by the solar cycle as revealed by the composite mean difference projection. Geophysical Research Letters 34, L14703.

Carroll, M.L., Ambrose Jr, W.G., Locke V, W.L., Ryan, S.K., Johnson, B.J., 2014. Bivalve growth rate and isotopic variability across the Barents Sea Polar Front. Journal of Marine Systems 130, 167–180.

Carroll, M.L., Denisenko, S.G., Renaud, P.E., Ambrose Jr, W.G., 2008. Benthic infauna of the seasonally ice-covered western Barents Sea: Patterns and relationships to environmental forcing. Deep Sea Research Part II: Topical Studies in Oceanography 55, 2340–2351.

Carslaw, K.S., Harrison, R.G., Kirkby, J., 2002. Cosmic rays, clouds, and climate. Science 298, 1732–1737.

Castagnoli, G.C., Bonino, G., Attolini, M.R., Galli, M., Nanni, T., 1987. The Schwabe cycle in the thermoluminescence profile of an Ionian Sea core. Il Nuovo Cimento C 10, 315–322.

Christensen, H., Kanneworff, E., 1985. Sedimenting phytoplankton as major food source for suspension and deposit feeders in the Oresund. Ophelia 24, 223–244.

Cortese, G., Dolven, J.K., Bjorklund, K.R., Malmgren, B.A., 2005. Late Pleistocene-Holocene radiolarian paleotemperatures in the Norwegian Sea based on artificial neural networks. Palaeogeography, Palaeoclimatology, Palaeoecology 224, 311–332.

Dahlback, A., 2002. Recent changes in surface ultraviolet solar radiation and stratospheric ozone at a high Arctic site, UV radiation and Arctic ecosystems. In: UV Radiation and Arctic Ecosystems, Hessen, D.O. (Ed.), Springer Berlin, pp. 3–22.

Dahlgren, T.G., Weinberg, J.R., Halanych, K.M., 2000. Phylogeography of the ocean quahog (*Arctica islandica*): influences of paleoclimate on genetic diversity and species range. Marine Biology 137, 487–495.

Damon, P.E., Eastoe, C.J., Hughes, M.K., Kalin, R.M., Long, A., Peristykh, A.N., 1998. Secular variation of delta ^{14}C during the Medieval solar maximum; a progress report. Radiocarbon 40, 343–350.

Dima, M., Lohmann, G., Dima, I., 2005. Solar-induced and internal climate variability at decadal time scales. International Journal of Climatology 25, 713–733.

Epplé, V.M., Brey, T., Witbaard, R., Kuhnert, H., Pätzold, J., 2006. Sclerochronological records of *Arctica islandica* from the inner German Bight. The Holocene 16, 763–769.

Floyd, L.E., Cook, J.W., Herring, L.C., Crane, P.C., 2003. SUSIM'S 11-year observational record of the solar UV irradiance. Advances in Space Research 31, 2111–2120.

Frisia, S., Borsato, A., Preto, N., McDermott, F., 2003. Late Holocene annual growth in three Alpine stalagmites records the influence of solar activity and the North Atlantic Oscillation on winter climate. Earth and Planetary Science Letters 216, 411–424.

Ghil, M., Allen, M.R., Dettinger, M.D., Ide, K., Kondrashov, D., Mann, M.E., Robertson, A.W., Saunders, A., Tian, Y., Varadi, F., Yiou, P., 2002. Advanced Spectral Methods for Climatic Time Series. Reviews of Geophysics 40, 1–41.

Gleissberg, W., 1944. A table of secular variations of the solar cycle. Terrestrial Magnetism and Atmospheric Electricity 49, 243–244.

Gnevyshev, M.N., 1977. Essential features of the 11-year solar cycle. Solar Physics 51, 175–183.

Gray, L.J., Beer, J., Geller, M., Haigh, J.D., Lockwood, M., Matthes, K., Cubasch, U., Fleitmann, D., Harrison, G., Hood, L., 2010. Solar influences on climate. Reviews of Geophysics 48, RG4001.

Gray, L.J., Haigh, J.D., Harrison, R.G., 2005. The influence of solar changes on the Earth's climate. Hadley Centre technical note 62, 1–81.

Häder, D.-P., Kumar, H.D., Smith, R.C., Worrest, R.C., 2003. Aquatic ecosystems: effects of solar ultraviolet radiation and interactions with other climatic change factors. Photochemical & Photobiological Sciences 2, 39–50.

Häder, D.P., Kumar, H.D., Smith, R.C., Worrest, R.C., 2007. Effects of solar UV radiation on aquatic ecosystems and interactions with climate change. Photochemical & Photobiological Sciences 6, 267–285.

Haigh, J.D., 1996. The impact of solar variability on climate. Science 272, 981–984.

Hale, G.E., 1908. On the probable existence of a magnetic field in sun-spots. Terrestrial Magnetism and Atmospheric Electricity 13, 159–160.

Halfar, J., Steneck, R., Schöne, B., Moore, G.W.K., Joachimski, M., Kronz, A., Fietzke, J., Estes, J., 2007. Coralline alga reveals first marine record of subarctic North Pacific climate change. Geophysical Research Letters 34, L07702.

Harder, J.W., Fontenla, J.M., Pilewskie, P., Richard, E.C., Woods, T.N., 2009. Trends in solar spectral irradiance variability in the visible and infrared. Geophysical Research Letters 36, L07801.

Hathaway, D.H., 2010. The solar cycle. Living Reviews in Solar Physics 7, 1–65.

Helbling, E.W., Villafane, V.E., 2002. UV radiation effects on phytoplankton primary production: a comparison between Arctic and Antarctic marine ecosystems, UV Radiation and Arctic Ecosystems. In: UV Radiation and Arctic Ecosystems, Hessen, D.O. (Ed.), Springer Berlin, pp. 203–226.

Hurrell, J.W., Kushnir, Y., Ottersen, G., Visbeck, M., 2003. An overview of the North Atlantic Oscillation. Geophysical Monograph 134, 1–36.

Huth, R., Bochnicek, J., Hejda, P., 2007. The 11-year solar cycle affects the intensity and annularity of the Arctic Oscillation. Journal of Atmospheric and Solar-Terrestrial Physics 69, 1095–1109.

Ineson, S., Scaife, A.A., Knight, J.R., Manners, J.C., Dunstone, N.J., Gray, L.J., Haigh, J.D., 2011. Solar forcing of winter climate variability in the Northern Hemisphere. Nature Geoscience 4, 753–757.

IPCC, 2013. Climate Change 2013: The Physical Science Basis. Contribution of Working Group I to the Fifth Assessment Report of the Intergovernmental Panel on Climate Change. Cambridge University Press, Cambridge, United Kingdom and New York, NY, USA.

Ivany, L.C., Brey, T., Huber, M., Buick, D.P., Schöne, B.R., 2011. El Niño in the Eocene greenhouse recorded by fossil bivalves and wood from Antarctica. Geophysical Research Letters 38, L16709.

Johnson, M.A., Proshutinsky, A.Y., Polyakov, I.V., 1999. Atmospheric patterns forcing two regimes of arctic circulation: A return to anticyclonic conditions? Geophysical Research Letters 26, 1621–1624.

Jones, P.D., Jonsson, T., Wheeler, D., 1997. Extension to the North Atlantic oscillation using early instrumental pressure observations from Gibraltar and south-west Iceland. International Journal of Climatology 17, 1433–1450.

Kern, A.K., Harzhauser, M., Soliman, A., Piller, W.E., Mandic, O., 2013. High-resolution analysis of upper Miocene lake deposits: Evidence for the influence of Gleissberg-band solar forcing. Palaeogeography, Palaeoclimatology, Palaeoecology 370, 167–183.

Kirkby, J., 2007. Cosmic rays and climate. Surveys in Geophysics 28, 333–375.

Kodera, K., 1995. On the origin and nature of the interannual variability of the winter stratospheric circulation in the northern hemisphere. Journal of Geophysical Research 100, 14077–14087.

Kodera, K., 2002. Solar cycle modulation of the North Atlantic Oscillation: Implication in the spatial structure of the NAO. Geophysical Research Letters 29, 59–51.

Kodera, K., 2003. Solar influence on the spatial structure of the NAO during the winter 1900–1999. Geophysical Research Letters 30, 1–4.

Labitzke, K., 1987. Sunspots, the QBO, and the stratospheric temperature in the north polar region. Geophysical Research Letters 14, 535–537.

Lamb, H.H., 1972. Climate: Present, Past And Future. In: Volume 1: Fundamentals And Climate Now, Lamb, H.H. (Ed.), Methuen & Co Ltd, pp. 212–253.

Lean, J., Beer, J., Bradley, R., 1995. Reconstruction of solar irradiance since 1610: Implications for climate change. Geophysical Research Letters 22, 3195–3198.

Mann, M., Lees, J., 1996. Robust estimation of background noise and signal detection in climatic time series. Climatic Change 33, 409–445.

Marsh, N., Svensmark, H., 2000. Low cloud properties influenced by cosmic rays. Physical Review Letters 85, 5004–5007.

Meehl, G.A., Arblaster, J.M., Matthes, K., Sassi, F., van Loon, H., 2009. Amplifying the Pacific Climate System Response to a Small 11-Year Solar Cycle Forcing. Science 325, 1114–1118.

North, G.R., Wu, Q., Stevens, M.J., 2004. Detecting the 11-year solar cycle in the surface temperature field. In: Solar Variability and Its Effects on Climate, Pap, J.M., Fox, P. (Eds.), American Geophysical Union, pp. 251–259.

Patterson, R.T., Chang, A.S., Prokoph, A., Roe, H.M., Swindles, G.T., 2013. Influence of the Pacific Decadal Oscillation, El Niño-Southern Oscillation and solar forcing on climate and primary productivity changes in the northeast Pacific. Quaternary International 310, 124–139.

Patterson, R.T., Prokoph, A., Chang, A., 2004. Late Holocene sedimentary response to solar and cosmic ray activity influenced climate variability in the NE Pacific. Sedimentary Geology 172, 67–84.

Proshutinsky, A.Y., Johnson, M.A., 1997. Two circulation regimes of the wind-driven Arctic Ocean. Journal of Geophysical Research 102, 12493–12514.

Ram, M., Stolz, M., Koenig, G., 1997. Eleven year cycle of dust concentration variability observed in the dust profile of the GISP2 ice core from Central Greenland: Possible solar cycle connection. Geophysical Research Letters 24, 2359–2362.

Rasmussen, T.L., Forwick, M., Mackensen, A., 2012. Reconstruction of inflow of Atlantic Water to Isfjorden, Svalbard during the Holocene: Correlation to climate and seasonality. Marine Micropaleontology 94/95, 80–90.

Raspopov, O.M., Dergachev, V.A., Kolström, T., 2004a. Hale Cyclicity of Solar Activity and Its Relation to Climate Variability. Solar Physics 224, 455–463.

Raspopov, O.M., Dergachev, V.A., Kolström, T., 2004b. Periodicity of climate conditions and solar variability derived from dendrochronological and other palaeoclimatic data in high latitudes. Palaeogeography, Palaeoclimatology, Palaeoecology 209, 127–139.

Rind, D., 2002. The Sun's Role in Climate Variations. Science 296, 673–677.

Rodolfo Rigozo, N., Nordemann, D.J.R., da Silva, H.E., de Souza Echer, M.P., Echer, E., 2007. Solar and climate signal records in tree ring width from Chile (AD 1587–1994). Planetary and Space Science 55, 158–164.

Roig, F.A., Le-Quesne, C., Boninsegna, J.A., Briffa, K.R., Lara, A., Grudd, H., Jones, P.D., Villagran, C., 2001. Climate variability 50,000-years ago in mid-latitude Chile as reconstructed from tree rings. Nature 410, 567–570.

Ruzmaikin, A., 1999. Can El Niño amplify the solar forcing of climate? Geophysical Research Letters 26, 2255–2258.

Sakshaug, E., Johnsen, G., Kristiansen, S., von Quillfeldt, C., Rey, F., Slagstad, D., Thingstad, F., 2009a. Phytoplankton and primary production. In: Ecosystem Barents Sea, Sakshaug, E. (Ed.). Tapir Academic Press, Trondheim, pp. 167–207.

Sakshaug, E., Johnsen, G., Volent, Z., 2009b. Light. In: Ecosystem Barents Sea, Sakshaug, E. (Ed.). Tapir Academic Press, Trondheim, pp. 117–138.

Schlesinger, M.E., Ramankutty, N., 1992. Implications for global warming of intercycle solar irradiance variations. Nature 360, 330–333.

Schöne, B.R., Dunca, E., Fiebig, J., Pfeiffer, M., 2005a. Mutvei's solution: An ideal agent for resolving microgrowth structures of biogenic carbonates. Palaeogeography, Palaeoclimatology, Palaeoecology 228, 149–166.

Schöne, B.R., Houk, S.D., Freyre Castro, A.D., Fiebig, J., Oschmann, W., Kröncke, I., Dreyer, W., Gosselck, F., 2005b. Daily growth rates in shells of *Arctica islandica*: Assessing sub-seasonal environmental controls on a long-lived bivalve mollusk. Palaios 20, 78–92.

Schöne, B.R., Oschmann, W., Rössler, J., Castro, A.D.F., Houk, S.D., Kröncke, I., Dreyer, W., Janssen, R., Rumohr, H., Dunca, E., 2003. North Atlantic Oscillation dynamics recorded in shells of a long-lived bivalve mollusk. Geology 31, 1037–1040.

Schöne, B.R., Pfeiffer, M., Pohlmann, T., Siegismund, F., 2005c. A seasonally resolved bottom-water temperature record for the period AD 1866–2002 based on shells of *Arctica islandica* (Mollusca, North Sea). International Journal of Climatology 25, 947–962.

Schwabe, M., 1844. Sonnenbeobachtungen im Jahre 1843. Von Herrn Hofrath Schwabe in Dessau. Astronomische Nachrichten 21, 233–236.

Sinha, R.P., Klisch, M., Gröniger, A., Häder, D.-P., 2001. Responses of aquatic algae and cyanobacteria to solar UV-B. Plant Ecology 154, 221–236.

Stuiver, M., Braziunas, T.F., 1993. Sun, ocean, climate and atmospheric $^{14}CO_2$: an evaluation of causal and spectral relationships. The Holocene 3, 289–305.

Stuiver, M., Quay, P.D., 1980. Changes in atmospheric carbon-14 attributed to a variable sun. Science 207, 11–19.

Sverdrup, H.U., 1953. On conditions for the vernal blooming of phytoplankton. Journal du Conseil 18, 287–295.

Thompson, D.W.J., Wallace, J.M., 1998. The Arctic oscillation signature in the wintertime geopotential height and temperature fields. Geophysical Research Letters 25, 1297–1300.

Torrence, C., Compo, G.P., 1998. A Practical Guide to Wavelet Analysis. Bulletin of the American Meteorological Society 79, 61–78.

van Loon, H., Meehl, G.A., Shea, D.J., 2007. Coupled air-sea response to solar forcing in the Pacific region during northern winter. Journal of Geophysical Research 112, D02108.

Vos, H., Brüchmann, C., Lücke, A., Negendank, J.F.W., Schleser, G.H., Zolitschka, B., 2004. Phase Stability of the Solar Schwabe Cycle in Lake Holzmaar, Germany, and GISP2, Greenland, between 10,000 and 9,000 cal. BP. In: The Climate in Historical Times, Springer, pp. 293–317.

Wanamaker Jr, A., Kreutz, K., Schöne, B., Maasch, K., Pershing, A., Borns, H., Introne, D., Feindel, S., 2009. A late Holocene paleo-productivity record in the western Gulf of Maine, USA, inferred from growth histories of the long-lived ocean quahog (*Arctica islandica*). International Journal of Earth Sciences 98, 19–29.

Wängberg, S.-A., Selmer, J.-S., Gustavson, K., 1998. Effects of UV-B radiation on carbon and nutrient dynamics in marine plankton communities. Journal of Photochemistry and Photobiology B: Biology 45, 19–24.

Wessel, S., Aoki, S., Winkler, P., Weller, R., Herber, A., Gernandt, A., 1998. Tropospheric ozone depletion in polar regions. A comparison of observations in the Arctic and Antarctic. Tellus 50B, 34–50.

White, W.B., Lean, J., Cayan, D.R., Dettinger, M.D., 1997. Response of global upper ocean temperature to changing solar irradiance. Journal of Geophysical Research 102, 3255–3266.

Willson, R.C., Hudson, H.S., 1991. The Sun's luminosity over a complete solar cycle. Nature 351, 42–44.

Witbaard, R., Duineveld, G.C.A., De Wilde, P.A.W.J., 1999. Geographical differences in growth rates of *Arctica islandica* (Mollusca: Bivalvia) from the North Sea and adjacent waters. Journal of the Marine Biological Association of the United Kingdom 79, 907–915.

Witbaard, R., Jansma, E., Sass Klaassen, U., 2003. Copepods link quahog growth to climate. Journal of Sea Research 50, 77–83.

Wunsch, C., 1999. The Interpretation of Short Climate Records, with Comments on the North Atlantic and Southern Oscillations. Bulletin of the American Meteorological Society 80, 245–255.

Supporting Publication VI

Climate Service – Definition and Function

Lars Beierlein[1], Rosie M. Sheward[2,3]

[1]Alfred Wegener Institute Helmholtz Centre for Polar and Marine Research, Bremerhaven, Germany

[2]School of Environmental Sciences, University of East Anglia, Norwich, UK

[3]Now at: Ocean and Earth Science, National Oceanography Centre, Southampton, University of Southampton, Southampton, UK

Published (2013) in: Climate change in the marine realm: an international summer school in the framework of the European Campus of Excellence. Dummermuth, A. and Grosfeld, K. (editors). *Berichte zur Polar- und Meeresforschung, Alfred Wegener Institute for Polar and Marine Research 662, 72–75*.

Climate Service – Definition and Function

Within the last 50 years the global population has risen from two to seven billion people (UN World Population Prospects, 2011). This growth will continue in the future, resulting in environmental and social challenges that we are already starting to encounter. Currently 600 million people do not have access to clean drinking water (WHO and WMO, 2012). Health is currently a key issue in some developing nations, where e.g., incidences of malaria are increasing due to changes in weather patterns and temperatures. Millions of acres of land are degraded, reducing the yield of crops and leading to issues of hunger and malnutrition. Overfishing of oceans has led to serious concerns about the numbers of particular fish species and people feeding on them as well as for the ecosystems themselves (FAO, 2005). Pollution concerns from fossil fuel burning, the use of agricultural chemicals and industrial waste are often key local issues and can impact as well as people worldwide. Accompanying the growth of population in general by the year 2100 about 80 per cent of the world's population will live in urban areas (Grubler et al., 2007). Most of the megacities worldwide are sited in coastal areas with even increasing pressure in these areas. The burning of fossil fuels from industry and other sources and the resulting emission of greenhouse gases (CO_2, N_2O, CH_4, etc.) cause global temperature to rise, leading to complex and drastic changes in the Earth's climate system. Decreasing Arctic sea-ice, rising sea level and changing weather patterns for example will all most likely feature in our future climate. Since the Earth system is a highly complex and interacting system, all these changes are (to some extent) coupled. The most prominent example is the interaction between the atmosphere and the oceans, which constantly tries to reach an equilibrium state. Therefore, the emission of carbon dioxide (CO_2) to the atmosphere also results in an increase in CO_2 in the oceans, which lowers the pH of the water. However, the consequences of ocean acidification on marine organisms and ecosystems are difficult to predict and it is likely that some species will be more adversely affected than others. Research suggests that corals have a high extinction risk, along with other species that generate calcium carbonate shells. This could have severe impacts for marine biodiversity, food webs and the function of the oceans as a sink for CO_2.

These are only examples of the impact of climate change on the Earth system. Some other likely impacts include increased aridity in already dry regions of the world, leading to the spreading of deserts and increasing drought events that already impact millions of people. Decreases in the amount of precipitation are likely in most sub-

tropical land regions (IPCC, 2007). As a result, agricultural productivity will also decline in some areas of the world (IPCC, 2007). Areas that already get a considerable amount of rain are likely to encounter even more rainfalls as a result of climate change, hence increasing flood risks in many areas (Climate Change, 2007: Working Group II: Impacts, Adaptation and Vulnerability, 3.4.3 Floods and droughts). Extreme weather events are also becoming more frequent and causing more damage than ever before (IPCC, 2007). People have been deforesting areas for decades constantly increasing the pressure on these habitats. Global deforestation continues at an alarming rate – 13 million hectares of forest are destroyed annually, equal to the size of Portugal (UNEP). Tropical rainforests are some of the most severely impacted areas, but they are crucial for delivering rainfall to vast areas of some continents, exacerbating the local impact of climate change as a result and decreasing tropical biodiversity.

All those topics are big challenges not only for our generation but also for the generations to come. However, mankind has also already achieved great progress in a variety of global issues. The use and production of substances that deplete the ozone layer have been almost eliminated and there is almost no more lead in today's petrol due to the implementation of the Kyoto protocol in national jurisdiction. We have decreased the production and use of persistent organic pollutants (POPs), reduced world poverty from more than 50% in 1981 to about 20% in 2009 (Geneva Convention on Long-Range Transboundary Air Pollution, 1979 and ratification of the 1998 Aarhus Protocol on Persistent Organic Pollutants) and have started the first steps in a decarbonisation process in order to reduce CO_2 emissions, e.g., by the investment in and increase of renewable energy technologies (wind, sun, etc.).

Within the last decade, the number of multi-national climate agreements such as for example the Kyoto protocol has increased dramatically. But does it really help tackling the problems related to climate change? Why do the results of scientific research fail to reach policy makers and decision takers and the general public? Why does the key scientific message become distorted along the way? Why is it so difficult to agree on measures to counteract climate change and its impacts? Why do people not trust science? One of the biggest problems in science communication is to communicate uncertainties as scientists aim to be as precise as possible when translating or simplifying their results for the general public and policy makers. Climate change science is a particularly important area that everyone should be aware of and understand. However, there are a number of reasons why scientists have not been

successful in better convincing society to act against climate change. Sometimes it is difficult for scientists to translate the scientific results in a comprehensible language in order to explain them to non-specialists, journalists, governmental representatives and the general public. Stakeholders, who use science output, may not have a scientific background. This can make it challenging to take appropriate decisions about climate change policy. Journalists can sensationalise science, which in turn can make it difficult for the public to understand that there are uncertainties and assumptions in the different projections for the future climate. It is not always easy the public to recognise that they can 'trust' scientists, as research will sometimes yield conflicting results in different studies so that reports seesaw from one view to another. However, it is also important that society tries to put aside preconceived ideas and misunderstandings and tries to approach science with an open mind. Science is always an on-going process that is changing with new findings and developments. The message may not always be clear or the same as what has been communicated at some time prior, but attempting to understand 'why' is just as important as the 'end result'.

In order to move science communication forward for the benefit of all parties involved, it is important that any communication is accessible for the intended audience and that any disagreements are discussed respectfully. It is also crucial for scientists to increase outreach and public engagement activities. The transfer of scientific knowledge should be a self-evident part of their work, interacting with all sectors of society and educating people about their research and how it relates to the 'big picture' of climate change research. A useful contribution could be to increase a target related communication through popular media as television, social media and the internet.

To close the gap between science and society, and given that the awareness of the importance of climate with regard to many sectors of society (agriculture, food security, water, health, energy, tourism etc.) is growing a new concept called 'climate services' has been conceived. Its fundamental objective is to help society (business, public service) to cope with climate risks and opportunities, strengthening the cooperation between (climate change) sciences and different interested parties that rely on climatic and scientific information. For example, economists need current and future climate information to make sound investments as it helps to better assess risks associated with different decisions. Thus all segments of society will benefit from climate services – governments, industry, economy, businesses as e.g., insurance

companies (risk evaluation), the media, educators and the general public – and all will be affected in some way by future climate changes.

Even though the relevance of managing climate risks is an increasingly important consideration to many entities, the concept of climate services is still evolving. Climate service investigates the need of society for advice regarding questions related to climate change. Climate service links climate researchers and climate advisors, integrates research data from natural and social sciences on the climate system and prepares them for the needs of clients. Climate service provides information to customers via products, which are sector specific and tailored to suit the clients needs. And finally climate service also coordinates feedback from practitioners to science.

Climate services first and foremost must meet the users needs to transfer scientific knowledge target-oriented. Climate communication is one important aspect and should include provision of choices and solutions that people can employ in their daily activities.

The main challenges of climate services will be to provide balanced, credible, cutting-edge scientific and technical information and to engage a diversity of users to express their needs in order to be able to act as real service providers. Climate services must serve to strengthen scientific standards and improve local and regional projections of climate change so that the most appropriate decisions can be made to minimise adverse future climate impacts and risks. The key purpose of climate services is to reduce society's vulnerability to climate change impacts and to maintain – and if possible improve – the adaptability of natural, societal and economic systems to any future changes.

In summary, the future climate of our planet is uncertain due to its complexity. However, we observe rise in global mean temperature with different extent crucially depending on the geographical region. We expect further increase in global temperature rise and there will be a range of influences on ecosystems at all levels impacting on society through food provision, health, economic security and water availability – many of which are already daily challenges for millions of people around the world. Pressure on environmental resources will increase in severity with the projected increase in population in the next 50–100 years. Inequality between the rich and poor, those who consume few resources and those who consume many is not decreasing, and as many nations aspire to further improve their development, it is a

time-sensitive issue for future generations to develop management strategies for reducing carbon emissions. Climate services will help to form productive relationships between scientists and those who use science, such as economists, governments, media and society leading to make informed decisions that benefit all of the society.

But what can you do? Science is something that we are all taught in school and we all learn about science through the media and our daily lives as well, although at times you may not realise it. However – how much do you think about what you learn? Science by its nature is unbiased and objective, but newspapers, television or the internet may not be. Next time you read or hear something about science, take a minute to think about it, and not just accept it as fact. After all, that is what scientists do every day! Where has the information come from? Who has written it and for what purpose? How does it relate to you or where you live? Asking questions like this will mean that you start to really understand the information that you pick up all the time. Misconceptions in climate change science are easy to form if you are not aware of the origin of the information and – as the next generation – it will be you who must live with the consequences of our changing climate. Understanding some of the science now and sharing it with those around you, asking questions and getting involved whenever you can – at school or in the community – will make you a better equipped member of our future society.

References

(please note that references have been formatted according to style of journal)

Climate Change (2007) Impacts, Adaptation and Vulnerability. Contribution of Working Group II to the Fourth Assessment Report of the Intergovernmental Panel on Climate Change [M.L. Parry et al. (eds.)]. Cambridge University Press.

FAO (2005) Review of the state of world marine fishery resources.

Grubler A., O'Neill B., Riahi K., Chirkov V., Goujon A., Kolp P., Prommer I., Scherbov S., Slentoe E. (2007) Regional, national, and spatially explicit scenarios of demographic and economic change based on sres. Technological forecasting and social change 74: 980–1029.

IPCC (2007) AR4, "Summary for Policymakers: C. Current knowledge about future impacts".

The Geneva Convention on Long-Range Transboundary Air Pollution (1979).

The Aarhus Protocol on Persistent Organic Pollutants (POPs) (1998). Guidance document on best available techniques for reducing emissions of POPs from major stationary sources adopted on 18 December 2009.

United Nations (1993) Agenda 21: Combating Deforestation (Ch.11). 300pp. ISBN: 978-92-1-100509-7.

United Nations, Department of Economic and Social Affairs, Population Division (2011) World Population Prospects: The 2010 Revision, Highlights and Advance Tables Working Paper No. ESA/P/WP.220.

World Health Organization and World Meteorological Organization (2012) Atlas on health and climate. 68 pp. ISBN: 978-92-4-156452-6.

5 Synthesis & Conclusions

This Section summarizes the main conclusions of this thesis by answering the questions raised in the three main objectives (Section 2). The specific results and conclusions of manuscripts II to V (Section 4) are examined and discussed in the wider context of the project aim. For more detailed explanations on results and discussions pertaining to specific issues, please refer to the indicated manuscripts (Section 4).

5.1 Main Conclusion A: Preservation & Taphonomy

Question A1
Is confocal Raman microscopy (CRM) a valid tool for the visualization of internal growth patterns in modern and fossil bivalve shells?
Answer A1
Yes, CRM is a reliable visualization tool that produces comparable results from modern specimens and superior results in fossil bivalve specimens when compared to commonly used visualization techniques (Mutvei staining and fluorescence microscopy).

In order to investigate whether CRM is a suitable or even superior – with respect to resolution and efficiency – tool for visualizing internal shell growth patterns, I compared the results of standardized growth indices (SGI) derived from CRM maps, Mutvei´s solution staining and fluorescence microscopy (FL) images, using modern and fossil shells of *Arctica islandica* and *Pygocardia rustica* (Manuscript II).

SGI time-series from the hinge plate of a modern *A. islandica* shell (ID: Ai1276R) were produced via all three visualization techniques and compared in order to calibrate the potential new tool. I found that the CRM SGI series correlate strongly with the FL series ($r = 0.98$; $P < 0.0001$; $N = 57$; age 5–62) and the Mutvei series ($r = 0.96$; $P < 0.0001$; $N = 57$; age 5–62) and that the Mutvei and FL series are also strongly correlated ($r = 0.97$; $P < 0.0001$; $N = 57$; age 5–62) (Figure 5 in Manuscript II). Therefore I consider CRM an equally reliable method to visualize internal growth structures in

modern aragonite shells. Furthermore, CRM maps clearly show annual growth increments throughout the entire hinge plate when applied to fossil *A. islandica* (ID: AI-CoCr-01) and *P. rustica* (ID: RGM609.096) shells where the FL and Mutvei staining approaches of both specimens resulted in digital images of very low contrast (Figures 3 and 4 in Manuscript II). In the ontogenetically older areas particularly, where growth increments become most narrow, a clear distinction between increments was no longer possible when using FL and Mutvei staining and consequently, I was not able to reliably measure the internal growth pattern over the entire hinge plate.

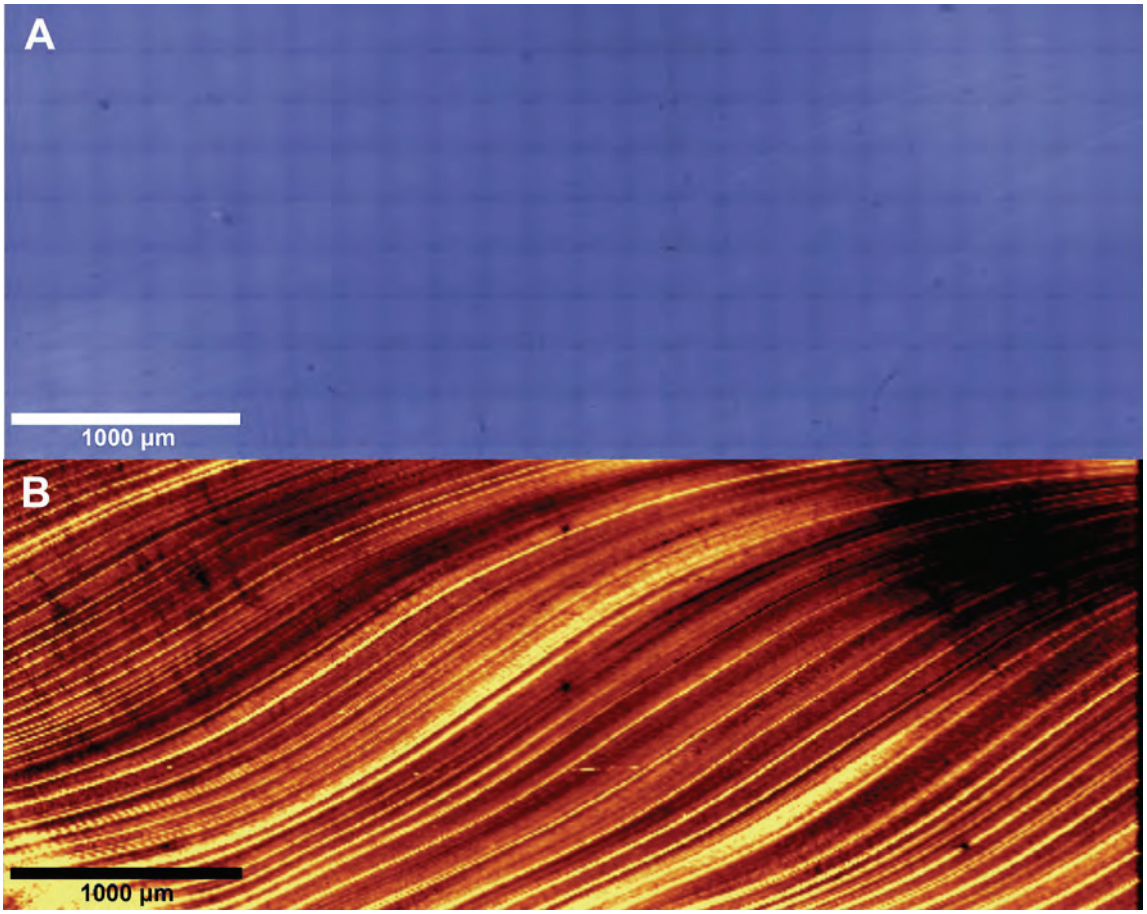

Figure 16. Stacked mosaic (squares due to lens effect of individual images) reflected-light microscopy image (A) in comparison to CRM map (B) in Pliocene *A. islandica* specimen AI-StRi1-BK2b from Stirone River, Italy (see Section 3.1). Internal growth patterns only visible by CRM approach (B).

In summary, I have shown that CRM is a reliable and valuable tool to visualize internal growth patterns in both modern and fossil bivalve shell specimens of *A. islandica* and *P. rustica*. CRM performs as good as established methods (Mutvei staining and FL) in modern shells. Regarding fossil shells, CRM reveals growth patterns where established methods fail, thus enabling a much more precise record of

annual and even sub-annual growth increments and the interpretation of their palaeo-environmental information. I therefore also consider CRM-based growth data suitable for cross-dating applications, such as those used to compile master chronologies from multiple specimen archives. Furthermore, CRM constitutes an alternative non-destructive approach that does not required any pre-treatment of the shell cross-section and makes the preparation of a second cross-section for geochemical analysis redundant.

I can therefore strongly recommend the use of CRM in samples where further geochemical analysis will be undertaken and as the best technique available for the imaging of annual growth increments in fossil bivalve shells (Figure 16).

Question A2

Does the recrystallization from pristine aragonite to calcite affect the stable isotope ($\delta^{18}O$ & $\delta^{13}C$) composition of a fossil *A. islandica* shell? What influence will this have on palaeo-temperature reconstructions?

Answer A2

Yes, recrystallization ('neomorphism') does have a severe impact on the isotopic composition ($\delta^{18}O$ & $\delta^{13}C$) of shell carbonate in fossil *A. islandica* specimens. Even the smallest amounts of undetected recrystallized calcite included in stable isotope analysis can easily lead to false palaeo-environmental conclusions.

The study presented in Manuscript III deals with one of the most important considerations when using stable oxygen isotopes ($\delta^{18}O$) for palaeo-environmental reconstructions in *A. islandica* shells. It is widely agreed that recrystallization from aragonite to calcite in a biogenic archive such as a bivalve shell would inhibit any possibility for its use in subsequent biogeochemical analysis. However, in Manuscript III I have presented the first continuous measurements throughout a shell section where pristine aragonite and re-precipitated secondary calcite were in direct contact in a commonly used biogenic archive (*A. islandica*). Using this I have analysed the direct impact of recrystallization on the most commonly used proxy $\delta^{18}O$, and its effect on palaeo-water temperature reconstructions.

I initially used CRM to identify carbonate polymorphs on a small spatial scale (a few hundred nm; Nehrke et al., 2012) to show that CRM maps can identify growth related structures in recrystallized shell calcite. These 'ghost structures' (i.e., relict textures), as referred to in the literature (Martin et al., 1986; Maliva et al., 2000), indicate a slow recrystallization process (Wardlaw et al., 1978) and may be associated with organic-depleted winter growth lines (Martin et al., 1986), providing pathways for hydrothermal/diagenetic fluids through the shell material.

The areas identified by CRM as pristine aragonite appear to preserve the original isotopic composition at the time of shell growth. In contrast, the recrystallized calcite appears to reflect the isotopic composition of fluids circulating within an ‘open system’, most likely meteoric water due to the strongly negative $\delta^{18}O$ values.

Furthermore, I was able to show that even the smallest fractions of recrystallized calcite within samples for isotope measurements result in misleading interpretations of palaeo-environment. The palaeo-temperature reconstruction in Manuscript III impressively demonstrates how important it is to check for alterations on very small scales. Even an advanced method such as CRM might not be able to detect such small scale diagenesis, due to the fact that recrystallization occurs in 3-dimensional space throughout the shell carbonate and CRM can only scan and map 2-dimensional surfaces. Hence, the shell surface might be aragonitic but the shell portion underneath might not. However, such minor traces of calcite would also not show up during a XRD diagenesis check, which emphasises the difficulty in assessing diagenesis and demonstrates the need for a reliable standard procedure to check for taphonomic alterations by finding new methods and/or applying multi-method approaches.

In conclusion, I highlight the need for careful interpretation of carbonate-based water temperature reconstructions such as those presented in Manuscript III, as small-scale diagenesis can significantly impact measured $\delta^{18}O$ and $\delta^{13}C$ and substantially distort the derived palaeo-climatic or palaeo-environmental interpretation. This study clearly shows the importance of a precise and careful check for any kind of alteration within the shell carbonate prior to any sampling or analysis.

Finally, it is an intention of mine to point out that there is a severe lack of acknowledgement and discussion in the literature regarding ‘neomorphism’ in more recent sclerochronological studies using carbonate biogenic archives (e.g., bivalves or corals). In order to guarantee that isotope analysis is preferentially performed on

material that has not undergone any recrystallization the community must ensure that steps are taken to assess the degree of 'neomorphism' in specimens assigned for biogeochemical analysis and for most accurate results.

5.2 Main Conclusion B: Seasonal Palaeo-temperatures

Question B1

Did sub-fossil *A. islandica* shells from the Dicksonfjord, Svalbard, record palaeo-water temperatures in their shell carbonate ($\delta^{18}O$)? If so, what are the reconstructed absolute water temperatures and seasonal amplitude for the early Holocene Climate Optimum?

Answer B1

Yes, sub-fossil *A. islandica* shells from the Dicksonfjord recorded water temperatures (2.8°C to 15.2°C), resulting in a palaeo-seasonality of 12.4°C for the assumed growing season (April to August) during the HCO.

To investigate the potential of early Holocene *A. islandica* bivalve shells for the reconstruction of palaeo-temperatures and palaeo-seasonality during the HCO interval I measured the stable oxygen isotope values ($\delta^{18}O_{shell}$) in three sub-fossil shells of *A. Islandica* from the Dicksonfjord, Svalbard. Samples were taken for isotope analysis along the growth trajectory with an exceptional high spatial resolution (up to 200 individual samples per ontogenetic year). Measured oxygen isotope are subject to possible fluctuations in palaeo-salinity, variations in seawater chemistry ($\delta^{18}O_{seawater}$) as well as changes in ice volume and the length of the growing season, all of which were considered and accounted for where possible.

Based on confocal Raman microscope (CRM) scans (c.f., Manuscripts II and III) I was able to show that all shells consisted of pristine aragonite and therefore radiocarbon dating ($^{14}C_{AMS}$) and stable oxygen isotope analysis ($\delta^{18}O$) isotope results could be considered reliable. Radiocarbon dating ($^{14}C_{AMS}$) determined that these specimens lived during the early Holocene Climate Optimum (9,954–9,782 cal yrs BP). Stable oxygen isotope ($\delta^{18}O_{shell}$) profiles of six ontogenetic years from three shells show

distinct seasonal patterns with amplitudes of 2.7‰ to 2.9‰ (Figure 2 in Manuscript IV).

Reconstructed maximum and minimum palaeo-temperatures of 15.2°C and 2.8°C for the assumed shell growth period (April to August) imply a palaeo-seasonality of about 12.4°C for the early Holocene at Svalbard. This is the first unique palaeo-environmental description of a fjord setting during the Holocene Climate Optimum at Spitsbergen and coincides with temperature distribution of modern *A. islandica* (Figure 17). Furthermore, the average water temperature of 9.1°C argues that the HCO at Spitsbergen was 6°C warmer than present and hence distinctly exceeds most previous global HCO temperature estimates (+ 1–3°C). I have however confirmed studies that indicate an amplified warming effect (+ 4–6°C) at high northern latitudes.

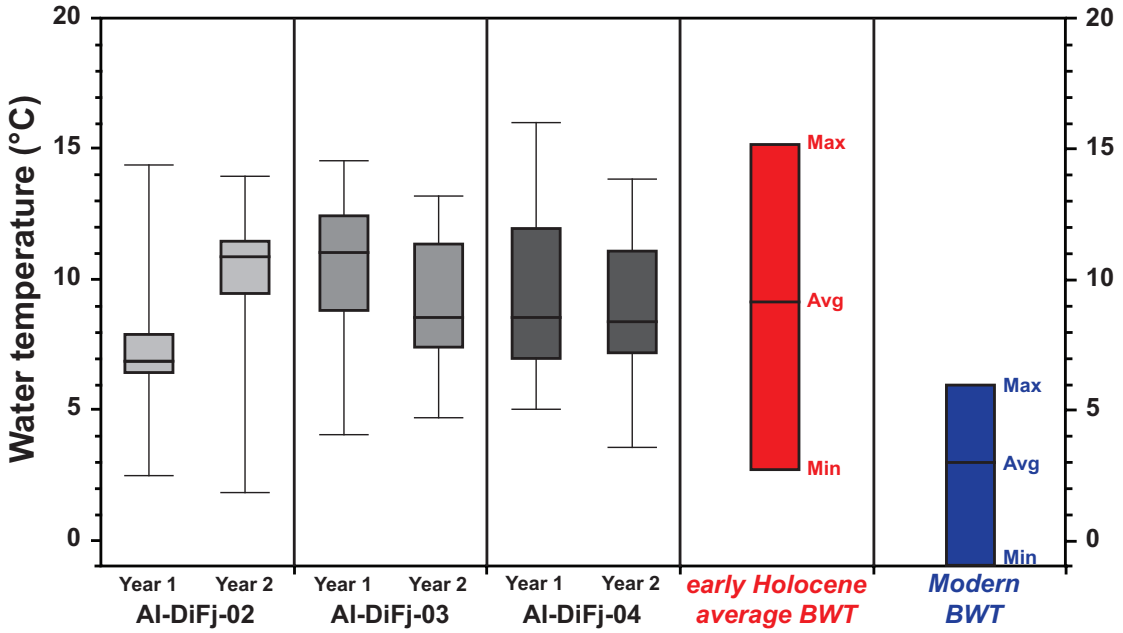

Figure 17. Reconstructed bottom water temperatures (BWTs) and palaeo-seasonality. Palaeo-temperatures derived from stable oxygen isotope values ($\delta^{18}O_{shell}$) of six individual ontogenetic years of specimens AI-DiFj-02, AI-DiFj-03 and AI-DiFj-04. Individual years are given as box-and-whisker plots with box giving the first quartile, median and third quartile (horizontal lines from top to bottom). Upper and lower whiskers give maximum and minimum of all data. Reconstructed early Holocene BWTs represent average values based on all six ontogenetic years. Modern MWT based on data listed in Table 1 in Manuscript IV.

5.3 Main Conclusion C: Decadal variability

Question C1

Do early Holocene *A. islandica* shells from the Dicksonfjord, Svalbard contain significant year-to-year variabilities within the internal growth record? What are the most likely potential environmental/climate drivers of any identified oscillations in shell growth?

Answer C1

Yes, a significant and pronounced quasi-decadal 11-year cyclicity could be identified in all *A. islandica* shells from the Dicksonfjord, Svalbard. Since there is a well-recognised 11-year cyclicity in the sun´s magnetic field (Schwabe cycle), potential mechanistic links between solar activity and shell growth via a biological (i.e., primary production) and UV radiation-induced amplification mechanism are presented and discussed.

Manuscript V presents the results of the frequency analysis of the growth records of six individual early Holocene (9,800 cal yrs BP) *A. islandica* bivalve shells, which have been derived from raised beach deposits in the Dicksonfjord, Svalbard (79°N). I identify a pronounced 11-year periodicity in the growth of the shells, which is likely attributed to the solar sunspot cycle (Figure 18). Although the direct change in solar forcing is likely to be small, it is clear that variability in the Sun's energy impacts upon a multitude of climatic, oceanographic and biological processes, each of which may cause an indirect physiological response in benthic organisms that is incorporated into their shells. I propose a first theoretical explanation for a connection between solar irradiance and bivalve growth via a potential amplifying mechanism such as UV radiation.

I propose a feasible mechanistic link between irradiance and shell growth via atmospheric processes, where UV-B radiation is negatively correlated to phytoplankton productivity, acting to amplify the initial irradiance change during periods of solar maxima (Figure 19). The 11-year and other solar signals have often been identified within biological and non-biological climate archives with no further explanation for the mechanisms that link the initial solar activity and the organism

growth. It is essential to understand the potential factors influencing shell growth in order to reliably distinguish between the effects of natural versus anthropogenic climate change. Therefore, although I recognise that the causal link I propose is a strongly simplified scenario, I hope that Manuscript V will generate debate along the scientific community who use biogenic archives for climatic and environmental reconstructions.

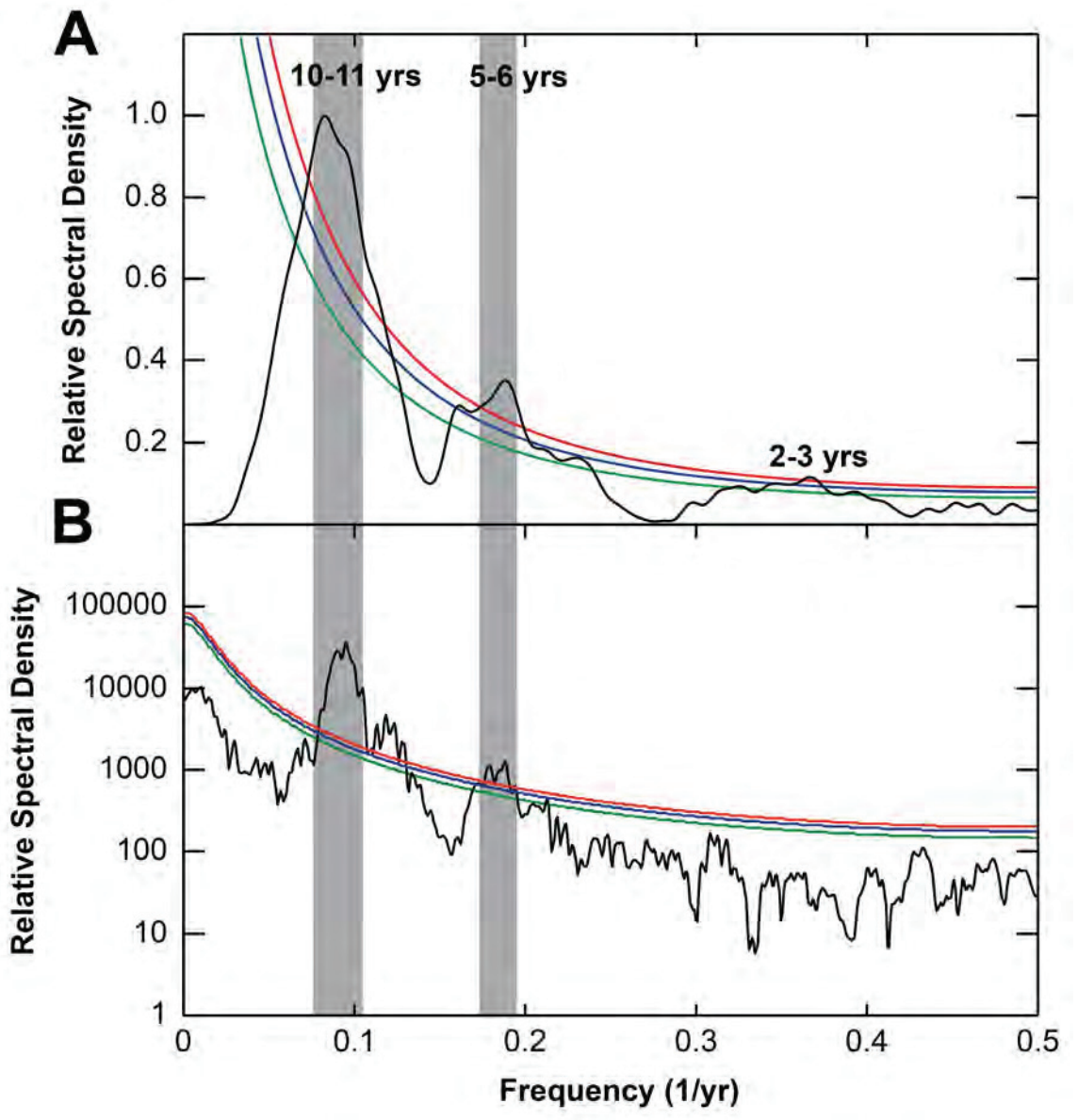

Figure 18. Comparison of spectral density 'fingerprints' in the form of stacked early Holocene *A. islandica* (all six shells) growth increment MTM (A) and sunspot number MTM (B) time-series (CE 1749–2012). Both MTMs share significant peaks at 11–10 years and 5–6 years respectively (highlighted by grey bars). Green (90%), blue (95%) and red (99%) lines being significance levels. Note that for illustration purposes the sunspot MTM has been plotted to a logarithmic scale.

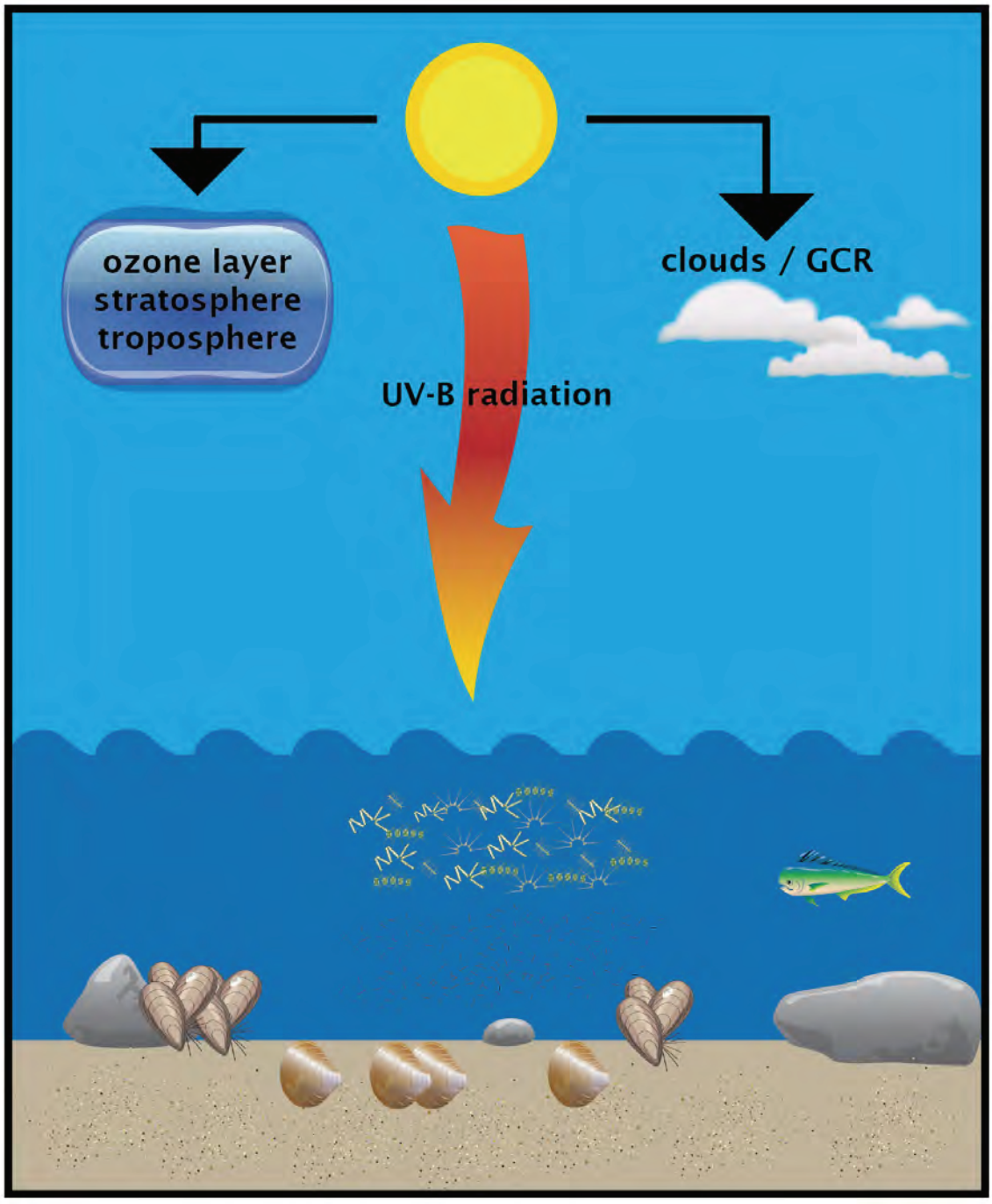

Figure 19. Schematic illustration showing the hypothesized mechanistic/causal link between solar activity and marine bivalve shell growth. Decadal changes in UV-B radiation associated with the Schwabe sunspot cycle negatively influence phytoplankton productivity, i.e., the food source of the bivalve. In this model, phytoplankton inversely amplifies changes in solar activity. Phases of strong solar activity (maxima; high sunspot numbers) are associated with a maximum of emitted and incident solar irradiance and more UV-B radiation subsequently reaches Earth´s surface and penetrates the upper layer of the oceans. Since UV-B radiation in general has a negative effect on phytoplankton growth and abundance this results in reduced abundance and quality of food for benthic communities and particularly deposit feeders such as *A. islandica*, a main driver of shell growth. The illustrated scenario of high solar activity during a solar maximum would result in less strong bivalve shell growth.

Further work on high-resolution biogenic archives at the high latitudes is necessary to explore some of the potential connections highlighted in Manuscript V. I am confident that with a reliable and established explanation for the connection between solar activity and bivalve shell growth, shell records derived from high latitudes might also be used as potential proxy for past solar activity. In addition, longer time-series data from the instrumental period will hopefully in time shed light on physical climate and ocean mechanisms associated with solar cycles.

5.4 Future Challenges & Perspectives

Arctica islandica is an amazing archive of past climatic and past environmental conditions (see Schöne (2013) for a comprehensive summary). A variety of different proxies can be used for reconstructions on different sub-annual (seasonal: Manuscript IV) to decadal (Manuscript V) and even multi-centennial time scales (Butler et al., 2013). However, in my opinion the immense potential of *A. islandica* as a climate recorder has yet to be fully exploited. Sclerochronology is a highly interdisciplinary field of science that brings together many disciplines, including climatology, oceanography, palaeontology and geology, geochemistry, biology and ecology. Since scientists usually bring in expertise of one or two of these fields it is essential that future projects involve collaborators covering as many of the above mentioned fields as possible to exploit the true potential of sclerochronology and also *A. islandica* as a biogenic archive of past environmental conditions. For the work I have presented in my thesis, there are a number of recommendations that would benefit this work and should be the focus of future studies.

First, a reliable dating method for absolute ages further back than 50,000 years (i.e., the maximum time period for $^{14}C_{AMS}$ radiocarbon dating) urgently needs development. (Bio-) stratigraphy is a powerful approach but will always only provide low-resolution (often several hundred thousand to millions of years) time windows. In my opinion, other dating options (e.g., including U- and Th-series; Hillaire-Marcel, 2009) are not (yet) reliable enough. Without precise dating, it is not possible to conduct studies similar to those presented in this thesis on older fossil bivalve specimens.

Manuscript III demonstrates the significant influence that minor recrystallization patches within the shell carbonate of fossil *A. islandica* might have on palaeo-environmental reconstructions and how difficult it is to identify them. The development

of a standard procedure that should be strictly followed when working on fossil specimens should be a matter of priority. Since no established method so far is able to meet this requirement, a multi-method approach that combines the strengths of different techniques and compensates for individual approach weaknesses is recommended. CRM should be considered an excellent addition to the conventional sclerochronology tool arsenal, due to its ability to reliably identify both taphonomic alterations and visualize growth patterns in modern and especially in fossil shell carbonate (Manuscripts II and III). Future studies that apply CRM to visualize growth patterns or non-biogenic laminated structures (e.g., stalagmites) may shed light onto new archives and growth record data that have so far remained unused.

Although daily increments in *A. islandica* have been reported (Schöne et al., 2005c), there is no reliable method to-date to visualize them in several consecutive ontogenetic years. If successfully established, this would help to decipher sub-annual growth rates. The ultimate aim would be to create annual growth models (as done in Schöne et al., 2005c) for different populations at different localities in order to more precisely assign biogeochemical measurements taken sub-annually but also to identify drivers of daily growth. This would provide sclerochronology with a new temporal dimension that would greatly exceed seasonality, already a remarkable feature of *A. islandica*.

As the results in Manuscript V indicate, there might be an indirect connection between shell growth and solar activity amplified by a biological process such as phytoplankton productivity inversely coupled to decadal changes in UV radiation. As of today, no explanation has been given for the mechanistic link between the 11-year cyclicity in shell growth and other biogenic archives. Any direct or indirect influence of solar activity on bivalve growth is too important to be neglected or even ignored in publications. If we want to use such biogenic archives for palaeo-environmental studies, we need to understand all processes involved in driving shell growth on all spatial (local, regional, global) and temporal (tidal to multi-centennial) scales. This particularly applies to modern studies that seek to reliably distinguish between natural and anthropogenic driven climate change. This also applies for linear/multivariate regression and frequency analyses that observe correlations between shell growth and an environmental, climatic or atmospheric time-series of any kind – the mechanisms linking them need to be investigated and scrutinized rather than, for example, automatically linking every significant 5 to 7 year signal in a biogenic archive to NAO.

A potential key topic for future research is crystal structures (e.g., Füllenbach et al., 2014 for the freshwater gastropod *Viviparus viviparus*), as it potentially records changes in stress of the animal, related to environmental conditions such as water temperature or pH. Advances in resolution and the sophistication of technical equipment (e.g., NanoSIMS and Electron backscatter diffraction (EBSD) techniques in Karney et al., 2012) might hopefully finally provide insights in the processes of biomineralization on micro- and nano-scales.

$\delta^{18}O$ values and growth increment widths have been used successfully in this thesis and are well-established proxy records in bivalve shells and other biogenic archives. However, the calibration and advancement of new and existing proxies (such as Mg/Ca ratios in foraminifera and coralline algae as a salinity-independent proxy for water temperatures) would be highly beneficial to the field of sclerochronology. Future advances in $\delta^{44}Ca$ or clumped isotopes will perhaps overcome current problems in calibration (Hippler et al., 2013; Eagle et al., 2013; Henkes et al., 2013) and become reliable future proxies for palaeo-temperatures. Trace and minor elements as well as advances in the examination of Rare Earth Elements (REE) might also yield the potential for completely new proxies.

As results from Manuscript IV have shown, it is possible to reveal palaeo-environmental information from early Holocene bivalve shells that otherwise would not be accessible. The similarities between the climate of the HCO and future temperature predictions make this a particularly important interval for understanding the mechanisms of climate change in the high latitudes and better predicting the impacts of future global warming on the natural environment. Continued research into the HCO, and other comparable warm intervals, particularly at the sub-annual resolution presented here, will further our understanding of both the environmental conditions that were typical of warm periods but also, importantly, the biological responses experienced by a range of marine and terrestrial organisms.

Climate archives with a sub-annual temporal resolution at high latitudes in the northern North Atlantic realm are rare. Due to changing climatic conditions over geological time-scales and related changes in the bio-geographic distribution of suitable archive species, it is challenging to provide continuous master chronologies for time spans such as the entire Holocene. However, my study has shown the potential of individual shell chronologies as well as cross-dated floating chronologies to provide valuable insights into palaeoceanographic and palaeo-environmental

conditions at single points in time. The production of cross-dated chronologies in bivalves and other bio-archives to compliment those already produced by dendrochronologists would greatly improve our understanding of high latitude past climates that are expected to be much more vulnerable to future climate change.

Lastly, I urge a much greater effort in sourcing, combining and comparing sclerochronological proxy data for use with numerical model (GCMs) prediction. Those models are our only tool for reliably predicting future climate change scenarios, yet they lack information on absolute annual temperatures and especially information on seasonality from past warm phases. The calibration data that the sclerochronological community can provide is essential to verify those models and can only be assessed by looking at high-resolution climate archives such as bivalve shells and *A. islandica*. Greater collaboration with the modelling community will hopefully further refine both global and region climate projections and enable societies to better equip themselves for the reality of a warmer future.

6 Appendix

Appendix 1

Locality	Epoch	Stage/Age	Species	# of shells	Used in Manuscript	Provider
Dicksonfjord, Svalbard	Holocene		*A. islandica, S. groenlandicus*	11	IV & V	Otto Salvigsen
Eggum, Lofoten, Norway	Holocene (?)		*A. islandica*	5	I	Carin Andersson Dahl
Stirone River, Italy	Pleistocene	Calabrian	*A. islandica*	23	II	Sergio Raffi, Daniele Scarponi
Coralline Crag, UK	Pliocene	Piacenzian	*A. islandica*	5	II	Peter Long
Tjörnes Beds, Iceland	Pliocene	Zanclean	*A. islandica*	8	III	Lovísa Ásbjörnsdóttir
North Sea, Netherlands, Belgium, Germany	Pleistocene, Pliocene, Miocene, Oligocene	Gelasian, Piacenzian, Zanclean, Burdigalian, Chattian	*A. islandica, P. rustica*	7	II	Frank Wesselingh
Ile de France, Greenland	Pleistocene	Gelasian	*A. islandica*	18	---	Ole Bennike

Appendix 1. Shell origin of all shells analysed in this dissertation.

7 References

ACIA, 2004. Impacts of a Warming Arctic – Arctic Climate Impact Assessment. Cambridge University Press, Cambridge, UK, pp. 1039.

Aldridge, D.C., 1999. The morphology, growth and reproduction of Unionidae (Bivalvia) in a Fenland waterway. Journal of Molluscan Studies 65, 47–60.

Bathurst, R.G.C., 1964. The replacement of aragonite by calcite in the molluscan shell wall. Approaches to Paleoecology, 357–376.

Beaugrand, G., 2004. The North Sea regime shift: Evidence, causes, mechanisms and consequences. Progress in Oceanography 60, 245–262.

Beaugrand, G., Reid, P.C., Ibanez, F., Lindley, J.A., Edwards, M., 2002. Reorganization of North Atlantic marine copepod biodiversity and climate. Science 296, 1692–1694.

Benton, M., Harper, D., 2009. Introduction to paleobiology and the fossil record. Wiley-Blackwell, Oxford, pp. 608.

Bertolani Marchetti, D., Accorsi, C.A., Pelosio, G., Raffi, S., 1979. Palynology and stratigraphy of the Plio-Pleistocene sequence of the Stirone River (Northern Italy). Pollen et spores 21, 149–167.

Birks, C.J.A., Koc, N., 2002. A high-resolution diatom record of late-Quaternary sea-surface temperatures and oceanographic conditions from the eastern Norwegian Sea. Boreas 31, 323–344.

Birks, H.H., 1991. Holocene vegetational history and climatic change in west Spitsbergen-plant macrofossils from Skardtjørna, an Arctic lake. The Holocene 1, 209–218.

Black, B.A., 2009. Climate-driven synchrony across tree, bivalve, and rockfish growth-increment chronologies of the northeast Pacific. Marine Ecology Progress Series 378, 37–46.

Brey, T., Arntz, W.E., Pauly, D., Rumohr, H., 1990. *Arctica* (*Cyprina*) *islandica* in Kiel Bay (Western Baltic): growth, production and ecological significance. Journal of Experimental Marine Biology and Ecology 136, 217–235.

Brey, T., Mackensen, A., 1997. Stable isotopes prove shell growth bands in the Antarctic bivalve *Laternula elliptica* to be formed annually. Polar Biology 17, 465–468.

Buchardt, B., Simonarson, L.A., 2003. Isotope palaeotemperatures from the Tjörnes beds in Iceland: evidence of Pliocene cooling. Palaeogeography, Palaeoclimatology, Palaeoecology 189, 71–95.

Buddemeier, R.W., Maragos, J.E., Knutson, D.W., 1974. Radiographic studies of reef coral exoskeletons: Rates and patterns of coral growth. Journal of Experimental Marine Biology and Ecology 14, 179–199.

Butler, P.G., Richardson, C.A., Scourse, J.D., Wanamaker Jr, A.D., Shammon, T.M., Bennell, J.D., 2010. Marine climate in the Irish Sea: analysis of a 489-year marine master chronology derived from growth increments in the shell of the clam *Arctica islandica*. Quaternary Science Reviews 29, 1614–1632.

Butler, P.G., Wanamaker Jr, A.D., Scourse, J.D., Richardson, C.A., Reynolds, D.J., 2013. Variability of marine climate on the North Icelandic Shelf in a 1357-year proxy archive based on growth increments in the bivalve *Arctica islandica*. Palaeogeography, Palaeoclimatology, Palaeoecology 373, 141–151.

Carré, M., Bentaleb, I., Blamart, D., Ogle, N., Cardenas, F., Zevallos, S., Kalin, R.M., Ortlieb, L., Fontugne, M., 2005. Stable isotopes and sclerochronology of the bivalve *Mesodesma donacium*: Potential

application to Peruvian paleoceanographic reconstructions. Palaeogeography, Palaeoclimatology, Palaeoecology 228, 4–25.

Castanheira, J.M., Graf, H.F., 2003. North Pacific-North Atlantic relationships under stratospheric control? Journal of Geophysical Research 108, 1–10.

Chan, P., Halfar, J., Williams, B., Hetzinger, S., Steneck, R., Zack, T., Jacob, D.E., 2011. Freshening of the Alaska Coastal Current recorded by coralline algal Ba/Ca ratios. Journal of Geophysical Research 116, G01032.

Clark, G.R., 1975. Growth Rhythms and the History of the Earth's Rotation, in: Rosenberg, G.D., Runcorn, S.K. (Eds.). Wiley and Sons, New York, pp. 103–117.

Coe, W.R., 1948. Nutrition, environmental conditions, and growth of marine bivalve mollusks. Journal of Marine Research 7, 586–601.

Comiso, J.C., Parkinson, C.L., Gersten, R., Stock, L., 2008. Accelerated decline in the Arctic sea ice cover. Geophysical Research Letters 35, L01703.

Craig, G.Y., Hallam, A., 1963. Size-frequency and growth-ring analyses of *Mytilus edulis* and *Cardium edule*, and their palaeoecological significance. Palaeontology 6, 731–750.

Craig, M.H., Kleinschmidt, I., Nawn, J.B., Le Sueur, D., Sharp, B.L., 2004. Exploring 30 years of malaria case data in KwaZulu-Natal, South Africa: Part I. The impact of climatic factors. Tropical Medicine & International Health 9, 1247–1257.

Cuif, J.-P., Dauphin, Y., Nehrke, G., Nouet, J., Perez-Huerta, A., 2012. Layered growth and crystallization in calcareous biominerals: Impact of structural and chemical evidence on two major concepts in invertebrate biomineralization studies. Minerals 2, 11–39.

Dahlgren, T.G., Weinberg, J.R., Halanych, K.M., 2000. Phylogeography of the ocean quahog (*Arctica islandica*): influences of paleoclimate on genetic diversity and species range. Marine Biology 137, 487–495.

Davenport, C.B., 1938. Growth lines in fossil Pectens as indicators of past climates. Journal of Paleontology 12, 514–515.

De Sherbinin, A., Schiller, A., Pulsipher, A., 2007. The vulnerability of global cities to climate hazards. Environment and Urbanization 19, 39–64.

Dettman, D.L., Lohmann, K.C., 1995. Microsampling carbonates for stable isotope and minor element analysis: Physical separation of samples on a 20 micrometer scale. Journal of Sedimentary Research 65A, 566–569.

Dettman, D.L., Reische, A.K., Lohmann, K.C., 1999. Controls on the stable isotope composition of seasonal growth bands in aragonitic fresh-water bivalves (unionidae). Geochimica et Cosmochimica Acta 63, 1049–1057.

Doney, S.C., Fabry, V.J., Feely, R.A., Kleypas, J.A., 2009. Ocean acidification: the other CO_2 problem. Marine Science 1, 169–192.

Eagle, R.A., Eiler, J.M., Tripati, A.K., Ries, J.B., Freitas, P.S., Hiebenthal, C., Jr, A.D.W., Taviani, M., Elliot, M., Marenssi, S., Nakamura, K., Ramirez, P., Roy, K., 2013. The influence of temperature and seawater carbonate saturation state on ^{13}C–^{18}O bond ordering in bivalve mollusks. Biogeosciences Discussions 10, 157–194.

Ebbesen, H., Hald, M., Eplet, T.H., 2007. Lateglacial and early Holocene climatic oscillations on the western Svalbard margin, European Arctic. Quaternary Science Reviews 26, 1999–2011.

Elliot, M., Labeyrie, L., Duplessy, J.-C., 2002. Changes in North Atlantic deep-water formation associated with the Dansgaard-Oeschger temperature oscillations (60–100 ka). Quaternary Science Reviews 21, 1153–1165.

Evans, J.W., 1972. Tidal growth increments in the cockle *Clinocardium nuttalli*. Science 176, 416–417.

Felis, T., Lohmann, G., Kuhnert, H., Lorenz, S.J., Scholz, D., Pätzold, J., Al-Rousan, S.A., Al-Moghrabi, S.M., 2004. Increased seasonality in Middle East temperatures during the last interglacial period. Nature 429, 164–168.

Fluteau, F., Ramstein, G., Besse, J., Guiraud, R., Masse, J.P., 2007. Impacts of palaeogeography and sea level changes on Mid-Cretaceous climate. Palaeogeography, Palaeoclimatology, Palaeoecology 247, 357–381.

Forsythe, G.T.W., Scourse, J.D., Harris, I., Richardson, C.A., Jones, P., Briffa, K., Heinemeier, J., 2003. Towards an absolute chronology for the marine environment: The development of a 1000-year record from *Arctica islandica*. Geophysical Research Abstracts Vol. 5, 06044.

Frank, D.C., Esper, J., Raible, C.C., Buntgen, U., Trouet, V., Stocker, B., Joos, F., 2010. Ensemble reconstruction constraints on the global carbon cycle sensitivity to climate. Nature 463, 527–530.

Friedrich, M., Remmele, S., Kromer, B., Hofmann, J., Spurk, M., Kaiser, K.f., Orcel, C., Küppers, M., 2004. The 12,460-year Hohenheim Oak and pine tree-ring chronology from central Europe: A unique annual record for radiocarbon calibration and paleoenvironment reconstructions. Radiocarbon 46, 1111–1122.

Füllenbach, C.S., Schöne, B.R., Branscheid, R., 2014. Microstructures in shells of the freshwater gastropod *Viviparus viviparus*: A potential sensor for temperature change? Acta Biomaterialia 10, 3911–3921.

Giannini, A., Cane, M.A., Kushnir, Y., 2001. Interdecadal changes in the ENSO teleconnection to the Caribbean Region and the North Atlantic Oscillation. Journal of Climate 14, 2867–2879.

Goewert, A., Surge, D., 2008. Seasonality and growth patterns using isotope sclerochronology in shells of the Pliocene scallop *Chesapecten madisonius*. Geo-Marine Letters 28, 327–338.

Grossman, E.L., Ku, T.-L., 1986. Oxygen and carbon isotope fractionation in biogenic aragonite: Temperature effects. Chemical Geology 59, 59–74.

Gruber, N., Keeling, C.D., Bates, N.R., 2002. Interannual variability in the North Atlantic Ocean carbon sink. Science 298, 2374–2378.

Hahn, S., Rodolfo-Metalpa, R., Griesshaber, E., Schmahl, W.W., Buhl, D., Hall-Spencer, J.M., Baggini, C., Fehr, K.T., Immenhauser, A., Slomp, C.P., 2012. Marine bivalve shell geochemistry and ultrastructure from modern low pH environments: environmental effect versus experimental bias. Biogeosciences 9, 1897–1914.

Hald, M., Ebbesen, H., Forwick, M., Godtliebsen, F., Khomenko, L., Korsun, S., Ringstad Olsen, L., Vorren, T.O., 2004. Holocene paleoceanography and glacial history of the West Spitsbergen area, Euro-Arctic margin. Quaternary Science Reviews 23, 2075–2088.

Hallmann, N., Burchell, M., Schöne, B.R., Irvine, G.V., Maxwell, D., 2009. High-resolution sclerochronological analysis of the bivalve mollusk *Saxidomus gigantea* from Alaska and British Columbia:

techniques for revealing environmental archives and archaeological seasonality. Journal of Archaeological Science 36, 2353–2364.

Henkes, G.A., Passey, B.H., Wanamaker, A.D., Grossman, E.L., Ambrose, W.G., Carroll, M.L., 2013. Carbonate clumped isotope compositions of modern marine mollusk and brachiopod shells. Geochimica et Cosmochimica Acta 106, 307–325.

Hetzinger, S., Halfar, J., Kronz, A., Steneck, R.S., Adey, W., Lebednik, P.A., Schöne, B.R., 2009. High-resolution Mg/Ca ratios in a coralline red alga as a proxy for Bering Sea temperature variations from 1902 to 1967. PALAIOS 24, 406–412.

Hillaire-Marcel, C., 2009. The U-series dating of (biogenic) carbonates. Earth and Environmental Science 5, 1–12.

Hippler, D., Witbaard, R., van Aken, H.M., Buhl, D., Immenhauser, A., 2013. Exploring the calcium isotope signature of *Arctica islandica* as an environmental proxy using laboratory- and field-cultured specimens. Palaeogeography, Palaeoclimatology, Palaeoecology 373, 75–87.

Hoefs, J., 1997. Stable Isotope Geochemistry. Springer Berlin, pp. 201.

Hudson, J.H., Shinn, E.A., Halley, R.B., Lidz, B., 1976. Sclerochronology: A tool for interpreting past environments. Geology 4, 361–364.

Hurd, B.H., Callaway, M., Smith, J., Kirshen, P., 2004. Climatic change and U.S. water resources: From modeled watershed impacts to national estimates. Journal of the American Water Resources Association 40, 129–148.

Hurrell, J.W., Hoerling, M.P., Folland, C.K., 2002. Climatic variability over the North Atlantic. International Geophysics 83, 143–151.

Hurrell, J.W., Kushnir, Y., Ottersen, G., Visbeck, M., 2003. An overview of the North Atlantic Oscillation. Geophysical Monograph 134, 1–36.

Huynen, M., Martens, P., Schram, D., Weijenberg, M.P., Kunst, A.E., 2001. The impact of heat waves and cold spells on mortality rates in the Dutch population. Environmental Health Perspectives 109, 463–470.

IPCC, 2013. Climate Change 2013: The Physical Science Basis. Contribution of Working Group I to the Fifth Assessment Report of the Intergovernmental Panel on Climate Change. Cambridge University Press, Cambridge, United Kingdom and New York, NY, USA.

Jones, D.S., 1980. Annual cycle of shell growth increment formation in two continental shelf bivalves and its paleoecologic significance. Paleobiology 6, 331–340.

Jones, D.S., 1983. Sclerochronology: Reading the record of the Molluscan Shell. Arnerican Scientist 71, 384–391.

Jones, D.S., Arthur, M.A., Allard, D.J., 1989. Sclerochronological records of temperature and growth from shells of *Mercenaria mercenaria* from Narragansett Bay, Rhode Island. Marine Biology 102, 225–234.

Jones, D.S., Thompson, I., Ambrose, W., 1978. Age and growth rate determinations for the Atlantic Surf Clam *Spisula solidissima* (Bivalvia: Mactracea), based on internal growth lines in shell cross-sections. Marine Biology 47, 63–70.

Kalis, A.J., Merkt, J., Wunderlich, J., 2003. Environmental changes during the Holocene climatic optimum in central Europe – human impact and natural causes. Quaternary Science Reviews 22, 33–79.

Karney, G.B., Butler, P.G., Speller, S., Scourse, J.D., Richardson, C.A., Schröder, M., Hughes, G.M., Czernuszka, J.T., Grovenor, C.R.M., 2012. Characterizing the microstructure of *Arctica islandica* shells using NanoSIMS and EBSD. Geochemistry, Geophysics, Geosystems 13, 1–14.

Koike, H., 1980. Seasonal dating by growth-line counting of the clam, *Meretrix lusoria*. University of Tokyo.

Koppe, C., 2005. Gesundheitsrelevante Bewertung von thermischer Belastung unter Berücksichtigung der kurzfristigen Anpassung der Bevölkerung an die lokalen Witterungsverhältnisse. University of Freiburg, pp. 214.

Krause-Nehring, J., Brey, T., Thorrold, S.R., 2012. Centennial records of lead contamination in northern Atlantic bivalves (*Arctica islandica*). Marine Pollution Bulletin 64, 233–240.

Lohmann, G., Schöne, B.R., 2012. Climate signatures on decadal to interdecadal time scales as obtained from mollusk shells (*Arctica islandica*) from Iceland. Palaeogeography, Palaeoclimatology, Palaeoecology, 152–162.

MacLachlan, S.E., Cottier, F.R., Austin, W.E.N., Howe, J.A., 2007. The salinity:$\delta^{18}O$ water relationship in Kongsfjorden, western Spitsbergen. Polar Research 26, 160–167.

Maliva, R.G., 1998. Skeletal aragonite neomorphism – quantitative modelling of a two-water diagenetic system. Sedimentary Geology 121, 179–190.

Maliva, R.G., Missimer, T.M., Dickson, J.A.D., 2000. Skeletal aragonite neomorphism in Plio-Pleistocene sandy limestones and sandstones. Sedimentary Geology 136, 147–154.

Marchitto, T.M., Jones, G.A., Goodfriend, G.A., Weidman, C.R., 2000. Precise Temporal Correlation of Holocene Mollusk Shells Using Sclerochronology. Quaternary Research 53, 236–246.

Marshall, J., Kushnir, Y., Battisti, D., Chang, P., Czaja, A., Dickson, R., Hurrell, J., McCartney, M., Saravanan, R., Visbeck, M., 2001. North Atlantic climate variability: Phenomena, impacts and mechanisms. International Journal of Climatology 21, 1863–1898.

Martin, G.D., Wilkinson, B.H., Lohmann, K.C., 1986. The Role of Skeletal Porosity in Aragonite Neomorphism–*Strombus* and *Montastrea* from the Pleistocene Key Largo Limestone, Florida. Journal of Sedimentary Research 56, 1–10.

Mary, C., Iaccarino, S., Courtillot, V., Besse, J., Aissaoui, D.M., 1993. Magnetostratigraphy of Pliocene Sediments From the Stirone River (Po Valley). Geophysical Journal International 112, 359–380.

Matthews, K.A., Grottoli, A.G., McDonough, W.F., Palardy, J.E., 2008. Upwelling, species, and depth effects on coral skeletal cadmium-to-calcium ratios (Cd/Ca). Geochimica et Cosmochimica Acta 72, 4537–4550.

Meehl, G.A., Washington, W.M., Collins, W.D., Arblaster, J.M., Hu, A., Buja, L.E., Strand, W.G., Teng, H., 2005. How much more global warming and sea level rise? Science 307, 1769–1772.

Meehl, G.A., Zwiers, F., Evans, J., Knutson, T., Mearns, L., Whetton, P., 2000. Trends in Extreme Weather and Climate Events: Issues Related to Modeling Extremes in Projections of Future Climate Change. Bulletin of the American Meteorological Society 81, 427–436.

Miller, G.H., Alley, R.B., Brigham-Grette, J., Fitzpatrick, J.J., Polyak, L., Serreze, M.C., White, J.W.C., 2010. Arctic amplification: can the past constrain the future? Quaternary Science Reviews 29, 1779–1790.

Mills, E., 2005. Insurance in a climate of change. Science 309, 1040–1044.

Myers, R.A., Hutchings, J.A., Barrowman, N.J., 1996. Hypotheses for the decline of cod in the North Atlantic. Marine Ecology Progress Series 138, 293–308.

Nehrke, G., Nouet, J., 2011. Confocal Raman microscope mapping as a tool to describe different mineral and organic phases at high spatial resolution within marine biogenic carbonates: case study on *Nerita undata* (Gastropoda, Neritopsina). Biogeosciences 8, 3761–3769.

Nehrke, G., Poigner, H., Wilhelms-Dick, D., Brey, T., Abele, D., 2012. Coexistence of three calcium carbonate polymorphs in the shell of the Antarctic clam *Laternula elliptica*. Geochemistry, Geophysics, Geosystems 13, Q05014.

Pannella, G., MacClintock, C., 1968. Biological and Environmental Rhythms reflected in Molluscan Shell Growth. Memoir 2, 64–80.

Patz, J.A., Campbell-Lendrum, D., Holloway, T., Foley, J.A., 2005. Impact of regional climate change on human health. Nature 438, 310–317.

Petit, J.R., Jouzel, J., Raynaud, D., Barkov, N.I., Barnola, J.M., Basile, I., Bender, M., Chappellaz, J., Davis, M., Delaygue, G., Delmotte, M., Kotlyakov, V.M., Legrand, M., Lipenkov, V.Y., Lorius, C., Pepin, L., Ritz, C., Saltzman, E., Stievenard, M., 1999. Climate and atmospheric history of the past 420,000 years from the Vostok ice core, Antarctica. Nature 399, 429–436.

Raman, C.V., Krishnan, K.S., 1928. A new type of secondary radiation. Nature 121, 501–502.

Rasmussen, T.L., Forwick, M., Mackensen, A., 2012. Reconstruction of inflow of Atlantic Water to Isfjorden, Svalbard during the Holocene: Correlation to climate and seasonality. Marine Micropaleontology 94/95, 80–90.

Richardson, C.A., 2001. Molluscs as archives of environmental change. Oceanography and Marine Biology 39, 103–164.

Rodwell, M.J., Rowell, D.P., Folland, C.K., 1999. Oceanic forcing of the wintertime North Atlantic Oscillation and European climate. Nature 398, 320–323.

Ropes, J.W., Jones, D.S., Murawski, S.A., Serchuk, F.M., Jearld Jr, A., 1984. Documentation of annual growth lines in ocean quahogs, *Arctica islandica* Linné. Fishery Bulletin 82, 1–19.

Roth, P.H., 1986. Mesozoic palaeoceanography of the North Atlantic and Tethys oceans. Geological Society, London, Special Publications 21, 299–320.

Sabine, C.L., Feely, R.A., Gruber, N., Key, R.M., Lee, K., Bullister, J.L., Wanninkhof, R., Wong, C., Wallace, D.W.R., Tilbrook, B., 2004. The oceanic sink for anthropogenic CO_2. Science 305, 367–371.

Salvigsen, O., Forman, S.L., Miller, G.H., 1992. Thermophilous molluscs on Svalbard during the Holocene and their paleoclimatic implications. Polar Research 11, 1–10.

Salzmann, U., Williams, M., Haywood, A.M., Johnson, A.L.A., Kender, S., Zalasiewicz, J., 2011. Climate and environment of a Pliocene warm world. Palaeogeography, Palaeoclimatology, Palaeoecology 309, 1–8.

Sarnthein, M., Van Kreveld, S., Erlenkeuser, H., Grootes, P.M., Kucera, M., Pflaumann, U., Schulz, M., 2003. Centennial-to-millennial-scale periodicities of Holocene climate and sediment injections off the western Barents shelf, 75°N. Boreas 32, 447–461.

Scaife, A.A., Folland, C.K., Alexander, L.V., Moberg, A., Knight, J.R., 2008. European climate extremes and the North Atlantic Oscillation. Journal of Climate 21, 72–83.

Schöne, B.R., 2008. The curse of physiology: challenges and opportunities in the interpretation of geochemical data from mollusk shells. Geo-Marine Letters 28, 269–285.

Schöne, B.R., 2013. Arctica islandica (Bivalvia): A unique paleoenvironmental archive of the northern North Atlantic Ocean. Global and Planetary Change 111, 199–225.

Schöne, B.R., Dunca, E., Fiebig, J., Pfeiffer, M., 2005a. Mutvei's solution: An ideal agent for resolving microgrowth structures of biogenic carbonates. Palaeogeography, Palaeoclimatology, Palaeoecology 228, 149–166.

Schöne, B.R., Fiebig, J., 2009. Seasonality in the North Sea during the Allerød and Late Medieval Climate Optimum using bivalve sclerochronology. International Journal of Earth Sciences 98, 83–98.

Schöne, B.R., Fiebig, J., Pfeiffer, M., Gle, R., Hickson, J., Johnson, A.L.A., Dreyer, W., Oschmann, W., 2005b. Climate records from a bivalved Methuselah (*Arctica islandica*, Mollusca; Iceland). Palaeogeography, Palaeoclimatology, Palaeoecology 228, 130–148.

Schöne, B.R., Freyre Castro, A.D., Fiebig, J., Houk, S.D., Oschmann, W., Kröncke, I., 2004. Sea surface water temperatures over the period 1884–1983 reconstructed from oxygen isotope ratios of a bivalve mollusk shell (*Arctica islandica*, southern North Sea). Palaeogeography, Palaeoclimatology, Palaeoecology 212, 215–232.

Schöne, B.R., Houk, S.D., Freyre Castro, A.D., Fiebig, J., Oschmann, W., Kröncke, I., Dreyer, W., Gosselck, F., 2005c. Daily growth rates in shells of *Arctica islandica*: Assessing sub-seasonal environmental controls on a long-lived bivalve mollusk. Palaios 20, 78–92.

Schöne, B.R., Kröncke, I., Houk, S., Castro, A., Oschmann, W., 2003a. The cornucopia of chilly winters: Ocean quahog (*Arctica islandica* L., Mollusca) master chronology reveals bottom water nutrient enrichment during colder winters (North Sea). Marine Biodiversity 32, 165–175.

Schöne, B.R., Oschmann, W., Rössler, J., Castro, A.D.F., Houk, S.D., Kröncke, I., Dreyer, W., Janssen, R., Rumohr, H., Dunca, E., 2003b. North Atlantic Oscillation dynamics recorded in shells of a long-lived bivalve mollusk. Geology 31, 1037–1040.

Schöne, B.R., Page, N., Rodland, D., Fiebig, J., Baier, S., Helama, S., Oschmann, W., 2007. ENSO-coupled precipitation records (1959–2004) based on shells of freshwater bivalve mollusks (*Margaritifera falcata*) from British Columbia. International Journal of Earth Sciences 96, 525–540.

Schöne, B.R., Pfeiffer, M., Pohlmann, T., Siegismund, F., 2005d. A seasonally resolved bottom-water temperature record for the period AD 1866–2002 based on shells of *Arctica islandica* (Mollusca, North Sea). International Journal of Climatology 25, 947–962.

Schöne, B.R., Radermacher, P., Zhang, Z., Jacob, D.E., 2013. Crystal fabrics and element impurities (Sr/Ca, Mg/Ca, and Ba/Ca) in shells of *Arctica islandica* – Implications for paleoclimate reconstructions. Palaeogeography, Palaeoclimatology, Palaeoecology 373, 50–59.

Schönwiese, C., 1992. Vulkanismus und Klimageschichte. Umweltwissenschaften und Schadstoff-Forschung 4, 239–245.

Scotese, C.R., Gahagan, L.M., Larson, R.L., 1988. Plate tectonic reconstructions of the Cretaceous and Cenozoic ocean basins. Tectonophysics 155, 27–48.

Serreze, M.C., Francis, J.A., 2006. The Arctic on the fast track of change. Weather 61, 65–69.

Shindell, D.T., Schmidt, G.A., Miller, R.L., Mann, M.E., 2003. Volcanic and solar forcing of climate change during the preindustrial era. Journal of Climate 16, 4094–4107.

Smith, E., Dent, G., 2005. Modern Raman Spectroscopy – A Practical Approach. Wiley, Hoboken, N.J., pp. 210.

Solomon, S., Qin, D., Manning, M., Chen, Z., Marquis, M., Averyt, K.B., Tignor, M., Miller, H.L., 2007. IPCC, 2007: climate change 2007: the physical science basis. Contribution of Working Group I to the fourth assessment report of the Intergovernmental Panel on Climate Change, pp. 1007.

Spann, N., Harper, E., Aldridge, D., 2010. The unusual mineral vaterite in shells of the freshwater bivalve *Corbicula fluminea* from the UK. Naturwissenschaften 97, 743–751.

Stenevik, E.K., Sundby, S., 2007. Impacts of climate change on commercial fish stocks in Norwegian waters. Marine Policy 31, 19–31.

Torrence, C., Compo, G.P., 1998. A Practical Guide to Wavelet Analysis. Bulletin of the American Meteorological Society 79, 61–78.

Trigo, R.M., Osborn, T.J., Corte-Real, J.o.M., 2002. The North Atlantic Oscillation influence on Europe: climate impacts and associated physical mechanisms. Climate Research 20, 9–17.

Tütken, T., Vennemann, T.W., 2011. Fossil bones and teeth: Preservation or alteration of biogenic compositions? Palaeogeography, Palaeoclimatology, Palaeoecology 310, 1–8.

Vörösmarty, C.J., Green, P., Salisbury, J., Lammers, R.B., 2000. Global water resources: vulnerability from climate change and population growth. Science 289, 284–284.

Wanamaker Jr, A., Kreutz, K., Schöne, B., Pettigrew, N., Borns, H., Introne, D., Belknap, D., Maasch, K., Feindel, S., 2008. Coupled North Atlantic slope water forcing on Gulf of Maine temperatures over the past millennium. Climate Dynamics 31, 183–194.

Wanamaker Jr, A.D., Kreutz, K.J., Schöne, B.R., Introne, D.S., 2011. Gulf of Maine shells reveal changes in seawater temperature seasonality during the Medieval Climate Anomaly and the Little Ice Age. Palaeogeography, Palaeoclimatology, Palaeoecology 302, 43–51.

Wardlaw, N., Oldershaw, A., Stout, M., 1978. Transformation of aragonite to calcite in a marine gastropod. Canadian Journal of Earth Sciences 15, 1861–1866.

Weidman, C.R., Jones, G.A., Lohmann, K.G., 1994. The long-lived mollusc *Arctica islandica*: A new paleoceanographic tool for the reconstruction of bottom temperatures for the continental shelves of the northern North Atlantic Ocean. Journal of Geophysical Research 99, 18305–18314.

Weslawski, J.M., Zajaczkowski, M., Kwasniewski, S., Jezierski, J., Moskal, W., 1988. Seasonality in an Arctic fjord ecosystem: Hornsund, Spitsbergen. Polar Research 6, 185–189.

Wetherald, R.T., Manabe, S., 2002. Simulation of hydrologic changes associated with global warming. Journal of Geophysical Research 107, 1–15.

Witbaard, R., 1996. Growth variations in *Arctica islandica* L. (Mollusca): a reflection of hydrography-related food supply. ICES Journal of Marine Science 53, 981–987.

Witbaard, R., Franken, R., Visser, B., 1997. Growth of juvenile *Arctica islandica* under experimental conditions. Helgoländer Meeresuntersuchungen 51, 417–431.

Erklärung gemäß § 6 (5) PromO

(vom 14. März 2007)

Name: Lars Beierlein

Anschrift: Lilienthalstraße 17, 27570 Bremerhaven

Bremerhaven, den .....

Ich erkläre hiermit eidesstattlich, dass ich

1. die vorliegende Doktorarbeit mit dem Titel “Predicting the future of northern North Atlantic shallow water ecosystems from fossil bio-archives” ohne unerlaubte fremde Hilfe angefertigt habe,
2. keine anderen als die von mir angegebenen Quellen und Hilfsmittel benutzt habe,
3. die den benutzten Werken wörtlich oder inhaltlich entnommenen Stellen als solche kenntlich gemacht habe.

_____

Unterschrift